Gene Expression Patterns in Human Prostate Stem Cell Differentiation

Emma Elizabeth Oldridge

PhD

University of York

Department of Biology

September 2012

ABSTRACT

The identification of phenotypic differences between stem cells (SCs) and their more differentiated counterparts is crucial for designing novel SC-based therapeutics for prostate cancer (CaP). RARRES1 and LXN were identified as two homologous genes whose expression was highly significantly down-regulated in the SC fraction compared to more differentiated epithelial cells. The overall aim of this study was to investigate the expression, regulation and function of the SC-silenced genes RARRES1 and LXN, and their potential interacting partner CPA4 in prostate epithelial differentiation and CaP.

We showed that RARRES1 and LXN were SC-silenced genes, whose expression was induced by the pro-differentiation agent all-*trans* retinoic acid (atRA). AtRA induced expression to a higher extent in the most differentiated cells than the SC fraction, suggesting that this sub-population was less responsive to atRA. Importantly, siRNA suppression of RARRES1 and LXN enhanced the SC properties of primary prostate cultures, as shown by a significant increase in their colony forming ability. Expression of both RARRES1 and LXN was co-ordinately repressed by DNA methylation in CaP cell lines and inhibition of RARRES1 and LXN increased the invasive capacity of primary prostate cultures, which also fully rescued an inhibitory effect induced by atRA. Despite their homology and adjacent location on chromosome 3, we provide evidence that RARRES1 and LXN reside within different sub-cellular compartments; RARRES1 is not a plasma membrane protein as previously supposed but is located in the endoplasmic reticulum, while LXN is localised to the nucleus of prostate epithelial cells.

These data provide novel results identifying two potential tumour suppressor genes as co-ordinately regulated, SC-silenced genes that function to suppress the invasion and colony forming ability of CaP cells. Work now should be focussed on determining whether re-administration of RARRES1 and LXN would be a valid differentiation strategy for the treatment, and potentially eradication, of CaP.

LIST OF CONTENTS

LIST OF FIGURES

LIST OF TABLES

ACKNOWLEDGEMENTS

Many thanks to my supervisor Professor Norman J. Maitland for giving me the opportunity to be part of the CRU laboratory and for his guidance throughout the four years of this PhD. I am also very grateful to Dr. Davide Pellacani for all of his support, advice and knowledge. I owe thanks to everyone at the CRU, past and present, for making the laboratory such a friendly work environment.

Thank you to my friends and family for supporting me throughout this project. In particular, Dad, Victoria and Nanna Julie, for your constant love and support. You helped me to keep going when things got tough. Thank you to David for always believing in me and keeping me sane! Finally, thank you to my mum. My wish and your wish was that you could have seen this thesis. I dedicate this work to you.

AUTHOR'S DECLARATION

I declare that this thesis represents my own unaided work, except where acknowledged otherwise in the text, and has not been submitted previously in consideration for a degree at this, or at any other university.

Emma Oldridge
September 2012

This work has been presented at the following scientific meetings:

June 2009	YCR Annual Scientific Meeting Harrogate, UK	Poster presentation
November 2009	SBUR/ESUR Joint Meeting 8th World Basic Urological Research Congress New Orleans, MS, USA	Poster presentation
June 2010	YCR Annual Scientific Meeting Harrogate, UK	Poster presentation
August 2010	AbCam Epigenetics, Stem Cells and Cancer Conference Copenhagen, Denmark	Poster presentation
November 2010	Young Prostate Researchers Symposium Cambridge, UK	Oral presentation
April 2011	Blue Skies Prostate Symposium Cambridge, UK	Oral presentation
June 2011	YCR Annual Scientific Meeting Harrogate, UK	Poster presentation
June 2012	YCR Annual Scientific Meeting Harrogate, UK	Poster presentation

Parts of this work have been/are under consideration for publishing:

Oldridge, E.E., Walker, H.F., Stower, M.J., Simms, M.S., Mann, V.M., Collins, A.T., Pellacani, D. and Maitland, N.J., 2013. Retinoic acid represses invasion and stem cell phenotype by induction of the metastasis suppressors RARRES1 and LXN. *Oncogenesis.* Submitted.

Pellacani, D., Oldridge, E.E., Collins, A.T. and Maitland, N.J., 2013. Prominin-1 (CD133) expression in the prostate and prostate cancer: a marker for quiescent stem cells. *Adv Exp Med Biol.* 777, 167-184.

In addition, the following review article was published during this PhD:

Oldridge, E.E., Pellacani, D., Collins, A.T. and Maitland, N.J., 2012. Prostate cancer stem cells: Are they androgen responsive? *Mol Cell Endocrinol.* 360, 14-24.

1. INTRODUCTION

1.1. Prostate anatomy

The human prostate is a small glandular organ located at the base of bladder, surrounding the urethra. The prostate has an important role in the male reproduction system, producing a slightly alkaline fluid containing protein secretions essential for sperm function, such as polyamines, prostatic acid phosphatise (PAP) and prostate specific antigen (PSA). The walnut-shaped gland is a lobar structure composed of four distinct anatomical regions (McNeal, 1981) (Figure 1):

- The anterior **peripheral zone** (PZ) is the largest of the zones and surrounds the urethra.
- The posterior **central zone** (CZ) is the second largest zone, forms the majority of the prostatic base and contains the ejaculatory ducts.
- The **transitional zone** (TZ) surrounds the urethra and represents only 5% of the prostatic volume, yet is the exclusive zone where benign prostatic hyperplasia (BPH) occurs.
- The **anterior zone** (AZ) is composed of muscular and fibrous tissue but lacks any glandular structures.

1.1.1. Prostate development

The prostate undergoes a considerable amount of growth and differentiation during development in the embryo, the first year of life and during puberty. In the embryo, the prostate develops from the urogenital sinus in response to testosterone stimulation, to form multi-layered epithelium surrounded by stroma. Epithelial growths then invade the stromal compartment to produce branched ductal structures, which form the immature acini. During puberty, the multi-layered epithelium differentiates to produce a mature epithelium bilayer under the influence of a testosterone surge.

The onset of prostate development is mainly dependent on the presence of androgens (Cunha et al., 1987), although, exposure to oestrogens can alter prostate development by modifying the expression of genes such as *NKX3.1* and *HOX13* (Huang et al., 2004; Prins and Putz, 2008). Retinoids also function to control the proliferation and differentiation of prostate epithelium (Peehl et al., 1993; Seo et al., 1997).
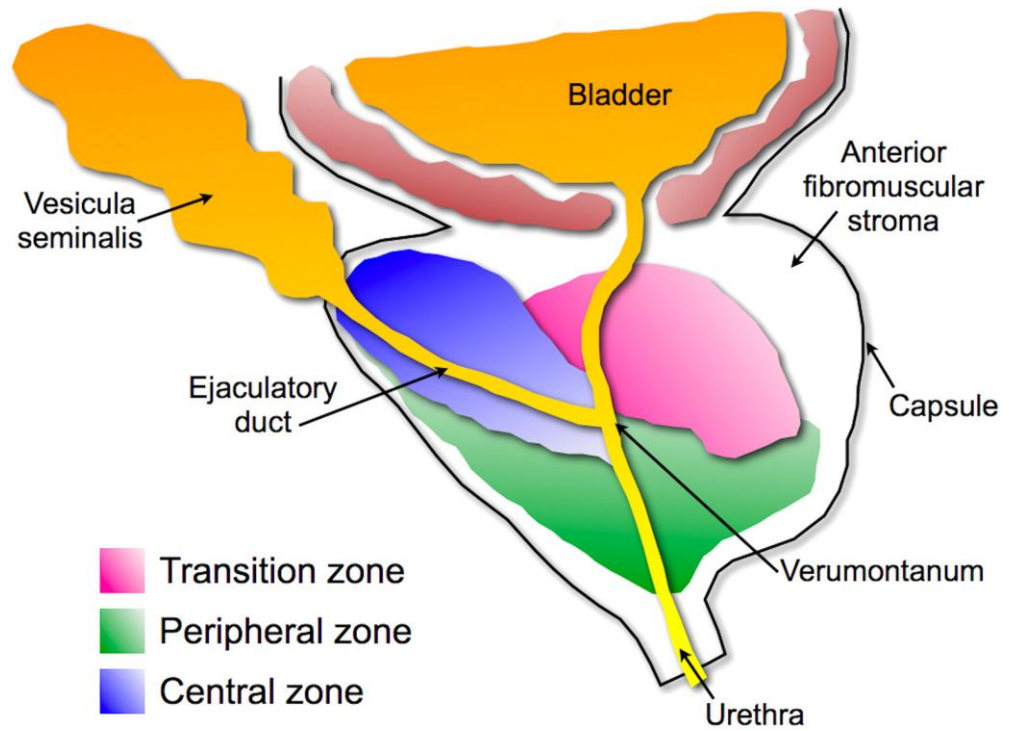
Figure 1. Schematic of the anatomical zones of the human prostate gland.
The adult prostate gland encapsulates the initial 3 cm of the urethral tube descending from the bladder, linking the urethra and ejaculatory ducts at a junction called the verumontanum. Little if any disease develops in the central zone, which houses the ejaculatory ductal tube from the vesicular seminalis. The peripheral zone surrounds the descending penile urethra and is the primary site of pre-cancerous and cancerous lesions. The transition zone is the only site of BPH and houses the transitional urethra composed of descending bladder and prostatic urethral sections. Modified from (Schauer and Rowley, 2011).

1.2. Disorders of the prostate

Three of the four zones within the prostate are composed of epithelial glandular structure and are susceptible to a number of different disorders of the prostate:

1) Prostatitis

This is the most common disorder, which arises principally in the CZ, due to inflammation of the prostate gland. This inflammation can be caused by acute and chronic bacterial infections or non-infectious causes such as stress, autoimmunity or physical injury. The incidence rate of prostatitis in adult men is 2-10% (Krieger, 2004). Evidence suggests that inflammation of the prostate is a major contributory factor to the initiation of BPH in older men (Lee and Peehl, 2004; Kramer and Marberger, 2006; Kramer et al., 2007; Nickel, 2008; Sciarra et al., 2008).

2) Benign Prostatic Hyperplasia (BPH)

This age-related disease is characterised by non-malignant hypertrophy in the gland, which originates exclusively in the TZ. Trans-urethral resections of the prostate (TURP) are often carried out in patients with BPH to alleviate symptoms associated with an enlarged prostate, such as increased frequency of urination due to pressure on the bladder or constriction of the urethra (Schroder and Blom, 1989) (Figure 2).

3) Prostate Intraepithelial Neoplasia (PIN)

PIN represents the pre-invasive end of the continuum of cellular proliferations within the prostatic epithelium and is most commonly found in the PZ of the prostate (Bostwick et al., 2004). It is characterised by cellular proliferations within pre-existing ducts and acini with cytologic changes mimicking cancer, including nuclear and nucleolar enlargement (Bostwick et al., 2004). As in cancer, abnormal cellular proliferation occurs causing destruction of the bi-layered basal-luminal cell stratification, but the basement membrane remains intact. High-grade PIN is considered a precursor to prostate cancer (CaP), which develops in the majority of patients after 10 years (Sakr et al., 1993; Bostwick et al., 2004) and a number of studies have found a high predictive value of PIN for CaP (Table 1).

4) Prostate Cancer (CaP)

The PZ comprises 70% of the prostate mass and is the site where the majority of malignant prostate adenocarcinomas are believed to initiate. The remaining cancers originate in the CZ or TZ. CaP will be discussed in more detail in Section 1.4.

Number of men	Patients with cancer on repeated biopsy (%)	Reference
100	35	(Davidson et al., 1995)
48	47.9	(Raviv et al., 1996)
53	27	(Langer et al., 1996)
66	58	(Shepherd et al., 1996)
43	51	(Park et al., 2001)
245	32	(Kronz et al., 2001)
88	43	(Igel et al., 2001)
104	22	(Vukovic et al., 2003)
190	30.5	(Gokden et al., 2005)
423	36	(Marshall et al., 2011)
336	23	(Schlesinger et al., 2005)

Table 1. Cancer detection in patients with high-grade PIN.
Adapted from (Bostwick et al., 2004).
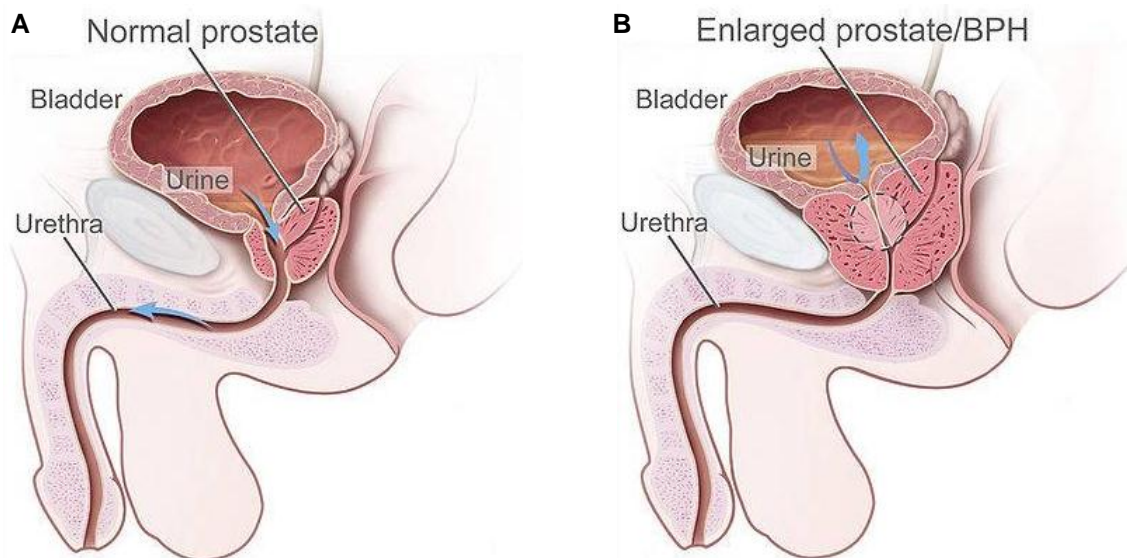
Figure 2. Schematic illustration of the normal prostate and BPH.
(a) Normal prostate. **(b)** BPH causes uncontrollable cell proliferation resulting in an enlarged prostate. This presses on the urethra and bladder affecting the upper part of the urethra, causing a reduction in urinary flow. Adapted from (National Cancer Institute).

1.3. Cellular organisation of the prostate epithelium

The normal, mature, human prostate shows a high level of cellular organisation. Three phenotypically distinct cell types are apparent within an epithelium bilayer: secretory luminal cells, relatively undifferentiated basal cells and rare, scattered neuroendocrine (NE) cells (Figure 3). The prostate gland is dependent on androgens for its development and growth, and so the integrity of prostatic epithelium is predominantly androgen-dependent. In contrast, the basal compartment is androgen-independent, but androgen-responsive, whereby androgens are not required for the survival of these cells.

The undifferentiated basal layer is the most proliferative compartment, lacks any secretory activity and adheres strongly to basement membrane (BM), which provides a structural barrier between the epithelium and the underlying stromal compartment. Basal cells express p63 (Signoretti et al., 2000), CD44 (Liu et al., 1997) and low levels of androgen receptor (AR). The compartment also displays expression of mitosis suppressors, like p27^{kip} and markers of cell proliferation, such as c-Met (van Leenders et al., 2003). Basal cells also express the oestrogen receptor (ER)β and proliferate under oestrogen therapy (Aumuller, 1983), but this effect on proliferation could equally be attributed to ER signalling via the stroma (Risbridger et al., 2010).

A stromal cellular compartment lies beneath the BM which secretes growth factors, such as epidermal growth factor (EGF) and fibroblast growth factor (FGF) and a proportion of stromal cells are androgen-responsive and express AR. The crucial role of the prostatic stromal cells in determining cell fate within the epithelium cannot be discounted, stromal cells are responsible for directing epithelial cell development, maintenance and differentiation (Hall et al., 2002; Berry et al., 2008).

The columnar luminal layer overlies the basal layer and in contrast, is composed of terminally differentiated epithelial cells which are the 'factory' within the epithelium, generating secretory products like PSA and PAP. They express CD57 (Signoretti et al., 2000), are dependent on androgens for their survival (Kyprianou and Isaacs, 1988) and consequently express high levels of AR (Bonkhoff and Remberger, 1993). Basal and luminal cell types can be discriminated on the basis of their expression of specific cytokeratins (CK). For example, basal cells express CK 5 and CK 14, whereas CK 8 and CK 18 are predominantly expressed by the luminal cells (Sherwood et al., 1991).

A small proportion of terminally-differentiated and androgen-insensitive NE cells are scattered throughout the epithelium bilayer (Bui and Reiter, 1998), which secrete NE peptides, such as bombesin, calcitonin, and parathyroid hormone-related peptide (Rumpold et al., 2002). Despite the fact that NE-like cells are routinely found in CaP, with increased prevalence in late stage metastatic disease (Abrahamsson et al., 1989; Bohrer and Schmoll, 1993; Jiborn et al., 1998; Ahlgren et al., 2000; Huang et al., 2006), their precise function is unknown. The relationship of

NE cells to basal and luminal cell types has remained unclear, although current evidence suggests that they represent a post-mitotic cell type that is derived from luminal secretory cells (Bonkhoff et al., 1991; Bonkhoff et al., 1994; Bonkhoff et al., 1995).

A

Secretory luminal layer

Secretory duct

Basal layer

Ductal lumen

Prostatic fluid

B

Neuroendocrine Cell

EPITHELIUM

Luminal Layer

Basal Layer

Basement Membrane

STROMA
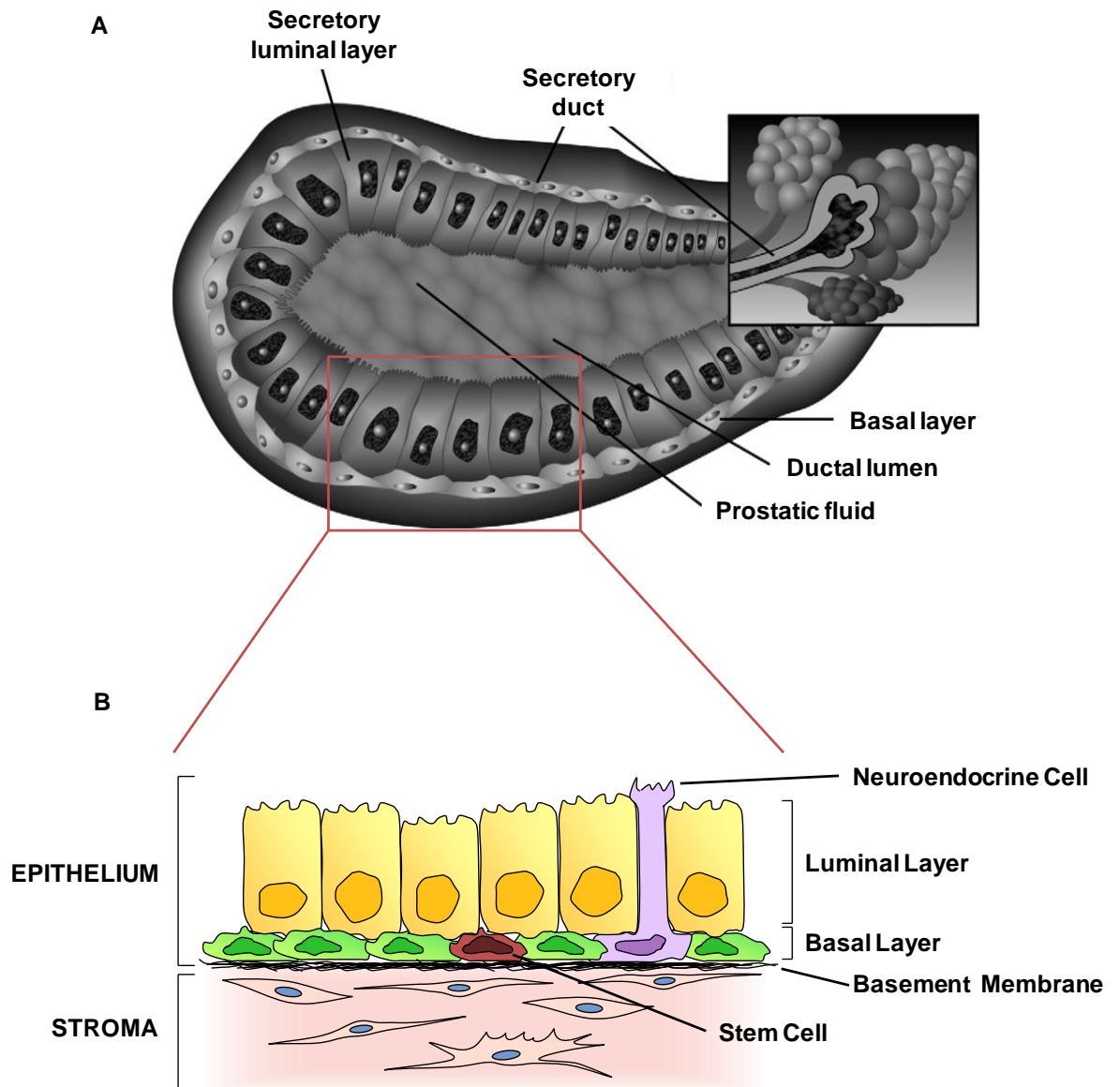
Stem Cell

Figure 3. Organisation of the normal prostate.
(a) The bi-layered prostate consists of an undifferentiated basal layer of cells and a differentiated luminal layer of cells. **(b)** Within the basal layer resides the rare population of stem cells and scattered neuro-endocrine cells. Modified from (Collins and Maitland, 2006; Oldridge et al., 2012).

1.3.1. Prostate epithelial stem cells

Stem cells (SCs) are defined by two fundamental properties: self-renewal (the ability to maintain an undifferentiated state through numerous cell divisions) and multipotency (the potential to differentiate into various specialised cell types). Compared to totipotent embryonic SCs, which have the potential to differentiate into any tissue in the body, multipotent adult SCs have limited differentiation potential and are committed to differentiate along the specific lineages of the tissue in which they reside. The slow cycling prostate SC is often maintained in a quiescent state for prolonged periods. Upon entry from G0 phase into the active cell cycle, SCs can undergo asymmetric or symmetric division to maintain, deplete or increase SC numbers (Figure 4) (Morrison and Kimble, 2006).

Haematopoietic SCs (HSCs) were the first adult SC to be isolated and consequently have been the focus of the majority of SC biology in previous years (Baum et al., 1992). Only more recently have adult SCs in the slow-growing prostate been recognised (Hudson et al., 2000; Collins et al., 2001).

Adult SCs possess several distinctive features, on the basis of which they can be identified. They usually represent a small subpopulation of quiescent cells with a large nuclear: cytoplasmic ratio. They can be induced to proliferate by precise stimuli generated by the SC niche or imported soluble factors (Watt and Hogan, 2000) and have a high proliferative potential. Moreover, adult SCs give rise to rapidly proliferating transit-amplifying (TA) cells that then commit to differentiation (Miller et al., 2005a).

The first convincing demonstration that a population of long-lived androgen-independent SCs exist within the prostate epithelium originated from androgen cycling experiments in the rodent. These experiments demonstrated that, upon androgen withdrawal (castration) the prostate involuted, leading to apoptosis of the majority of luminal (androgen-dependent) cells. Some of the basal cells survived and were responsible for the regeneration of the prostate once androgens were re-administered some time later (English et al., 1987; Evans and Chandler, 1987; Kelly and Yin, 2008). These results led Isaacs and Coffey to hypothesise that a population of long-lived androgen-independent SCs must exist and proposed a SC model for the organisation of the prostate epithelium (Isaacs and Coffey, 1989) (Figure 5). These epithelial SCs reside within a 'SC niche', which provides the support and signals necessary for continued maintenance of this rare cell type (Miller et al., 2005b).

Human prostate epithelial SCs were originally identified and isolated by taking into account their association with BMs. These putative SCs were shown to express higher levels of $\alpha_2\beta_1$-integrin ($\alpha_2\beta_1$-integrin^{high}) compared to other cell populations in the CD44$^+$ basal layer and consequently were isolated on the basis of their adhesion to type I collagen (Collins et al., 2001). Later, it was shown that a small subset of these basal $\alpha_2\beta_1$-integrin^{high} cells also expressed the human

CD133 cell surface antigen ($\alpha_2\beta_1$-integrin^{high}CD133$^+$) (Figure 6). This small $\alpha_2\beta_1$-integrin^{high}CD133$^+$ quiescent population constituted <0.1% of cells and exhibited important SC characteristics: they had a high proliferative potential *in vitro* and could reform functional prostate acinar structures *in vivo* (Richardson et al., 2004). Molecular characterisation of these cells revealed that they did not express *AR* at mRNA level (Maitland et al., 2011b), indicating that they were not dependent on androgens for their survival, nor were they androgen-responsive.

A   **B**   **C**

TA

SC

Symmetric   **Asymmetric**   **Symmetric**

Deplete SC numbers   Maintain SC numbers   Increase SC numbers
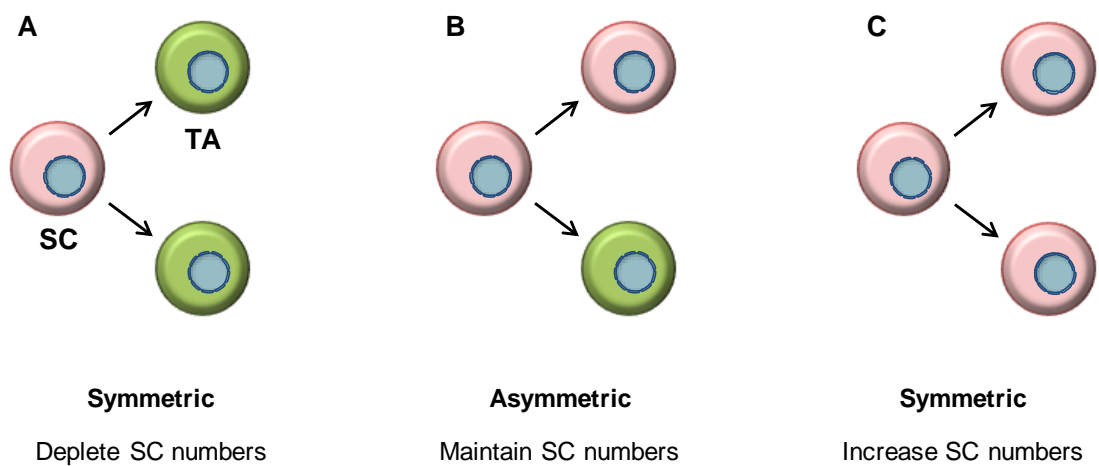
Figure 4. Stem cells can undergo asymmetric or symmetric division.
(a) Asymmetric division results in one daughter SC and a differentiated TA progenitor cell, **(b)** symmetric division produces either two identical daughter SCs or **(c)** two identical TA cells; the divisions maintain, deplete or increase SC numbers respectively.
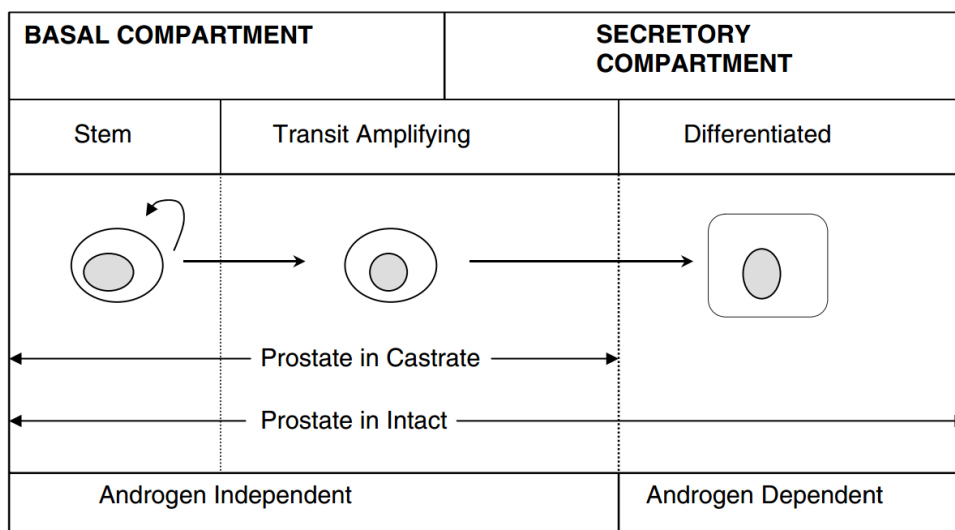
Figure 5. Stem cell model for the organisation of the prostate epithelium.
In the absence of androgens, SCs within the basal layer give rise to TA cells which differentiate in the presence of androgen to secretory luminal cells. Adapted from (Collins and Maitland, 2006).
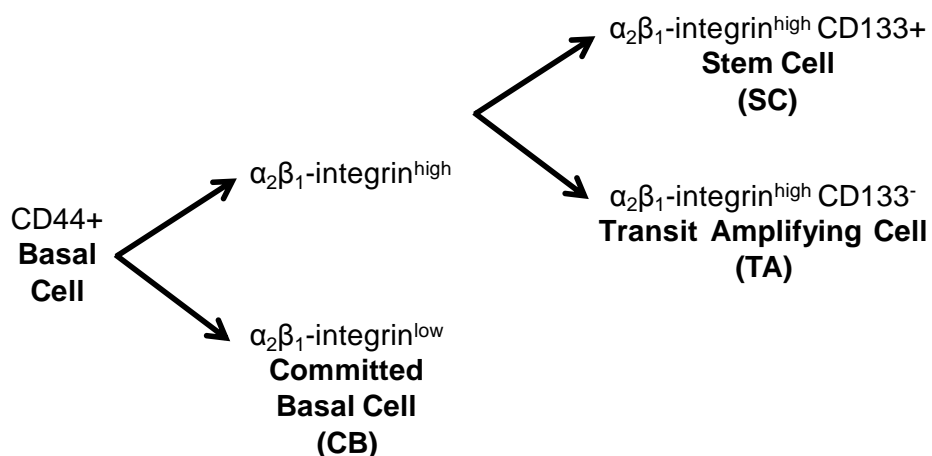
Figure 6. Fractionation of basal prostate epithelial cultures.
Cells can be separated into committed basal cell (CB; $\alpha_2\beta_1$-integrin^{low}), TA cell ($\alpha_2\beta_1$-integrin^{high}CD133$^-$) and SC ($\alpha_2\beta_1$-integrin^{high}CD133$^+$) populations based on the expression of $\alpha_2\beta_1$-integrin and CD133.

1.3.2. Epithelial hierarchy within the prostate epithelium

A number of observations strongly support the hypothesis that basal and luminal cells within the prostatic epithelium are linked in a hierarchical pathway, which is most accurately described as a continuum of cells with different stages of change and different proliferative potentials. The basal compartment possesses a further level of cellular heterogeneity, consisting of several cell types with variable differentiation states (Figure 7).

1) The SC model for the organisation of the prostate epithelium initially suggested that three discernible cell types were arranged in an expanding hierarchy: a SC, a TA cell (shares basal characteristics with the SC, but is cycling) and a differentiated cell (Isaacs and Coffey, 1989). The model proposed that within the adult prostate epithelium, a population of androgen-independent multipotent SCs exist in the basal compartment. These are able to give rise to all populations within the epithelium through a hierarchical pathway to androgen-responsive TA cells, which in turn are driven to differentiate to androgen-dependent luminal cells by circulating androgens and stromal factors (Bonkhoff and Remberger, 1996).

2) CK expression patterns have also provided evidence of epithelial cells within the normal prostate that are phenotypically intermediate between basal and luminal cells. A TA subpopulation of basal cells have been identified that co-express both basal and luminal cytokeratin markers (Verhagen et al., 1988; Verhagen et al., 1992; Robinson et al., 1998; Xue et al., 1998; Hudson et al., 2001; Lang et al., 2001; van Leenders et al., 2001).

3) The late differentiation stage PSA-Pb promoter was activated in differentiated cells, derived from primary prostate SCs transduced with lineage-tracking lentiviruses, demonstrating the capacity of the basal SC to differentiate through a hierarchy of cells (Frame et al., 2010).

4) Most recently, *in situ* lineage tracking studies of human prostate tissues show that all the prostate epithelial cell types have a common clonal origin (Blackwood et al., 2011; Gaisa et al., 2011).
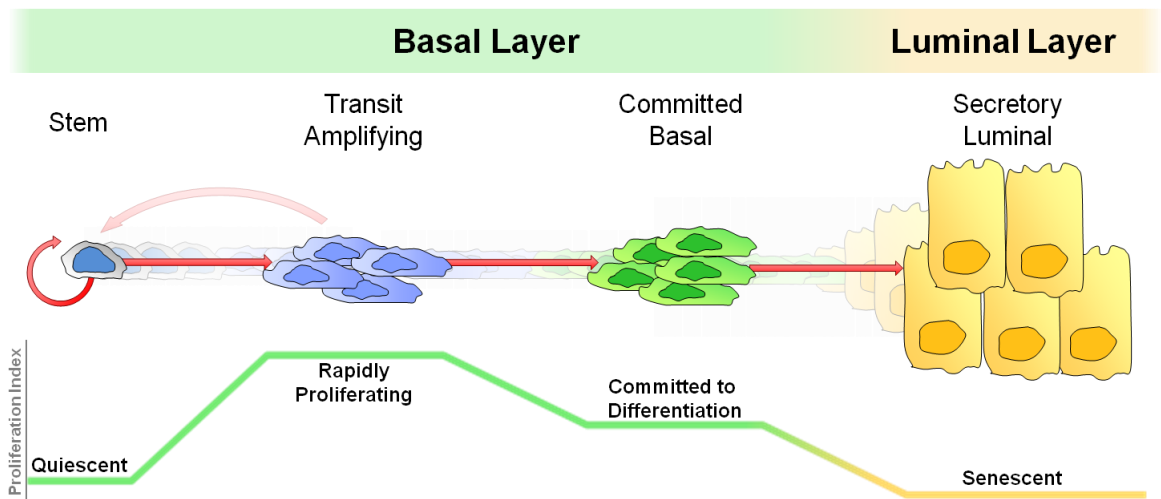
Figure 7. Hierarchical pathway of human prostate epithelium.
Predominantly quiescent SCs produce proliferating TA progeny, which mainly commit to differentiation producing CB cells. CB cells then further differentiate to secretory luminal cells which are largely senescent. Adapted from (Oldridge et al., 2012).

1.4. Prostate cancer

CaP is regarded as a slow-growing proliferative disease. However, the aetiology of CaP is still a matter of debate, which can be attributed to the high level of heterogeneity seen in the disease. In addition to PIN being considered a precursor to CaP, Proliferative Inflammatory Atrophy (PIA) is hypothesised to give rise to CaP, either directly (Franks, 1954), or indirectly via development into PIN (De Marzo et al., 1999). PIA was a term proposed by De Marzo et al. (1999) to designate discrete foci of proliferative glandular epithelium with the morphological appearance of simple atrophy (Ruska et al., 1998) or post-atrophic hyperplasia (Cheville and Bostwick, 1995), occurring in association with inflammation.

CaP is characterised by an imbalance of the differentiation process that leads to the accumulation of aberrantly differentiated luminal cancer cells (Nagle et al., 1987). As the disease progresses to adenocarcinoma, a number of characteristics are apparent:

- Tissue architecture of the prostate begins to degrade (Gleason, 1966).
- Loss of the characteristic glandular structure.
- Destruction of the BM.
- Considerable decrease in basal cells (<1%).
- AR^+ luminal cells constitute the majority of cells (>99%) (Grisanzio and Signoretti, 2008).
- Luminal cells are highly proliferative in the diseased state (De Marzo et al., 1998).

1.4.1. Cancer stem cells

There are two main models which may explain the initiation and development of CaP. The **prevailing model** views the tumour as a homogeneous tissue with every cell type possessing the ability to initiate tumour formation. A minimum of two independent mutation events within the cell would be required to initiate tumourigenesis. Traditional CaP treatments work on the basis of this model.

A series of transplant experiments initially proved that cancers are composed of a heterogeneous population of cells, which differ in their potential to self-renew and reconstitute the original tumour upon transplantation (Brunschwig, 1961; Bruce and Van Der Gaag, 1963; Hamburger and Salmon, 1977; Sabbath and Griffin, 1985). These early observations led to the **SC hypothesis**, which states that within a heterogeneous tumour cell population there exists a rare subset of 'cancer SCs' (CSCs) with tumour-initiating and sustaining characteristics.

The SC hypothesis is the more widely accepted view of the initiation of cancer and a number of studies have demonstrated that sub-populations of tumour cells from a number of tissues,

including the prostate (Collins et al., 2005), have CSC characteristics (Table 2). The majority of these putative CSCs have been identified using normal SC markers, suggesting that CSCs and their normal SC counterparts share many phenotypic markers. In fact, CSCs are analogous to normal SCs in that they both have extensive proliferative potential, the ability to give rise to new tissues and can divide symmetrically and asymmetrically (Reya et al., 2001). Unlike the bulk of the cells in a tumour, SCs have a high capacity for self-renewal, enabling them to be maintained throughout the life time of a host. This allows them to acquire the multiple mutational hits required for the development of cancer (Vogelstein and Kinzler, 1993).

Tissue	Reference
Haematopoietic system	(Bonnet and Dick, 1997)
Breast	(Al-Hajj et al., 2003)
Brain	(Singh et al., 2003; Singh et al., 2004)
Multiple myeloma	(Matsui et al., 2004)
Pancreas	(Li et al., 2007)
Liver	(Ma et al., 2007)
Colon	(Ricci-Vitiani et al., 2007)
Head and neck squamous cell carcinoma	(Prince et al., 2007)
Lung	(Eramo et al., 2008)
Ovary	(Zhang et al., 2008)
Melanoma	(Fang et al., 2005; Schatton et al., 2008)
Endometrium	(Rutella et al., 2009)
Bladder	(He et al., 2009)
Cervix	(Feng et al., 2009)

Table 2. Cancer stem cells have been discovered in a number of different tissues.

1.4.2. Prostate cancer stem cells

It has been the prevailing view that the CSC in CaP arises from the androgen-dependent AR^+ luminal compartment, as this constitutes the majority of cells in CaP. Studies in murine models have shown that CaP can indeed arise from luminal cells (Ma et al., 2005; Korsten et al., 2009; Wang et al., 2009). Other studies suggest that CaP is derived from intermediate progenitors that have acquired the ability to self-renew (Verhagen et al., 1992; van Leenders and Schalken, 2001). However, there is consistently strong evidence from several independent studies supporting the proposal that the disease arises from a SC population residing in the basal compartment (Collins et al., 2005; Brown et al., 2007; Hurt et al., 2008; Goldstein et al., 2010; Liao et al., 2010; Rajasekhar et al., 2011).

Human prostate CSCs have been identified and isolated in our lab from different grades of human prostate CaP biopsies, based on the expression of normal epithelial SC markers ($CD44^+\alpha_2\beta_1^{hi}CD133^+$) and constituted only 0.1% of cells in the tumour (Collins et al., 2005). Only this most primitive cell population was able to self-renew *in vitro.* Moreover, under differentiating conditions, $AR^+ PAP^+ CK\ 18^+$ luminal cells could be identified in these cultures, suggesting that they were derived from the more primitive population.

Aldehyde dehydrogenase (ALDH) has also been used as a marker for cancer stem/progenitor cells in human CaP cell lines (Yu et al., 2007a) and in the murine prostate (Burger et al., 2009). A subpopulation of human CaP PC-3M cells with high ALDH activity ($ALDH^{hi}\alpha2/\alpha6/\alpha v$-integrin$^+CD44^+$) showed both enhanced clonogenicity and invasiveness *in vitro* and enhanced tumourigenicity and increased metastatic ability *in vivo* (van den Hoogen et al., 2010).

Results from the murine CaP models suggest the co-existence of multiple CSCs in the mouse. However, the current evidence is overwhelming in the human system, in implicating a basal cell as the CSC for human CaP. The ultimate evidence for CSC properties is serial xenotransplantation. Our own recent experiments (Maitland et al., 2011b) have confirmed that the strongest tumour initiating fraction, where fewer than 100 cells are required to initiate new tumour growth in immuno-compromised mice, has a purely basal phenotype.

Long-lived prostate SCs are considered excellent candidates for the CSC as they are the only cell within a tumour that has the capacity for extensive self-renewal and regeneration (Leong et al., 2008). These properties permit their maintenance over the lifetime of the host, facilitating the accumulation of the essential genetic and epigenetic changes. In contrast to the SCs, there is less opportunity for mutations to accumulate in the shorter-lived differentiated cells.

1.4.3. Epidemiology of prostate cancer

CaP is the most commonly diagnosed cancer in men in the UK, accounting for over a quarter of all new male cancer diagnoses (Figure 8a) and attributable for 13% of cancer-related deaths in males in 2009, second only to lung cancer (Figure 8b). CaP incidence dramatically increases with age; over 95% of all diagnoses occur in men over the age of 60 (Figure 8c).

Familial CaP is an hereditary disease which accounts for 10-20% of all cases of the disease in the general population (Stanford and Ostrander, 2001). It is commonly defined as a family in which there are:
1)   two first-degree (father, brother, son) relatives or
2)   one first-degree and at least two second-degree (grandfather, uncle, nephew, half-brother) relatives with CaP.

Hereditary CaP, a subset of familial CaP, may account for 5-10% of all cases of the disease in the general population (Stanford and Ostrander, 2001). It describes families in which there is a pattern of Mendelian inheritance of rare susceptibility genes, characterised by at least one of the following criteria:
1)   three or more first-degree relatives with CaP,
2)   three successive generations with CaP or
3)   two siblings with CaP diagnosed at <55 years.

The last 20 years have seen a vast increase in CaP incidence, primarily due to the introduction of serum testing for PSA levels and an increase in male life expectancy (Quinn and Babb, 2002). However, since the early 1990s, mortality rates have overall decreased (Office for National Statistics; General Register Office for Scotland; Northern Ireland Statistics and Research Agency), which could also be attributed to PSA testing (Office for National Statistics).

1.4.4. Diagnosis of prostate cancer

Current screening and diagnosis of CaP relies on the quantification of PSA levels in serum (Placer and Morote, 2011). In the normal prostate, PSA functions as a serine protease to maintain the fluidity of seminal fluid (Lilja, 1985). However, increased serum levels of PSA is linked to CaP progression (Hudson et al., 1989). The PSA test is not infallible, with a 5% rate of false positives and 2% rate of false negatives (Brawer, 1999). By requesting that all participants undergo biopsy, the Prostate Cancer Prevention Trial (PCPT) has determined the specificity and sensitivity of PSA testing. Among 5112 men in the placebo arm of this trial, a PSA level >4 ng/ml (the traditional threshold level) had a specificity of 93% and a sensitivity of 24% (Thompson et al., 2006; Lilja et al., 2008). PSA occurs in blood in stable complexes with protease inhibitors (complexed PSA; cPSA) or as free PSA (fPSA). Calculating the percentage of non-complexed fPSA has shown evidence of increasing the diagnostic accuracy, compared to detecting total PSA levels (Catalona et al., 1998; Morote et al., 2002).

The major issue surrounding the use of PSA as a diagnostic marker is that PSA shows detectable expression levels in other tissues, including breast, lung and ovary (Smith et al., 1995). Also, high PSA levels can be the result of other conditions including PIN, inflammation or infection (Ferrero Doria et al., 1997) and a proportion of men exhibiting 'normal' PSA levels do have CaP (Thompson et al., 2004). Consequently, the use of PSA levels as a diagnostic test should be approached with caution, and combined with further tests for accurate diagnosis.

Once high PSA levels in the serum is diagnosed, multiple biopsies are taken and the tissue is most commonly graded according to the Gleason tumour grading system (Figure 9) (Gleason, 1966; Gleason, 1992). According to this Gleason grading system, two areas of the tissue with the most prevalent grade are given a score between one and five. The score is then added together to give a Gleason score between two and ten. This method of histologically grading prostate tissue biopsies following diagnosis is used to identify optimal treatments. Recently, the Gleason grading system was upgraded to accommodate changes in the Gleason system and achieve a consensus (Epstein, 2010). The modified Gleason system proposed that Gleason grades 2-4 should rarely be diagnosed on needle biopsy (Epstein, 2000), all cribriform cancer designated as Gleason grade 4 and poorly formed glands should also be designated as Gleason grade 4.

A

- 25.2% Prostate
- 14.2% Lung
- 14.0% Bowel
- 4.7%
- 4.1%
- 3.5%
- 3.3%
- 3.0%
- 3.0%
- 21.5%

Legend:
- Prostate
- Lung
- Bowel*
- Bladder
- Non-Hodgkin Lymphoma
- Kidney
- Malignant Melanoma
- Oesophagus
- Stomach
- Leukaemia
- Other Sites**

B

- 23.5% Lung
- 13.0% Prostate
- 10.6% Bowel
- 6.2%
- 4.7%
- 4.0%
- 3.8%
- 3.1%
- 3.0%
- 2.9%
- 25.3%

Legend:
- Lung
- Prostate
- Bowel*
- Oesophagus
- Pancreas
- Bladder
- Stomach
- Leukaemia
- Kidney
- Non-Hodgkin Lymphoma
- Other Sites**

Introduction

C
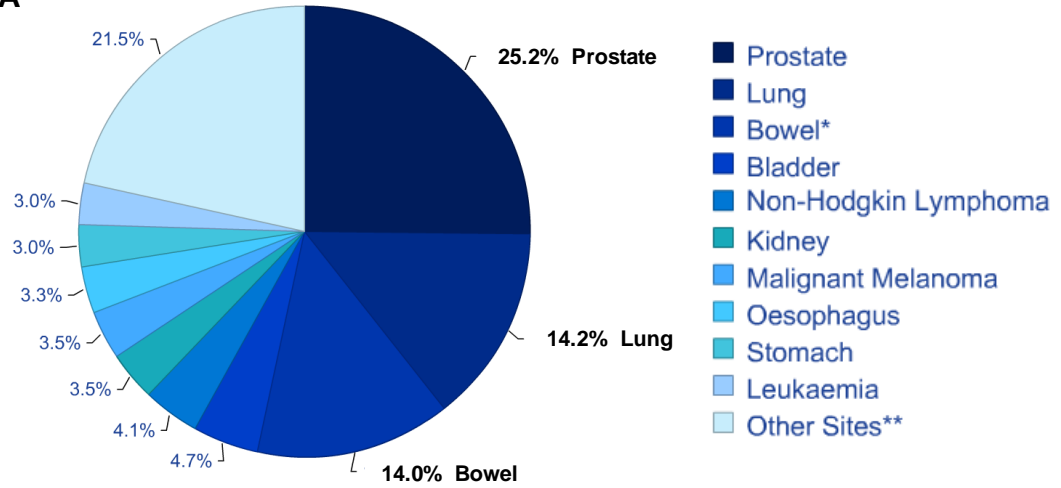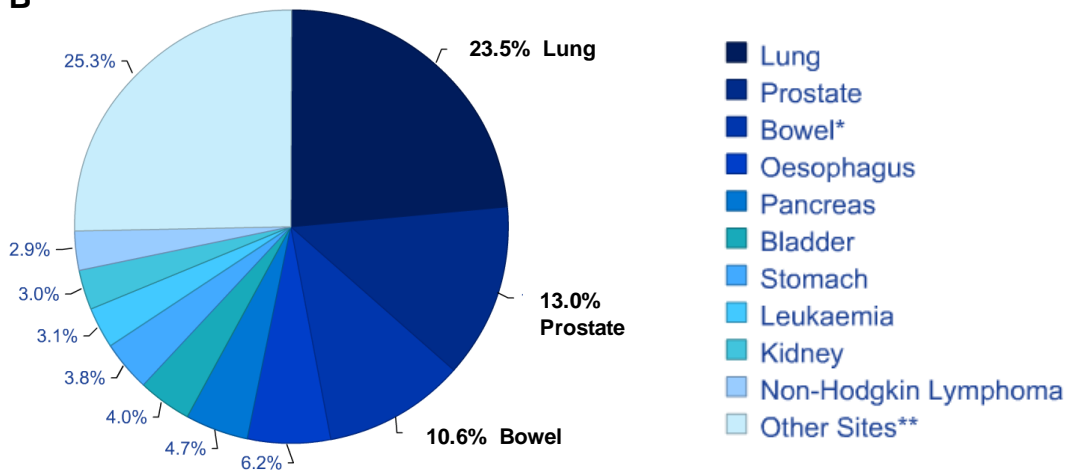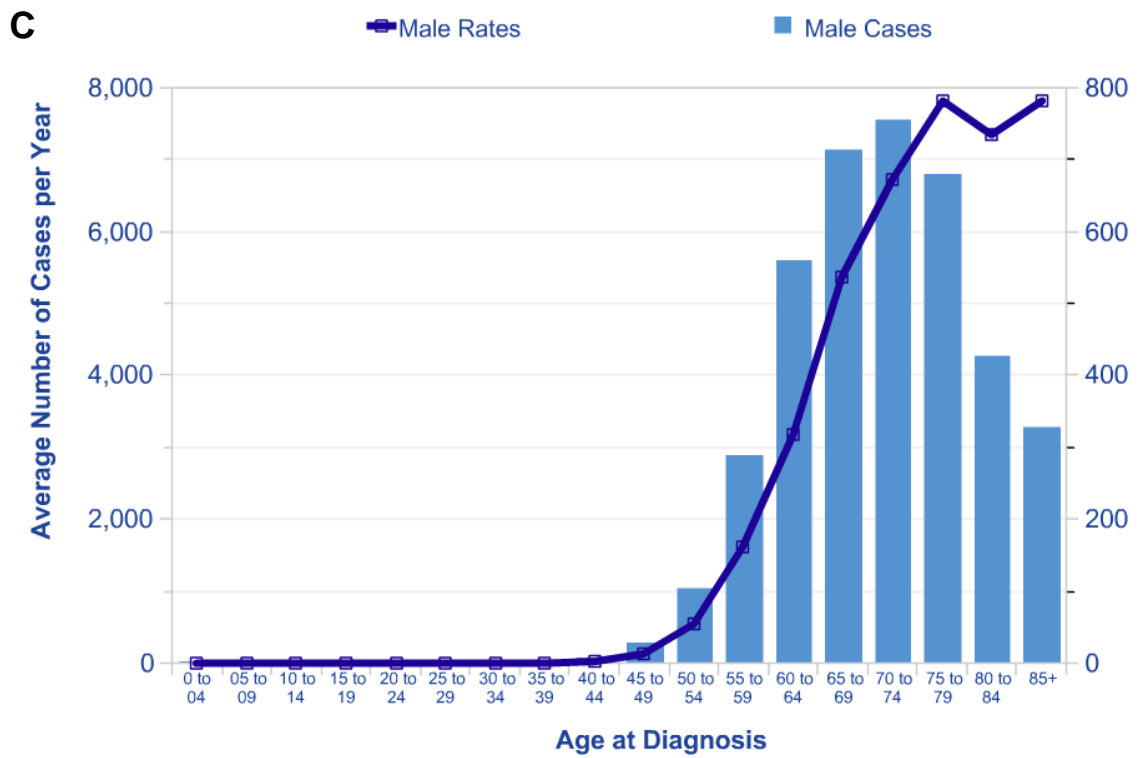
Figure 8. Epidemiology of prostate cancer.
(a) The most common cancers in males in the UK in 2009. **(b)** The ten most common causes of cancer death in males in the UK in 2009. **(c)** The average number of new cases per year and age-specific incidence rates of CaP in the UK between 2007 and 2009. Modified from (Cancer Research UK).
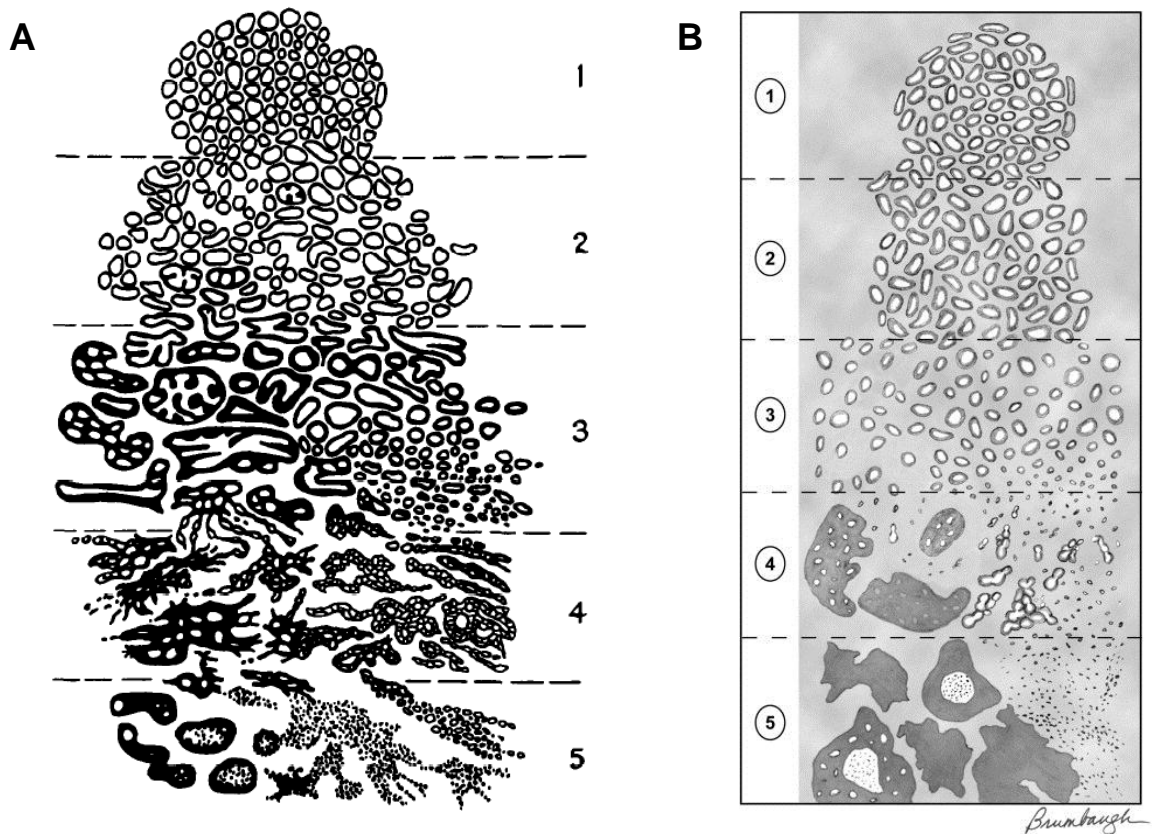
Figure 9. The Gleason grading system for prostatic adenocarcinoma.
(a) The original Gleason system describes histological patterns of prostate biopsies which are graded from 1 (simple round glands, closely-packed in rounded masses with well-defined edges) to 5 (anaplastic adenocarcinoma in ragged sheets). **(b)** The modified Gleason system. Adapted from (Gleason, 1966; Gleason, 1992; Epstein, 2010).

1.4.5. Current treatments for prostate cancer

1.4.5.1. Low grade organ-confined prostate cancer

Current treatments for CaP depend on the stage of the disease. In low Gleason-graded tumours confined to the prostate, the tumour cells are usually well-differentiated and organised into glandular structures, so treatment can be as simple as surveillance of the disease.

1) Active surveillance

Some patients with a low grade or low volume tumour will never progress to a higher stage, so active surveillance may be the best treatment option. This involves monitoring PSA serum levels every three months and repeated biopsies every six to twelve months.

2) Radical prostatectomy

For tumours confined to the prostate gland, the most common and most successful treatment is surgery via radical prostatectomy (Bill-Axelson et al., 2005). This is usually successful at reducing progression of the disease but the cancer needs to be detected at an early stage before signs of spreading outside of the prostate. There are also possible side effects which include urinary impotence and sexual dysfunction (Catalona et al., 1999).

3) Radiotherapy

An alternative for organ-confined CaP is radiation therapy, which involves applying ionising radiation to the tumour to control its growth, by either external beam radiation therapy or brachytherapy (Duchesne, 2011). External beam radiation therapy involves the use of an external source of ionising radiation targeted at the tumour. Brachytherapy involves the implantation of numerous small radioactive seeds into the prostate next to the tumour, either temporarily and emitting high doses of radiation (^{125}I, ^{103}Pd or ^{192}Ir) or as a permanent low dose implant. With brachytherapy, the radiation dose to surrounding tissues is low and so the numbers of undesired side-effects are reduced, whereas external beam radiation therapy is less invasive.

Within high Gleason-graded diseases, the cells are less differentiated and the tissue architecture is more compromised, indicative of spread outside of the prostate. This results in a poorer prognosis, as current treatments are largely ineffective.

1) Androgen deprivation therapy

For metastatic CaP, the current treatment of choice is androgen-deprivation therapy (ADT) through the administration of pharmacological drugs. These exploit the dependency of the tumour on androgens for growth, by removing circulating androgens or blocking their binding to the AR. The major types of hormone ablation therapy are described in Table 3.

Type of therapy	Mechanism of action	Example of Drug	Reference
Anti-androgen therapy	Binds to the AR and prevents ligand binding	Bicalutamide	(Iversen et al., 2000)
	Inhibits androgen-mediated transcription	Hydroxyflutamide	(Labrie et al., 1990)
LHRH-agonist	Desensitises the pituitary gland	Zoladex	(Peeling, 1989)
Oestrogen treatment	Inhibits 5-α reductase, which activates testosterone	Stilbestrol	(Bailar and Byar, 1970)
GnRH-antagonist	Binds to the GnRH-receptor, blocking 5-α reductase activity	Finasteride	(Rittmaster, 1994)
Androgen biosynthesis blockade	Blocks the CYP17 enzyme, preventing androgen production	Abiraterone	(de Bono et al., 2011)

Table 3. Types of hormone ablation therapy.

2) Chemotherapy

Cytotoxic chemotherapy is often used to treat advanced castration-resistant prostate cancer (CRPC), after failure of ADT. The most commonly used drugs include docetaxel, paclitaxel and vinblastine, which target dividing cells and prevents them from completing mitosis by inhibiting mitotic spindle assembly (Yvon et al., 1999). However, the tumour can become resistant to these cytotoxic agents and use of chemotherapeutic drugs prolong life expectancy by a matter of months only (Seruga and Tannock, 2011).

Current therapies for CaP have failed to account for the heterogeneous composition of the disease, and eliminate the differentiated bulk of cells within a tumour, resulting in an enrichment of a rare population of therapy-resistant CSCs. However, the nature of the CSC makes them very difficult to target, for example, their slow cycling rate and protection within the SC niche. The key to eradicating the CSC lies in identifying the phenotypic differences between malignant SCs and the bulk of differentiated cells in the prostate and exploiting these differences through differentiation therapy. SCs from both normal and cancerous tissues have been shown to be more resistant to chemotherapeutic reagents than more differentiated cell types (Harrison and Lerner, 1991; Phillips et al., 2006) and characteristically express multiple drug resistance (MDR) (Chaudhary and Roninson, 1991) and ATP-binding cassette (ABC) transporters (Zhou et al., 2001; Kim et al., 2002). In addition, there is now evidence of highly efficient DNA repair mechanisms, active anti-apoptotic pathways and slower cell cycle kinetics in SCs derived from solid tumours (Bao et al., 2006; Liu et al., 2006a; Chiou et al., 2008; Ma et al., 2008).

Differentiation therapy describes the process of inducing a quiescent SC to cycle and differentiate into amplifying progeny. Potential strategies of differentiation therapy include:

1)   **Activation of signalling cascades**. Exposure of human glioblastomas to bone morphogenetic protein 4 (BMP4) induces differentiation, reduces clonogenic ability and markedly reduces the size of the CD133^{+} CSC population (Piccirillo et al., 2006).

2)   **Inhibition of cell surface markers**. CD44 inhibition, through shRNA lentivirus particles, has been shown to promote the differentiation of a CD44^{+}CD24^{-} breast CSC population (Pham et al., 2011).

3)   **Compounds selectively targeted towards SC**. A high-throughput screening approach identified salinomycin as a compound that selectively kills CD44^{+}CD24^{-} breast CSCs (Gupta et al., 2009). Moreover, salinomycin treatment in mice inhibited tumour growth, induced cellular differentiation and caused a loss of breast CSC gene expression. The Src inhibitor, bosutinib, also controlled the development of mammary tumours by inducing differentiation (Hebbard et al., 2011).

4)   **AtRA treatment.** All-*trans* retinoic acid *(a*tRA) is one of the most thoroughly examined and clinically tested differentiation agents and has been shown to promote differentiation of SCs from a number of different tissues including human HSCs (Sammons et al., 2000; Luo et al., 2007), mouse embryonic SCs (Simandi et al., 2010), stem-like glioma cells (Campos et al., 2010), rabbit bone marrow-derived mesenchymal SCs (Su et al., 2010) and human breast CSCs (Ginestier et al., 2009).

Conversely, inhibition of retinoid signalling pathways has been shown to induce the expansion of human HSCs (Chute et al., 2006).

1.4.6. Castration-resistant prostate cancer

Androgens, such as testosterone and DHT (5α-dihydrotestosterone), act through the AR and are required for both normal and cancerous prostate development and function (Heinlein and Chang, 2004). The AR is a member of the steroid hormone receptor family of transcription factors (TFs) and regulates androgen responsive genes such as PSA.

Work in the early 1940s first demonstrated that CaP is initially dependent on androgens for growth and survival (Huggins et al., 1941). As a result, ADT has since been used as the main therapy to treat advanced and metastatic CaP (Denmeade and Isaacs, 2002). Unfortunately, approximately 15% of all patients will not respond to ADT and of those that do, the majority of tumours will become androgen-independent within 2-3 years of treatment, resulting in CRPC (Denmeade and Isaacs, 2002; Beltran et al., 2011). CRPC is incurable by current treatment strategies and patients typically have a median life expectancy of 12-24 months (Yap et al., 2011). Moreover, studies in a mouse model have demonstrated that ADT frequently leads to a more aggressive and metastatic disease (Gingrich et al., 1996).

It remains unclear whether CRPC is an inevitable development of CaP. The prevailing model proposes that CRPC arises through adaptation of previously androgen-dependent cells. Alternatively, the SC hypothesis suggests that CRPC occurs through activation and/or an increase in the number of ADT-resistant, androgen-independent SCs, which consequently repopulate the tumour with androgen-independent cells (Shen and Abate-Shen, 2010).

Both the normal prostate and CaP are androgen-dependent and AR plays a key role in maintaining the homeostasis of epithelial and stromal tissues. Following ADT, the dependence of the prostate on androgens is manifested by rapid apoptosis of epithelial cells and prostate regression, which requires paracrine signalling of pro-apoptotic factors from the stromal cells. CRPC retains AR expression and expresses AR target genes, suggesting that the receptor and pathway play an important role in its development (Gregory et al., 1998). CRPC has been shown to retain AR activity through a variety of different mechanisms (Figure 10; (Shen and Abate-Shen, 2010)) including:

1) **Amplification of *AR*** gene copy number resulting in an increased amount of the AR protein (Visakorpi et al., 1995; Koivisto et al., 1997; Linja et al., 2001).

2) **Mutations in the *AR* gene** predominantly caused by gain-of-function mutations that occur in the ligand-binding domain and produce a receptor that is more sensitive to

native ligand or can be activated by other steroid hormones (Taplin et al., 2003). In addition, constitutively active splice variants of the *AR* gene also occur in CRPC (Dehm et al., 2008; Guo et al., 2009; Hu et al., 2009).

3) **Ligand-independent activation of AR** by up-regulation of growth-factor signalling pathways such as PI3K, through *PTEN* deletion (Gao et al., 2006b) and MAPK pathways (Gao et al., 2006a).
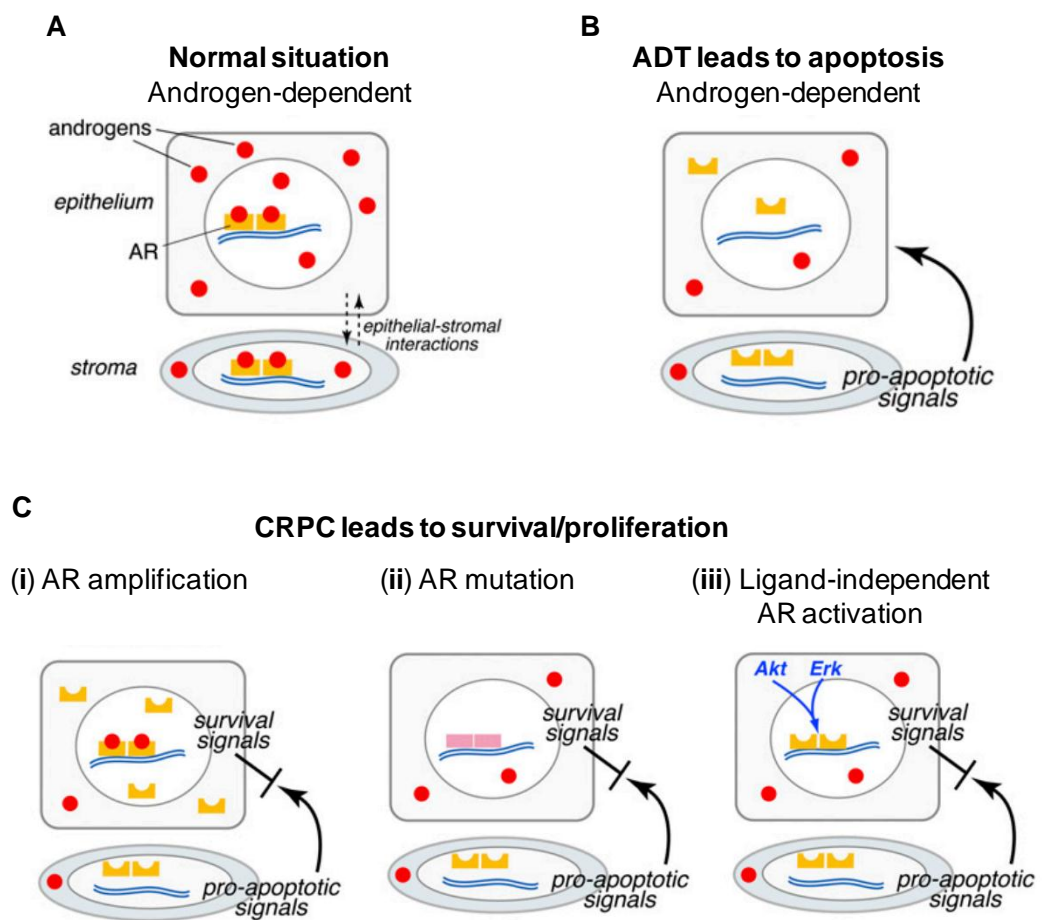
Figure 10. Mechanisms of retention of AR activity in castrate resistant prostate cancer.
(a) AR maintains homeostasis in the normal prostate. **(b)** ADT stimulates the stroma to produce pro-apoptotic stimuli which causes regression of the epithelial compartment. **(c)** Castration-resistance promotes survival of the epithelium by overcoming the pro-apoptotic signals from the stroma through a number of mechanisms, including: (i) amplification of the AR, (ii) mutation of the *AR* or (iii) activation of the AR by other signalling pathways. Adapted from (Shen and Abate-Shen, 2010).

1.4.7. Cancer cell invasion and metastasis

Whereas organ-confined primary CaP is curable in the vast majority of cases, metastatic CaP is largely incurable due to its systemic nature and the resistance of disseminated cancer cells to existing therapeutic agents. In fact, greater than 90% of mortality from cancer is due to metastases and not the primary malignant tumours (Valastyan and Weinberg, 2011). Distant metastases are established through a complex cascade of events termed the invasion-metastasis cascade (Figure 11):

1) **Primary tumour formation.** The development of a primary prostate tumour from a PIN lesion is a multistep pathway involving a number of molecular processes, genes and pathways, including telomere shortening, DNA damage, *PTEN* inactivation and *MYC* over-expression (Shen and Abate-Shen, 2010)

2) **Local invasion through the BM and stroma.** Individual tumour cells may invade via the protease-, stress-fibre-, and integrin-dependent "mesenchymal invasion" program or the protease-, stress-fibre-, and integrin-independent, Rho/ROCK-dependent "amoeboid invasion" program, depending on the microenvironment conditions (Friedl and Wolf, 2003). The best characterised alteration occurring upon invasion is the loss of the cell-to-cell adhesion molecule, E-cadherin, during an epithelial-to-mesenchymal (EMT) transition. Loss of E-cadherin results in dissociation of epithelial cell sheets into single cells, detachment of adherens and tight junctions and a loss of cell polarity. This causes cells to exhibit multiple mesenchymal attributes, including heightened invasiveness (Thiery et al., 2009). After penetration of the BM, the invasive cell infiltrates the stroma, which becomes increasingly 'reactive' and acquires many of the attributes of the stroma from tissues that are in the midst of wound healing or are inflamed (Grivennikov et al., 2010).

3) **Intravasation into the lymphatic system or blood vessels**. Metastatic carcinoma cells disseminate from the primary tumour via the circulation or lymphatic system (Gupta and Massague, 2006). Invasion into the lymphatic system is the most common route for most carcinomas, including CaP (Shridhar, 1979).

4) **Survival of transport in the circulation.** Viable circulating tumour cells (CTCs) have been detected and isolated in the bloodstream of patients with a range of different cancers including metastatic lung, pancreatic, breast, colon (Nagrath et al., 2007; Stott et al., 2010) and CaP (Ghossein et al., 1995)

5) **Arrest at a distant organ site.** Individual primary tumours form metastases in only a limited subset of secondary organs. For example, primary prostate tumours primarily

metastasise to bone (90%), with metastasis also occurring in the lung (46%), liver (25%), pleura (21%), and adrenals (13%) (Bubendorf et al., 2000).

6) **Extravasation into distant tissues.** Once lodged in the capillaries of distant organs, CTCs may initiate growth and form a colony that ruptures the vessel walls, thereby placing tumour cells in direct contact with the tissue (Al-Mehdi et al., 2000). Alternatively, CTCs may cross from the blood vessel into the tissue by extravasation.

7) **Survival and formation of micro-metastases in a foreign environment.** The microenvironment of the metastatic site usually differs vastly from the primary site. However, it has been proposed that cancer cells can address the problem of an incompatible microenvironment at the metastatic site via the establishment of a "pre-metastatic niche" (Psaila and Lyden, 2009).

8) **Proliferation at secondary sites forming detectable metastatic colonies.** By overcoming the incompatibility with the foreign microenvironment and activating self-renewal pathways, a small minority of disseminated carcinoma cells may succeed in completing the process of metastatic colonisation (Valastyan and Weinberg, 2011).

Not every cell in a tumour possesses the ability to metastasise to distant organs, and recent data has supported the notion that metastases directly arise from CSCs. Most notably, a distinct subset of $CD133^+CXCR4^+$ CSCs localised to the invasive edge of pancreatic carcinomas, exhibited significantly stronger migratory activity *in vitro* than non-CSCs and demonstrated *in vivo* metastatic activity to the liver (Hermann et al., 2007).
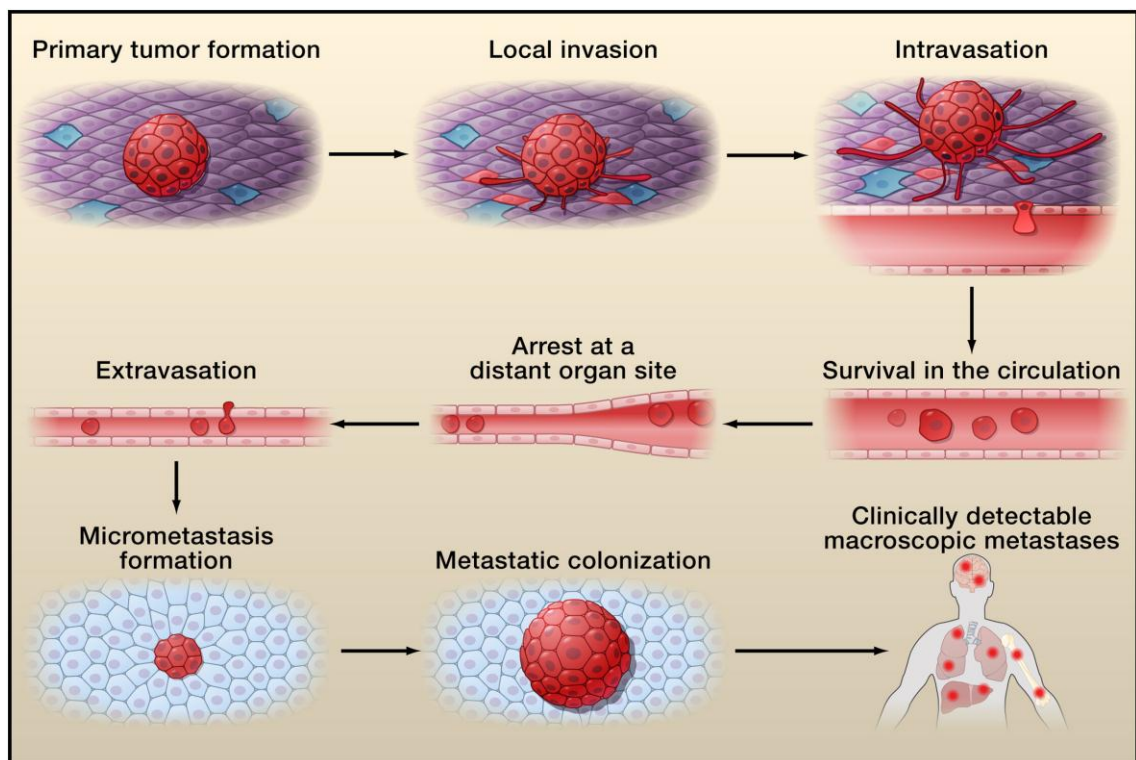
Figure 11. The stages of invasion and metastasis.
During metastasis, tumour cells initially invade adjacent tissue and exit the primary site through intravasation. Metastatic cancer cells then translocate through the circulation and enter a distant tissue through extravasation. Metastatic colonies are developed which adapt to survive and thrive in the microenvironment of a distant tissue. Adapted from (Valastyan and Weinberg, 2011).

1.4.8. Epithelial-to-mesenchymal transition

EMT is a trans-differentiation programme characterised by the loss of the differentiation characteristics of epithelial cells, including cell-cell adhesion, apical-basal motility and lack of motility. Instead, cells acquire mesenchymal features, which include motility, invasiveness and a heightened resistance to apoptosis (Polyak and Weinberg, 2009). EMT is critical for normal embryonic morphogenesis (Thiery et al., 2009) and wound healing (Savagner et al., 2005). However, EMT has become implicated as a means by which transformed epithelial cells can undergo metastasis and acquire the ability to invade, resist apoptosis and disseminate (Barrallo-Gimeno and Nieto, 2005; Klymkowsky and Savagner, 2009; Polyak and Weinberg, 2009; Thiery et al., 2009; Yilmaz and Christofori, 2009). EMT is coordinated by a set of TFs, including Slug, Snail, Twist, ZEB1, and ZEB2, which suppress the expression of epithelial markers and induce expression of markers associated with the mesenchymal state (Thiery et al., 2009). These transcriptional regulators have been shown, in experimental models of carcinoma formation, to be important for programming invasion and some have been found to provoke metastasis when ectopically over-expressed (Hanahan and Weinberg, 2011). In fact, EMT-inducing TFs are able to orchestrate most steps of the invasion-metastasis cascade apart from the final step of metastatic colonisation (Hanahan and Weinberg, 2011). The reversal of EMT, the mesenchymal-to-epithelial (MET) transition, may have a role in the reversion of disseminated mesenchymal tumour cells to a more epithelial state in distant metastases (Polyak and Weinberg, 2009).

EMT is implicated in progression to a metastatic disease and in acquisition of therapeutic resistance, both of which may be linked to the generation of cancer cells, which have undergone EMT, with SC-like characteristics. Two independent studies have shown that mammary cells that have experienced an EMT behave in many respects similarly to SCs isolated from normal or neoplastic cell populations (Mani et al., 2008; Morel et al., 2008). Furthermore, Mani et al. (2008) showed that most of the EMT-inducing TFs are expressed at higher levels in $CD44^{+}CD24^{-}$ mammary SC-like cells than differentiated cells. More recently, it has been shown that CaP cells with an EMT phenotype displayed stem-like cell features (Kong et al., 2010).

1.5. Regulation of gene expression in the prostate epithelium

Maintenance of prostate epithelial homeostasis is an equilibrium between self-renewal, proliferation and differentiation, which is regulated by changes in gene expression throughout the different cell types (Moore and Lemischka, 2006). Gene expression can be regulated either by controlling the level of transcription of mRNA from a gene or regulating the translation of mRNA into proteins. Transcriptional control of expression can involve regulation by specific TFs within the cell, which bind to their target sequences, genetic changes and mutations or epigenetic mechanisms.

TF regulation of expression within the prostate has been well studied and a number of TFs have been implicated in the regulation of expression within the prostate epithelium. It is well regarded that androgens and the AR undoubtedly play a pivotal role in prostate differentiation during embryonic (Kellokumpu-Lehtinen et al., 1979) and postnatal development (Kellokumpu-Lehtinen et al., 1981; Aumuller, 1991), as well as being essential for the survival of the luminal secretory cells in the adult prostate (English et al., 1987). Several other pathways are important in the development and differentiation of the prostate epithelium. These include, induction of Notch (Leong and Gao, 2008), Wnt (Verras et al., 2004; Lu et al., 2009) and Hedgehog (Berman et al., 2004; Karhadkar et al., 2004; Sanchez et al., 2004) signalling, which promote prostate epithelial cell proliferation and differentiation, even in the absence of androgens.

One of the lesser studied TFs in the prostate is the biologically active derivative of vitamin A (retinol), retinoic acid (RA). RA signalling controls the expression of *HOX* genes, and thus has a direct role in the early development of many organs and systems including heart, urogenital system, eyes, pancreas and lungs (Duester, 2008). RA is also known to play a crucial role in the development and homeostasis of a wide range of other tissues, including prostate (Peehl et al., 1993; Seo et al., 1997), bone (Karakida et al., 2011), neuron (Ito et al., 2011b) and liver (Huang et al., 2009), through regulating numerous genes involved in differentiation, proliferation and homeostasis (Bastien and Rochette-Egly, 2004). RA also stimulates apoptosis, by up-regulating the expression of caspase 7 and 9 (Donato and Noy, 2005).

The importance of retinoids during tissue development and homeostasis is apparent in vitamin A deficiency (VAD) syndrome, which causes congenital malformation during development and tissue degeneration, growth retardation and widespread squamous metaplasia after birth (Wilson et al., 1953). It is known that RA can either positively (Vezina et al., 2008) or negatively affect prostate formation and gland development (Aboseif et al., 1997), depending on the stage of prostate development. This suggests that RA plays a crucial role in development and differentiation of the prostate epithelium.

1.5.1. Retinoic acid signalling

The RA signal is transduced by a heterodimeric complex of retinoic acid receptors (RARs) and retinoid X receptors (RXRs). Both RAR and RXR families consist of 3 isoforms (α, β and γ), encoded by different genes (Leid et al., 1992; Kastner et al., 1997). RARs are activated by atRA and 9-*cis*-RA, whereas only 9-*cis*-RA activates RXRs. In the absence of ligand, RARs are primarily found in the nucleus bound to DNA (Bastien and Rochette-Egly, 2004). The RAR/RXR heterodimers bind to specific DNA sequences called RA response elements (RAREs) which are composed of 2 direct repeats of the PuG(G/T)TCA hexameric motif usually spaced by 5 bp (DR5), although 2 bp (DR2) or 1 bp (DR1) spaces do occur (Leid et al., 1992) (Figure 12).

Retinoids and their derivatives are hydrophobic in nature and consequently are stored and transported in complex with either cellular retinoid-binding proteins (CRBP) or cellular RA-binding proteins (CRABP) (Donovan et al., 1995). There are 2 isoforms of CRABP: CRABP1 and CRAPB2, which possess distinct distributions and functions. A number of studies have eluded to the fact that CRABP2, but not CRABP1, is a co-activator of the RAR (Delva et al., 1999; Dong et al., 1999). Both Delva et al. (1999) and Dong et al. (1999) concluded that CRABP1 might be able to sequester RA when RA levels exceed homeostasis (Wolf, 2000). It is also significant that RA can itself induce expression of the CRABP2 gene, but not the CRABP1 gene (Giguere et al., 1990; Durand et al., 1992; Astrom et al., 1994).

CRABP shuttles RA to the nucleus and binds to the RAR/RXR heterodimer, which is stabilised by cyclin D3 (Delva et al., 1999; Budhu and Noy, 2002; Despouy et al., 2003). RA binding causes conformational changes, which increase the receptors DNA affinity and causes dissociation of co-repressors such as NCoR, SMRT, and a histone deacetylase (HDAC) complex (Egea et al., 2001). This creates a new hydrophobic cleft surface where co-activators, such as the SRC/p160 family, p300/CBP and CARM-1, can bind (Glass and Rosenfeld, 2000; McKenna and O'Malley, 2002). These co-activators modify chromatin structure through histone acetyltransferase (HAT) or methyltransferase activity, resulting in decondensed and relaxed chromatin (Zhang and Reinberg, 2001). This facilitates the recruitment of transcriptional machinery (Dilworth and Chambon, 2001; Woychik and Hampsey, 2002) and allows the initiation of gene transcription to occur (Figure 12).

1.5.2. Genetic changes in cancer

In cancer, mutation events can occur within tumour suppressor genes or oncogenes, resulting in changes in their gene expression. Some examples of commonly mutated genes in CaP include *PTEN* (Li et al., 1997), *Rb* (Bookstein et al., 1990), *p27^{kip1}* (Tsihlias et al., 1998) and *p53* (Voeller et al., 1994). Loss of heterozygosity (LOH) is a frequent event in CaP progression (Abate-Shen and Shen, 2000) and is defined as the loss of normal function of one allele of a gene, in which the other allele was already inactivated. LOH at chromosomes *8p, 10q, 13q,* and *17p* are well-characterised events and losses of *6q, 7q, 16q,* and *18q* have also been reported in CaP, although they are not as well characterised (Latil et al., 1994; Zenklusen et al., 1994; Elo et al., 1995; Takahashi et al., 1995; Cooney et al., 1996; Cunningham et al., 1996; Latil et al., 1997; Macintosh et al., 1998; Saric et al., 1999; Murant et al., 2000). In addition, chromosomal gains at *8q* and *7* occur during CaP progression (Alcaraz et al., 1994; Bandyk et al., 1994; Van Den Berg et al., 1995).

Figure 12. Cellular mechanism of retinoic acid activation of gene expression.
(a) Vitamin A (retinol) is taken up from the blood and binds to cellular retinol binding protein (CRBP). Retinol is metabolised to retinal by retinol dehydrogenases (RoDH), which is further metabolised to retinoic acid (RA) by retinaldehyde dehydrogenases (RALDH). RA is transported to the nucleus bound to a cellular RA-binding protein (CRABP), where the RA ligand binds to a RAR/RXR heterodimer bound to a RARE DNA sequence, activating transcription of a target gene. **(b)** In the absence of ligand, RARs bound to RAREs located in the promoter of target genes repress transcription through their association with HDAC-containing complexes, tethered through co-repressors. **(c)** Upon RA ligand binding, the co-repressors dissociate, allowing the recruitment of co-activators that function to open chromatin. **(d)** The co-activators dissociate and the transcription machinery is recruited to initiate transcription. Adapted from (Maden, 2002; Bastien and Rochette-Egly, 2004).
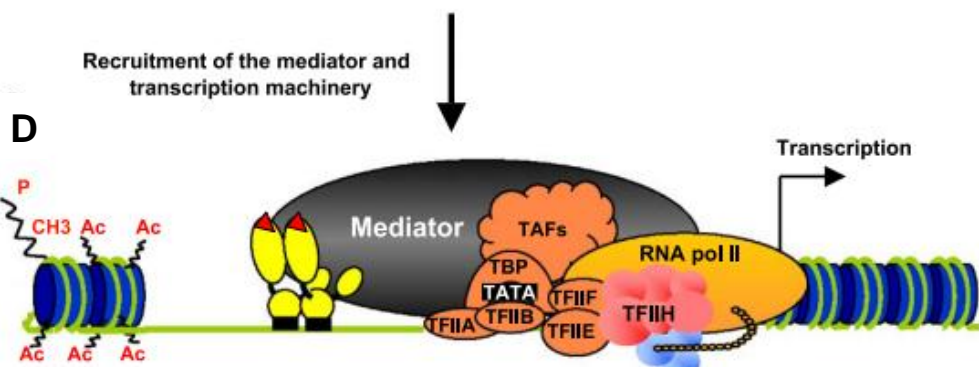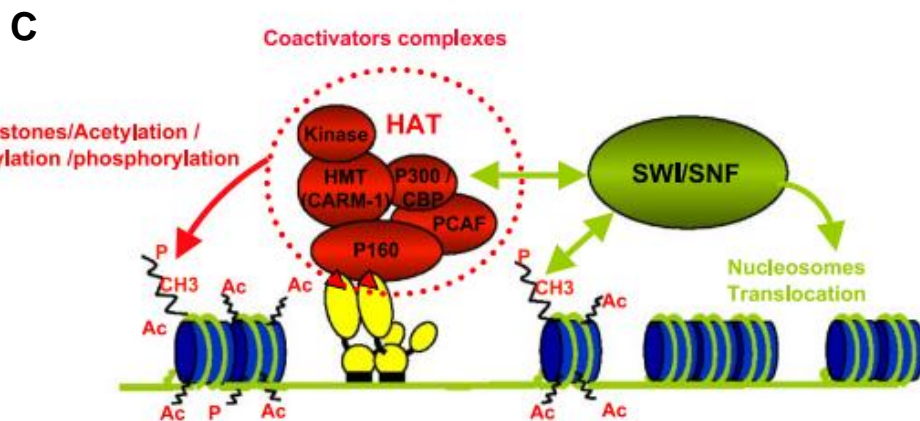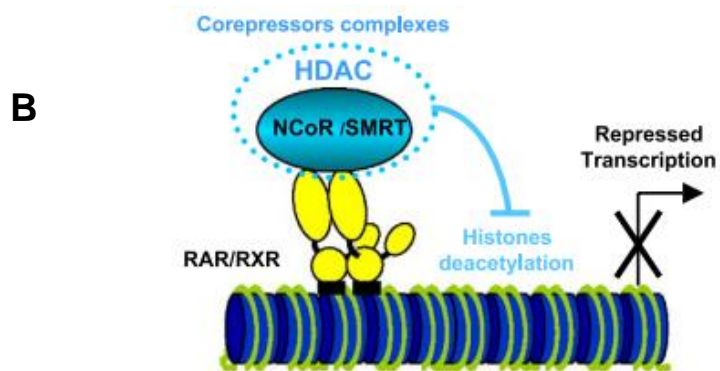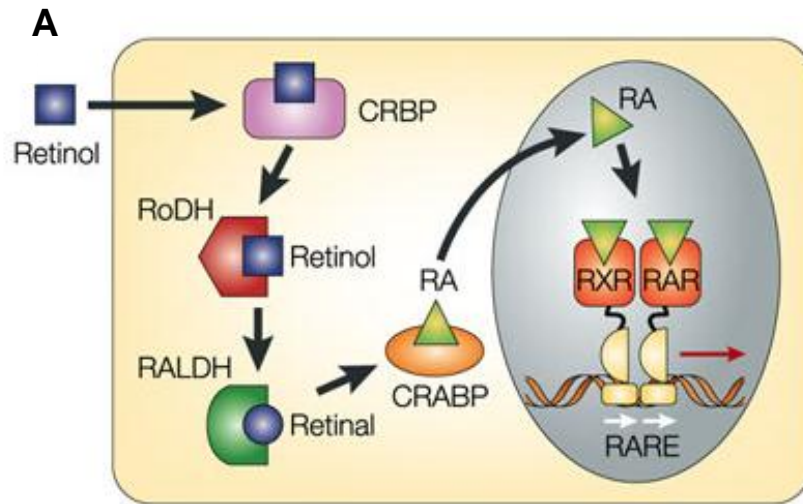
1.6. Epigenetic regulation mechanisms

Over the past century the genetic model of cancer has predominated, however the role of epigenetics in cancer development has exploded in the last few years and is now accepted as a mainstream area of cancer research. Epigenetics can be defined as heritable changes in gene expression that cannot be explained by changes in DNA sequence or gene copy number. The major epigenetic mechanisms include DNA methylation, chromatin remodelling (histone modifications and polycomb complexes) and small non-coding RNAs.

1.6.1. DNA methylation

DNA methylation was the first epigenetic modification to be identified and is the most studied to date. Until only recently, the only known epigenetic modification of DNA was 5-methylcytosine (**5mC**), which is a covalent modification that occurs when DNA methyltransferases (DNMT) catalyses the addition of a methyl group from S-adenosylmethionine to the 5'-carbon position of a cytosine pyrimidine ring preferentially at cytosine and guanine (CpG) dinucleotides. There are now known to be at least four different DNA modifications.

In 2009, ten-eleven translocation 1 (TET1) was shown to enzymatically oxidise 5mC to 5-hydroxymethylcytosine (**5hmC**) (Tahiliani et al., 2009). 5hmC was originally detected in mammalian DNA in 1972 (Penn et al., 1972). Although 5hmC may be a bona fide epigenetic mark, it is predicted that 5hmC may be an intermediate in the removal of 5mC and the low levels of 5hmC found in the genome suggest that it may be a short-lived entity (Branco et al., 2012). The demethylation pathway may involve even further oxidation of 5hmC to 5-formylcytosine (**5fC**) and 5-carboxylcytosine (**5caC**) by TET enzymes (He et al., 2011; Ito et al., 2011a). The biological significance of the 5mC oxidation derivatives is still yet to be established, but they are likely to be an essential intermediate in the process of active/passive demethylation and preclude/enhance the binding of several methyl-CpG-binding domain (MBD) proteins, effecting the recruitment of chromatin regulators. Furthermore, 5hmC has been mapped to both active and repressed genes and at bivalent transcriptionally-poised genes (Wu and Zhang, 2011; Dawson and Kouzarides, 2012).

5mC is found almost entirely within CpG dinucleotides (Bird, 2002), which are generally sparse in the genome. CpG islands are regions of DNA with a high C+G content that contain a higher frequency of clustered CpG dinucleotides relative to the bulk genome (Gardiner-Garden and Frommer, 1987). CpG islands are mostly located at the 5' end of genes, but are also found in intronic and extronic sequences of gene bodies (Bird, 1986). Based on Gardiner-Garden and Frommers' initial criteria (1987), CpG islands were first identified as being 200 bp in length. However, Takai and Jones (2002) modified the criteria and suggested that regions of DNA greater than 500 bp with a C+G equal to or greater than 55% and observed CpG/expected CpG

of 0.65 should be classed as CpG islands and were more likely to be associated with the 5' regions of genes.

In normal tissues, 5mC globally marks the vertebrate genome, but is rare within CpG islands that are usually unmethylated in normal cells. However, specific CpG islands are hypermethylated in normal tissues in a tissue-specific manner (Ghosh et al., 2010). DNA methylation is associated with the regulation of gene expression, but it also involved in a number of other processes including genomic imprinting, X chromosome inactivation, suppression of retrotransposon elements (Bird, 2002) and is crucial for normal mammalian development, as embryos that possess abnormal methylation levels die before birth (Li et al., 1992; Okano et al., 1999).

Two basic models for the mechanism of gene silencing by DNA methylation have evolved: a direct or an indirect mechanism (Figure 13). Direct inhibition may result from 5mC sterically blocking TFs binding to their cognate DNA sequence at the promoter. Indirect repression would be due to MBD proteins binding to methylated cytosines and recruiting co-repressors, to silence gene expression (Nan et al., 1997; Nan et al., 1998).

The current model for the establishment and inheritance of DNA methylation patterns relies on the original hypotheses of Riggs (1975) and Holliday and Pugh (1975). This model states that methylation patterns are established in germ cells and in developing embryos by *de novo* **methylation**, carried out by DNMT3A and DNMT3B, which methylate previously unmethylated CpG sites. Methylation patterns are then inherited between cell generations with high fidelity by **maintenance methylation**, primarily by DNMT1, which has a preference for hemimethylated sites generated during DNA synthesis. However, Jones and Liang (2009) have recently proposed a revised model for DNA methylation maintenance suggesting that the bulk of the methylation is carried out by DNMT1, which is the predominant DNA methylase in the cell (Walsh and Bestor, 1999). DNMT3A and DNMT3B then complete the methylation process and correct errors left by the DNMT1 enzyme.

DNA demethylation can occur through a progressive passive mechanism, either by not methylating the new DNA strand after replication or via inhibition or a lack of DNMTs. Alternatively, an active enzyme-mediated mechanism involving 5hmC and TET proteins can result in DNA demethylation, which still remains poorly understood (Wu and Zhang, 2011). It is now emerging that there is considerable cross-talk between DNA methylation and histone modifications during inactivation of the chromatin. For example, it has recently been shown that histones packaged with nucleosomes containing the H3Lys27Me3 chromatin mark, causes the recruitment of DNMTs to induce methylation (Schlesinger et al., 2007).
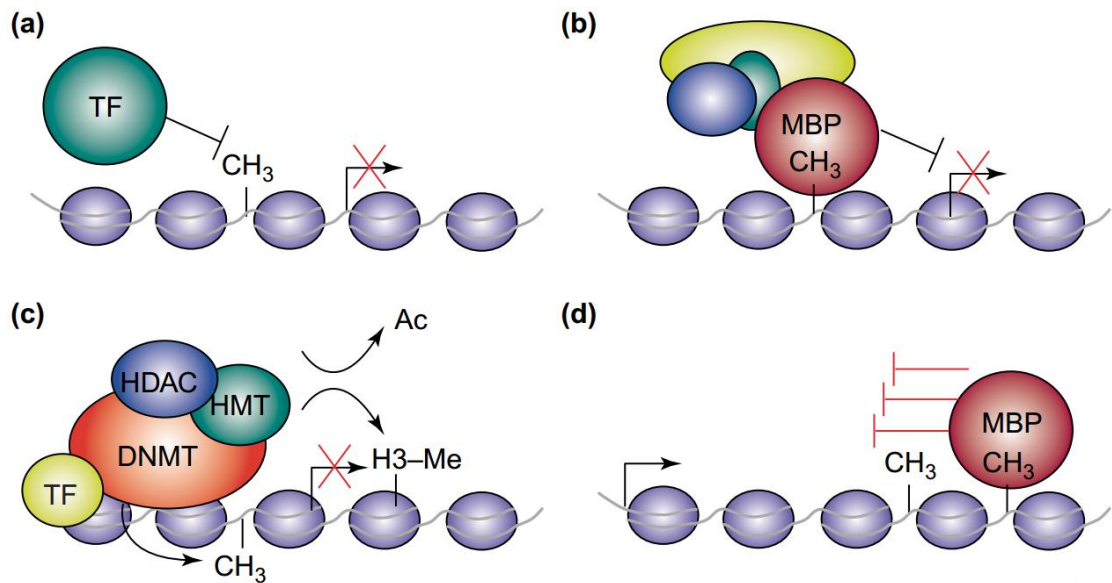
Figure 13. Mechanisms of transcriptional repression by DNA methylation.
(a) DNA methylation in the cognate DNA-binding sequences of some TFs can inhibit their binding to DNA. **(b)** Methyl-CpG-binding proteins (MBPs) recognise 5mC DNA and recruit co-repressor molecules to repress transcription and modify surrounding chromatin. **(c)** DNMT enzymes are linked to HDACs and histone methyltransferases (HMT), so the addition of 5mC to DNA is coupled to transcriptional repression and chromatin modification. **(d)** DNA methylation within the genes body can repress transcriptional elongation through the involvement of MBPs. Adapted from (Klose and Bird, 2006).

1.6.2. Histone modifications and chromatin remodelling

The packaging of DNA into highly compacted chromatin is achieved through the winding of DNA around an octamer of two subunits of each of the core histones: H2A, H2B, H3, H4 and linker H1, forming nucleosomes. Chromatin is presented in two forms (Grewal and Jia, 2007):

- highly condensed **heterochromatin** that is transcriptionally silent
- less condensed **euchromatin**, which is transcriptionally active.

The core histone domain is flanked by protruding N- and C-terminal tails, which are targets for several covalent modifications that determine histone-DNA interaction. These include methylation, acetylation, phosphorylation, poly-ADP ribosylation, ubiquitination and glycosylation, form a 'histone code' (Figure 14) (Jenuwein and Allis, 2001).

Acetylation and methylation, of lysine residues in the majority of cases, are two of the best-studied histone modifications and both can result in either gene activation or gene silencing depending on the nature and position of the alteration. For example, mono-, di- or tri-methylation of H3K4, H3K36 and H3K79 results in active gene transcription, but methylation of H3K9, H3K27 and H4K20 usually results in gene silencing (Li et al., 2008).

Lysine residues can also be acetylated, a process catalysed by HATs (Roth et al., 2001). This removes the positive charge on the histone tails and results in a reduced affinity between histones and DNA, consequently opening the chromatin and enhancing transcription. HDACs act to deacetylate these lysine residues, resulting in condensed chromatin and repression of transcription in the majority of cases (Figure 15) (Shukla et al., 2008). A number of HDACs have been identified which are grouped into four classes: class I (HDAC 1-3, 8), class II (HDAC 4-7, 9, 10), class III (SIRT 1-7) and class IV (HDAC 11) (Minucci and Pelicci, 2006; Epping and Bernards, 2009).

Polycomb group (PcG) proteins were originally identified in *Drosophila melanogaster*, as repressors of *HOX* genes (Lewis, 1978; Struhl, 1981) and when mutated resulted in activation of silenced *HOX* genes. PcG proteins form two multimeric complexes in humans: Polycomb repressive complex 1 or 2 (PRC1 or PRC2), which function to silence gene expression. PcG proteins are implicated in cell proliferation, SC identity, cancer, genomic imprinting and X inactivation (Schuettengruber et al., 2007). The PcG proteins and DNA methylation have been mechanistically linked; the PcG protein EZH2 has been shown to serve as a recruitment platform for DNMTs (Vire et al., 2006).
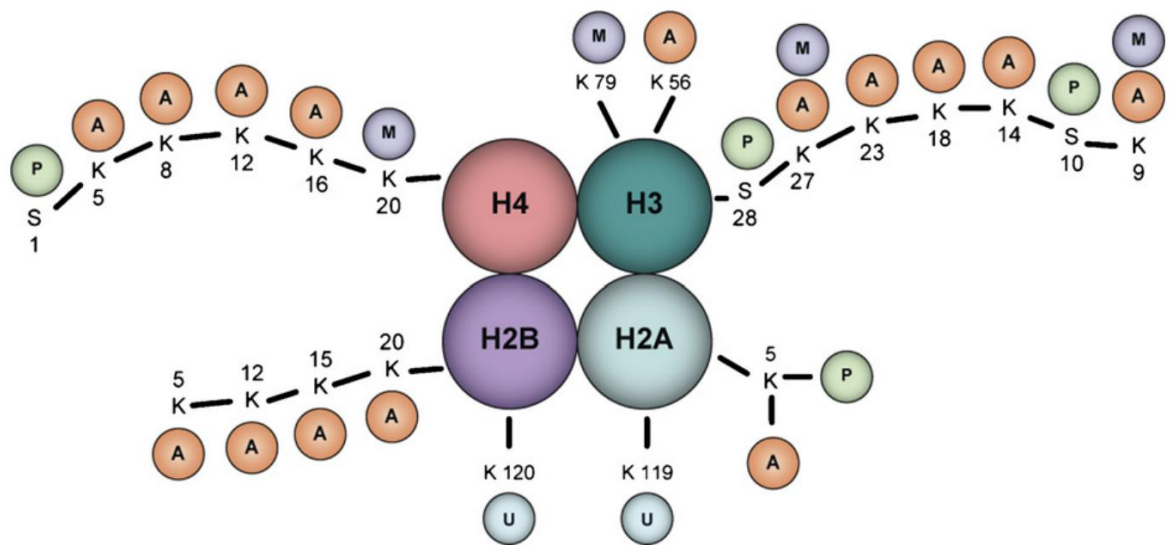
Figure 14. Schematic representation of a nucleosome and histone modifications.
The N-terminal tails of the core histones (H2A, H2B, H3 and H4) contain post-translational modifications of histones: acetylation (A), methylation (M), phosphorylation (P), and ubiquitination (U). Several lysines (e.g. Lys 9) can be either acetylated or methylated. Modified from (Shukla et al., 2008).
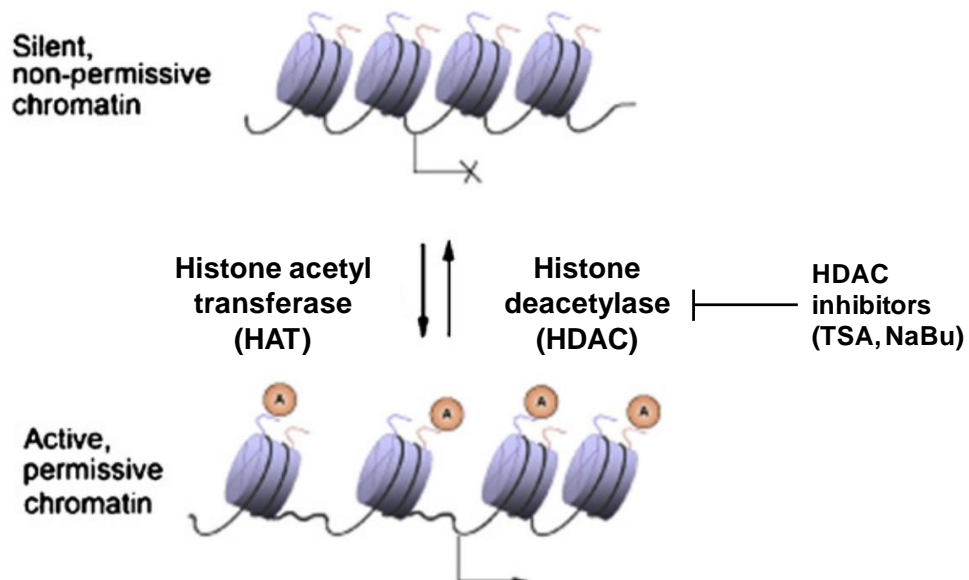
Figure 15. The balance between histone acetylation and deacetylation determines the level at which a gene is transcribed.
The acetylation of histones leads to an open, transcriptionally permissive chromatin. Histone acetylation is a reversible modification and acetyl groups are removed by several HDACs. Modified from (Shukla et al., 2008).

1.6.3. MicroRNAs

MicroRNAs (miRNAs) are a class of small non-coding RNA, around 18-25 nucleotides in length, that are transcribed from DNA into RNA. They are synthesised (pri-miRNA) and processed (pre-miRNA) in the nucleus, before they are exported to the cytoplasm. In the cytoplasm they are cleaved to form mature miRNA, which bind mRNAs with complementary sequences and alter their expression through an RNA-induced silencing complex (RISC). MiRNA expression is frequently altered in cancer and miRNAs can act as oncogenes when over-expressed or tumour suppressors when silenced (Calin and Croce, 2006; Garzon et al., 2009).

MiRNAs can regulate both normal SCs and CSCs, including prostate CSCs (Croce and Calin, 2005; Yu et al., 2007b; Shimono et al., 2009; Melton et al., 2010; Liu et al., 2011a), and deregulation of miRNAs has been implicated in tumourigenesis (Esquela-Kerscher and Slack, 2006). Liu et al. (2011a) recently showed that miRNA-34a, a p53 target, is down-regulated specifically in CD44^{+} prostate CSCs and expression of miRNA-34a in CD44^{+} prostate CSCs inhibits tumour regeneration and metastases in mice.

1.6.4. Epigenetic therapy in cancer

As epigenetic modifications have such a prominent effect on the progression of cancer, a number of drugs that function to reverse epigenetic abnormalities have been tested as potential cancer therapies.

1.6.4.1. DNA demethylating agents

Cytosine analogues (Figure 16) are known to possess DNA demethylating activity and pharmacologically inhibit the biologically active DNMTs (DNMT1, DNMT3A and DNMT3B) (Jones and Taylor, 1980). These analogues initially displayed a high toxicity and so were unsuitable for clinical use, however, they have since shown to achieve therapeutic efficacy at a lower dose. Consequently, two inhibitors, azacytidine (Vidaza; Celgene) and 5-Aza-2'-Deoxycytidine (5-Aza-dC), also known as decitabine (Dacogen; Eisai), have recently gained approval by the FDA for myelodisplastic syndrome, which leads to leukaemia. This paves the way for refining the use of low-dose regimens not only for leukaemia but also for solid tumours (Baylin and Jones, 2011).

5-Aza-dC is a cytosine analogue in which the pyrimidine ring carbon 5 is replaced with nitrogen, and when incorporated into DNA (by base-pairing with guanine) it cannot be methylated. Consequently, almost complete demethylation of genomic DNA occurs after two cell cycles (Haaf, 1995).
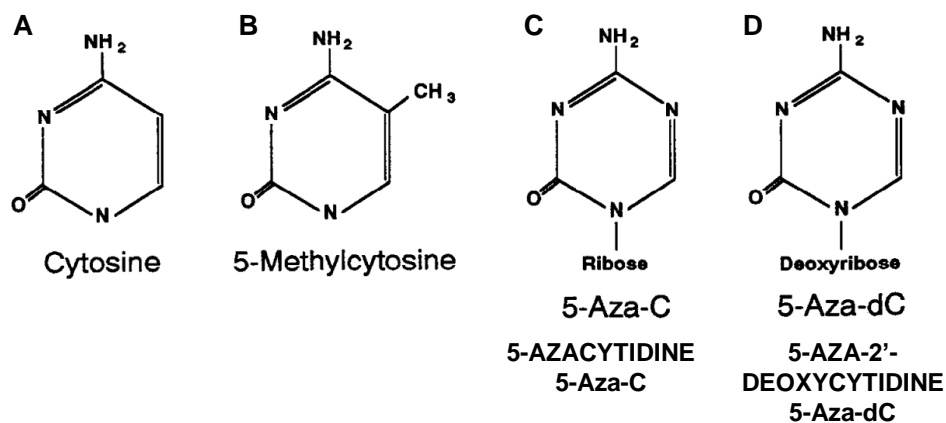
Figure 16. Structure of cytidine and its analogues.
Adapted from (Haaf, 1995).

1.6.4.2. HDAC inhibitors

Deacetylation of histones can be reversed by treating cells with HDAC inhibitors (HDACIs), which include trichostatin A (TSA), sodium butyrate (NaBu) and valproic acid. HDACIs have received extensive investigation in a number of clinical trials. The FDA have recently approved the use of vorinostat (Zolinza; Merck) and romidepsin (Istodax; Celgene) for their remarkable efficacy in cutaneous T cell lymphoma (Baylin and Jones, 2011).

Another translational area of HDACIs is their use in overcoming SC resistance mechanisms to traditional cancer therapies. Multiple HDACIs were shown to reverse therapeutic resistance to chemotherapeutic reagents in cultured cancer stem-like cells (Sharma et al., 2010). This suggests that HDACIs could be used as a combination therapy to sensitise against current treatments, although, considerable pre-clinical work is necessary before the efficacy of this combinatorial treatment is sought.

1.6.5. Epigenetic changes in prostate cancer

1.6.5.1. DNA methylation

It is widely established that there is a link between DNA methylation and cancer development, with methylation changes occurring early and ubiquitously in cancer (Jaenisch and Bird, 2003). A striking feature of carcinogenesis is that the majority of malignant tumours show a global hypomethylation of sparse CpG sites, compared to their normal counterparts (Feinberg and Vogelstein, 1983). Genome-wide DNA hypomethylation of DNA has been found to induce tumour formation in mice, by promoting chromosomal instability (Gaudet et al., 2003). Metastatic CaP has been shown to exhibit global hypomethylation (Bedford and van Helden, 1987), which has been linked with chromosome instability and disease progression (Schulz et al., 2002). In addition to global hypomethylation occurring at sparse CpG sites, a number of genes are found to be up-regulated through hypomethylation of CpG islands located within their promoters in CaP (Table 4).

Hypermethylation at the promoters of specific genes is also found in almost all malignant tumours. The best characterised epigenetic alteration in CaP is DNA hypermethylation and substantial evidence supports the view that DNA hypermethylation has a major role in the initiation and development of CaP. More than 50 genes that are hypermethylated in CaP have been characterised (Jeronimo et al., 2011). *GSTP1* is the most commonly methylated gene in CaP, and its inactivation occurs as an early event in cancer progression (Nakayama et al., 2004). Hypermethylation of *GSTP1* was found to be absent in normal prostate epithelium, but present in 70% of PIN lesions and more than 90% of adenocarcinomas (Nakayama et al., 2003). Other genes, also known to be frequently hypermethylated at their CpG islands in CaP are shown in Table 5. Frequent promoter hypermethylation of some genes is also found in PIN and normal prostate tissue, suggesting that epigenetic alterations are early events in CaP progression (Kang et al., 2004; Woodson et al., 2004; Henrique et al., 2006).

Many of the genes frequently repressed by hypermethylation in CaP are usually expressed predominantly in the more undifferentiated cells in the normal prostate. For example, *GSTP1* is expressed only in the basal compartment of normal prostate (Moskaluk et al., 1997) and *CD44* is expressed mainly in basal cells (Liu et al., 1997; Alam et al., 2004).

	Hypomethylated Gene	Reference
CAGE	Cancer/testis antigen	(Cho et al., 2003)
CYP1B1	Cytochrome P450 1B1	(Tokizane et al., 2005)
HPSE	Heparanase	(Ogishima et al., 2005)
PLAU	Urokinase-type plasminogen activator	(Pakneshan et al., 2003)
WNT5a	Wingless-related MMTV integration site 5A	(Wang et al., 2007)
CRIP1	S100 calcium-binding protein P	(Wang et al., 2007)
S100P	Cysteine-rich protein 1	(Wang et al., 2007)

Table 4. Genes showing frequent regulation by DNA hypomethylation in prostate cancer.

	Hypermethylated Gene	Reference
GSTP1	Glutathione S-transferase P1	(Lee et al., 1994)
APC	Familial adenomatous polyposis	(Maruyama et al., 2002)
RARβ	Retinoic acid receptor β	(Nakayama et al., 2001)
RASSF1α	Ras association domain family protein 1 isoform A	(Liu et al., 2002)
TIMP3	TIMP metallopeptidase inhibitor 3	(Yamanaka et al., 2003)
MGMT	O-6-methylguanine DNA methyltransferase	(Yegnasubramanian et al., 2004)
MDR1	Multidrug resistance receptor 1	(Ellinger et al., 2008)
PTGS2	Prostaglandin-endoperoxide synthase 2	(Yegnasubramanian et al., 2004)
CD44	Cluster of differentiation 44	(Lou et al., 1999; Kito et al., 2001)

Table 5. Genes showing frequent regulation by DNA hypermethylation in prostate cancer.

1.6.5.2. Chromatin Remodelling

Several histone modifying enzymes are deregulated in CaP, including the EZH2 histone methyltransferase PcG protein, which trimethylates H3K27, dimethylates H3K9 (Cao et al., 2002), is involved in DNA methylation (Vire et al., 2006) and is over-expressed in CRPC (Varambally et al., 2002). EZH2 over-expression is associated with hypermethylation and repression of genes involved in EMT (Chen et al., 2005), tumour suppression and metastasis (Beke et al., 2007) and is associated with a high proliferative rate and CaP aggressiveness (Bachmann et al., 2006). LSD1 (or histone demethylase 1a) acts as a transcriptional co-repressor by removing mono- or dimethyl groups from H3K4, promotes cell proliferation (Scoumanne and Chen, 2007) and is associated with CRPC (Metzger et al., 2005; Kahl et al., 2006). A number of HDACs are also up-regulated in CaP (Patra et al., 2001), including HDAC1 (Halkidou et al., 2004).

1.6.5.3. MicroRNAs

In CaP, miRNA deregulation affects epigenetic reprogramming, blockade of apoptosis, promotion of cell cycle, migration and invasion and is an alternative mechanism sustaining androgen-independent growth (Coppola et al., 2010; Jeronimo et al., 2011).

1.6.6. Epigenetic changes in stem cells

Epigenetic modifications are essential for the normal function of SCs and early progenitor cells, but can be highly deregulated in cancers. Epigenetic regulation plays a crucial role in the maintenance of the hierarchical structure of tissues, since it is involved in both SC maintenance and fate determination (Ansel et al., 2003; Hsieh and Gage, 2004; Fan et al., 2005; Roloff and Nuber, 2005; Sen et al., 2010). The tumour suppressor gene *p16ink4A* is one of the most common and earliest epigenetically silenced genes in a range of cancers, including breast, colon and lung. Recent experiments with knockout mice have revealed that germ line loss of this gene increases SC life span, consistent with the proposed role of epigenetic modifications facilitating early abnormal clonal expansion of cells at risk for cancer (Jones and Baylin, 2007). It is also known that the PcG protein, Bmi1, maintains the self-renewal of a number of SCs, including HSCs (Park et al., 2003), neural SCs (Molofsky et al., 2003), mammary SCs (Liu et al., 2006b) and prostate SCs (Lukacs et al., 2010). Recently, it was shown that the Bmi1 pathway is one of the key regulatory mechanisms of the 'stemness' function of normal SCs and CSCs (Glinsky, 2008).

SCs exhibit an epigenetic landscape with a highly dynamic bivalent chromatin state, in which active and repressive chromatin marks are closely positioned. Bivalent domains were initially proposed as areas of chromatin responsible for silencing developmental genes in embryonic SCs, whilst keeping them poised for activation during differentiation (Bernstein et al., 2006). Moreover, this bivalent chromatin state has also been shown to be associated with HSCs or progenitor cells prior to differentiation (Cui et al., 2009). Evidence has suggested that a bivalent SC-like chromatin pattern in important regulatory genes in SCs or progenitor cells may leave these genes vulnerable to aberrant DNA hypermethylation and heritable gene silencing, during tumour initiation and progression (Ohm et al., 2007).

The key question is whether epigenetic modifications are the driving force for the development of cancer, or if they are a secondary event. If indeed they are, reversion of malignancy would be more achievable. As epigenetic modifications are found so early in tumourigenesis it is plausible that epigenetic changes in SCs may be the instigator for cancer. Feinberg *et al.* (2006) proposed that epigenetic abnormalities might play a seminal role in the earliest steps of cancer initiation. He proposed that cancer arises in three steps: (1) epigenetic disruption of progenitor cells, (2) an initial mutation and (3) genetic and epigenetic plasticity (Figure 17). The initial step involves an epigenetic change occurring in a stem/progenitor cell leading to a polyclonal altered population of neoplasia-ready cells. It is proposed that 'tumour-progenitor genes', that may normally regulate SC characteristics, promote this initial epigenetic change. This tumour-progenitor gene (or genes) may constitute part of an epigenetic network with positive and negative feedback. The second step is an initiating genetic mutation within this epigenetically altered progenitor-cell pool, which has traditionally always been thought of as the first step in

carcinogenesis. Finally, the cell must acquire an ability to stably evolve its phenotype both genetically and epigenetically leading to the development of a primary cancer.
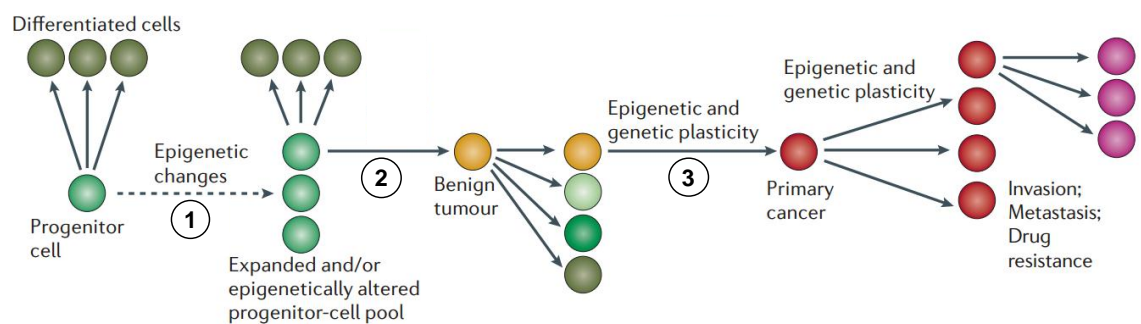
Figure 17. The epigenetic progenitor model of cancer.
This model proposes that cancer arises in 3 steps: (1) Epigenetic alteration of stem/progenitor cells within a tissue. (2) Initial genetic mutation within the altered progenitor pool. (3) Epigenetic and genetic plasticity leading to the development of cancer. Adapted from (Feinberg et al., 2006).

1.7. Identification of a prostate cancer stem cell signature

To identify new strategies of SC differentiation therapy, the phenotypic differences between SCs and their differentiated progeny needs to be sought. Birnie et al. (2008) have identified an expression signature of genes that are over-expressed in prostate SCs compared to more differentiated CB cells, using an Affymetrix microarray. More importantly, classes of genes that were lowly expressed in the SC compartment were identified. These classes of genes could be exploited by future differentiation therapies through restoration of their expression or function. Two of the most significantly down-regulated genes in the SC compartment were the two homologous genes RARRES1 and LXN. RARRES1 has a known role in CaP progression and LXN has been identified as a SC regulator; these genes were consequently selected based on their expression in the microarray and their expression, regulation and function was investigated in greater detail in this study.

1.7.1. Retinoic acid receptor responder 1 (RARRES1)

The *RARRES1* gene is located on the long arm of chromosome 3 adjacent to the *LXN* gene, at 3q25.32 (Figure 18). The gene is 35.38 kb in length, contains one open reading frame, but through alternative splicing codes for 2 protein isoforms of 228 (26 kDa) and 294 (33 kDa) amino acids.

RARRES1, or Tazarotene Induced Gene 1 (TIG1), was originally identified as the most up-regulated gene induced by the RAR β/γ - specific retinoid, tazarotene, in human skin raft cultures and psoriatic lesions (Nagpal et al., 1996). Gene expression was not induced by RXR specific retinoids, indicating that RARRES1 expression is mediated through the RAR pathway in the skin. Similarly, RARRES1 expression has been shown to be induced by the vitamin D3 pro-differentiation agent 1,25-dihydroxyvitamin D in the human colon carcinoma cell line, Caco-2 (Wood et al., 2004). Expression of RARRES1 is generally low in malignant cancer cell lines and is known to be repressed by DNA methylation in a number of cancers, including CaP (Youssef et al., 2004; Zhang et al., 2004; Kwong et al., 2005; Mizuiri et al., 2005; Ellinger et al., 2008; Yanatatsaneejit et al., 2008; Son et al., 2009; Tamura et al., 2009; Peng et al., 2012).

The cellular localisation of RARRES1 has only been speculated upon. Sequence analysis initially predicted RARRES1 to be a transmembrane protein with a small N-terminal intracellular region, a single membrane-spanning hydrophobic region and a long C-terminal extracellular region (Jing et al., 2002). More recently, RARRES1 was proposed to be a type III transmembrane protein based purely on its N-glycosylation status, with its long C-terminal domain facing the cytoplasm (Sahab et al., 2011). RARRES1 was only very recently shown to be exclusively secreted by plexiform neurofibroma Schwann cells, but not by normal Schwann cells, derived from non-neoplastic peripheral nerve (Chen et al., 2012). RARRES1 protein has

previously been detected in the conditioned media of adenocarcinomic human alveolar basal epithelial (A549) cells (Caccia et al., 2011), Hela cells, colorectal carcinoma (Colo205) cells and hepatocellular carcinoma (Hep3B) cells (Wu et al., 2010).

A functional role for the suppression of RARRES1 expression in cancer cell lines was confirmed by studies on a metastatic CaP cell line (PC-3M), where it acted as a metastasis suppressor (Jing et al., 2002). A decrease in RARRES1 expression increased the malignant characteristics of prostate cells and xenograft tissues; expression was found to reduce the invasiveness of malignant PC-3M cells *in vitro* and reduced tumour size *in vivo* in nude mice. A similar effect on invasion has been seen in Epstein-Barr virus-infected nasopharyngeal carcinoma cells (Kwok et al., 2009) and breast carcinoma SUM-159 cells (Peng et al., 2012).

The expression of RARRES1 is closely associated with differentiation and staging of colorectal adenocarcinoma cells (Wu et al., 2006). In normal colorectal mucosal tissue, it was found that RARRES1 protein expression is highest in terminally-differentiated luminal epithelial cells. RARRES1 plays a role in controlling the proliferation and differentiation of adult adipose-derived mesenchymal SC (Ohnishi et al., 2009), suggesting it might have a role in SC differentiation. Furthermore, over-expression of RARRES1 in endometrial tumour cells and colon cancer cell lines resulted in suppression of colony forming ability (Takai et al., 2005).

The mechanism of action of RARRES1 in suppressing invasion in cancer progression is currently unknown. The 30% sequence similarity between the C-terminal region of RARRES1 and LXN suggests that RARRES1 may also function as a carboxypeptidase inhibitor (Aagaard et al., 2005). In fact, RARRES1 has only recently been described to interact with the cytosolic carboxypeptidase AGBL2 to regulate the α-tubulin tyrosination cycle in the HEK 293 cell line (Sahab et al., 2011).
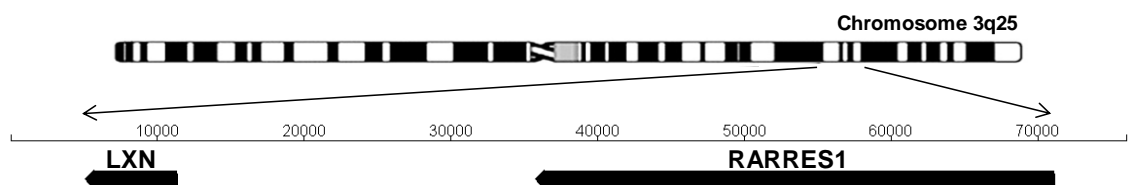
Figure 18. Adjacent location of the RARRES1 and LXN genes.
RARRES1 and *LXN* are located adjacent on the long arm of chromosome 3 at the region 3q25.32-q25.33. Despite their adjoining location, each gene is controlled by an individual promoter.

1.7.2. Latexin (LXN)

Latexin (LXN), or Tissue/Endogenous Carboxypeptidase Inhibitor (TCI/ECI), was initially discovered as a marker of neurons in the lateral neocortex of developing and adult rats (Arimatsu, 1994). The human *LXN* gene is 6.28 kb in length and codes for one 222 amino acid protein (26 kDa), which displays 84% sequence identity to the rat LXN protein (Liu et al., 2000). The adjacent location of *RARRES1* and *LXN*, and also their sequence homology, suggests the cluster emerged via gene duplication and subsequent divergence (Aagaard et al., 2005). However, the principal differences reside in the termini of the proteins, particularly in the existence of a putative N-terminal transmembrane domain in RARRES1, that is absent in LXN. In addition, both genes share high sequence homology with cysteine protease inhibitors (Aagaard et al., 2005).

The intracellular localisation of LXN in human cells is unknown, but an early study in rat mast cells indicated a cytoplasmic granular distribution that was not associated with lysosomal structures (Uratani et al., 2000). Similar to RARRES1, LXN expression has only recently been shown to be repressed by DNA methylation in medullablastoma, gastric carcinoma, melanoma and CaP (Muthusamy et al., 2006; Anderton et al., 2008; Li et al., 2011; Kloth et al., 2012).

LXN has also been identified as a quantitative trait gene responsible for negatively regulating HSC numbers in mice (Liang et al., 2007). LXN-deficient HSCs have been shown to possess an enhanced colony forming ability (Mitsunaga et al., 2011) and modulation of LXN expression in gastric carcinoma cell lines affected colony forming ability in a similar manner (Li et al., 2011). Little is known about the biological function of LXN, but it is thought to modulate SC pool size by decreasing HSC replication and increasing HSC apoptosis (Liang and Van Zant, 2008). It has been proposed that LXN regulates replication and apoptosis in SCs by inhibiting carboxypeptidase A (CPA), participating in intracellular signalling pathways or regulating protein aggregation. Various studies have shown LXN to have a role in inflammation, in the transmission of pain in mice and in protein aggregation (Aagaard et al., 2005; Jin et al., 2006; Pallares et al., 2007). It has also recently been found that LXN is involved in BMP-2-induced chondrocyte differentiation and plays an important role in skeletogenesis and skeletal regeneration (Kadouchi et al., 2009).

LXN could also function via blocking the action of proteinases, as it has been described as the only known endogenous CPA inhibitor in mammals (Normant et al., 1995). Recombinant rat LXN was first shown to inhibit proteolytic activity of CPA *in vitro* (Normant et al., 1995). The mechanism of inhibition of CPA4 by LXN is unknown at present, but the structure of LXN in complex with CPA4 has been resolved (Pallares et al., 2005) (Figure 19). This structure showed that LXN is comprised of two topologically equivalent α/β-fold subdomains, packed tightly against each other, similar to that of the cysteine protease inhibitor, cystatin C (Pallares et al., 2005). The human CPA4 protein shows the characteristic α/β-hydrolase fold of A/B

metallocarboxypeptidases (MCPs) and resembles a funnel-like structure, with the active site cleft at the bottom of this 'funnel'. In the LXN/CPA4 complex, LXN sits on top of this 'funnel rim' at the interface between its two subdomains and via only relatively few interactions.

Unbiased analysis of Affymetrix gene-expression array data from our laboratory identified classes of genes whose expression was significantly down-regulated in the SC population from both benign and malignant human CaP compared to more differentiated epithelial cells (Birnie et al., 2008). This analysis identified the homologous genes *RARRES1* and *LXN* as two of the most highly-significantly down-regulated genes in the SC compartment, whose expression increased through differentiation to CB cells.
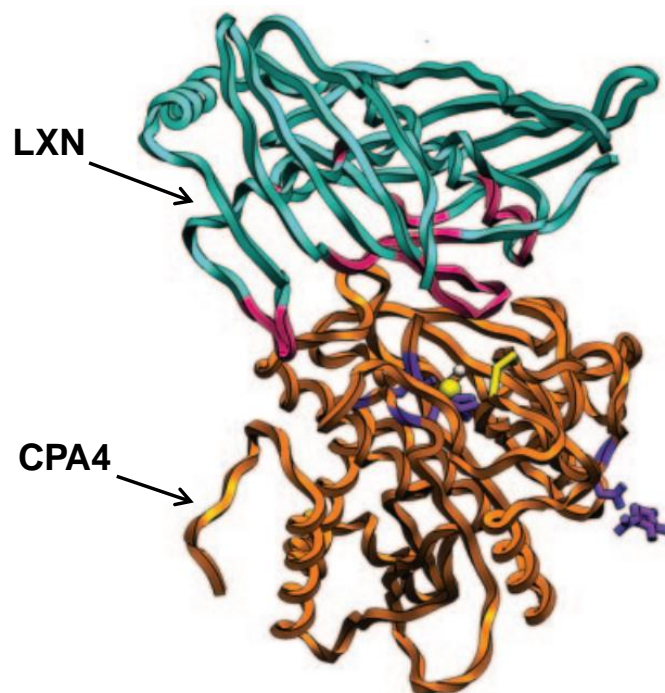
Figure 19. Structure of LXN in complex with human CPA4.
Ribbon plot of the LXN (cyan) and human CPA4 (hCPA4; orange) enzyme complex. LXN segments contacting hCPA4 are in magenta. Protein residues coordinating the catalytic zinc ion (yellow sphere) in CPA4 are violet, as is the glycosylation site (Asn148A). Modified from (Pallares et al., 2005).

1.7.3. Carboxypeptidase A4 (CPA4)

Carboxypeptidases are members of the MCP family, which hydrolyse and remove carboxy-terminal amino acids in polypeptides and proteins via catalysis, involving a tightly-bound catalytic Zn^{2+} ion (Vendrell et al., 2000). MCPs can be classified into the A/B and N/E subfamilies based on structural and sequence similarities. A/B MCPs are synthesised and secreted as inactive zymogens, possessing an additional inhibitory 90 amino acid long pro-domain at the amino-terminus, which blocks access to the active site cleft. Activation of the MCP occurs through proteolytic cleavage of the pro-domain, resulting in its release from the active site (Vendrell et al., 2000). A/B MCPs can be classified further upon the basis of their substrate specificity, with the prototypical CPA having a preference for hydrophobic amino acids. The mammalian CPA family contains six members, termed CPA1-6, all with diverse functions.

The *CPA4* gene comprises a 31.05 kb DNA sequence, containing an open reading frame encoding a 421 amino acid protein (Huang et al., 1999). The inactive zymogen pro-CPA4 (47 kDa) is cleaved into an active CPA4 protease (35 kDa) by trypsin cleavage (Tanco et al., 2010). Expression of CPA4 is apparent in a wide range of tissues, including prostate, ovary, brain, cervix and thymus; however, the level of expression in these adult tissues is extremely low. CPA4 is located at a putative CaP-aggressive locus on chromosome 7q32 (Witte et al., 2000) and a non-synonymous coding single-nucleotide polymorphism (G303C) on the CPA4 gene was found to be associated with an increased risk of aggressive disease in younger men (Ross et al., 2009). CPA4 also lies in a 120 kb gene cluster interval with CPA1, CPA2 and CPA5 (Bentley et al., 2003). The CPA family lies only 100 kb proximal to a cluster of imprinted genes *MEST*, *MESTIT1* and *COPG2IT1*, yet only the single gene, *CPA4*, is found to be imprinted in normal prostate and BPH tissue (Bentley et al., 2003; Kayashima et al., 2003).

CPA4, originally termed CPA3, was first identified as a gene up-regulated by NaBu in the androgen independent CaP cell line, PC3 (Huang et al., 1999). CPA4 induction in these cells was mediated via transactivation of p21 by NaBu. A recent publication by Tanco et al. (2010) identified that the substrate specificity of CPA4 included chromogranin A and neurotensin, which have recognised roles in CaP progression (Kadmon et al., 1991; Sehgal et al., 1994) and differentiation (Swift et al., 2010).

1.8. Prostate models

1.8.1. Prostate epithelial cell lines

Established cell lines are the traditional model for studying CaP as they confer significant advantages over other models: (1) they can be maintained for extended passages, (2) they are easily manipulated, (3) they can be adapted to culture under different conditions and (4) they are readily transfectable. A number of well characterised cell lines used in this project representing benign, malignant and metastatic models of CaP isolated from various tissues are described in Table 6.

1.8.2. Primary prostate epithelial cultures

Cell lines are an adequate model for optimising protocols, testing hypotheses and generating preliminary data, but they do not accurately represent the *in vivo* situation. In fact, the long-term culture of cells in serum-containing media can induce chromosomal changes (Lee et al., 2006; Izadpanah et al., 2008) and DNA hypermethylation often occurs during the establishment of immortal cell lines (Jones et al., 1990; Kawai et al., 1994; Jaenisch and Bird, 2003; Meissner et al., 2008). As a result of the limitations of cell line models, it is important to use primary culture models of CaP as they are a 'near to the patient' model. However, it must be noted that patient biopsies for the derivation of primary cultures can be difficult to obtain and have a limited lifespan *in vitro*. The epithelial cultures used are derived from biopsies taken with consent and ethical approval from patients undergoing radical prostatectomy, TURP or cystectomy.

Cell Line	Origin	Method of immortalisation	Reference	Increasing Malignancy
PNT1a / PNT2-C2	Normal prostate cells originating from young male organ donors	Transfection with SV40 large T antigen	(Berthon et al., 1995)	
BPH-1	TURP of a BPH tissue	Transfection with SV40 large T antigen	(Hayward et al., 1995)	
P4E6	Well-differentiated early Gleason 4 CaP tissue	Transfection with human papillomavirus-16 *E6* gene	(Maitland et al., 2001).	
RC165N/ hTERT	Primary benign tissues of African-American CaP patients	Telomerase	(Miki et al., 2007).	
Bob	TURP of CRPC tissue	Spontaneous	(Attard et al., 2009)	
Serbob	TURP of CRPC tissue	Spontaneous	(Attard et al., 2009)	
PC346C	Advanced, but not metastatic, prostate adenocarcinoma removed via TURP and subcutaneously implanted into athymic mice	Transfection with retrovirus	(Marques et al., 2006)	
LNCaP	Left supraclavicular lymph node metastasis		(Horoszewicz et al., 1980)	
VCaP	Bone metastasis		(Korenchuk et al., 2001)	
DU145	Isolated from the brain of a patient with CaP metastasis		(Stone et al., 1978)	
PC3	Bone metastasis from grade 4 prostate adenocarcinoma		(Kaighn et al., 1979)	

Table 6. Cell line models of prostate cancer.

1.8.3. *In vivo* mouse models

Following the testing of hypotheses and potential therapies using *in vitro* assays, the results must be validated on an animal model to determine efficacy *in vivo*. CaP spontaneously arises in the dog (Waters and Bostwick, 1997), but for other species genetic manipulation must be used to develop valid models for CaP. Transgenic mouse models such as TRAMP and LADY are a common way to study CaP *in vivo* (Greenberg et al., 1995; Kasper et al., 1998). An alternative possibility is the orthotopic transplantation (xenografts) of tumourigenic human CaP cells into immune-compromised mice models, such as NOD/SCID or RAG2$^{-/-}$γC$^{-/-}$ mice (Shultz et al., 1995), which are the model of choice to study CSC *in vivo*.

While mice share significant similarities to humans, there are also distinct differences. In contrast to human prostate, the murine prostate structure is much simpler and consists of a luminal-like epithelium in direct contact with BM, containing a discontinuous layer of relatively few basal cells and a less complex and sparse stroma (El-Alfy et al., 2000; Tsujimura et al., 2002). In addition, anatomically the mouse prostate comprises four paired lobes, whereas the human prostate is a single gland divided into four distinct zones (Roy-Burman et al., 2004). Although the architecture of mouse and human prostates are dissimilar, the study of the murine prostate has been of invaluable assistance in prostate SC research. In addition, mouse models provide essential information about the efficacy and toleration of potential treatments *in vivo*, but this may not be fully predictive of the response in a human.

1.9. Aims of research

There is a need for novel therapeutic strategies to tackle advanced CaP, since traditional treatments such as ADT and chemotherapy fail to kill the rare SC component of a tumour. The identification of genes that are differentially expressed between SCs and differentiated cells, in particular, classes of genes whose expression is significantly down-regulated in the SC fraction, is crucial for designing new SC-based therapies.

The two homologous genes RARRES1 and LXN have recently been identified as SC-silenced genes within the prostate epithelium (Birnie et al., 2008). The main aim of this project was to investigate the expression, regulation and function of these SC-silenced genes, and their potential interacting partner, CPA4, in prostate epithelial differentiation.

More specifically, the objectives of the study were to:

- Determine if RARRES1 and LXN were differentially expressed between SC, TA and CB cells and between BPH and CaP and elucidate the potential mechanisms of their regulation.

- Examine the expression and epigenetic regulation of their potential interacting protein CPA4 in the same cell models.

- Explore the roles of RARRES1 and LXN as potential tumour suppressor genes in CaP.

- Investigate the function of RARRES1 and LXN in SC differentiation.

Restoration of expression or function of RARRES1 and LXN within the SC population could act as a differentiation therapy, whereby the SC pool is depleted leaving the remaining differentiated cells susceptible to current therapies. Expression could be restored by exploiting the mechanism responsible for repressing their expression within the SC, or by transfecting over-expression vectors into the SC population. It is hypothesised that RARRES1 and LXN may function by binding to and inhibiting the carboxypeptidase CPA4. Therefore, if CPA4 is artificially supressed within the SC compartment, by shRNA or direct inhibitors, this would recapitulate the effect of restoration of RARRES1 and LXN expression.

By answering these questions and furthering our understanding of the regulation of RARRES1, LXN and CPA4, novel therapeutics against the SC phenotype within cancer may be found.

2. MATERIALS AND METHODS

2.1. Mammalian cell culture

2.1.1. Maintenance of mammalian cell lines

Cells were routinely passaged in T25 or T75 flasks at 37°C with 5% CO_2 and medium constituents were purchased from Invitrogen, unless otherwise stated. A commercial preparation of 0.05% (v/v) trypsin-EDTA in PBS (Invitrogen) was used to sub-culture cells, which were split 1:2-1:10 depending on the growth characteristics of individual cell lines. All cells were maintained in a humidified atmosphere at 37°C in the presence of 5% CO_2 in air. Details of cell lines used, their origin and culture conditions are shown in Table 7.

2.1.2. Isolation and maintenance of primary epithelial cultures

Patient prostate tissue was obtained from patients undergoing TURP or radical prostatectomy, with informed patient consent and approval from the York Research Ethics Committee. BPH or CaP diagnosis was confirmed by histological examination of adjacent tissue fragments. Patient tissue details can be found in Appendix 3.

Patient tissues were chopped with a scalpel, pieces retained for histology and digested with 200 U/mg collagenase (Lorne Laboratories) dissolved in 2.5 ml Keratinocyte Serum-Free Medium (KSFM with 5 ng/ml human EGF and 50 µg/ml bovine pituitary extract supplements (Invitrogen)) and 5 ml Roswell Park Memorial Institute-1640 medium (RPMI, Invitrogen), supplemented with 100 U/ml antibiotic/antimycotic solution and 2 mM L-Glutamine (Invitrogen) overnight at 37°C, with shaking at 80 RPM. The digestion was then triturated by passing through a 5 ml pipette and blunt needle and centrifuged at 2000 RPM for 10 min to sediment cells. To wash out the collagenase, two washing steps with PBS were performed: the supernatant was removed, 10 ml PBS was added, the cell pellet was re-centrifuged at 2000 RPM for 10 min and the procedure repeated. After resuspending the cell pellet in RPMI media supplemented with 10% foetal calf serum (FCS) (PAA) and 2mM L-Glutamine (**R10**), cells were centrifugally fractionated at 800 RPM for 1 min to remove stromal cells (supernatant). The pellet consisting of the acini-containing epithelial cells were treated with 5 ml 0.05% trypsin-EDTA for 30 min at 37°C with shaking at 80 RPM. Trypsin-EDTA was inactivated with R10 medium, and epithelial cells centrifuged at 1500 RPM for 3 min. Cells were routinely co-cultured on type I Collagen-coated 100 mm plates (BD Biosciences) with mouse STO fibroblast feeder cells in stem cell media (**SCM**), to maintain an undifferentiated basal population of cells. SCM is constituted of Keratinocyte Serum-Free Medium, 5 ng/ml human EGF, 50 µg/ml bovine pituitary extract, 2 ng/ml leukaemia inhibitory factor (Chemicon), 100 ng/ml cholera toxin (Sigma), 1 ng/ml granulocyte macrophage colony stimulating factor (Miltenyi Biotec), 2 ng/ml stem cell factor

(First Link UK Ltd) and 2 mM L-Glutamine. 0.05% trypsin-EDTA was used to sub-culture cells, which were split 1:2-1:6 depending on the growth characteristics of individual patient samples, to a maximum passage of 8.

2.1.3. Generation and maintenance of xenografts

Xenografts were generated by subcutaneously engraftment of patient CaP tissue into the left flank of RAG2$^{-/-}$γC$^{-/-}$ mice, supplemented with a 5α-DHT tablet (Innovative Research of America) for slow release of androgens (90 days), which was subcutaneously placed under the right flank. Once the tumour volume had exceeded a width of 15 mm, tumours were removed and a small piece was passaged on by re-engraftment into a different mouse. The remaining tissue was used in experiments, fixed in 10% formalin or snap-frozen in OCT embedding medium (Thermo Scientific), for histology or DNA extraction. This was performed by Dr. Anne Collins or Paul Berry.

2.1.4. Embedding and sectioning of snap-frozen xenograft tissue

Xenograft tissue was initially washed in PBS, placed in a plastic tissue freezing mould and covered with OCT embedding medium. The mould containing the tissue was then snap-frozen in liquid nitrogen, to form a block of frozen OCT with the tissue in the centre and placed at -80°C until required. When sections were needed, snap frozen tissue was removed from the -80°C freezer and immediately placed on a Cryostat CM1950 (Leica) cutting key at -22°C. Sections were cut at 10 µm, collected on a frost-free glass slide (Fisher Scientific) and frozen at -80°C until required. This was performed by Katy Hyde.

Cell Line	Origin	Culture media	Reference
PNT2-C2	Clone derived at York	R10	(Berthon et al., 1995)
PNT1a	Obtained with kind permission from Dr. P Berthon	R10	(Berthon et al., 1995)
BPH-1	Obtained with kind permission from Dr. Simon Hayward	RPMI, 5% (v/v) FCS, 2 mM L-Glutamine (**R5**)	(Hayward et al., 1995)
RC165N/ hTERT	Obtained with kind permission from Dr. Jun Miki	KSFM , 50µg/ml bovine pituitary extract, 5ng/ml human EGF, 2mM L-Glutamine	(Miki et al., 2007)
P4E6	Derived at York	Keratinocyte Serum-Free Medium (KSFM, Invitrogen), 2% (v/v) FCS, 2mM L-Glutamine, 5ng/ml human EGF (Invitrogen), 50µg/ml bovine pituitary extract (Invitrogen) (**K2**)	(Maitland et al., 2001)
Bob	Obtained with kind permission from Dr. David Hudson	SCM	(Attard et al., 2009)
SerBob	Obtained with kind permission from Dr. David Hudson	SCM, 10% (v/v) FCS	(Attard et al., 2009)
PC3	ECACC	Ham's F-12 medium (Lonza Laboratories), 7% (v/v) FCS, 2 mM L-Glutamine (**H7**)	
DU145	ATCC	R10	
VCaP	ATCC	R10	
LNCaP	ECACC	R10	
PC346C	Obtained with kind permission from Prof. Chris Bangma	1:1 mix of Dulbecco's Modified Eagle's Medium (DMEM) and Ham's F-12 medium, 100 µg/ml streptomycin, 100 U/ml penicillin G, 2% FCS, 0.01% (w/v) BSA (Sigma), 10 ng/ml EGF (Sigma), 1% (v/v) ITS-G (GIBCO), 0.1 nM R1881 (DuPont-New England Nuclear), 1.4 µM hydrocortisone (Sigma), 1 nM triiodothyronine (Sigma), 0.1 mM phosphoethanolamine (Sigma), 50 ng/ml cholera toxin (Sigma), 0.1 µg/ml fibronectin (Sigma), 20 µg/ml fetuin (Sigma)	(Dubbink et al., 1996)
MDA-MB-231	ATCC	DMEM, 10% (v/v) FCS, 2 mM L-Glutamine (**D10)**	
STO	ATCC	D10	

Table 7. Table listing the cell lines used, their origin and culture conditions.

2.1.5. Cryopreservation of mammalian cells

For storage in liquid nitrogen, mammalian cells were trypsinised, sedimented by centrifugation at 1500 RPM for 3 min and suspended in freezing medium at a concentration of 1-2 x 10^6 cells per ml. 1 ml aliquots of the cell suspension were aliquoted into cryovials and the vials stored at -80°C for at least 24 hours, until transfer to liquid nitrogen. After thawing, cells were diluted into 15 ml of R10 culture medium, sedimented by centrifugation and plated in either T25 flasks (cell lines) or 100 mm collagen-I coated plates (primary cultures).

2.1.6. Irradiation of fibroblasts

For inactivation by irradiation, mouse STO fibroblast cells were trypsinised at 80-90% confluency and sedimented by centrifugation at 1500 RPM for 3 min. Cells were then resuspended in 10 ml SCM per 100 cm^2 of culture surface and treated with a radiation dose of 60 Gy. Cells could be stored at 4°C for up to 5 days before use. This was routinely performed by Caty Hyde, Sandra Klein or Richard Bingham.

2.1.7. Fetal calf serum hormone depletion

2 g of Norvid A charcoal (Sigma) was added to 100 ml FCS and incubated at 4°C overnight, to remove steroid hormones and other lipid-based hormones. The mixture was centrifuged at 5000 RPM for 10 min to sediment the charcoal, and the supernatant re-centrifuged repeatedly at 5000 RPM for 10 min until the supernatant cleared. The FCS was then filtered using a 0.2 µM filter and stored at 4°C until use.

2.1.8. Determination of live cell number using a haemocytometer

To determine live cell counts, 10 µl 0.4% Trypan Blue Stain (Sigma-Aldrich) was diluted 1:1 with 10 µl cell suspension. Total cell number (blue and non-stained cells) and live cell number (non-stained cells) were then counted using a haemocytometer (Neubauer).

2.1.9. Determination of viable cell number using the Vi-Cell cell viability analyser

Cells were trypsinised and sedimented by centrifugation at 1500 RPM for 3 min. Pellets were resuspended in 500 µl PBS, placed on ice and analysed on a Vi-Cell Cell Viability Analyser (Beckman Coulter). The average number of total and viable cells was quantified from 50 images.

2.2. Primary culture enrichment

Primary prostate epithelial cultures were enriched for three subpopulations of cells at different differentiation states, based on the expression of $\alpha_2\beta_1$-integrin and CD133 as described previously (Collins et al., 2001; Richardson et al., 2004):

- An undifferentiated population of cells with SC characteristics, which expressed high levels of $\alpha_2\beta_1$-integrin and CD133 ($\alpha_2\beta_1$-integrin^{high}CD133$^+$).
- TA progeny, which expressed high levels of $\alpha_2\beta_1$-integrin, but did not express CD133 ($\alpha_2\beta_1$-integrin^{high}CD133-).
- Committed to differentiation CB cells, which expressed low levels of $\alpha_2\beta_1$-integrin and did not express CD133 ($\alpha_2\beta_1$-integrin^{low}CD133-).

The enriched subpopulations will henceforth be described as SC, TA and CB cell populations.

2.2.1. Enrichment of $\alpha_2\beta_1$-integrin expressing cells

Cultured primary prostate epithelial cultures were grown to approximately 80% confluency and harvested using 0.05% trypsin-EDTA. Type I collagen-coated 100 mm plates were blocked with 0.3% BSA (0.3% bovine serum albumin in PBS, heated denatured at 80°C for 5 min) for 1 hour at 37°C. 3 ml cell suspension was plated out onto blocked plates and incubated at 37°C for 20 min (cells from 3 x 100 mm plates were combined onto 1 blocked plate). Media was collected and the plates were rinsed 5 times with 5 ml PBS, which was also retained. The collected media and washes were spun at 1500 RPM for 5 min to pellet the cells expressing low levels of $\alpha_2\beta_1$-integrin ($\alpha_2\beta_1$-integrin^{low}; CB). The $\alpha_2\beta_1$-integrin^{high} adherent cells were harvested by incubation with 0.05% trypsin-EDTA and used for CD133 cell isolation.

2.2.2. Enrichment of CD133 expressing cells

To isolate CD133-expressing cells from established primary prostate epithelial cultures, the Direct CD133 Cell Isolation Kit (Miltenyi Biotec) was used. $\alpha_2\beta_1$-integrin^{high} cells were isolated (as described in Section 2.2.1) and up to 10^8 cells were resuspended in 300 µl magnetic-activated cell sorting (MACS) buffer (2 mM EDTA, 0.5% (v/v) FCS in PBS), 100 µL FcR blocking reagent (Miltenyi Biotec) and 100 µL CD133 beads (Miltenyi Biotec) and incubated at 4°C for 30 min. Cells were washed with 3 ml MACS buffer, centrifuged at 1500 RPM for 5 min and the cell pellet was resuspended in 500 µl MACS buffer. Magnetic cell labelling and cell separation on MACS MS columns were performed according to the manufacturer's instructions. Briefly, the MS column was equilibrated with 500 µl MACS buffer and cells bound to magnetic beads were passed through the column. Following three wash steps with 500 µl MACS buffer to collect the CD133$^-$ fraction, 1 ml MACS buffer was added to the column and the CD133$^+$ cells were eluted from the beads with a plunger. The procedure was then repeated by passing cells over a second MS column to increase purity of the CD133$^+$ population from 70-75% to 95%. The CD133$^-$ and CD133$^+$ cells were sedimented by centrifugation at 1500 RPM for 3 min, the

supernatant carefully aspirated and the cell pellets were frozen at -80°C to use for RNA and DNA extraction or resuspended in SCM and plated on 8 well BioCoat collagen-I coated chamber slides (BD Bioscience) for immunofluorescence.

2.3. Drug treatment of cells

2.3.1. Treatment of cell lines with NaBu, TSA and 5-Aza-dC

Cell lines or primary cultures were plated at a density of 5×10^4 cells per well into uncoated (cell lines) or collagen-I coated (primary cultures) 24 well plates, 24 hours prior to treatment. Cells were treated with 10 mM NaBu dissolved in PBS, or 0.6 µM TSA dissolved in dimethyl sulfoxide (DMSO) for 48 hours, or 1 µM 5-Aza-dC dissolved in DMSO for 96 hours (replacing media containing drug every 24 hours).

2.3.2. Treatment of cell lines and primary cultures with atRA

Cell lines or primary cultures were plated at a density of 5×10^4 cells per well into uncoated (cell lines) or collagen-I coated (primary cultures) 24 well plates, 24 hours prior to treatment. Cells were treated with 10 nM - 1 µM atRA dissolved in DMSO for 24 - 96 hours. Cell lines were grown in charcoal-stripped medium for 24 hours prior to treatment. Medium containing atRA was left on cell lines for the duration of the assay, but the medium on primary cultures was changed after 48 hours.

2.4. Luciferase assay

Primary cultures were plated at a density of 1×10^4 into collagen-I coated 96 well plates, with 10 µl STO feeder cells, 24 hours prior to treatment. Cells were transfected with the Cignal RARE reporter (luc) kit (SABiosciences), which contained a luciferase reporter plasmid, with active regulatory elements composed of a TATA box element and a tandem array of RAREs. Cells were transfected using the TransIT-2020 transfection reagent (Invitrogen) (see Section 2.5.3.3). Cells were also transfected with a non-inducible firefly luciferase reporter as a negative control and a constitutively expressing GFP construct, pre-mixed with a constitutively expressing firefly luciferase construct, as a positive control. 24 hours after transfection with the plasmid, cells were treated with 250 nM – 1 µM atRA (see Section 2.3.2) or a DMSO control. After a further 24 hours, luciferase expression was measured using the Dual-Glo system (Promega) following the manufacturer's protocol. Briefly, Stop & Glo substrate was diluted 1:100 (v/v) into Stop & Glo buffer to create Stop & Glo reagent. To lyse cells, 100 µl lysis buffer containing luciferase substrate was added to cells grown in 100 µl cell medium in a 1:1 ratio (v/v) in 96 well plates, mixed by pipetting and incubated for 10 min at RT. Firefly luciferase activity was measured on a

Polarstar Optima micro-plate reader (BMG). To quench firefly luciferase activity and provide a substrate for Renilla luciferase, 100 µl Stop & Glo reagent was then immediately added to the wells (1:1 (v/v) with initial culture medium volume), mixed by pipetting, and Renilla luciferase activity was measured after 10 min. Renilla luciferase acts as an internal control for monitoring transfection efficiencies and monitoring cell viability.

2.5. Transfection of mammalian cells

2.5.1. Transfection of cell lines with siRNA

DharmaFECT 2 transfection reagent (Dharmacon) was used to transfect cell lines with Silencer Select scrambled, RARRES1 or LXN siRNA (Applied Biosystems). PNT1a and PC3 cells were plated at a density of 0.5-2 x 10^5 cells per well into 24 well (RNA, cell motility assay) or 6 well (protein) plates 24 hours prior to transfection. A 50 µM working stock siRNA solution was prepared in RNase-free ddH$_2$O. In separate tubes siRNA (tube 1) and DharmaFECT 2 (tube 2) were diluted into OptiMEM reduced serum medium (Fisher Scientific Ltd) in a polystyrene tube according to Table 8, gently pipetted to mix and incubated at RT for 5 min.

	Tube 1		Tube 2		Medium (µl)	Total medium (µl)
	5 µM siRNA (µl)	optiMEM (µl)	DharmaFECT (µl)	optiMEM (µl)		
24 well	1	49	1	49	400	500
6 well	4	196	4	196	1600	2000

Table 8. The amounts of siRNA and transfection reagent used to transfect cell lines.

Tubes 1 and 2 were combined, gently mixed by pipetting and incubated at RT for 20 min to allow siRNA-liposomal complex formation. R10 (PNT1a) or H7 (PC3) culture medium was then added to complete the transfection mix. Medium was removed from cells, washed once with PBS and the siRNA transfection medium added to each well. The siRNA final concentration was 10 nM and the specific siRNAs used were Silencer Select (Applied Biosystems) siRNAs targeting RARRES1 (siRNA ID:s11812), LXN (siRNA ID: s230651) or Negative control #1. Cells were harvested at 24, 48 and 72 hours for RNA extraction or at 48, 72 and 96 hours for protein extraction.

2.5.2. Transfection of primary cells with siRNA

Oligofectamine transfection reagent (Invitrogen) was used to transfect primary cultures with scrambled siRNA, RARRES1 siRNA or LXN siRNA. Cells were plated at a density of 5×10^4 - 1.5×10^6 cells per well into 24 well (RNA), 6 well (protein) or 10 cm (invasion assay or colony forming assays) plates, 24 hours prior to transfection. A 20 µM working stock siRNA solution was prepared in RNase-free ddH$_2$O. In separate tubes, siRNA (tube 1) and Oligofectamine (tube 2) were diluted into OptiMEM reduced serum medium in a polystyrene tube, according to Table 9, gently pipetted to mix and incubated at RT for 10 min.

	Number of cells	Tube 1		Tube 2		OptiMEM Medium (µl)	SiRNA/ Oligofect amine mix (µl)	SCM Medium (µl)
		5 µM siRNA (µl)	optiMEM (µl)	Oligofect amine (µl)	optiMEM (µl)			
24 well	5×10^4	1.25	62.5	0.5	49	44	81	500
6 well	2×10^5	5	250	2	68	175	325	2000
10 cm dish	1.5×10^6	40	2000	16	544	1400	2600	5000

Table 9. The amounts of siRNA and transfection reagent used to transfect primary cultures.

Tubes 1 and 2 were combined, gently mixed by pipetting and incubated at RT for 25 min to allow siRNA-liposomal complex formation. OptiMEM medium was initially added to cells, followed by the siRNA/oligofectamine mix and cells were incubated at 37°C in 5% CO$_2$ for 4 hours. SCM was then added to cells and the plates incubated for a further 4 h. Medium was removed from cells, washed once with PBS and fresh SCM was added to cells. Cells were incubated and then harvested at 24, 48 and 72 hours for RNA extraction, or at 48, 72 and 96 hours for protein extraction. Fresh SCM was added every two days. The siRNAs used were as described in Section 2.5.1, but the final concentration was 50 nM.

2.5.3. Transfection with cDNA expression vectors

2.5.3.1. Bacterial transformation with plasmid DNA

Aliquots of DH5α or Top10 chemically competent *E. coli* cells (Fisher Scientific Limited) were thawed on ice for 30 min before transformation. 1-5 ng pReceiver-M45 (RARRES1), pEZ-M06 (LXN) and pReceiver-M06 (control vector with eGFP) cDNA expression plasmid DNA (GeneCopoeia) was added to each vial and left on ice for 30 min. Cells were heat-shocked for 30 seconds at 42°C without shaking, and then placed on ice for 2 min, followed by the addition of 250 µl of RT super optimal broth (SOC) medium (Invitrogen). Vials were incubated at 37°C for 1 hour in a shaking incubator. Cells were plated in lysogeny broth (LB) agar plates (1% (w/v) tryptone, 0.5% (w/v) yeast extract, 1% (w/v) NaCl, 1.5% (w/v) agar) containing 30 µg/ml Kanamycin and incubated for 24 hours at 37°C, before colony screening. This was performed by Hannah Walker.

2.5.3.2. Bacterial cultures, plasmid isolation and purification

A single colony from a freshly streaked selective plate inoculated a starter culture of 5 ml LB medium (1% (w/v) tryptone, 0.5% (w/v) yeast extract, 1% (w/v) NaCl, pH 7.0) containing 30 µg/ml Kanamycin and was incubated for 8 hours at 37°C, with vigorous shaking (300 RPM). The starter culture was diluted 1:500 to 1:1000 (v/v) into selective LB liquid media, in a flask with a volume of at least four times the volume of the culture, and cultures were grown at 37°C overnight with vigorous shaking (300 RPM). To harvest the bacterial cells, cultures were centrifuged at 2900 RPM for 10 min using a Heraeus Megafuge 1.0R centrifuge (Thermo Scientific) and supernatant discarded. The EndoFree Maxi kit (Qiagen) was used to generate Endofree plasmid DNA according to manufacturer's instruction.

Briefly, cell pellets were resuspended using 10 ml Buffer P1 (50 mM Tris-Cl pH 8.0, 10 mM EDTA, 100 µg/ml RNase A). 10 ml Buffer P2 (200 nM NaOH, 1% SDS (w/v)) was added to the mixture, mixed thoroughly by vigorously inverting the tube five times and left at RT for 5 min. Cold Buffer P3 (3 M potassium acetate, pH 5.5) was added and immediately mixed by vigorously inverting the tube five times, until a clear phase and a precipitate could be visible. The lysate was poured into the barrel of a QIAfilter cartridge and incubated at RT for 10 min. After the lysate was passed through the column using a plunger, 2.5 ml Buffer ER was added to the filtered lysate, the tube was inverted 10 times and incubated on ice for 30 min. A QIAGEN-tip 500 was equilibrated with 10 ml Buffer QBT (750 mM NaCl, 50 mM MOPS, pH 7.0, 15% isopropanol (v/v), 0.15% Triton X-100 (v/v)), the filtered supernatant was applied to the QIAGEN-tip to promote plasmid binding to the resin and washed twice with 30 ml Buffer QC (1.0 M NaCl, 50 mM MOPS pH 7.0, 15% isopropanol (v/v), 0.15% Triton X-100 (v/v)). Plasmid DNA was eluted using 15 ml QN buffer (1.6 M NaCl, 50 mM MOS pH 7.0, 15% isopropanol (v/v)), precipitated by adding 0.7 volumes (10.5 ml) of isopropanol and centrifuged at 14,000 RPM for

30 min at 4°C, using a Heraeus Multifuge X1R centrifuge (Thermo Scientific). The DNA pellet was washed with endotoxin-free 70% ethanol (v/v) at RT, re-centrifuged, supernatant removed and the DNA pellet air-dried for 10 min and then resuspended in ddH$_2$O. The plasmid DNA was diluted down to 1000 ng/µl for use to transfect into mammalian cells. This was performed by Hannah Walker.

2.5.3.3. Transfection of cell lines with plasmid DNA

TransIT-2020 transfection reagent was used to transfect cell lines with pReceiver-M45 (RARRES1), pEZ-M06 (LXN) and pReceiver-M06 (control vector with eGFP) cDNA expression plasmid DNA. 0.1-2 x 10^5 cells per ml were plated in 24 well plates (RNA), 6 well plates (protein) or 8 well chamber slides (immunofluorescence) 24 hours prior to transfection so cells were at least 50% confluent at transfection. TransIT-2020 reagent was warmed to RT and vortexed gently before use. For each well to be transfected (details of volumes for each plate are described in Table 10), 100-2500 ng plasmid DNA was diluted into OptiMEM reduced serum medium in a polystyrene tube, and gently pipetted to mix. TransIT-2020 reagent was then added to the tube, and the mixture gently pipetted to mix. The DNA-reagent mix was incubated at RT for 30 min to allow complexes to form and then transferred into culture wells containing R10 (for PNT1a and LNCaP cells) or H7 (for PC3 cells) culture medium, drop-wise to different areas of the well. Culture plates or slides were rocked to evenly distribute the DNA-reagent complexes, and incubated for 6 hours at 37°C. After 6 hours, the culture medium containing the DNA-reagent complexes was removed, cells were rinsed with PBS and fresh culture medium was added to stop any cytotoxic effects from the reagent. Cells were then incubated for a further 18-90 hours before results were analysed.

	Cell suspension (µl)	Opti-MEM medium (µl)	1 µg/µl DNA stock (µl)	TransIT-2020 reagent (µl)	Culture medium (µl)
8 well chamber slide	100	9	0.1	0.3	92
24 well plate	500	50	0.5	1.5	50
6 well plate	2500	250	2.5	7.5	250

Table 10. The amounts of plasmid DNA and transfection reagent used to transfect cell lines.

2.6. Isolation and analysis of mammalian cell RNA

2.6.1. RNA Extraction

RNA was extracted from cells using the RNeasy Mini Kit (QIAGEN). Up to 5×10^6 cells were washed once in PBS and incubated with 0.05% trypsin-EDTA at 37°C. Trypsin was blocked with R10 medium, centrifuged at 1500 RPM for 3 min and the supernatant aspirated. Pelleted cells were resuspended in 350 µl Buffer RLT containing 3.5 µl β-mercaptoethanol and vortexed to mix. The cell lysate was pipetted into a QIAshredder homogeniser column (QIAGEN) and centrifuged at 13,000 RPM for 2 min. 350 µl 70% ethanol diluted in DEPC-treated water was added to the homogenised lysate and mixed well by pipetting. The sample was transferred to an RNeasy spin column and centrifuged at 13,000 RPM for 15 seconds. The column was washed with 700 µl Buffer RW1 and spun at 13,000 RPM for 15 seconds, followed by washing with 500 µl Buffer RPE. The column was further washed with 500 µl Buffer RPE and spun at 13,000 RPM for 2 min, and then spun at 13,000 RPM for 1 min with a new 2 ml collection tube to remove any residual ethanol from the column. The flow-through was discarded after every wash step. RNA was eluted with 30 µl RNase-free water after centrifugation at 13,000 RPM for 1 min. RNA concentration and quality checks were performed using a NanoDrop ND-1000 spectrophotometer (Thermo Scientific). RNA samples were routinely stored at -80°C.

2.6.2. cDNA Synthesis

Total RNA (50 ng / 500 ng) was reversed transcribed in a total volume of 14.25 µl, mixed with 0.75 µl ddH$_2$0 and 0.75 µl Random primers (Invitrogen) and heated to 70°C for 10 min. 14.25 µl reaction mix consisting of 6 µl 5 x First strand buffer (Invitrogen), 3 µl 0.1 M DTT (Invitrogen), 3 µl 10 mM dNTPs (Invitrogen), 0.75 µl ddH$_2$O, 1.5 µl Superscript III enzyme (Invitrogen) was added and incubated at 45°C for 2 hours. Complementary DNA (cDNA) was purified by ethanol (EtOH) precipitation, with the addition of 15 µl 3 M NaCl and 120 µl 100% EtOH and samples placed at -80°C for 30 min. Samples were centrifuged at 13,000 RPM for 10 min in a benchtop centrifuge and supernatant removed. The pelleted cDNA was washed in 100 µl 70% EtOH and re-centrifuged at 13,000 RPM for 5 min. The supernatant was removed, the pellet was dried using a Eppendorf Concentrator 5301 (Eppendorf) at 30°C for 5 min and resuspended in 30 µl DEPC-treated ddH$_2$O.

cDNA was purified using the QIAquickPCR Purification Kit (QIAGEN), as described in the QIAquick spin handbook. Briefly, 150 µl Buffer PB was added to the PCR sample, mixed by pipetting, transferred in the Spin Column and spun at 13,000 RPM for 1 min. Flow-through was discarded and the sample washed with 750 µl Buffer PE and re-spun at 13,000 RPM for 1 min. Flow-through was again discarded and the tube re-spun for 1 min to remove any residual EtOH. 30 µl ddH$_2$O was added to the column, incubated for 1 min at RT and then centrifuged at 13,000 RPM for 1 min to elute the purified cDNA. cDNA concentration and quality checks were

Materials and Methods

performed using a NanoDrop spectrophotometer and cDNA samples were routinely stored at -20°C.

2.6.3. Quantitative reverse-transcriptase PCR (qRT-PCR)

Quantitative reverse-transcriptase PCR (qRT-PCR) was performed in 10 μl reactions constituted of 5 μl Taqman Gene Expression Master Mix (Applied Biosystems) or SsoFast Probes Supermix (Bio-Rad), 0.5 μl TaqMan gene expression assays (Applied Biosystems) and 4.5 μl cDNA (30 ng) diluted in ddH$_2$0. All reactions were run in triplicate wells on MicroAmp Optical (Applied Biosystems) or FrameStar white-tubed (4titude) 96 well plates. Primers used were TaqMan gene expression assays (Table 11).

Gene	TaqMan Primer	Gene	TaqMan Primer
RARRES1	Hs00161204_m1	γ-actin	Hs03044422_g1
LXN	Hs00220138_m1	EEF1A1	Hs00265885_g1
CPA4	Hs00275311_m1	TPT1	Hs02621289_g1
RPLPO	Hs99999902_m1	YWHAZ	Hs03044281_g1
GAPDH	Hs99999905_m1	PPIA	Hs99999904_m1
18S	Hs03003631_g1	HPRT1	Hs99999909_m1
HUWE1	Hs00948075_m1	β-2M	Hs99999907_m1
β-actin	Hs99999903_m1		

Table 11. Primers used for TaqMan qRT-PCR analysis.

Reactions were run on an ABI Prism 7000 Sequence Detection System and analysed using the 7000 System SDS Software (Applied Biosystems), or on a CFX96 Real-Time PCR Detection System and analysed using the Bio-Rad CFX Manager 2.0 (Bio-Rad) and Microsoft Excel. Standard thermal cycling conditions included a hot start of 10 min at 95°C followed by 40 cycles of 95°C for 15 seconds and 60°C for 1 min (ABI Prism 7000) or 2 min at 95°C followed by 40 cycles of 95°C for 5 seconds and 60°C for 5 seconds (Bio-Rad CFX96). Analyses were carried out using the delta-delta C_T method (Schmittgen and Livak, 2008) for relative quantification and expression levels standardised to GAPDH, RPLPO or 18S.

2.6.4. Standard curve qRT-PCR for absolute quantification

qRT-PCR was performed as described in Section 2.6.3. Reactions were run on a CFX96 Real-Time PCR Detection System, and analysed using the Bio-Rad CFX Manager 2.0. A best-fit standard curve of RARRES1 and LXN expression was constructed using 10-fold serial dilutions of cDNA expression plasmids, in triplicate (RARRES1: EX-Z1865-M45; LXN: EX-V0043-M06). The standard curve was graphically represented as a semi-log regression line plot of C_T value

vs. log of input nucleic acid. Expression levels in unknown samples was interpolated from the equation of the standard curve and normalised to a calibrator sample, set at 1.

2.7. Analysis of DNA methylation by pyrosequencing

2.7.1. Identification of CpG islands

Regions of genomic sequence spanning 10,000 bp downstream and 3000 bp upstream of the RARRES1 and LXN transcription start sites were analysed for regions that were rich in CG dinucleotides (CpG islands), using the EMBOSS CpGPlot software. The presence and location of CpG islands fitting specific criteria within each gene and their promoters was determined:

- the observed-to-expected CpG ratio was greater than 0.6.
- the percentage of CG dinucleotides was greater than 50%.
- the CpG island was greater than 50 bp in length.

The Ensembl database was utilised to determine if the CpG islands contained any known SNPs.

2.7.2. Isolation of mammalian cell genomic DNA from cells and tissues

Genomic DNA (gDNA) was extracted from cell cultures using the DNeasy Blood and Tissue Kit (Qiagen). Briefly, up to 5×10^6 cells were washed once in PBS and incubated with 0.05% (v/v) trypsin-EDTA at 37°C. Trypsin was blocked with R10 medium, centrifuged at 1500 RPM for 3 min and the supernatant aspirated. Pelleted cells were resuspended in 200 µl PBS containing 20 µl proteinase K and 4 µl RNase A (100 mg/ml), vortexed to mix and incubated for 2 min at RT. 200 µl Buffer AL was added to the cell suspension, mixed thoroughly by vortexing and incubated at 56°C for 10 min to lyse the cells. 200 µl EtOH was added to the tube and vortexed to mix. The cell lysate was pipetted into a DNeasy mini spin column and centrifuged at 8000 RPM for 1 min. The flow-through was discarded and the column placed into a new collection tube, 500 µl Buffer AW1 was added and the tube centrifuged at 8000 RPM for 1 min. The flow-through was discarded and the column placed into another collection tube. 500 µl Buffer AW2 was added and the tube centrifuged at 13,000 RPM for 3 min to remove any residual ethanol from the column. gDNA was eluted with 200 µl buffer EB, after centrifugation at 8000 RPM for 1 min.

gDNA was extracted from primary prostate tissues using the same DNeasy Blood and Tissue Kit, but with a different protocol by Dr. Davide Pellacani. Briefly, up to 20 mg of tissue was cut into small pieces and incubated with 180 µl Buffer ATL and 20 µl proteinase K, mixed thoroughly by vortexing and incubated at 56°C until the tissue was completely lysed after 2 hours. After vortexing for 15 seconds, 200 µl Buffer AL was added and the sample was re-vortexed. 200 µl absolute EtOH was added, vortexed to mix and the sample was pipetted into a

DNeasy mini spin column and centrifuged at 8000 RPM for 1 min. The flow-through was discarded and the column placed into a new collection tube, 500 µl Buffer AW1 was added and the tube centrifuged at 8000 RPM for 1 min. The flow-through was discarded and the column placed into another collection tube, 500 µl Buffer AW2 was added and the tube centrifuged at 13,000 RPM for 3 min to dry the DNeasy membrane. gDNA was eluted with 200 µl Buffer AE, after centrifugation at 8000 RPM for 1 min.

gDNA was extracted from SC samples and snap frozen xenograft tissue sections using the QIAamp DNA micro kit (Qiagen) according to the manufacturer's instruction, due to the low cell number. Briefly, 100 µl ATL buffer was added to the cell pellet, supplemented with 10 µl Proteinase K and 100 µl Buffer AL and mixed by pulse-vortexing for 15 seconds. 1 µl carrier RNA was added and the lysate incubated at 56°C for 10 min shaking. 50 µl absolute EtOH was added, mixed by pulse-vortexing for 15 seconds and incubated for 3 min at RT. The lysate was transferred to a QIAamp MinElute Column and centrifuged at 8000 RPM for 1 min. 500 µl buffer AW1 was added to the column, centrifuged, 500 µl Buffer AW2 was added and re-centrifuged. After each spin, the flow-through was discarded and a new collection tube used. To dry the membrane, the column was spun at 14,000 RPM for 3 min, 20 µl Buffer AE was added to the membrane, incubated at RT for 5 min and spun at 14,000 RPM for 1 min to elute the gDNA. This step was repeated so the DNA was eluted in 40 µl buffer AE. DNA concentration and quality checks were performed using a Nanodrop spectrophotometer and DNA samples were routinely stored at -20°C.

2.7.3. Bisulphite conversion of gDNA

To allow determination of the methylation status of gDNA, unmethylated cytosines were bisulphite converted to uracil using the EpiTect Bisulphite Kit (Qiagen). Briefly, 85 µl bisulphite mix (containing sodium bisulphite) and 35 µl DNA protect buffer were added to 20 µl, of up to 1 µg, DNA (diluted in RNase-free water). The tubes were inverted several times to mix and samples were placed in the thermal block cycler GeneAmp PCR system 9700 (Applied Biosystems), using the following thermal profile: 99°C for 5 min, 60°C for 25 min, 99°C for 5 min, 60°C for 85 min, 99°C for 5 min, 60°C for 175 min and samples were left at RT indefinitely.

After conversion, 560 µl buffer BL was added to the reaction, the tubes were vortexed to mix and briefly centrifuged. The mixture was transferred to an EpiTect spin column, centrifuged at 13000 RPM for 1 min and 500 µl buffer BW wash buffer was added, followed by re-centrifugation. 500 µl buffer BD desulfonation buffer was then added and after incubation for 15 min at RT, the column was centrifuged. The column was washed twice with 500 µl buffer BW and centrifuged at 13000 RPM for 1 min. The flow through was discarded after every centrifugation step. The column was placed in a new collection tube and centrifuged at 13,000 RPM for 1 min to remove any residual liquid. The DNA was eluted from the column with 20 µl elution buffer EB and centrifuged at 13,000 RPM for 1 min. This step was repeated to increase

the yield of DNA. The concentration and quality checks of bisulphite converted DNA were performed using a Nanodrop spectrophotometer and DNA samples were routinely stored at -20°C.

2.7.4. PCR amplification for pyrosequencing

RARRES1 and LXN were amplified by PCR, using specific primers (see Appendix 2) spanning their CpG islands and Platinum Taq DNA Polymerase (Invitrogen). These primers were designed specific for bisulphite-converted gDNA using the PyroMark Assay Design Software (Qiagen), were HPLC-purified and biotinylated at the 5'-end of the reverse primer.

2.7.4.1. RARRES1 PCR amplification

Briefly, bisulphite converted template DNA (10 ng) was mixed with 0.625 µl of 50 mM magnesium chloride ($MgCl_2$; 1.25mM), 0.5 µl of 10 µM specific primers (200 nM), 0.5 µl of 10 mM dNTPs (200 µM), 2.5 µl of 10 X PCR buffer and 0.1 µl Platinum Taq enzyme mix (0.5 U/reaction) in a total volume of 25 µl. Samples were placed in the thermal block cycler GeneAmp PCR system 9700 (Applied Biosystems) using the following thermal profile: 1 cycle at 94°C for 5 min, 45 cycles of 30 seconds at 94°C, 30 seconds at 55°C and 30 seconds at 72°C and a final elongation step of 5 min at 72°C.

2.7.4.2. LXN nested PCR amplification

As optimisation of a single PCR assay failed to produce high quality PCR products for pyrosequencing, a nested PCR approach was used. For the first PCR reaction, LXN was amplified using specific primers (see Appendix 2) and Platinum Taq Polymerase. Briefly, bisulphite converted template DNA (20 ng) was mixed with 0.5 µl of 50 mM $MgCl_2$ (1 mM), 0.5 µl of 10 µM specific primers (200 nM), 0.5 µl of 10 mM dNTPs (200 µM), 2.5 µl of 10 X PCR buffer and 0.1 µl Platinum Taq enzyme mix (0.5 U/reaction), in a total volume of 25 µl. Samples were placed in the thermal block cycler GeneAmp PCR system 9700 (Applied Biosystems), using the following thermal profile: 1 cycle at 94°C for 5 min, 35 cycles of 30 seconds at 94°C, 30 seconds at 55°C and 30 seconds at 72°C and a final elongation step of 5 min at 72°C. The LXN DNA product was purified from the reaction mixture using the QIAquickPCR Purification Kit, as described in the QIAquick spin handbook. Briefly, 150 µl Buffer PB was added to the PCR sample, mixed by pipetting and spun at 13,000 RPM for 1 min. Flow-through was discarded and the sample washed with 750 µl Buffer PE and re-spun at 13,000 RPM for 1 min. Flow-through was again discarded and the tube re-spun for 1 min, to remove any residual ethanol. 30 µl ddH$_2$O was added to the column, incubated for 1 min at RT and then centrifuged at 13,000 RPM for 1 min to elute the purified DNA. DNA concentration and quality checks were performed using a Nanodrop spectrophotometer. For the second PCR reaction, the pyrosequencing primers (which bound within the product from PCR 1), described in Appendix 2,

were used. Briefly, bisulphite converted template DNA (10 ng) was mixed with 0.875 µl of 50 mM $MgCl_2$ (1.75 mM), 0.5 µl of 10 µM specific primers (200 nM), 0.5 µl of 10 mM dNTPs (200 µM), 2.5 µl of 10 X PCR buffer and 0.1 µl Platinum Taq enzyme mix (0.5 U/reaction), in a total volume of 25 µl. Samples were placed in the thermal block cycler GeneAmp PCR system 9700 (Applied Biosystems), using the following thermal profile: 1 cycle at 94°C for 5 min, 45 cycles of 30 seconds at 94°C, 30 seconds at 55°C and 30 seconds at 72°C and a final elongation step of 5 min at 72°C

2.7.4.3. GSTP1 PCR amplification

Briefly, bisulphite converted template DNA (10 ng) was mixed with 0.75 µl of 50 mM $MgCl_2$ (1.5mM), 0.5 µl of 10 µM specific primers (200 nM), 0.5 µl of 10 mM dNTPs (200 µM), 2.5 µl of 10 X PCR buffer and 0.1 µl Platinum Taq enzyme mix (0.5 U/reaction) in a total volume of 25 µl. Samples were placed in the gradient thermal cycler TC-5120 (Techne) using the following thermal profile: 1 cycle at 94°C for 5 min, 45 cycles of 30 seconds at 94°C, 30 seconds at 55°C and 40 seconds at 72°C and a final elongation step of 5 min at 72°C.

2.7.5. Agarose gel electrophoresis

In order to confirm the quality of the PCR products and specificity of the amplification, each product was run on 2% (w/v) TAE agarose gel using GelRed nucleic acid stain (1:10,000 (v/v); Biotium), to visualise. 2 µl PCR product, 3 µl ddH_2O and 1 µl DNA loading dye (4 mg Ficolt 400, 0.1 M EDTA, 0.1% (w/v) SDS, 0.05% (w/v) bromophenol blue and 0.05% (w/v) xylene cyanol) were mixed and loaded onto the gel run in TAE buffer (0.04 M Tris-acetate, 0.001 M EDTA, pH 8.0), for a minimum of 1 hour at 80 V. 100 bp MW DNA ladders (Invitrogen) were run in adjacent lanes for sizing. Gels were visualised using the GeneSnap ID software (Syngene).

2.7.6. Pyrosequencing analysis

To analyse methylation status, the DNA products were analysed on a Pyromark Q24 Pyrosequencer (Qiagen), according to the manufacturer's protocol. Briefly, a mixture of 50 µl streptavidin-coated Sepharose beads, 1 ml PyroMark binding buffer and 450 µl ddH_2O was prepared and mixed to form a homogenous solution. 60 µl sepharose bead mix was added to 20 µl PCR product in each well of a 24 well plate, to bind and immobilise the biotinylated PCR amplicons and the plate was agitated on an Orbis Microplate shaker (Mikura) at 1400 RPM, for at least 10 min. Template DNA-sepharose bead complexes were isolated from all wells, in parallel, using the PyroMark Q24 vacuum workstation, whereby a vacuum was applied which held the beads on probes. The probes were then dipped into 70% EtOH, Pyromark denaturation solution to separate the complementary strand from the biotinylated strand, and PyroMark washing buffer to wash and neutralise the immobilised biotinylated single-stranded DNA (ssDNA). The vacuum was then removed and the ssDNA released from the probes into a

PyroMark Q24 plate containing 0.3 µM sequencing primer (specific for the CpG island of interest), diluted in PyroMark annealing buffer to enhance hybridisation of the sequencing primer. The plate containing ssDNA-sequencing primer mix was heated to 80°C for 5 min, left to cool to RT and then analysed on the pyrosequencer. Nucleotide incorporation into the sequence generated light in a luciferase-catalysed reaction, proportional to the number of nucleotides incorporated, which produced a peak on a pyrogram. The nucleotide sequence was then determined from the signal peaks in the pyrogram trace and the percentage methylation at each CpG site plotted on a bar chart. Tost and Gut (2007) detailed additional information on DNA methylation analysis by pyrosequencing.

2.8. Chromatin Immunoprecipitation (ChIP)

2.8.1. Chromatin preparation

10^7 - 10^8 cells were trypsinised, sedimented and resuspended in 5 ml R10 (PNT2-C2 and LNCaP) or H7 (PC3) culture medium. Cells were fixed with 1% formaldehyde for 10 min at RT. 0.125 M glycine was added to stop fixation for 5 min at RT and cells were centrifuged at 1000 RPM for 5 min at 4°C. Cells were washed twice with 20 ml cold PBS and re-centrifuged for 3 min. Pellets were resuspended in cold swelling buffer (5 mM PIPES pH 8, 85 mM KCl) supplemented with NP-40 (final concentration of 0.2% (v/v)) and complete EDTA-free protease inhibitor cocktail (PIC; Roche). The cell suspension was incubated on ice with gentle shaking for 20 min. The suspension was centrifuged at 1500 RPM for 10 min at 4°C and resuspended in IP buffer TSE 150 (0.1% (w/v) SDS, 1% (v/v) Triton X-100, 2 mM EDTA, 20 mM Tris-HCl pH 8, 150 mM NaCl), supplemented with a PIC. The chromatin was sonicated using a Sonopuls HD 2070 ultrasonic homogeniser (Bandelin), for 20 cycles of 30 seconds on / 40 seconds off at maximum power. Chromatin was centrifuged at 14000 RPM for 30 min at 4°C, aliquoted and routinely stored at -80°C.

2.8.2. Sonication control DNA extraction

A sample of the sonicated chromatin was purified using a phenol/chloroform extraction to corroborate correct chromatin disruption by sonication. 20 µl of the sonicated chromatin was added to 230 µl TE / 1% SDS buffer (10 mM Tris pH 8, 1 mM EDTA, 1% (w/v) SDS) and incubated at 65°C overnight, rocking. 250 µl TE buffer (10 mM Tris pH 8, 1 mM EDTA) was added to the sonication control, supplemented with 10 µg glycogen (Roche) and 100 µg proteinase K (Invitrogen) and incubated for 2 hours at 37°C. 44 µl lithium chloride (5 M LiCl) was added and a phenol/chloroform extraction performed. Briefly, 500 µl phenol/chloroform solution was added, vortexed to mix and centrifuged at 15000 RPM for 15 min at RT. The upper phase was transferred to a new tube, 1 ml EtOH (100%) was added, tubes were inverted five times and incubated at -20°C overnight. The tubes were centrifuged at 14,000 RPM for 15 min

at 4°C, pellet was rinsed in 1 ml EtOH (70%) and re-centrifuged. The supernatant was removed and the DNA pellet dried for 20 min at 45°C in an Eppendorf Concentrator 5301. The pellet was resuspended in 100 µl TE buffer, concentration and quality verified using a NanoDrop spectrophotometer and run on a 0.75% (w/v) TAE agarose gel using GelRed nucleic acid stain (1:10,000 (v/v) dilution) to visualise. 5 µl PCR product, 7.5 µl ddH$_2$O and 2.5 µl DNA loading dye were mixed and loaded onto the gel run in TAE buffer, for a minimum of 1 hour at 80 V. 100 bp and 1 kB MW DNA ladders (Invitrogen) were run in adjacent lanes for sizing. Gels were visualised using the GeneSnap ID software.

2.8.3. Immunoprecipitation

Protein A-sepharose beads (Sigma) were blocked by incubating them in an IP buffer TSE 150 solution, containing yeast tRNA (Sigma; initially denatured at 95°C for 5 min), to a final concentration of 1 µg/ml and BSA (Sigma), to a final concentration of 250 µg/ml, while rotating at 4°C for 4 hours. Beads were centrifuged at 3000 RPM for 1 min, rinsed three times with IP buffer TSE 150 and stored at 4°C.

Chromatin was cleaned up by incubating 50 µl of 50% pre-blocked protein A-sepharose beads with 20 µg (per immunoprecipitation) of chromatin in a total volume of 1 ml IP buffer TSE 150, supplemented with a PIC for 1.5 hours at 4°C while rotating. The suspension was centrifuged for 1 min at 3000 RPM and supernatant kept in a separate tube. 20 µl of the supernatant was retained, to be used as INPUT control, then the rest was divided and incubated with primary antibody (Table 12) at 4°C overnight, shaking.

Primary antibody	Species	Isotype	Conc. (mg/ml)	Origin	Working dilution
Histone 3	Rabbit	IgG	1	Abcam	1:100
H3K4me2	Rabbit	IgG	1	Millipore	1:100
H3K27me3	Rabbit	IgG	-	Millipore	1:100
IgG control	Rabbit	IgG	1	Millipore	1:100

Table 12. Description of primary antibodies used for chromatin immunoprecipitation.

2.8.4. Recovery of the immunoprecipitated complexes

Antibody-protein-DNA complexes were recovered by incubation with 50 µl of 50% pre-blocked protein A sepharose beads for 1.5 hours at 4°C. Beads were sedimented by centrifugation at 3000 RPM for 1 min at RT and washed once with 1 ml IP buffer TSE 150, IP buffer TSE 500 (0.1% (w/v) SDS, 1% (v/v) Triton X-100, 2 mM EDTA, 20 mM Tris-HCl pH 8 and 500 mM NaCl),

washing buffer (10 mM Tris-HCl pH 8, 0.25 M LiCl, 0.5% (v/v) NP-40) and twice with 1 ml TE buffer. DNA was eluted by adding 100 µl of elution buffer (1% (w/v) SDS, 10 mM EDTA, 50 mM Tris-HCl pH 8), vortexed to mix and incubated at 65°C for 15 min. Beads were centrifuged at 13,000 RPM for 1 min and the supernatant transferred to a separate tube. Beads were rinsed with 150 µl TE/1% SDS buffer, vortexed to mix, centrifuged at 13,000 RPM and the supernatant pooled with the previous one.

2.8.5. Immunoprecipitated DNA extraction

Immunoprecipitated DNA was incubated at 65°C overnight, rocking. 250 µl TE buffer was added to the sonication control, supplemented with 10 µg glycogen and 100 µg proteinase K and incubated for 2 hours at 37°C. 44 µl lithium chloride (5 M LiCl) was added and DNA was purified by phenol/chloroform extraction, as described in Section 2.8.2. The pellet was resuspended in 150 µl ddH$_2$0, the concentration and quality verified using a NanoDrop spectrophotometer and DNA stored at -20°C.

2.8.6. Quantitative PCR analysis

Standard curve and primer efficiency analysis were initially performed, to confirm the amplification of a single product and that the amplification efficiency was between 90-110%. Reactions for quantitative PCR (qPCR) experiments were prepared in MicroAmp Optical 96-Well Reaction Plates (Applied Biosystems) using 7.5 µl of Power SYBR Green 2 X master mix (Applied Biosystems), 3 µl of cDNA, 0.6 µl of 10 µM forward primer, 0.6 µl of 10 µM reverse primer and ddH$_2$O, up to a total volume of 15 µl. qPCR amplification experiments were run in triplicate on an ABI 7000 real-time PCR instrument, using the following thermal profile: 1 cycle at 50°C for 15 min, 1 cycle at 95°C for 2 min, 40 cycles of 15 seconds at 95°C and 30 seconds at 60°C. To determine the efficiency of the primers, a dissociation step was added at the end of each cycle: 95°C for 15 seconds, 60°C for 20 seconds and 95 °C for 15 seconds. The enrichment of immunoprecipitated DNA was analysed using eight specific primers spanning the CPA2 gene, CPA4 promoter and CPA4 gene. The percentage of immunoprecipitation (% IP) was calculated by taking into account the dilution factor and the level of amplification obtained from unprecipitated chromatin input DNA.

$$\% \, \text{IP} = \frac{\left[2^{-\text{Ct of IP}}\right] \times X \times Y}{\left[\, 2^{-\text{Ct of INPUT}}\right] \times Z \times Y} \times 100$$

Where X is the dilution factor of the amount of chromatin used, proportional to the number of antibodies used, Y is the dilution factor of the DNA used for qPCR (a factor of 50 as 3 µl was used, from 150 µl total DNA) and Z is the dilution factor of the amount of input chromatin (a factor of 50 as 20 µl was used, from 1 ml total chromatin).

2.9. Analysis of protein expression

2.9.1. Cell lysis

Cells were washed once in PBS and whole cell lysates were prepared, by direct lysis with CytoBuster protein extraction reagent (Novagen). 300 µl reagent was added to a 6 well plate, with the addition of a PIC and incubated on ice for 5 min. Cell debris was scraped, pooled into the reagent and centrifuged at 4°C at 16,000 g for 5 min, using a Hettich Mikro 220R Centrifuge (SLS). The supernatant was removed to a pre-chilled tube and routinely stored at -80°C.

2.9.2. BCA assay

Whole cell protein lysates were quantified using the Bicinchoninic acid assay (BCA) protein assay kit (Thermo Scientific), according to manufacturers' instructions. Briefly, 25 µl of BSA standards, or unknown samples, were pipetted in triplicate into a 96 well plate. 200 µl working reagent was added to each well, the plate was mixed on a plate shaker for 30 seconds and the plate incubated at 37°C for 30 min. The absorbance was read at 562 nm on a POLARstar OPTIMA microplate reader (BMG Labtech), after cooling the plate to RT. A best-fit standard curve of BSA standard concentration vs. absorbance was constructed and interpolated, to find the protein concentration in the unknown samples.

2.9.3. SDS-PAGE gel electrophoresis

For samples to be probed for LXN, 20 µg protein lysate was mixed in a 1:4 (v/v) ratio with 4 x SDS loading buffer (10% (v/v) glycerol, 62.5 mM Tris-HCl pH 6.8, 1% (w/v) SDS, 65 mM DTT and bromophenol blue to colour), vortexed for 10 seconds and heated to 100°C for 15 min in a Grant QBD2 heating block (Grant). The samples were then re-vortexed for 10 seconds and centrifuged for 10 seconds. Samples were loaded up to a maximum volume of 50 µl onto a 10% Tris-SDS acrylamide gel, cast using the Bio-Rad Protean II system and run at 100 V.

For samples to be probed for RARRES1, 20 µg protein lysate was mixed in a 1:2 (v/v) ratio with 2 x SDS urea loading buffer (10% (v/v) glycerol, 62.5 mM Tris-HCl pH 6.8, 1% (w/v) SDS, 65 mM DTT, 8 M urea and bromophenol blue to colour), vortexed for 10 seconds and heated to 100°C for 15 min. The samples were then re-vortexed for 10 seconds and centrifuged for 10 seconds. Samples were loaded up to a maximum volume of 50 µl onto a 10% Tris-SDS acrylamide gel, containing 5 M urea, cast using the Bio-Rad Protean II system and run at 100 V in 1 x SDS running buffer (25 mM tris, 0.19 M glycine and 3.5 mM SDS). Biotinylated (Cell Signalling Technology) and Kaleidoscope (Bio-Rad) MW ladders were run in adjacent lanes for sizing and visualisation of protein transfer. RARRES1 (Abnova) and LXN (R+D Systems) full-length recombinant protein were also run in adjacent lanes as positive controls.

2.9.4. Western blot

Immobilon-P membrane (Millipore) was wet with methanol for 30 seconds, washed with dH_2O and equilibrated in transfer buffer (48 mM tris, 39 mM glycine and 10% (v/v) methanol) for 10 min. Gels were transferred immediately onto the membrane at 100 V for 2 hours at RT, or 30 V overnight at 4°C. Membranes were air-dried, re-wet with methanol and washed twice in TBS (150 mM NaCl and 50 mM Tris-HCl at pH 7.4). Membranes were blocked with 5% (w/v) non-fat skimmed milk (Marvel) for 1 hour at RT and then incubated with primary antibodies (Table 13) in 1% (w/v) Marvel at RT. Membranes were washed three times in TBST (150 mM NaCl, 50 mM Tris-HCl and 0.1% (v/v) Tween-20, pH 7.4). Peroxidase-labelled secondary antibodies (1:3000 (v/v); Cell Signalling Technologies/Boehringer) and 1:5000 (v/v) anti-biotin-HRP (Cell signalling technologies) diluted in 1% (w/v) marvel were added for 1 hour at RT. Membranes were washed four times in TBST and coated with HRP substrate (Roche), equilibrated to RT. Membranes were exposed to hyperfilm ECL (GE Healthcare) and manually processed using Kodak GBX developer and fixer solutions (SLS).

Primary antibody	Species	Isotype	Conc. (mg/ml)	Origin	Working dilution	Incubation time
RARRES1	Rabbit	IgG	0.2	Santa Cruz Biotechnology	1:200	1 h
LXN	Rabbit	IgG	0.15	Sigma	1:500	4 h
CPA4	Mouse	IgG1	1	Sigma	1:1000	1 h
HA tag	Mouse	IgG2a	0.2	Santa Cruz Biotechnology	1:1000	1 h
β-actin	Mouse	IgG2a	-	Sigma	1:5000	1 h

Table 13. Description of primary antibodies used for western blotting.

2.9.5. Stripping western blot

Each membrane was stripped in stripping buffer (20 mM Tris-HCl pH 6.8, 0.1% (w/v) SDS and 20 mM DTT) for 30 min at 55°C, with shaking and washed three times in TBST. The membrane was blocked and reprobed, as detailed above, with β-actin antibodies as an internal control to ensure equal loading and to obtain quantitative protein expression intensities using Image J software (National Institutes of Health, http://rsbweb.nih.gov/ij/).

2.10. Cell function assays

2.10.1. Wound healing assay

PNT1a cells were plated at a density of 5 x 10^4 cells per well in a 24 well plate and incubated at 37°C for 24 hours. Cells were treated with 10 nM siRNA (Section 2.5.1) or cDNA expression vectors (Section 2.5.3.3) and incubated at 37°C for 48 hours. Using a 1 ml pipette tip, a wound was created in the cell monolayer, cells were washed with PBS and fresh R10 media was added. Migration into the wound was monitored and 10 x images were taken on an Evos XL transmitted light microscope (AMG), 18 hours after wounding and the percentage of wound closure was calculated. The width of the wound at 0 and 18 hours was measured using Volocity software, the average (of 10 points) taken and the relative percentage wound closure at 18 hours with respect to 0 hours was calculated.

2.10.2. Matrigel invasion assay

Cells were transfected with siRNA (Section 2.5.1 and 2.5.2) or over-expression vectors (Section 2.5.3.3), 24 hours prior to commencing the invasion assay. Control PNT1a and MDA-MB-231 cells were grown to ~90% confluency in T75 flasks. Cells were harvested with trypsin-EDTA and counted using a Haemocytometer. Cell culture inserts (BD Biosciences) were coated with 50 µl of 750 µg/ml Matrigel BM matrix (BD Biosciences), diluted in media (RPMI for PNT1a/LNCaP, DMEM for MDA-MB-231 or KSFM for primary cells) and left to polymerise for at least 2 hours at 37°C. Cells were seeded onto Matrigel-coated 0.8 µM porous cell culture inserts and non-Matrigel control inserts, in triplicate, at a density of 2.5 x 10^5 cells per insert, unless otherwise stated. The inserts were transferred onto a plate containing R10 medium as the chemo-attractant and incubated at 37°C for 48 hours.

Cells were washed in PBS and the non-invading cells removed from the upper surface of the membrane, by scrubbing with a cotton bud. Cells on lower surface of the membrane were fixed in 500 µl ice-cold methanol at RT for 20 min. The bottom membrane of the insert was removed with a scalpel and mounted onto frost–free glass slides, using Vectashield mounting medium containing DAPI (Vector laboratories). Slides were examined under a Nikon Eclipse TE300 fluorescent microscope (Nikon) and four random images from each of the three replicate membranes were taken at 20 x magnification. Nuclei were counted by eye, or using the cell count analysis function on the ImageJ software. Invasion/motility ratios were calculated to determine the number of invasive cells relative to migratory cells.

2.10.3. Clonogenic recovery assay

Primary cultures were treated with siRNA as described in Section 2.5.2. Cells were trypsinised and plated at 100 cells per well, diluted in 2 ml SCM, in a 6 well collagen-I coated plate, in

triplicate. 500 µl irradiated STOs were added per well and plates were incubated at 37°C in 5% CO_2. Medium was changed every 2 days and STOs were added when sparse. When colonies greater than 32 cells started to emerge (usually after 10-14 days), medium was removed and cells were washed with 1 ml PBS. To distinguish epithelial colonies from STOs, the cells were fixed with 2 ml crystal violet stain (1% (w/v) crystal violet, 10% (v/v) ethanol and 89% (v/v) PBS) and the number of colonies containing greater than 32 cells (5 population doublings) per well were counted visually under the 10 x objective of a Leica DM IL LED microscope (Leica Microsystems). The percentage colony forming efficiency (CFE) was calculated, by dividing the number of colonies by the number of cells plated and multiplying by 100. Relative CFE was calculated by setting the CFE for each media sample at 100%.

2.11. Flow cytometry analysis

2.11.1. Analysis of cell surface marker expression

Primary cells were simultaneously analysed for the expression of CD44, CD49b, CD24 and CD133. Cells were trypsinised, sedimented by centrifugation and resuspended in 60-80 µl MACS buffer, per 10^6 cells. Cell suspensions were incubated with MACS FcR blocking buffer and the appropriate antibody, as described in Table 14, for 10 min at RT, in the dark. Cells were washed in 2 ml MACS buffer and centrifuged at 1300 RPM for 3 min. Cells were resuspended in 1 ml MACS buffer, placed on ice and analysed on a CyAn ADP flow cytometer (Dako Cytomation). Immediately before analysis, 1 µl Sytox Blue dead cell stain (Invitrogen) was added to each cell suspension at 1:1000 (v/v) dilution, to differentiate live and dead cells. As a control, cells not labelled with any antibody were analysed. Unlabelled cells were resuspended in 2 ml MACS buffer prior to analysis, of which 1 ml was analysed on the flow cytometer and Sytox Blue was added to the other 1 ml suspension. To prevent bleaching of the fluorescence, cells were protected from light where possible during the procedure. CD44 fluorescence was recorded in the FITC channel, CD49b and CD24 in the PE channel, CD133 in the APC channel and Sytox Blue in the Violet1 channel.

Antibody	Conjugation	Working dilution	Origin of antibody	MACS buffer (µl)	MACS FcR Block (µl)	Antibody (µl)
Unlabelled	-	-	-	80	20	-
CD44	FITC	1:10	Miltenyi Biotec	70	20	10
CD49b	PE	1:10	AbD Serotec	70	20	10
CD133	APC	1:10	Clone 293C2, Miltenyi Biotec	70	20	10
CD24	PE	1:5	BD Bioscience	60	20	20

Table 14. Description of antibodies used for cell surface membrane expression by FACS.

All results were analysed using the Summit software (Beckman Coulter). An initial gate (R1) was set in a pulse width histogram, to include all single cells and exclude doublets. A second gate (R2) was applied to the FSlin/SSlog histogram, to include the cell population of interest and exclude cell debris. A third gate (R3) was applied to the Violet1 histogram, to include all live cells and exclude dead cells. For statistical significance, at least 10,000 events were collected.

2.11.2. Cell cycle analysis

Primary cells were trypsinised, sedimented by centrifugation and resuspended in 5 ml R10 medium per 10^6 cells. Cells were centrifuged at 1300 RPM for 5 min and the pellet resuspended in 1 ml PBS. To fix the cells, 2.5 ml ice-cold 70% EtOH was added to the cell suspension whilst vortexing, to prevent clustering of cells. Cells were incubated on ice for 30 min and centrifuged at 1300 RPM for 5 min. The pellet was washed in 5 ml PBS and re-centrifuged. The pellet was then resuspended in 400 μl PBS, 50 μl RNase A (1 mg/ml final concentration) and 50 μl propidium iodide (PI; 400 μg/ml final concentration) and incubated at 37°C for 30 min. Cells were then placed on ice, analysed on a CyAn ADP flow cytometer (Dako Cytomation) and PI fluorescence was recorded in the PE channel. To prevent bleaching of the fluorescence, cells were protected from light where possible during the procedure.

All results were analysed using the Summit software. Two initial gates were set in an FSlin/SSlog (R1) and PElin/PEarea (R2) histogram, to include the cell population of interest and exclude cell debris. Four further gates were applied to the PE histogram, to include all cells in G0/G1 phases (R3), G2/M phases (R4), S phase (R5) and apoptotic cells (R6). For statistical significance, at least 10,000 events were collected.

2.11.3. Caspase 3 apoptosis assay

PC3 cells were trypsinised and sedimented by centrifugation at 1300 RPM for 3 min. Cells were resuspended in 8 ml PBS, split into 4 separate tubes: (1) Unlabelled (PBS only), (2) CaspACE only, (3) Sytox blue only and (4) CaspACE + Sytox blue and re-centrifuged at 1300 RPM for 3 min. The supernatant was removed, 2 μl CaspACE-FITC apoptosis marker (Promega) was diluted 1:500 (v/v) into 1 ml PBS and 100 μl diluted CaspACE reagent was added to each cell pellet (except unlabelled and Sytox blue only). Cells were incubated at 37°C, in the dark, for 20 min. Cells were then washed in 2 ml PBS and centrifuged at 1300 RPM for 3 min. Cells were resuspended in 1 ml MACS buffer, placed on ice and analysed on a CyAn ADP flow cytometer (Dako Cytomation). Immediately before analysis, 1 μl Sytox Blue dead cell stain was added to each cell suspension at 1:1000 (v/v) dilution, to differentiate live and dead cells (except unlabelled and CaspACE only). To prevent bleaching of the fluorescence, cells were protected from light where possible during the procedure. CaspACE fluorescence was recorded in the FITC channel and Sytox Blue in the Violet1 channel.

All results were analysed using the Summit software. An initial gate (R1) was set in a pulse width histogram, to include all single cells and exclude doublets. A second gate (R2) was applied to the FSlin/SSlog histogram, to include the cell population of interest and exclude cell debris. Four further gates were applied to the FITC/Violet1 histogram, to include all dead (R3), apoptotic and dead (R4), live (R5) and apoptotic cells (R6). For statistical significance, at least 10,000 events were collected.

2.12. Cell localisation assays

2.12.1. Immunofluorescence

Immunofluorescence was performed in BD-Biocoat collagen I-coated (primary cultures) or BD-Falcon uncoated (cell lines) 8-well chamber slides (BD Bioscience). 200 µl cell suspensions were plated into chamber slides at 5×10^4 cells per well and incubated at 37°C for at least 24 hours. Cell medium was then aspirated. Cells were washed twice with PBS and fixed with 200 µl 4% (w/v) paraformaldehyde pH 7.4, for 20 min. Cells were washed three times with 500 µl PBS for 5 min and then permeabilised with 200 µl 0.5% (v/v) Triton X-100 for 20 min. Cells were washed a further three times with PBS and the immunofluorescence procedure continued, or the slides stored at 4°C. Cells were blocked with 200 µl 10% (v/v) goat serum, diluted 1% (w/v) BSA in PBS, for 30 min and then incubated with primary antibody, diluted in 1% (w/v) BSA in PBS, for 1 hour.

Cells were washed three times with 500 µl PBS for 5 min and then incubated with 200 µl secondary antibody, diluted in 1% BSA in PBS, for 45 min. After a final three washes with 500 µl PBS for 5 min, the chambers were removed from the slide, cells covered with Vectashield mounting medium with DAPI (Vector laboratories), a 0.13-0.17mm coverslip (SLS) added and then sealed with clear nail varnish. Slides were stored at 4°C until analysis on a Nikon Eclipse TE300 fluorescent microscope (Nikon), or a LSM 510 meta confocal microscope (Zeiss). Slides were gently agitated during incubations, which were performed at RT and protected from light where possible, to avoid bleaching of fluorescence. Secondary only controls, where the primary antibody was replaced with PBS and IgG controls, where the primary antibody was replaced by an isotype IgG control antibody, were performed. Dilutions of primary antibodies used for immunofluorescence are listed in Table 15. Secondary Alexa fluor 488 or 568 goat anti-rabbit, or goat anti-mouse IgG antibodies (Invitrogen) were used at 1:200 (v/v) dilution.

A more stringent nuclear fixation protocol was also used to detect nuclear LXN expression which was carried out as described above with the following modifications. Cells were fixed with 200 µl of a mixture of 2% (w/v) paraformaldehyde pH 7.4 and 0.2% (v/v) Triton X-100 for 20 min. Cells were then washed three times with 500 µl PBS for 5 min and permeabilised with 200

µl 0.5% (v/v) NP-40 for 20 min. All washing steps during the immunofluorescence procedure were performed with a PBS buffer containing 0.5% (w/v) BSA and 0.175% (v/v) Tween-20.

Primary antibody	Species	Isotype	Conc. (mg/ml)	Origin	Working dilution
HA tag	Rabbit	IgG	-	Sigma	1:50
Ki67	Rabbit	IgG	1	Abcam	1:500
LXN	Rabbit	IgG	0.15	Sigma	1:100
RAR α	Rabbit	IgG	0.2	Santa Cruz Biotechnology	1:100
RAR β	Rabbit	IgG	0.2	Santa Cruz Biotechnology	1:100
RAR γ	Rabbit	IgG	0.2	Santa Cruz Biotechnology	1:100
RARRES1	Rabbit	IgG	0.2	Santa Cruz Biotechnology	1:100
α1-Na/K-ATPase	Mouse	IgG1	1	Abcam	1:100
Cytokeratin 5	Mouse	IgG1	0.05	Vector laboratories	1:200
Cytokeratin 8	Mouse	IgG1	-	Sigma	1:200
Cytokeratin 18	Mouse	IgG1	-	Sigma	1:200
HA tag	Mouse	IgG2a	0.2	Santa Cruz Biotechnology	1:100
Protein Disulphide Isomerase (PDI)	Mouse	IgG2a	1	Abcam	1:100
IgG control	Rabbit	IgG	10	Sigma	Dependent on conc. of primary antibody
IgG control	Mouse	IgG1	0.5	R+D Systems	
IgG control	Mouse	IgG2a	0.5	R+D Systems	

Table 15. Description of primary antibodies used for immunofluorescence.

2.12.2. Cellular fractionation of plasma membrane and cytoplasm

PC3 cells grown in T25 flasks were washed twice with 5 ml PBS, scraped in 4 ml PBS and transferred to a universal tube. Cells were pelleted by centrifugation at 2300 RPM for 10 min. Supernatant was aspirated, pellet was resuspended in 200 µl ice cold Tris buffer (40 mM tris pH 7.4) supplemented with a PIC and incubated at 4°C for 10 min, with gentle shaking. The cell lysate was sonicated for 10 min, using the Bioruptor sonication system (Diagnode), for 10 cycles of 30 seconds on / 30 seconds off on ice, at low power. Unbroken cells (**UBC**) were pelleted by centrifugation at 2500 g for 10 min at 4°C. Supernatant was removed and

transferred to 1.5 ml Eppendorf tube. To disrupt the interactions between cytoskeletal and PM proteins, the supernatant was diluted with 800 µl ice cold 0.1 M sodium carbonate (pH 11) supplemented with a PIC and shaken for 1 hour at 4°C. To collect the carbonate treated membranes, the supernatant was ultracentrifuged at 100,000 g for 1 hour at 4°C (Rotor: TLA 100.3, ultracentrifuge TL100.) The supernatant was removed (**Wash 1**) and stored at -80°C. The pellet was re-suspended in 800 µl ice cold sodium carbonate supplemented with a PIC and shaken for 1 hour at 4°C. A second ultracentrifugation step at 100,000 g for 1 hour at 4°C was performed, to collect the remaining carbonate treated membranes. The supernatant was removed (**Wash 2**) and stored at -80°C. The membrane pellet was re-suspended in 200 µl ice cold 40 mM Tris (pH 7.4) and shaken for 10 min. A final ultracentrifugation step at 115,000 g for 20 min at 4°C was performed. The supernatant was removed (**Wash 3**), a SDS sample buffer was added to the plasma membrane pellet (**PM**) and stored -80, or continued with SDS-PAGE as described in Section 2.9.3. This was performed by Hannah Walker.

3. RESULTS

3.1. Expression patterns of RARRES1, LXN and CPA4 in prostate cell lines

3.1.1. RARRES1 and LXN expression is repressed in prostate cancer cell lines

RARRES1 has been proposed as a tumour suppressor gene, whose diminished expression is involved in the malignant progression of CaP (Jing et al., 2002). To determine the expression pattern of RARRES1 and LXN in a panel of benign prostate and CaP epithelial cell lines, quantitative analysis of RARRES1 (Figure 20a) and LXN (Figure 20c) mRNA expression was performed. qRT-PCR data demonstrated that RARRES1 was expressed at lower levels in CaP cell lines compared to benign cell lines. Furthermore, the expression status of RARRES1 correlated with the malignancy of the cell line; expression was highest in the least malignant cell line, PNT2-C2, but lowest in the most malignant cell lines, PC3 and LNCaP (undetectable after 40 cycles in the latter). In the benign cell lines, RARRES1 expression was more than 10-fold higher in PNT2-C2 cells than the PNT1a cell line. LXN mRNA expression also showed a similar trend to RARRES1, where expression correlated with the malignancy status of the cell line. LXN was expressed at higher levels in the benign cell lines PNT2-C2 and PNT1a than in the P4E6 and LNCaP cancer cell lines. In contrast to RARRES1, expression of LXN was low, but detectable, in the LNCaP cell line. However, LXN mRNA was not detected in the P4E6 cell line, even after 40 cycles of qRT-PCR. One exception was the highly malignant PC3 cell line, where LXN was over-expressed to levels almost 10-fold higher than that seen in the benign cell lines.

Protein expression of RARRES1 (Figure 20b) and LXN (Figure 20d) was analysed by SDS-PAGE and western blot analysis, in the same benign and cancer cell lines, and band intensities were quantified relative to a β-actin loading control. Recombinant protein was also loaded on each gel to ensure the antibodies were specific for the protein of interest. The expression patterns of RARRES1 and LXN, at the protein level, correlated well with that seen at the mRNA level, although the quantitative values differed slightly, i.e. RARRES1 protein expression was highest in the PNT2-C2 cell line and decreased with malignancy. RARRES1 expression in PC3 and LNCaP cell lysates was undetected at the protein level. There are 2 splice variants of RARRES1, producing a full-length 33 kDa isoform and shorter 26 kDa isoform. All cell lines analysed here expressed the full-length 33 kDa RARRES1 and not the shorter variant. As seen at the mRNA level, LXN protein expression was highest in the highly malignant PC3 cell line, followed by the benign cell lines PNT2-C2 and PNT1a and then the cancer cell lines LNCaP and P4E6. Taken together, these results showed that both RARRES1 and LXN expression was lower in cancer, compared to benign epithelial cell lines.
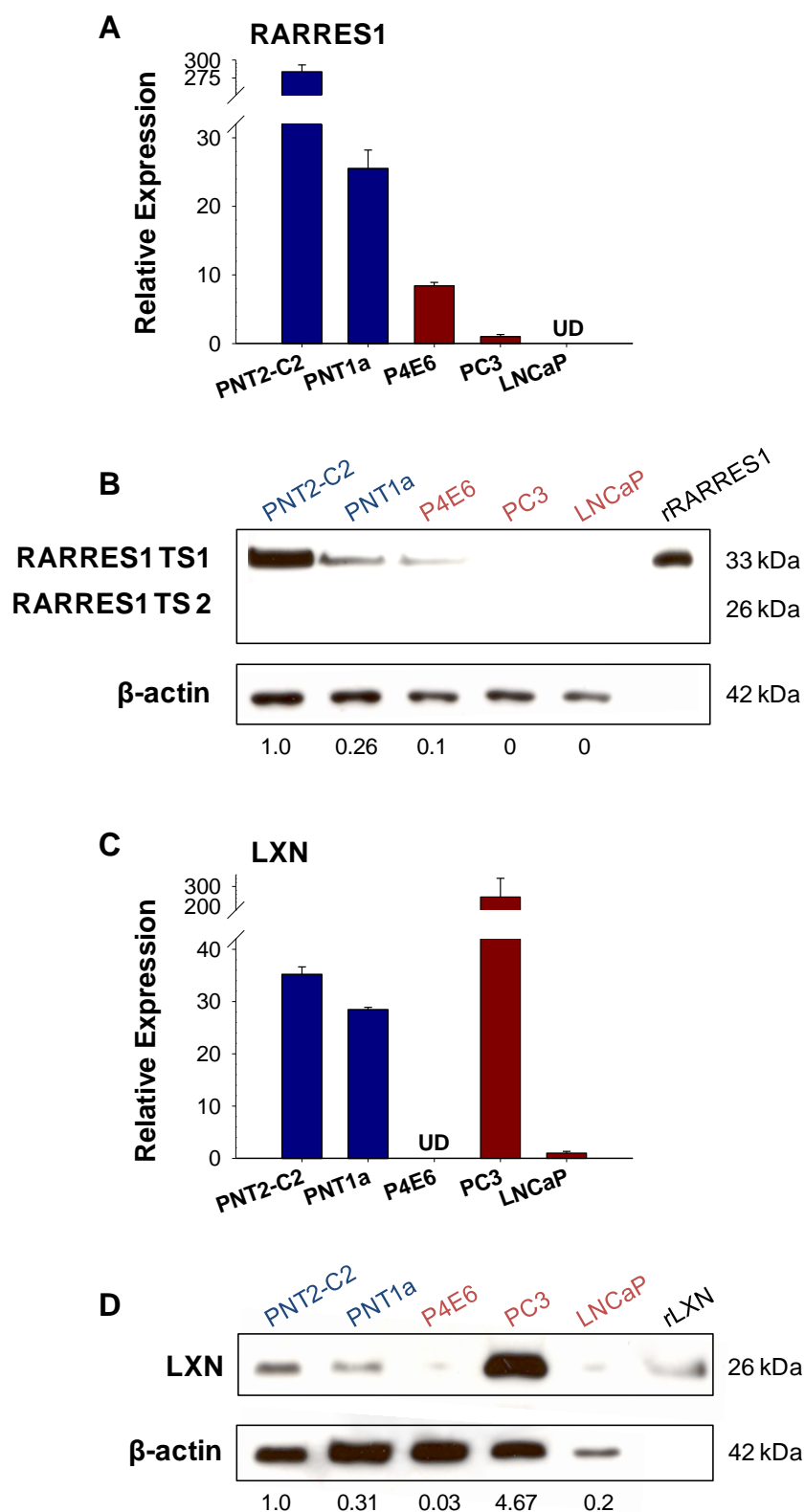
Figure 20. qRT-PCR and western blot analysis of RARRES1 and LXN expression in prostate epithelial cell lines.
mRNA expression of **(a)** RARRES1 and **(c)** LXN in benign (PNT2-C2 and PNT1a) and cancer (P4E6, PC3 and LNCaP) cell lines, relative to a GAPDH control gene and normalised to a calibrator sample (a: PC3, b: LNCaP; expression set at 1). (UD: expression undetectable after 40 cycles; n=3 technical replicates; error bars expressed as range of the mean). Protein expression of **(b)** RARRES1 (33 kDa) and **(d)** LXN (26 kDa) in benign and cancer cell lines. Full-length recombinant protein (rRARRES1, rLXN) was loaded on each gel, to confirm antibody specificity. Protein expression was quantified relative to a β-actin (42 kDa) loading control and relative to the PNT2-C2 cell line (set at 1; values below each blot).

3.1.2. CPA4 is ubiquitously expressed in prostate cell lines

CPA4 mRNA has previously been shown to be detectable in a number of prostate cell lines, but is expressed at extremely low levels in normal prostate tissue (Huang et al., 1999). To determine the expression pattern of CPA4, in panel of benign prostate and CaP epithelial cell lines, quantitative analysis of CPA4 mRNA expression was performed (Figure 21a). qRT-PCR data demonstrated that CPA4 expression was ubiquitous in the cell lines tested and, unlike RARRES1 and LXN, did not correlate with malignancy of the cell line. CPA4 mRNA expression was highest in the benign PNT1a cell line and lowest in the malignant LNCaP cell line, which was the calibrator sample for which expression was set at 1.

Protein levels of CPA4 were analysed by SDS-PAGE and western blot analysis, in the same benign and cancer cell lines and band intensities were quantified relative to a β-actin loading control (Figure 21b). The antibody used for western blot analysis was able to detect CPA4 in its zymogen pro-CPA4 form (47 kDa) and its active CPA4 form (35 kDa), which can be generated by trypsin cleavage (Tanco et al., 2010). A positive control LNCaP cell lysate, transfected with HA-tagged CPA4 expression vectors, was also loaded on each gel to ensure that the antibodies were specific for CPA4. The expression patterns of total CPA4, at the protein level, correlated well with those seen at the mRNA level. The exception was the LNCaP cell line, which showed the lowest mRNA expression of CPA4, but the highest levels of CPA4 protein expression.

CPA4 has recently been shown to be a soluble secreted protein in HEK 293T cells (Tanco et al., 2010), so CPA4 expression was analysed in conditioned media harvested at various time points, from the benign PNT1a cell line, which expresses the highest levels of CPA4 (Figure 21c). Increasing levels of CPA4 were secreted from the PNT1a cell line in the pro-form; and detectable levels of expression were not seen until 48 hours after a media change. Next, CPA4 expression was analysed in conditioned media extracted from a panel of benign and cancer cell lines after 72 hours (Figure 21d). CPA4 was secreted from all cell lines screened, in the pro-form. Expression of CPA4 in conditioned media roughly correlated with that seen in cell lysates, with expression being lowest in the P4E6 and PC3 cell lines and highest in the PNT1a and LNCaP cell lines.

Within cell lines, CPA4 was predominantly expressed in the inactive pro-form, but the active cleaved form of CPA4 was present in the PNT1a and LNCaP cell lines (Figure 21b). In the PNT1a cell line, the active form was expressed at equivalent amounts to the inactive form, but in the LNCaP cell line, pro-CPA4 was nearly 8-fold more abundant than active CPA4.

Figure 21. qRT-PCR and western blot analysis of CPA4 expression in prostate epithelial cell lines.
mRNA expression of **(a)** CPA4 in benign (PNT2-C2 and PNT1a) and cancer (P4E6, PC3 and LNCaP) cell lines, relative to a GAPDH control gene. (n=3 technical replicates; error bars expressed as range of the mean). Protein expression of **(b)** CPA4 in benign and cancer cell lines. Protein expression was quantified relative to a β-actin loading control (42kDa; values below each blot). **(c)** Protein expression of CPA4 in PNT1a cell line media, extracted from cells over a time course, and in **(d)** benign and cancer cell line media. A LNCaP cell lysate transfected with a HA-tagged CPA4 expression vector (+ve) was loaded on each gel to confirm antibody specificity.

A

CPA4

B

	PNT2-C2	PNT1a	P4E6	PC3	LNCaP
Pro-CPA4	0.24	0.28	0.02	0.11	1.0
Active CPA4	0	0.28	0	0	0.13
Total CPA4	0.24	0.56	0.02	0.11	1.13

C

PNT1a media

0hr	24hr	48hr	72hr	96hr
0	0	0.60	0.61	1.0

D

PNT2-C2	PNT1a	P4E6	PC3	LNCaP
0.62	1.0	0.33	0.30	0.65

Results
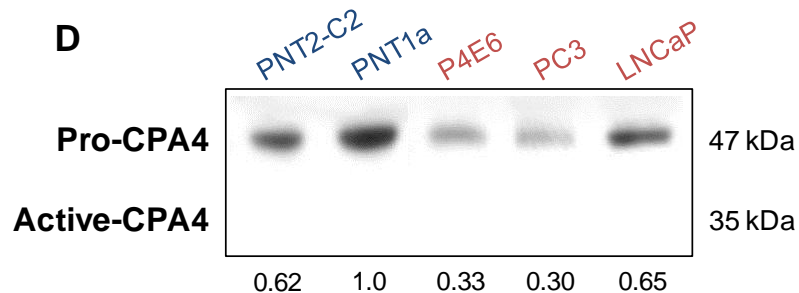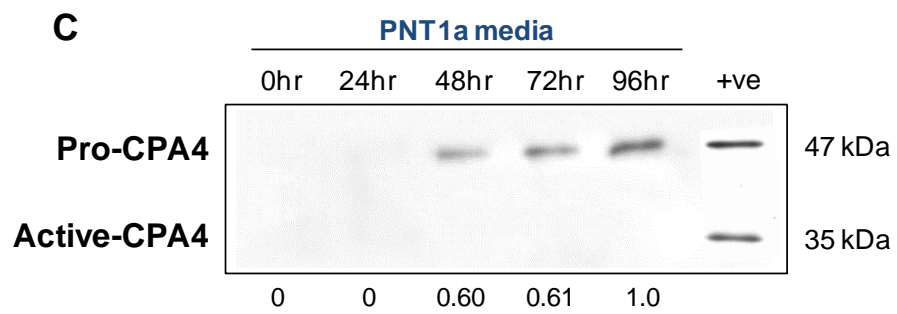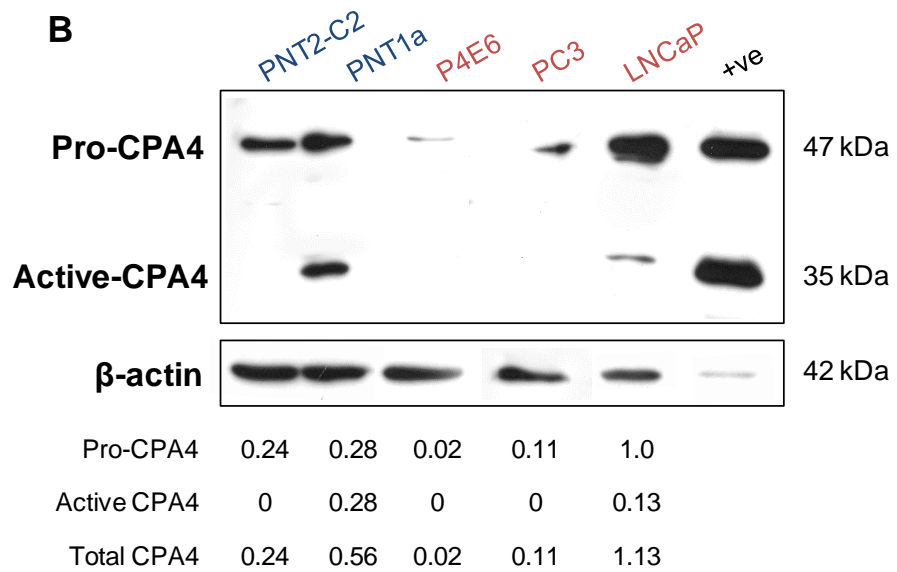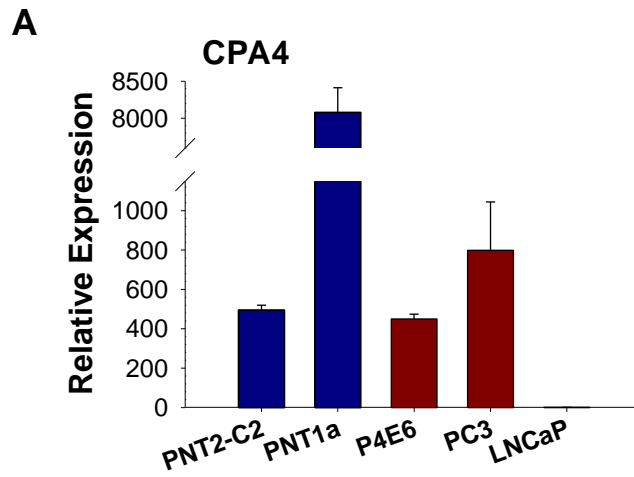
3.2. Expression patterns of RARRES1, LXN and CPA4 in primary prostate epithelial cultures

3.2.1. Microarray analysis identified RARRES1 and LXN as differentially expressed in primary prostate epithelial cultures

Affymetrix gene-expression array data, obtained in our laboratory and published by Birnie et al. (2008), was reanalysed to examine the relative expression of RARRES1, LXN and CPA4 in primary prostate epithelial cultures enriched for SCs and CB cells, derived from human CaP tissue (n=12) or human benign prostatic hyperplasia (BPH) tissues (n=7) (Figure 22a). CaP tissues analysed contained a minimum Gleason score 7 pathology, in which gene expression differences were most prominent.

The results show that RARRES1 and LXN were both significantly differentially expressed between the SC and CB populations from BPH alone samples and pooled BPH and CaP samples. When comparing SC and CB populations from CaP samples, only one of three probes (221872_at) for RARRES1 was significantly differentially expressed (Figure 22b). Moreover, this was the only probe that was specific for transcript one of RARRES1, suggesting that transcript one and not transcript two, is differentially expressed in SC and CB populations from CaP. The lack of significance could also be attributed to the high patient variability regularly seen between CaP samples. High variation in RARRES1 and LXN expression was most notable in the SC population from CaP samples.

In contrast, no significant differential expression was seen when comparing BPH and CaP populations of cells (Figure 22c). LXN was overall expressed at higher levels than RARRES1 in all subpopulations, but especially in the SC fraction. CPA4 showed ubiquitous expression between all cell populations, so CPA4 expression was not studied further in enriched primary prostate epithelial cultures.

Taken together, microarray analysis identified RARRES1 and LXN as significantly down-regulated in SC compared to CB primary prostate BPH epithelial cultures.

A
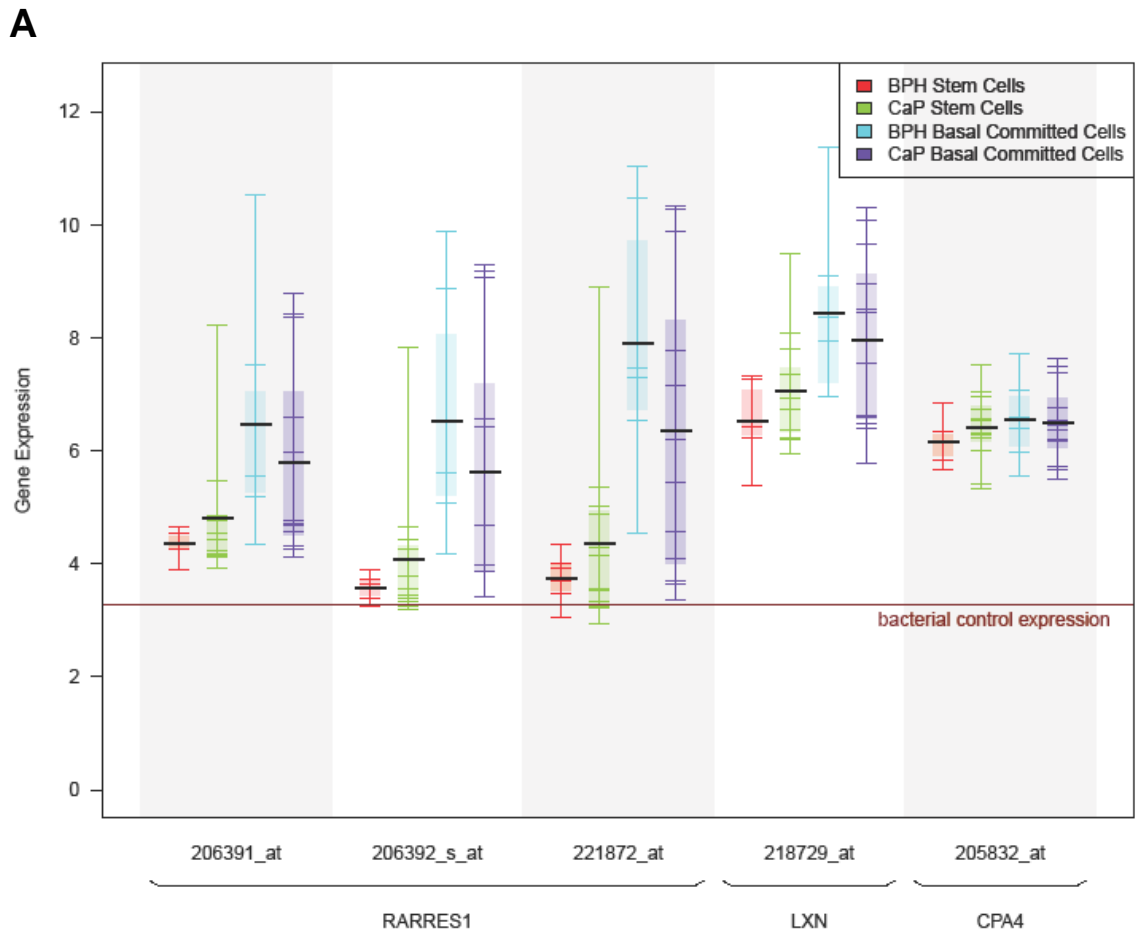
B

	Gene	Probe	BPH Stem vs BPH Comm	CaP Stem vs CaP Comm	Stem vs Comm
Stem vs Comm	**RARRES1**	206391_at	**0.046**	0.122	**0.011**
	RARRES1	206392_s_at	**0.010**	0.058	**0.002**
	RARRES1	221872_at	**0.002**	**0.038**	**0.0005**
	LXN	218729_at	**0.026**	0.119	**0.008**

P < 0.05
P < 0.01
P < 0.001

C

	Gene	Probe	BPH vs CaP	BPH Stem vs CaP Stem	BPH Comm vs CaP Comm
BPH vs CaP	**RARRES1**	206391_at	0.872	0.354	0.512
	RARRES1	206392_s_at	0.787	0.365	0.455
	RARRES1	221872_at	0.614	0.381	0.259
	LXN	218729_at	0.962	0.251	0.544

Figure 22. Reanalysis of Affymetrix gene-expression array data.
(a) Expression of RARRES1 and LXN in primary prostate epithelial cultures enriched for SC and CB cells derived from human BPH (n=7) and CaP (n=12) tissues, containing a minimum Gleason score 7 pathology. **(b)** Statistical significance values of stem vs. committed and **(c)** BPH vs. CaP were measured by the Student's T-test (Unpaired, two-tailed). Significance values are highlighted in red. Reanalysis of microarray data (Birnie et al., 2008) was performed by Dr. Davide Pellacani and Dr. Alastair Droop.

3.2.2. mRNA expression of RARRES1 and LXN is low in primary prostate epithelial cultures enriched for stem cells

To investigate differential expression of RARRES1 and LXN further, quantitative analysis of mRNA expression was performed, on a panel of BPH (n=5) and CaP (n=6) primary prostate epithelial cultures, enriched for SC, TA and CB cell populations.

We initially used a relative qRT-PCR analysis protocol, where the expression of RARRES1 and LXN was quantified relative to an RPLPO control gene (Figure 23a-d). These results showed that the expression of RARRES1 and LXN was higher in SC, decreased in TA and increased again in CB cultures. This was in contrast with the microarray analysis. A more in depth analysis showed that the C_T value of RPLPO was consistently higher in the SC population. This led us to the conclusion that due to the lower levels of expression of RPLPO in the SC population (higher C_T value), the expression of both RARRES1 and LXN was showing false high results.

To overcome this technical problem, we first selected different control genes. The microarray datasets created in our lab (Birnie et al., 2008) and a compendium of published microarray datasets were utilised to identify genes that showed low variation between a number of different cell types, including SCs (Figure 23e) (Bioinformatic analysis performed by Dr. Alastair Droop). This led to the identification of five potential control genes for relative qRT-PCR analysis: HUWE1, γ-actin, EEF1A1, TPT1 and YWHAZ. YWHAZ had previously been identified as a suitable control gene for qRT-PCR experiments in SCs (Fink et al., 2008; Curtis et al., 2010). Consequently, the viability of these control genes was sought along with other well-known control genes. From this data, HUWE1 showed the least variability between cell populations. However, the variation between cell populations was still greater than four C_T values in the majority of patient samples tested.

When calculating the relative expression of RARRES1 and LXN, relative to either RPLPO or HUWE1, it was apparent just how important the choice of endogenous control gene was (Figure 23f). In some samples, depending on the control gene that was used in the calculation, the expression pattern of LXN changed. The magnitude of expression of RARRES1 expression in the SC was also variable. However, higher expression levels were constantly seen in the SC compared to TA and CB fractions.

Consequently, absolute qRT-PCR was utilised to calculate absolute levels of gene expression of RARRES1 (Figure 24) and LXN (Figure 25). A standard curve was produced, using serial dilutions of a pure cDNA plasmid preparation of either RARRES1 (pReceiver-M45) or LXN (pEZ-M06), obtained from GeneCopoeia, which was then used to calculate the expression levels of RARRES1 and LXN in the unknown samples. To ensure that accurate results were obtained, the concentration and amount of input cDNA was precisely measured using a nanodrop spectrophotometer, to be identical for all samples in every well.

Results demonstrated that both RARRES1 and LXN were now expressed at lower levels in SCs, compared to their differentiated TA and CB counterparts. RARRES1 was significantly differentially expressed between SC and CB subpopulations derived from BPH cultures (Figure 24b). In contrast, although there was a trend showing that RARRES1 expression increased through differentiation, significantly differential expression was not observed between cell populations derived from CaP cultures (Figure 24c). Levels of RARRES1 expression were considerably lower in all populations derived from CaP compared to BPH. Moreover, RARRES1 expression was significantly lower in CB cells derived from CaP, than CB cells derived from BPH (Figure 24d). However, RARRES1 was not significantly differentially expressed in CB cells between BPH and CaP in the microarray analysis (Figure 22a). This could be attributed to: (1) the high variability in RARRES1 expression seen in CB cells from CaP samples in the microarray analysis, (2) the different samples analysed using the two techniques or (3) the difference in the sensitivity/normalisation of the two experiments. Furthermore, the most malignant CaP samples (Gleason grade 8 and 9, castrate-resistant) showed lower expression levels of RARRES1 than Gleason grades 6 and 7 CaP samples (Figure 24e).

Analogous to RARRES1, LXN was significantly differentially expressed between SC and TA cells derived from both BPH (Figure 25b) and CaP (Figure 25c). Although RARRES1 expression was at its highest in the most differentiated CB cells, the highest expression of LXN was seen in the highly proliferative TA population. Moreover, a 2-fold increase in average LXN expression was seen in the TA population from CaP compared to BPH samples. However, a higher level of variability was seen in this TA population, most probably due to the patient variability between CaP samples. Similar to RARRES1, the most malignant CaP samples showed the lowest expression levels of LXN in TA (Figure 25d) and CB (Figure 25e) cells.

Taken together, these results confirm the initial microarray data, and show that RARRES1 and LXN are expressed at significantly lower levels in prostate SC compared to TA and CB cells. In addition, RARRES1 expression is significantly down-regulated in CB cells from CaP cultures compared to CB from BPH cultures. In conjunction with the repression of RARRES1 seen in malignant cell lines, this repression in CaP compared to BPH supports a 'metastasis suppressor' function for RARRES1 in CaP.
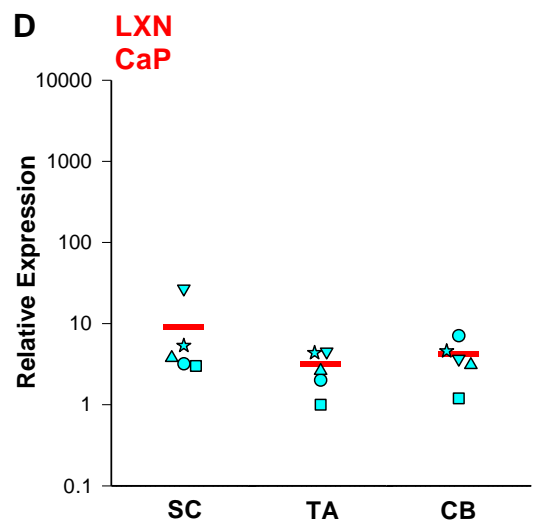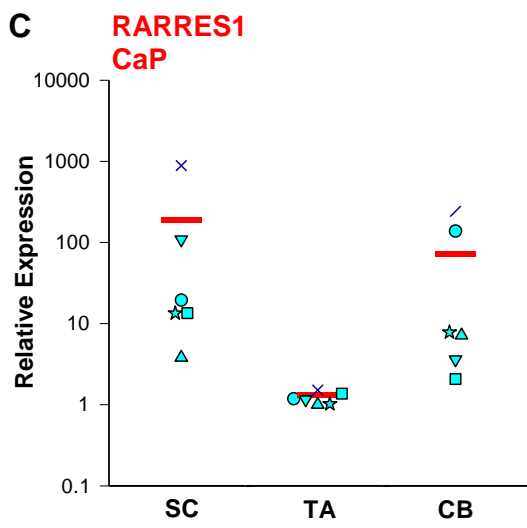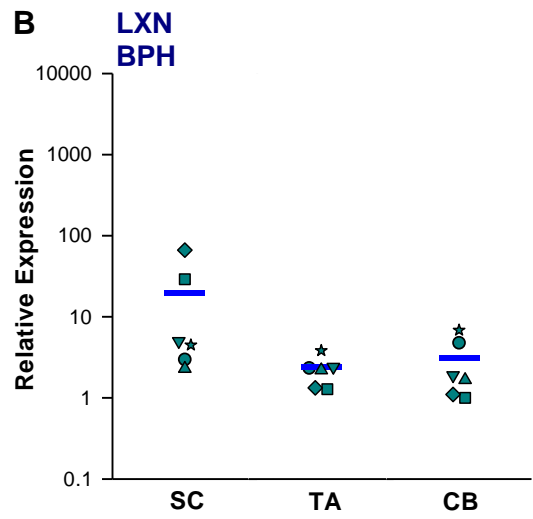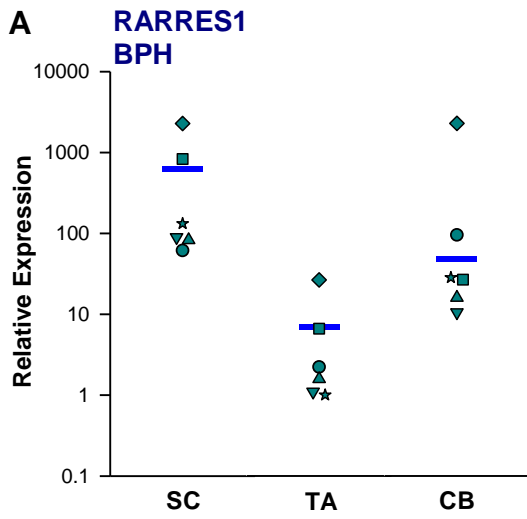
A RARRES1 BPH

B LXN BPH

C RARRES1 CaP

D LXN CaP

BPH	
●	Y003/10
■	Y048/10
▲	Y052/10
▼	Y040/10
★	Y030/10
◆	Y061/10

CaP	
●	PE671
■	Y089/09
▲	PE665
▼	H031/11 RB
★	H031/11 LM
╱	PE667

E

	HUWE1	β-actin	18S	γ-actin	GAPDH	EEF1A1	TPT1	YWHAZ	RPLPO	PPIA	HPRT1	β-2M
					Range in CT Values between SC, TA and CB enriched cell populations							
YO61/10	4.25	5.78	-	5.97	6.18	6.55	6.40	6.47	6.60	-	-	-
YO40/10	4.16	6.38	-	6.90	6.96	6.89	7.16	6.86	6.99	-	-	-
PE665	1.63	1.51	-	2.26	1.19	1.58	1.24	1.17	1.75	-	-	-
YO52/10	4.88	5.61	-	6.49	6.47	6.75	7.12	7.48	6.42	-	-	-
YO59/10	-	6.67	5.37	-	5.79	-	-	-	7.06	6.23	7.16	7.10
YO89/09	-	4.04	4.98	-	5.93	-	-	-	6.92	5.81	6.19	6.50
AVERAGE	3.73	5.00	5.17	5.40	5.42	5.44	5.48	5.49	5.96	6.02	6.67	6.80

F

		Relative Expression Values			
		RARRES1		LXN	
		RPLPO	HUWE1	RPLPO	HUWE1
YO61/10	SC	86.40	16.96	49.83	9.78
	TA	1.00	1.00	1.00	1.00
	CB	1.07	0.95	0.83	0.73
YO59/10	SC	3198.10	287.42	6.14	0.55
	TA	1.00	1.00	1.00	1.00
	CB	1.99	2.31	0.64	0.74
YO40/10	SC	52.45	7.41	1.04	0.15
	TA	1.00	1.00	1.00	1.00
	CB	10.13	8.19	0.76	0.61
PE665	SC	3.81	3.70	1.45	1.41
	TA	1.00	1.00	1.00	1.00
	CB	7.17	3.87	1.18	1.09
YO52/10	SC	131.51	45.19	50.04	0.08
	TA	1.00	1.00	1.00	1.00
	CB	3.14	1.28	0.52	0.35

Figure 23. Relative qRT-PCR analysis of RARRES1 and LXN expression in enriched subpopulations from primary prostate epithelial cultures.
Relative qRT-PCR data showing average fold change in **(a, c)** RARRES1 and **(b, d)** LXN gene expression relative to a RPLP0 internal control in SC, TA and CB populations, derived from BPH (n=6) (a, b) and CaP (n=6) (c, d) epithelial cultures. Average expression denoted by a horizontal line (Blue: BPH; Red: CaP). **(e)** Table showing range of C_T values for 12 endogenous control genes between SC, TA and CB populations from a number of patient samples obtained by qRT-PCR. HUWE1 shows the least variation in C_T value (pink). **(f)** Table showing the relative expression of RARRES1 and LXN between SC, TA and CB populations using RPLPO or HUWE1 as endogenous control genes. Table shows higher expression (pink) or lower expression (blue) in SC compared to TA populations.
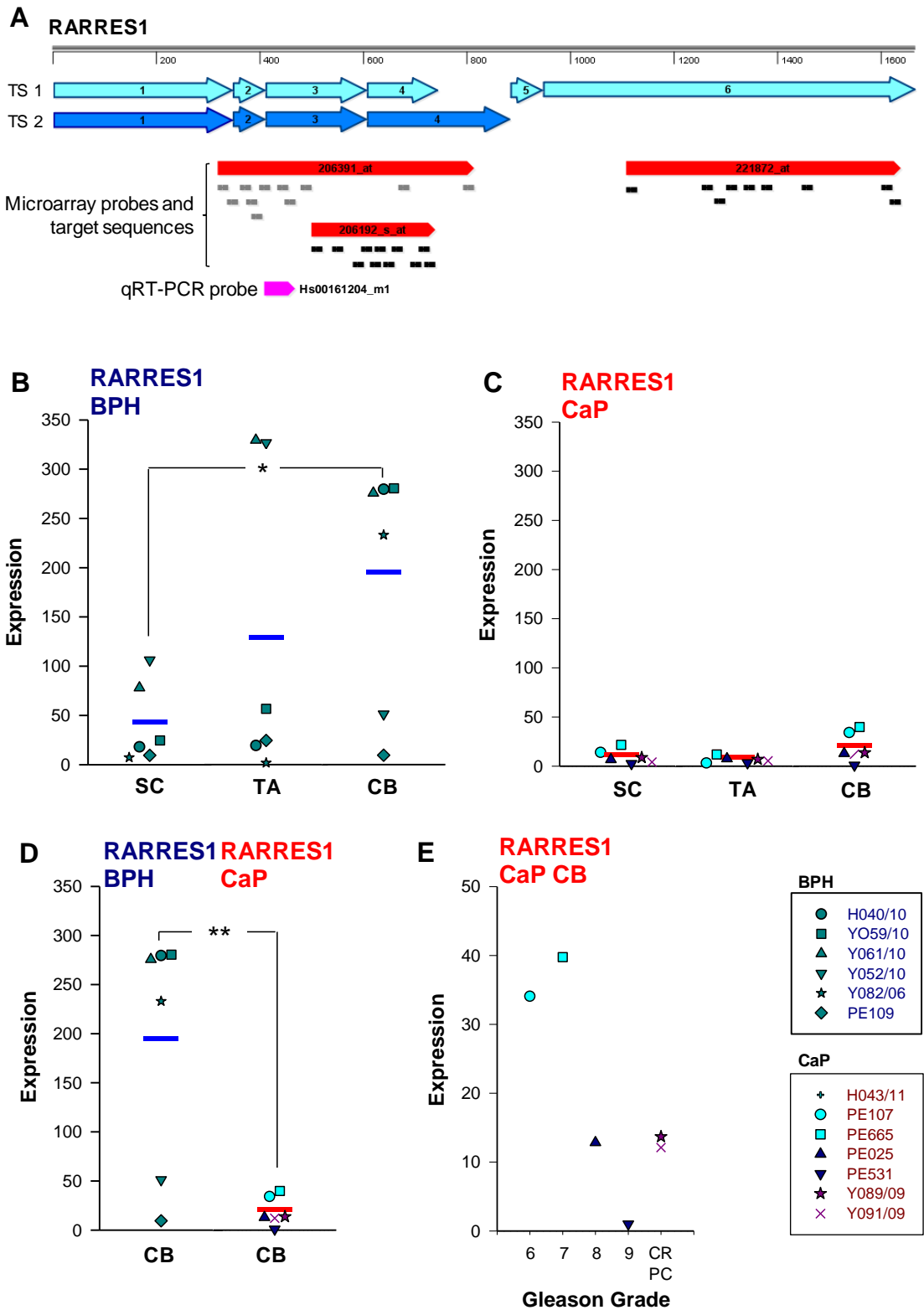
Figure 24. Absolute qRT-PCR analysis of RARRES1 expression in enriched sub-populations from primary prostate epithelial cultures.
(a) Diagrams depicting the relative location of primers used for microarray and qRT-PCR analysis within the RARRES1 gene. Each exon is depicted by a numbered arrow. **(b)** Absolute gene expression of RARRES1 in SC, TA and CB populations derived from BPH (n=5) and **(c)** CaP (n=6). **(d)** Expression values of RARRES1 in CB cells derived from BPH and CaP were plotted on the same scale for comparison. **(e)** Correlation of CaP Gleason grade with expression in CB cells. Average expression denoted by a horizontal line (Blue: BPH; Red: CaP). Statistical significance values were measured by the Mann-Whitney test (* $p < 0.05$, ** $p < 0.01$).
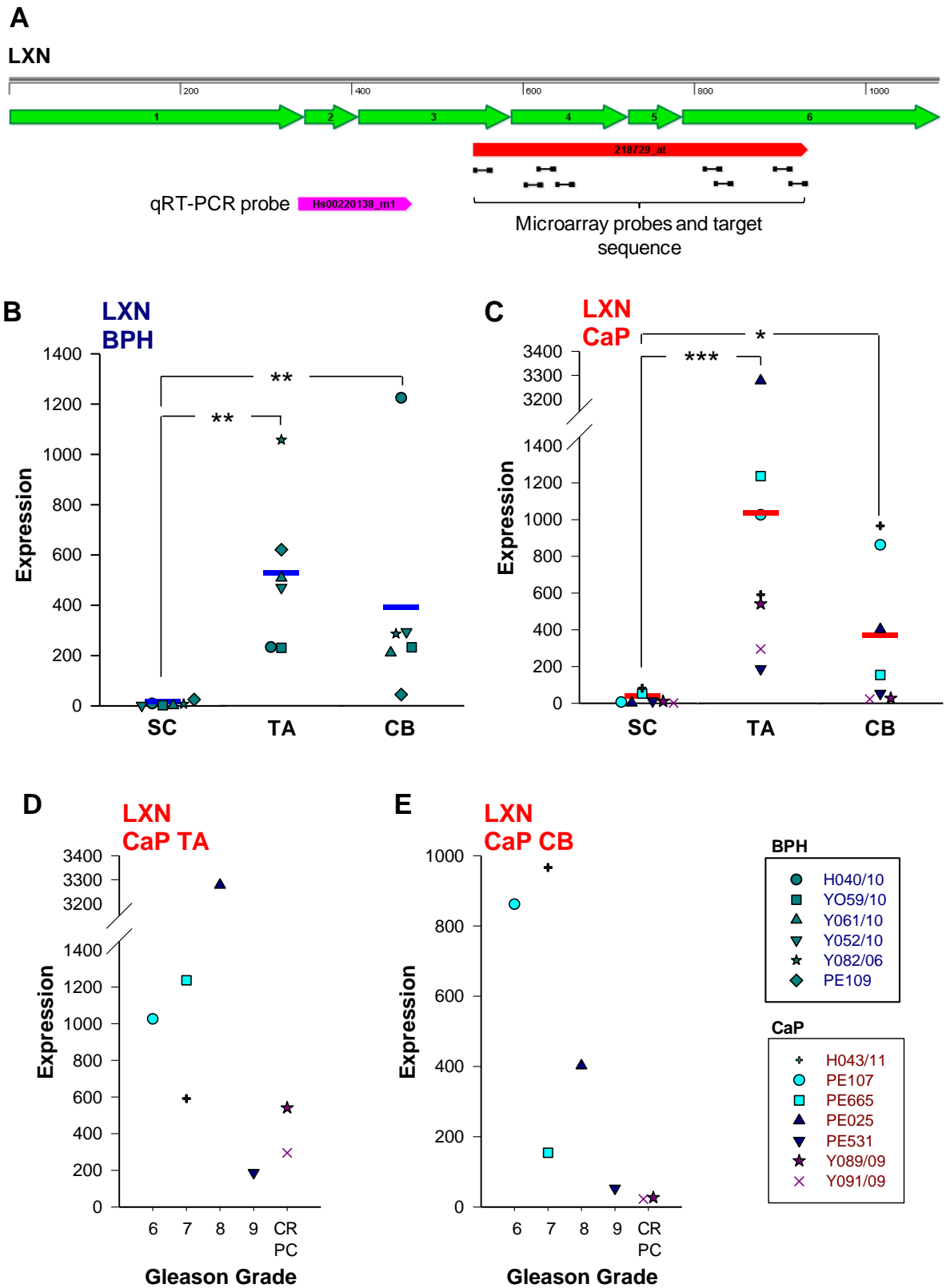
Figure 25. Absolute qRT-PCR analysis of LXN expression in enriched sub-populations from primary prostate epithelial cultures.
(a) Diagram depicting the relative location of primers used for microarray and qRT-PCR analysis within the LXN gene. Each exon is depicted by a numbered arrow. **(b)** Absolute gene expression of LXN in SC, TA and CB populations derived from BPH (n=5) and **(c)** CaP (n=6). **(d)** Correlation of CaP Gleason grade with expression in TA and **(e)** CB cells. Average expression denoted by a horizontal line (Blue: BPH; Red: CaP). Statistical significance values were measured by the Mann-Whitney test (* p<0.05, ** p<0.01).

3.2.3. Protein expression of RARRES1 and LXN is low in primary prostate epithelial cultures enriched for stem cells

Since RARRES1 and LXN mRNA was expressed at significantly lower levels in SC than TA and CB cultures, from BPH and CaP, protein expression of RARRES1 and LXN was next measured in SC, TA and CB populations from malignant (H103/11) and non-malignant BPH (H094/11) primary prostate epithelial cultures, by fluorescence microscopy.

Overall, the expression of RARRES1 (Figure 26a) and LXN (Figure 26b) emulated the pattern seen at the mRNA level; expression was low in SCs and increased through differentiation. The majority of cells in the SC population derived from BPH and CaP cultures did not express RARRES1. Around 25% of cells from both samples showed weak staining for RARRES1. Almost all cells from the TA and CB populations derived from BPH demonstrated a more intense cytoplasmic expression of RARRES1.

In the SC population derived from BPH and CaP cultures, LXN expression was absent or at very low levels in around 50% of cells, and expressed, but still at low levels in the other 50%. Only one anomalous SC from the BPH culture showed high levels of LXN expression that was located to the nucleus and cytoplasm. In parallel with the mRNA expression data, LXN expression was at its highest in the TA population in both cultures. Furthermore, expression was higher in the TA population derived from CaP than BPH. In all cells tested, except the anomalous SC, LXN expression was localised to the nucleus of primary prostate epithelial cultures.

Taken together, RARRES1 and LXN protein is expressed at lower levels in SC, than TA and CB cultures, from BPH and CaP. Interestingly, when expressed, RARRES1 shows cytoplasmic expression, but LXN is located in the nucleus within the primary prostate epithelial hierarchy.

A RARRES1

B LXN

C
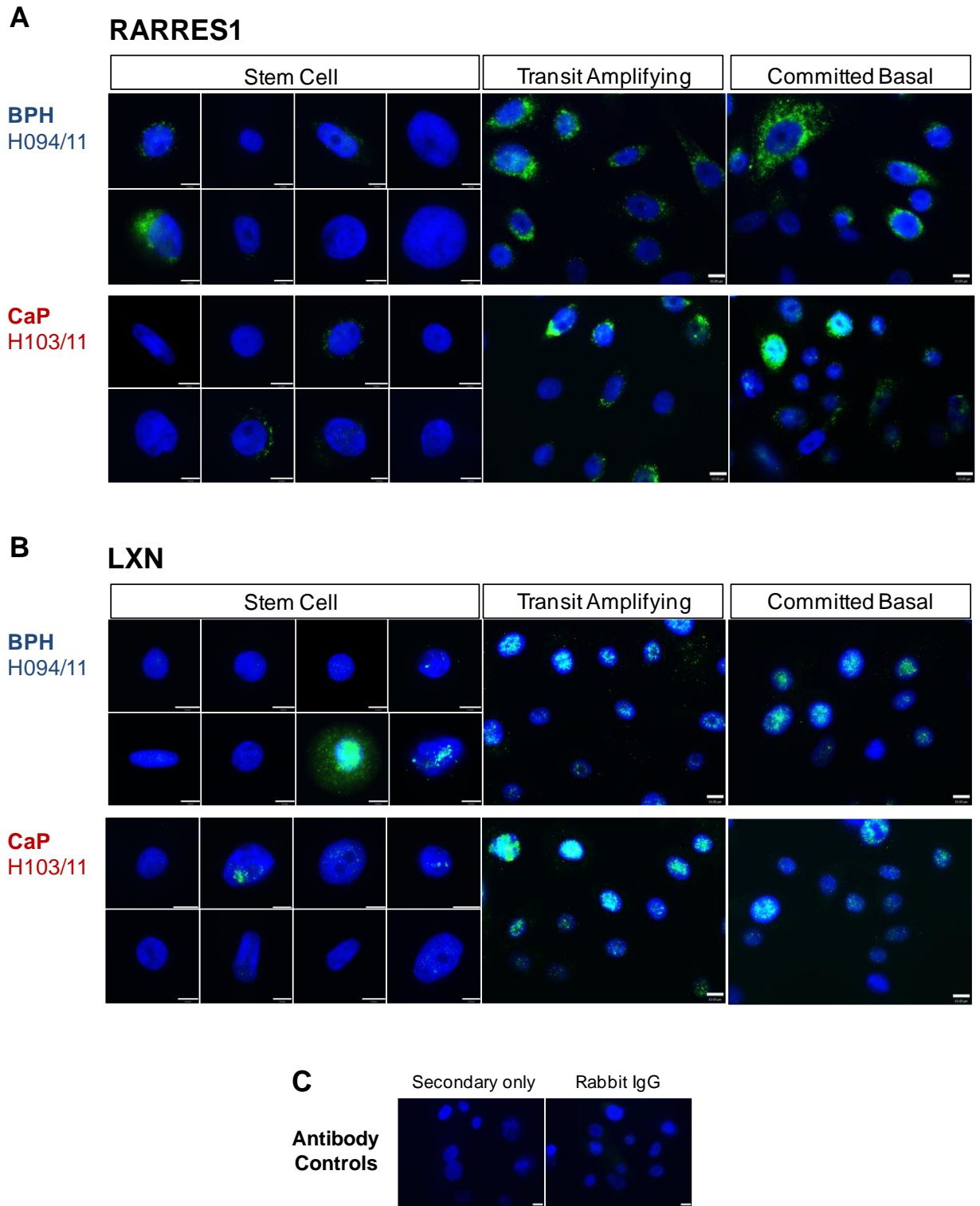
Figure 26. Immunofluorescence images of RARRES1 and LXN expression in enriched sub-populations from primary prostate epithelial cultures.
(a) RARRES1 and **(b)** LXN expression was detected by immunofluorescence in SC, TA and CB cells derived from BPH (H094/11) and CaP (H103/11) epithelial cultures. Cells were counterstained with DAPI to enable nuclear visualisation. White scale bar represents 10 µm. **(c)** Antibody controls using Rabbit IgG, instead of primary antibody and secondary antibody only.

3.3. Regulation of RARRES1, LXN and CPA4 by histone acetylation

3.3.1. CPA4 Expression is induced by HDAC inhibitors in prostate epithelial cell lines

CPA4 was initially identified as a gene induced by NaBu in the PC3 cell line (Huang et al., 1999). Along with TSA, NaBu is a well characterised general HDACI and chromatin remodeller, which functions to relax chromatin by inducing the acetylation of histones, leading to transcriptional activation of a small number of genes. To investigate whether CPA4 was potentially regulated by chromatin structure in a larger panel of prostate epithelial cell lines, and to determine if RARRES1 and LXN were regulated in the same way, a panel of benign prostate and prostate cancer cell lines were treated with 0.6 µM TSA or 10 mM NaBu for 48 hours. RNA was extracted from cells and mRNA expression levels of RARRES1, LXN and CPA4 were quantified using qRT-PCR.

Results showed that treatment with TSA and NaBu induced CPA4 expression in all benign and cancer cell lines. CPA4 expression was significantly induced by NaBu in PNT2-C2 (84-fold), P4E6 (23-fold) and PC3 (53-fold) cell lines but not in the LNCaP cell line (2-fold increase) (Figure 27a). The more potent HDACI, TSA, significantly induced CPA4 in all cell lines tested and increased expression to a greater extent than NaBu in PC3 and LNCaP cell lines (PNT2-C2: 71-fold; P4E6: 4-fold; PC3: 166-fold; LNCaP: 277-fold) (Figure 27d).

In contrast to CPA4, the mRNA expression of RARRES1 and LXN showed no significant increase after HDAC inhibition with NaBu (Figure 27b, c), or TSA (Figure 27e, f). In the majority of cell lines tested, RARRES1 and LXN expression decreased or remained constant after treatment with both HDACIs. The exception was LXN expression in P4E6 cells after treatment with NaBu (Figure 27c), where LXN expression increased after treatment. Taken together, these results indicate that CPA4 may be regulated by chromatin structure, in particular by histone acetylation.
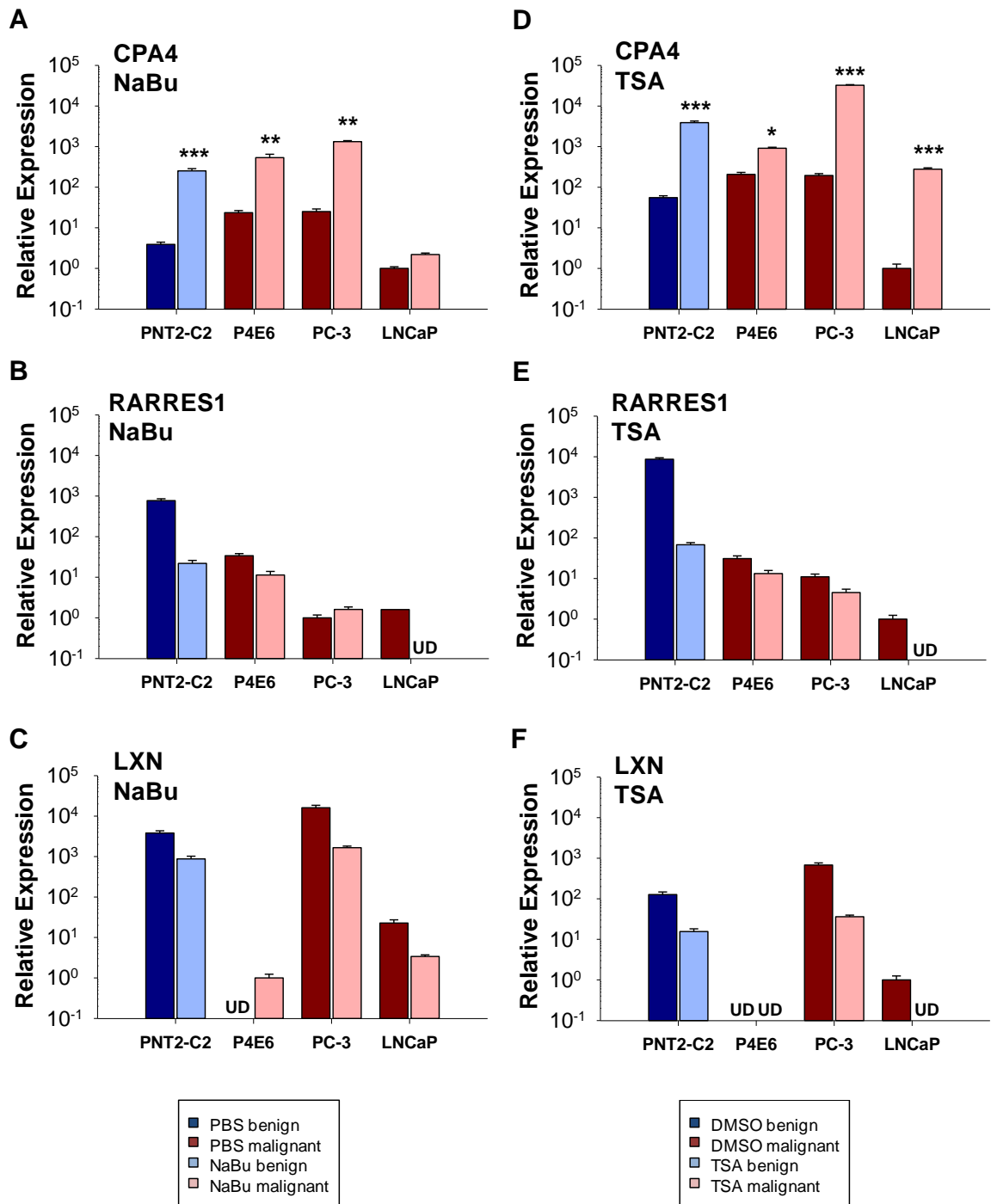
Figure 27. qRT-PCR analysis of RARRES1, LXN and CPA4 expression after treatment of prostate epithelial cell lines with HDAC inhibitors.

mRNA expression of **(a, d)** CPA4, **(b, e)** RARRES1 and **(c, f)** LXN was analysed in benign (PNT2-C2) and cancer (P4E6, PC3 and LNCaP) cell lines after treatment with 10 mM NaBu or 0.6 µM TSA for 48 hours. Expression was relative to a GAPDH control gene and plotted on a $\log_{10}$ scale to enable optimal visualisation; UD: expression undetectable after 40 cycles; error bars expressed as standard deviation of n=2 biological replicates. Statistical significance values were measured by the Student's T-test (Unpaired, two-tailed; * p<0.05, * p<0.01, *** p<0.001).

3.3.2. CPA4 expression is induced by HDAC inhibitors in primary prostate epithelial cultures

CPA4 expression was induced by HDACIs in prostate epithelial cell lines. To determine whether CPA4 expression was also induced by HDAC inhibition in primary prostate epithelial cultures, a panel of BPH (n=3) and CaP (n=3) primary prostate epithelial cultures were treated with the same HDACIs, under the same conditions as in cell lines: 0.6 µM TSA and 10 mM NaBu for 48 hours. RNA was extracted from cells and mRNA expression levels of CPA4 were quantified using qRT-PCR. RARRES1 and LXN expression was not examined in primary cultures as no induction of expression was seen in cell lines after treatment.

All BPH and CaP samples analysed showed a clear increase in CPA4 expression after treatment with both NaBu (Figure 28a) and TSA (Figure 28b), although the effect was not statistically significant due the high patient variability between samples. Average CPA4 expression after NaBu treatment was lower in BPH cultures (14-fold) compared to CaP cultures (36-fold). Average induction of CPA4 expression after TSA treatment was also lower in BPH cultures (8-fold) compared to CaP cultures (10-fold). Similar to the results seen in cell lines, basal cells were able to induce CPA4 to a higher level after NaBu treatment than after TSA treatment. However, the fold change of CPA4 after treatment was low, in comparison to the high magnitude of changes seen in cell lines.

Taken together, these results show that CPA4 may be regulated by chromatin structure, in particular by histone acetylation in primary prostate epithelial cultures as well as in prostate epithelial cell lines.
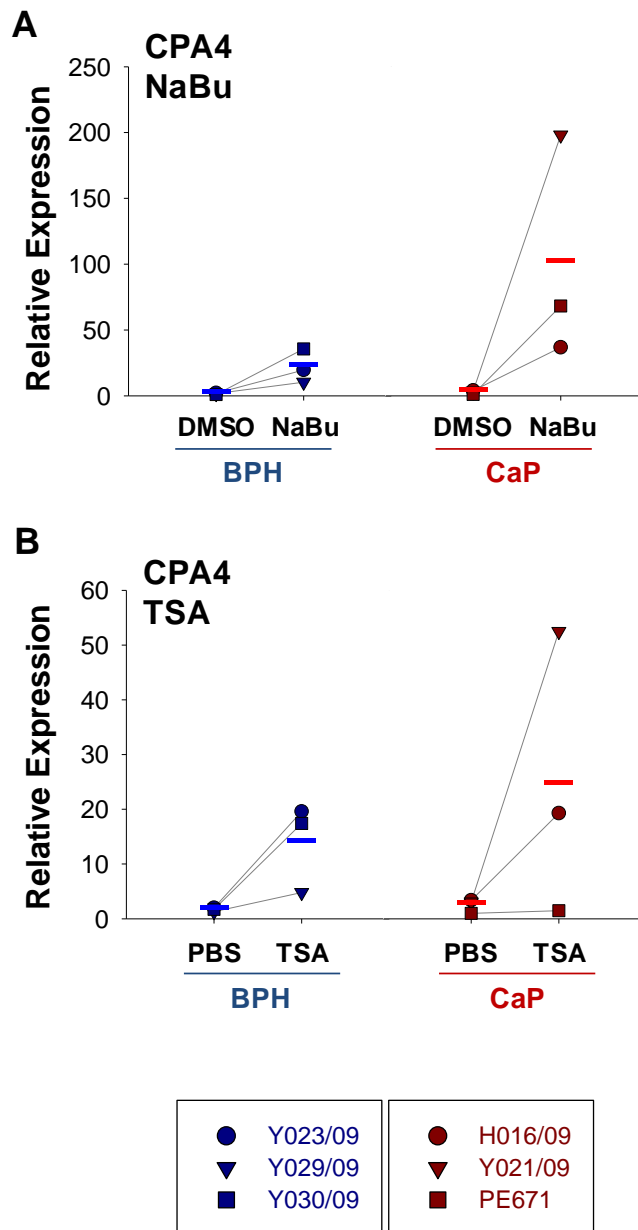
Figure 28. qRT-PCR analysis of CPA4 expression after treatment of primary prostate epithelial cultures with HDAC inhibitors.
mRNA expression of CPA4 was analysed in primary prostate epithelial cultures derived from BPH (n=3) or CaP (n=3) after treatment with **(a)** 10 mM NaBu or **(b)** 0.6 µM TSA for 48 hours. Expression was relative to a GAPDH control gene. Average expression is denoted by a horizontal line (Blue: BPH; Red: CaP). Lines join each sample to highlight the trend in expression with and without treatment.

3.3.3. CPA4 expression is regulated by chromatin structure in prostate epithelial cell lines

CPA4 expression was induced by HDACIs in prostate epithelial cell lines and primary prostate epithelial cultures. To directly determine whether CPA4 was regulated by chromatin structure, the chromatin status of the CPA4 promoter and gene body was determined by chromatin immunoprecipitation (ChIP) on a panel of cell lines (Figure 29a). Regions of active (euchromatin) and inactive chromatin (heterochromatin) were immunoprecipitated, using antibodies specific for the dimethylation of lysine 4 of histone H3 (H3K4Me2; euchromatin) or the trimethylation of lysine 27 of histone 3 (H3K27Me3; heterochromatin). DNA fragments were amplified by qPCR using specific primers spanning the CPA2 gene, CPA4 promoter and CPA4 gene (Figure 29b). Total histone 3 (H3), which is a core component of chromatin and is bound to the majority of DNA sequences in the genome, and negative IgG control antibodies were used as a positive and negative controls, respectively.

All cell lines tested showed an enrichment for active chromatin (H3K4Me2) within the CPA4 promoter, but PNT2-C2 cells showed the highest enrichment (0.16) compared to 0.05 in PC3 and LNCaP cells, which correlated with the high expression of CPA4 seen in this cell line. This maximum enrichment in PNT2-C2 cells was seen with the ChIP3 primer set, which is located around 2300 bp upstream of the CPA4 transcription start site.

The inactive chromatin mark (H3K27Me3) showed a maximum enrichment of 0.12 in the LNCaP cell line, which correlated with the low level of CPA4 transcriptional activity in these cells. In contrast, PNT2-C2 and PC3 cells express CPA4 to higher levels and showed a very low enrichment of only 0.01 for the inactive chromatin mark.

Taken together, these results suggest that changes in chromatin structure can result in changes in gene expression of CPA4; the highest expressing cells (PC3 and PNT2-C2) showed the highest levels of euchromatin, but the lowest expressing cell line (LNCaP) had the highest enrichment for heterochromatin.
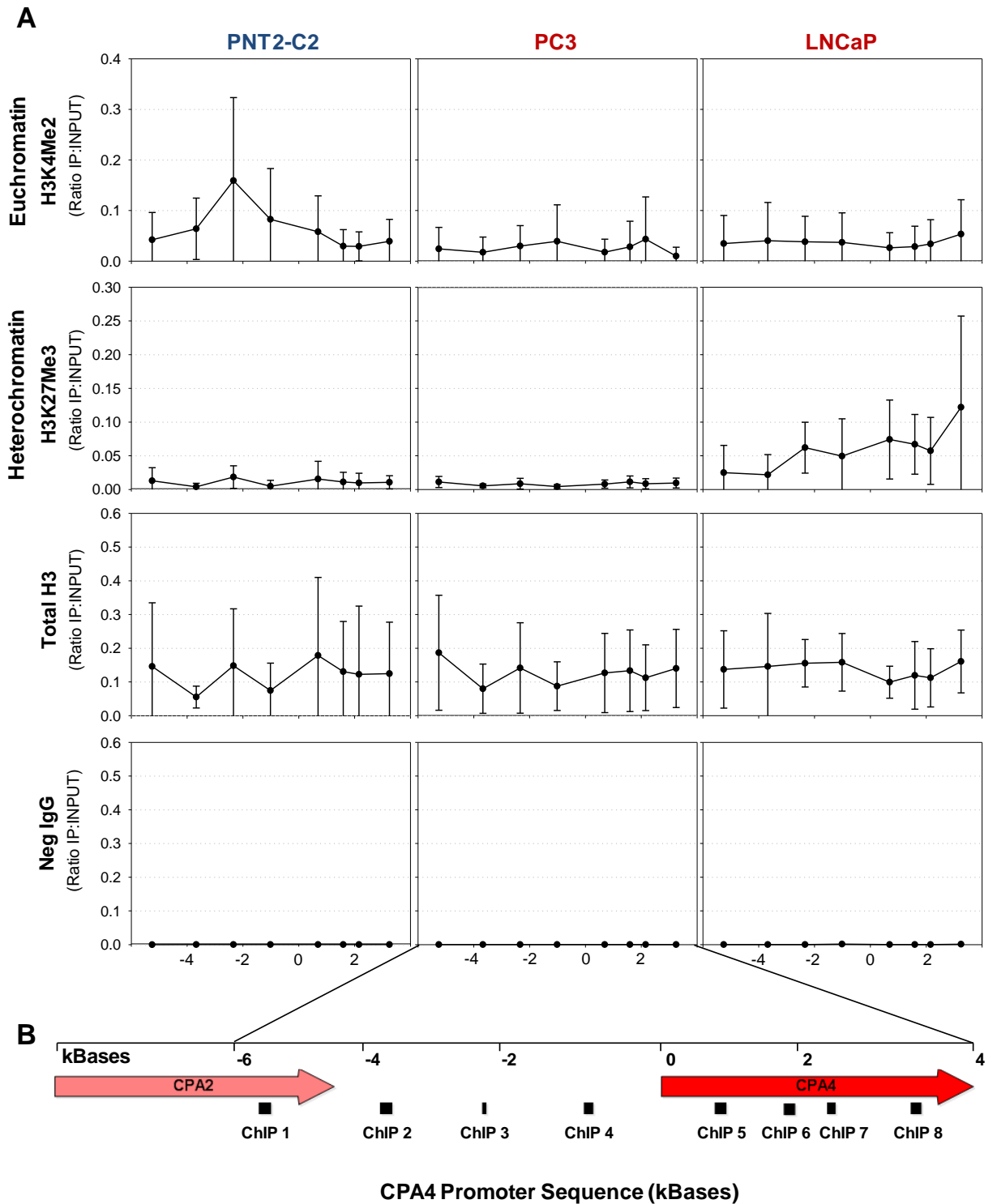
Figure 29. ChIP-qPCR analysis of CPA4 chromatin in prostate epithelial cell lines.
(a) Chromatin immunoprecipitation of CPA4 and its promoter using anti–histone H3 control (Total H3), anti-H3K4me2 (euchromatin), anti-H3K27me3 (heterochromatin) and rabbit IgG control (Neg IgG) antibodies in benign (PNT2-C2) and cancer (PC3, LNCaP) cell lines. **(b)** The position of primers used for qPCR, with respect to CPA4 and CPA2. X axes: CPA4 promoter sequence, 0 kB: CPA4 transcription start site; Y axes: ratio of immunoprecipitated DNA relative to input DNA; error bars expressed as standard deviation of n=4 biological replicates.

3.4. Regulation of RARRES1, LXN and CPA4 by DNA methylation

3.4.1. RARRES1 and LXN expression is induced by a DNA demethylating agent in prostate epithelial cell lines

RARRES1 had previously been shown to be silenced by DNA methylation in human cancers including CaP (Youssef et al., 2004; Zhang et al., 2004) and expression was induced by a DNA demethylating agent in a number of cell lines (Youssef et al., 2004), including PC3 and LNCaP (Zhang et al., 2004). To investigate whether LXN and CPA4 were also induced by a DNA demethylating agent, a panel of benign prostate and CaP epithelial cell lines were treated with 1 µM 5-Aza-dC for 96 hours. RNA was extracted and mRNA expression changes of RARRES1, LXN and CPA4 were quantified using qRT-PCR.

Treatment with 5-Aza-dC induced RARRES1 expression significantly in all cancer cell lines tested (P4E6: 78-fold; PC3: 37-fold; LNCaP: expression became detectable) (Figure 30a). Treatment with 5-Aza-dC induced LXN expression significantly in two out of three cancer cell lines tested (P4E6: 8045-fold; LNCaP: 92-fold), but not in the PC3 cell line, where LXN was over-expressed at basal levels (Figure 30b). In the benign PNT2-C2 cell line, a decrease in RARRES1 expression and a marginal increase in LXN expression (2-fold) was seen after 5-Aza-dC treatment.

In contrast to RARRES1 and LXN, treatment with 5-Aza-dC induced CPA4 expression marginally (to a maximum of 3-fold) in all benign and cancer cell lines (Figure 30c). However, this was: (1) not significant, (2) not the magnitude of fold change we would expect to see of a gene regulated by DNA methylation or (3) as high as the expression changes seen after HDACI treatment.

Taken together, these results suggest that RARRES1 and LXN are regulated by DNA methylation in CaP epithelial cell lines. However, they also suggest that CPA4 expression is regulated by chromatin structure, but not DNA methylation.
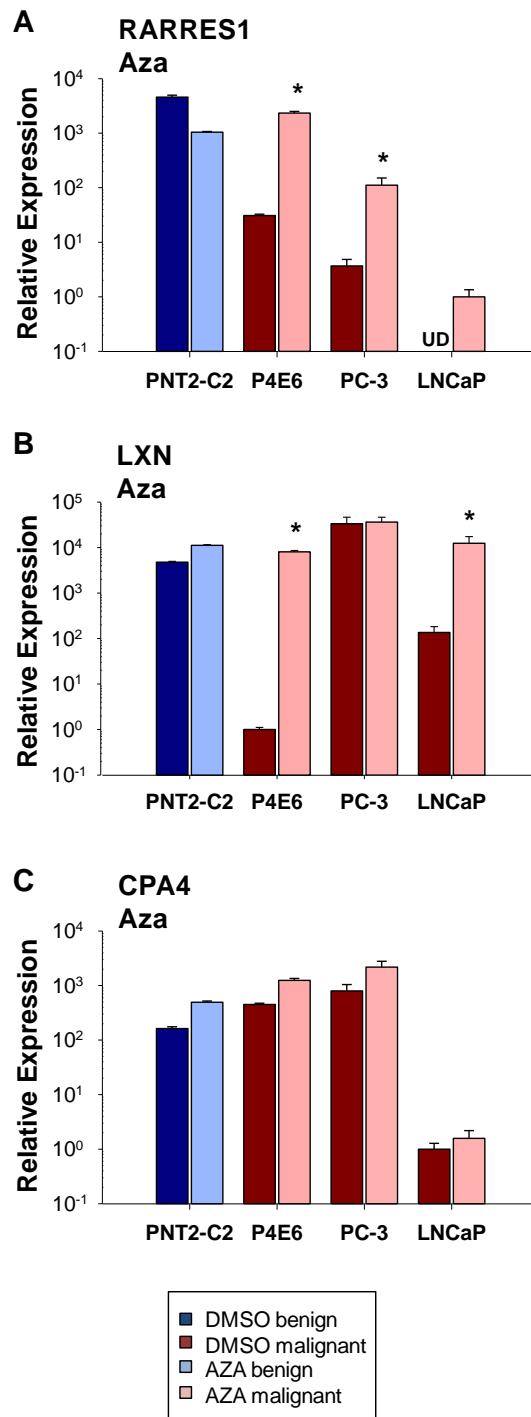
Figure 30. Analysis of RARRES1, LXN and CPA4 expression after treatment with a DNA demethylating agent in prostate epithelial cell lines.
mRNA expression of **(a)** RARRES1, **(b)** LXN and **(c)** CPA4 was analysed in benign (PNT2-C2) and cancer (P4E6, PC3 and LNCaP) cell lines, after treatment with 1 µM 5-Aza-dC (AZA) for 96 hours. Expression was relative to a GAPDH control gene and plotted on a $\log_{10}$ scale to enable optimal visualisation; UD: expression undetectable after 40 cycles; error bars expressed as standard deviation of n=2 biological replicates. Statistical significance values were measured by the Student's T-test (Unpaired, two-tailed; * $p < 0.05$).

3.4.2. RARRES1 and LXN expression is induced by a DNA demethylating agent in primary prostate epithelial cultures

RARRES1 and LXN expression was induced by a DNA demethylating agent in CaP epithelial cell lines. To determine whether RARRES1 and LXN expression was also induced by DNA demethylating treatment in primary prostate epithelial cultures, BPH (n=3) and CaP (n=3) primary cultures were treated with the same DNA demethylating agent, under the same conditions as in cell lines: 1 μM 5-Aza-dC for 96 hours. RNA was extracted from cells and mRNA expression levels of RARRES1 and LXN were quantified using qRT-PCR. CPA4 expression was not examined in primary cultures, as no induction of expression was seen in cell lines after treatment.

All BPH and CaP samples analysed showed an increase in RARRES1 expression after treatment though the effect was not statistically significant due the high patient variability between primary samples (Figure 31a). A differential effect between BPH and CaP was seen with the average RARRES1 increase being considerably higher in CaP cultures (14-fold), compared to BPH cultures (2-fold) after 5-Aza-dC treatment, though this was predominantly due to one CaP sample (PE671). In contrast, there was no difference in the average LXN expression after 5-Aza-dC treatment in both BPH and CaP cultures (Figure 31b). Moreover, unlike RARRES1, only two out of three BPH and two out of three CaP samples showed an increase in LXN expression after treatment.

Taken together these results suggest that LXN is not regulated by DNA methylation in primary prostate epithelial cultures, but RARRES1 may be in specific CaP samples.
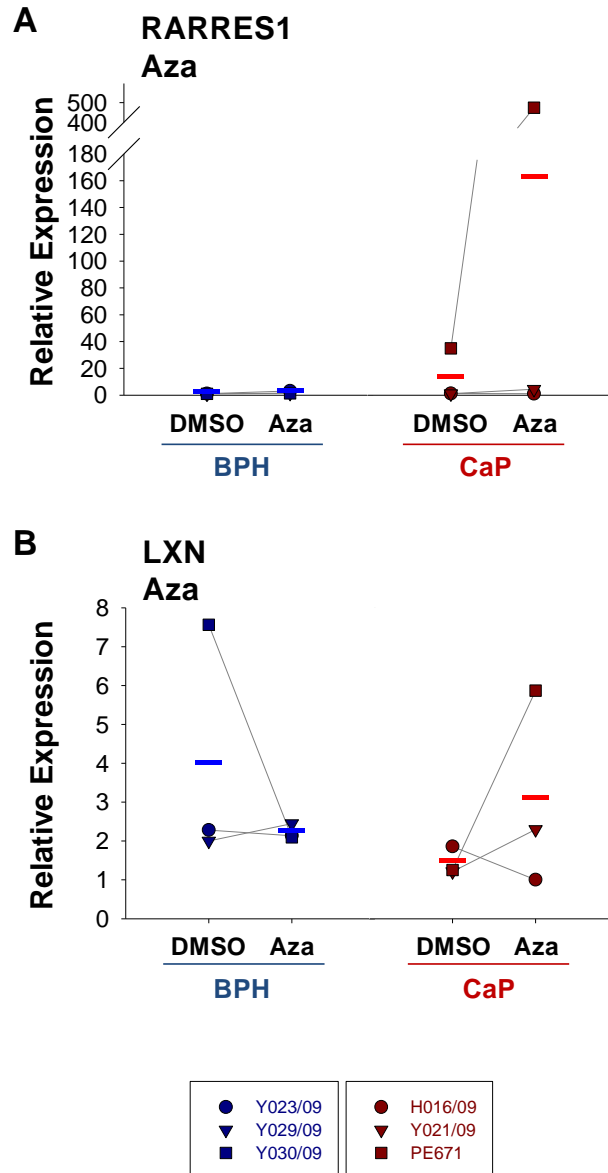
Figure 31. qRT-PCR analysis of RARRES1 and LXN expression after treatment of primary prostate epithelial cultures with a DNA demethylating agent.
mRNA expression of **(a)** RARRES1 and **(b)** LXN was analysed in primary epithelial cell cultures derived from BPH (n=3) or CaP (n=3), after treatment with 1 µM 5-Aza-dC (AZA) for 96 hours. Expression was relative to a GAPDH control gene; UD: expression undetectable after 40 cycles. Average expression denoted by a horizontal line (Blue: BPH; Red: CaP). Lines join each sample to highlight the trend in expression with and without treatment.

3.5. Pyrosequencing analysis of regulation of RARRES1 and LXN by DNA methylation

3.5.1. RARRES1 and LXN expression is repressed by DNA methylation in malignant prostate epithelial cell lines

Expression of RARRES1 and LXN was induced by a DNA demethylating agent in cancer cell lines. To determine whether RARRES1 and LXN could be directly marked by 5mC DNA methylation, the presence and location of CpG islands fitting specific criteria within each gene and their promoters was determined, using the EMBOSS CpG Plot software (Figure 32): (1) the observed-to-expected CpG ratio was greater than 0.6, (2) the percentage of GC dinucleotides was greater than 50% and (3) the CpG island was greater than 50 bp in length. The methylation of CPA4 was not determined, as no effect on expression was seen after treatment with a DNA demethylating agent. RARRES1 contained two CpG islands 16 bp apart, which were located upstream of the transcription start site and within exon 1 of the gene, spanning 255 bp and 581 bp, respectively. LXN contained one smaller 151 bp-long CpG island, within exon 1 of the gene.

The extent of DNA methylation surrounding the promoters of RARRES1 and LXN was quantified by pyrosequencing (Section 2.7.6), using assays designed within these CpG islands, spanning 11 and 6 CpG sites, respectively, in a panel of benign and CaP cell lines. The nucleotide sequence was determined from the signal peaks in the Pyrogram trace and the percentage methylation at each CpG site plotted on a bar chart (Figure 33a). Built-in quality controls to ensure the DNA had been fully bisulphite-converted were also performed (Figure 33b). Pyrosequencing was used as it is regarded as the gold-standard for DNA methylation analysis, as: (1) it is a highly sensitive technique, (2) it has the ability to quantify individual, consecutive CpG sites, (3) it enables the analysis of minimal changes in methylation levels and (4) it has a low rate of false positives.

To determine the specificity of the pyrosequencing assays, 100% methylated and 0% methylated EpiTect human control bisulphite-converted DNA (Qiagen) were utilised. Average methylation levels of RARRES1 (Figure 34a) and LXN (Figure 34b) in the 0% methylation control DNA were 4.2% and 5.2%, respectively. In the 100% methylation control DNA, methylation of RARRES1 was 88.0% and LXN was 76.7%. These results show that both assays were specific, with the RARRES1 assay having a broader range than the LXN assay. A cell line was described as being significantly hypermethylated if the average percentage of methylation was significantly more than that seen in the 0% methylated control DNA.

The RARRES1 promoter was significantly hypermethylated in three out of seven cancer cell lines: P4E6 (6%), PC3 (11%) and LNCaP (73%), but not in the majority of benign cell lines (Figure 35a). The exception was the benign PNT1a cell line, which was also significantly hypermethylated, although the average methylation was low at 6%. The LXN promoter was

significantly hypermethylated in four out of seven cancer cell lines: P4E6 (82%), DU145 (55%), Serbob (23%) and LNCaP (64%), but not in the majority of benign cell lines (Figure 35b). The exceptions were the benign PNT2-C2 (27%) and BPH-1 (8%) cell lines, which were also significantly hypermethylated, although the average methylation was low.

To confirm that the pyrosequencing technique was working correctly and that the cancer cell lines were truly cancerous, average percentage methylation levels of a GSTP1 control gene, in the same cell lines, were obtained from Dr. Davide Pellacani (Figure 35c). GSTP1 was chosen as a positive control for DNA methylation as it one of the most hypermethylated genes in CaP (Tokumaru et al., 2004). These results showed that GSTP1 was hypermethylated in four out of seven cancer cell lines, and showed the highest levels of methylation (95%) in the most luminal cell lines (VCaP and LNCaP).

A direct comparison of the expression of RARRES1 and LXN with the extent of DNA methylation confirmed that hypermethylation of RARRES1 (Figure 36a) and LXN (Figure 36b) correlated with a down-regulation of expression. Cell lines expressing high levels of mRNA (PNT2-C2) had low levels of promoter methylation, but the cell line with the lowest levels of mRNA (LNCaP) had the highest levels of promoter methylation of both RARRES1 and LXN.

Taken together, these results confirm that the expression of both RARRES1 and LXN is repressed by DNA methylation in CaP cell lines.
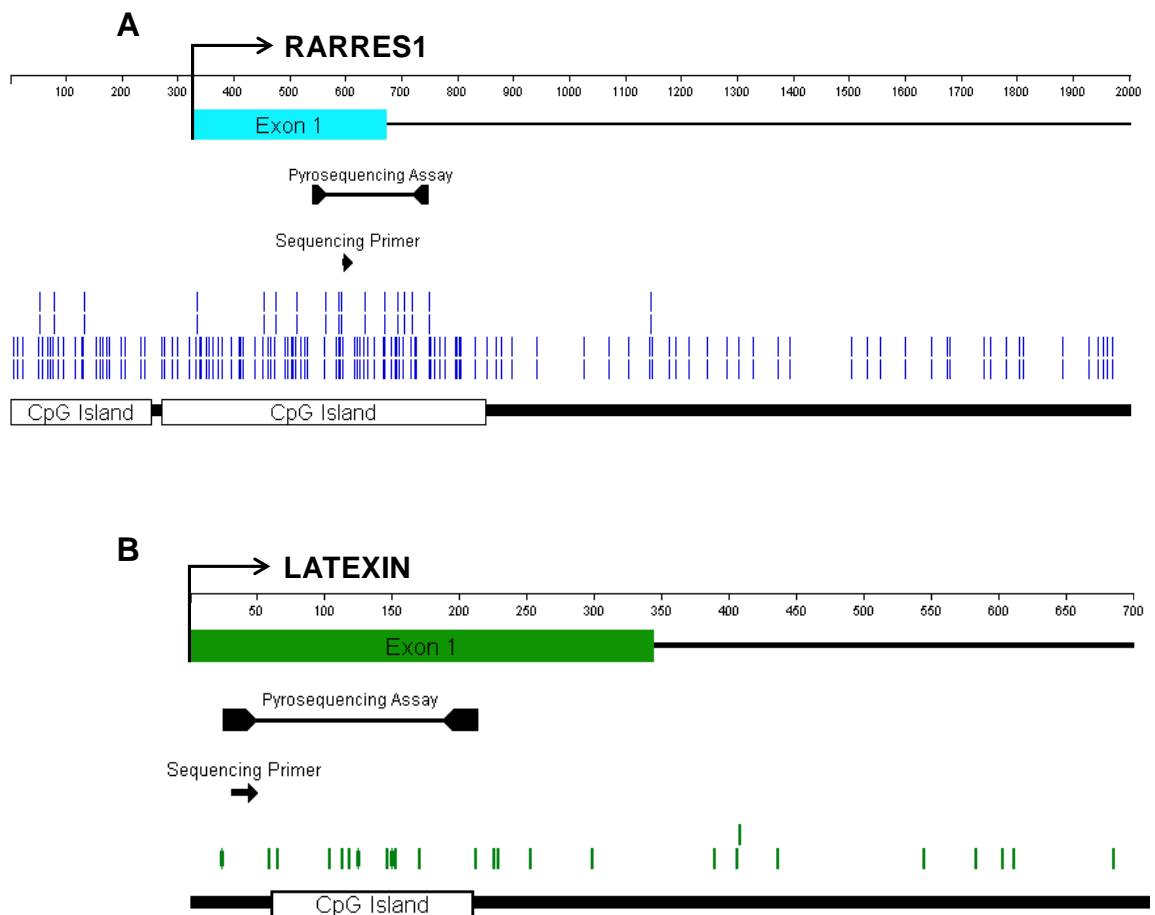
Figure 32. Location of CpG islands within the RARRES1 and LXN promoters.
(a) Diagram depicting the location of the CpG islands, relative to exon 1 of the RARRES1 and **(b)** LXN genes, identified by bioinformatics analysis using the EMBOSS CpGPlot software. PCR primers and sequencing primers used for pyrosequencing analysis are shown. Individual CpG sites are depicted by blue (RARRES1) or green (LXN) vertical lines.
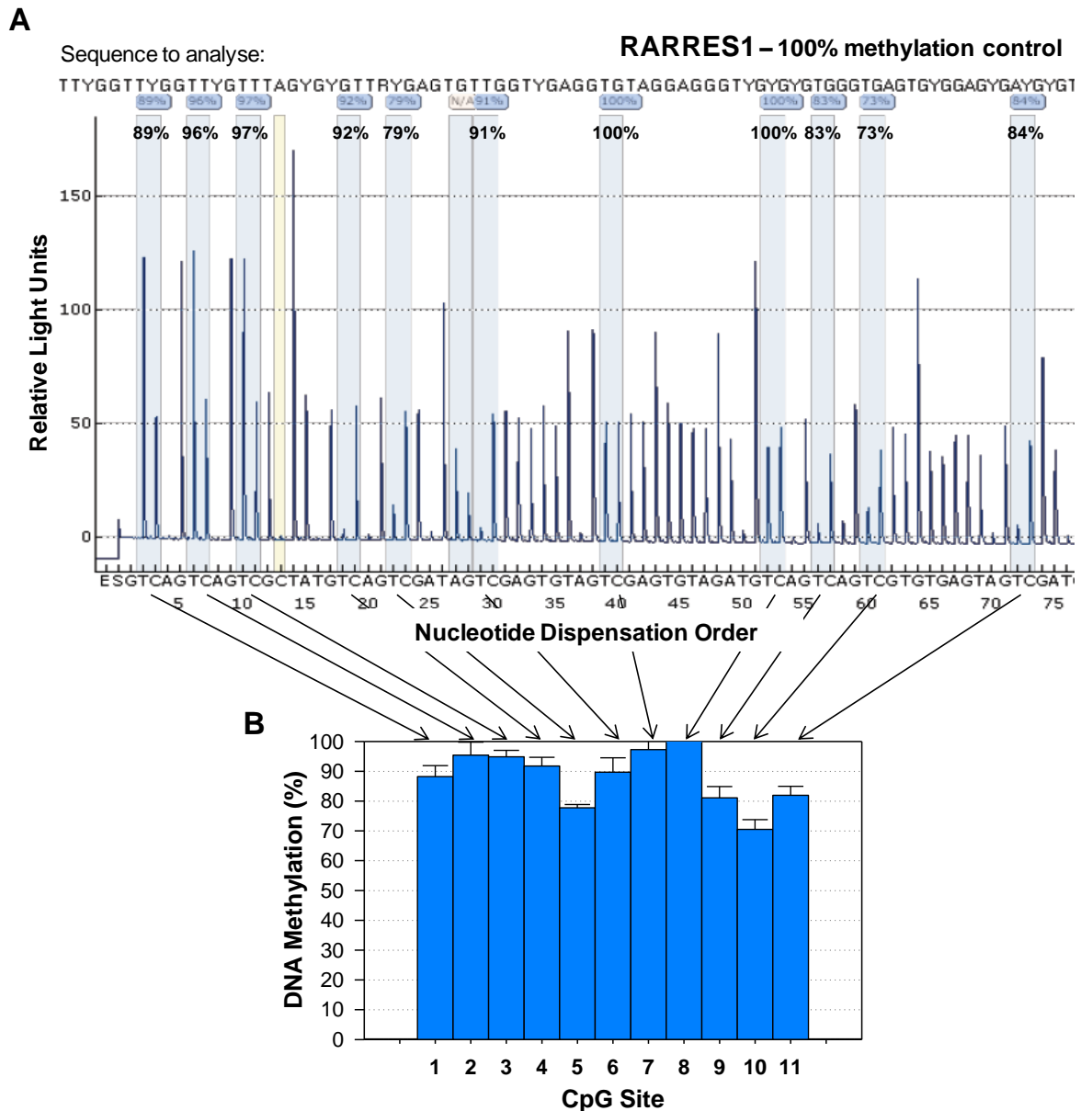
Figure 33. Representative pyrogram and bar chart showing levels of CpG methylation using pyrosequencing.
(a) Pyrosequencing pyrogram trace, produced by the PyroMark Q24 software, after analysis of the RARRES1 CpG island in 100% methylated control DNA. Highlighted areas in the trace indicate CpG positions (light blue) and built-in bisulphite treatment controls (C not followed by G; yellow shading). The methylation level of each CpG site is indicated in boxes above the trace. The software calculates the percentage of methylated C by quantifying the extent of C and T at each CpG site, post bisulphite conversion (indicate methylated C and unmethylated C, respectively). **(b)** Representative graphs show the percentage of promoter methylation at each CpG site as quantified by the pyrogram trace, calculated by the PyroMark Q24 software. Bars = individual CpG sites; black line = average of all individual CpG sites; error bars expressed as standard deviation of n=3 technical replicates.
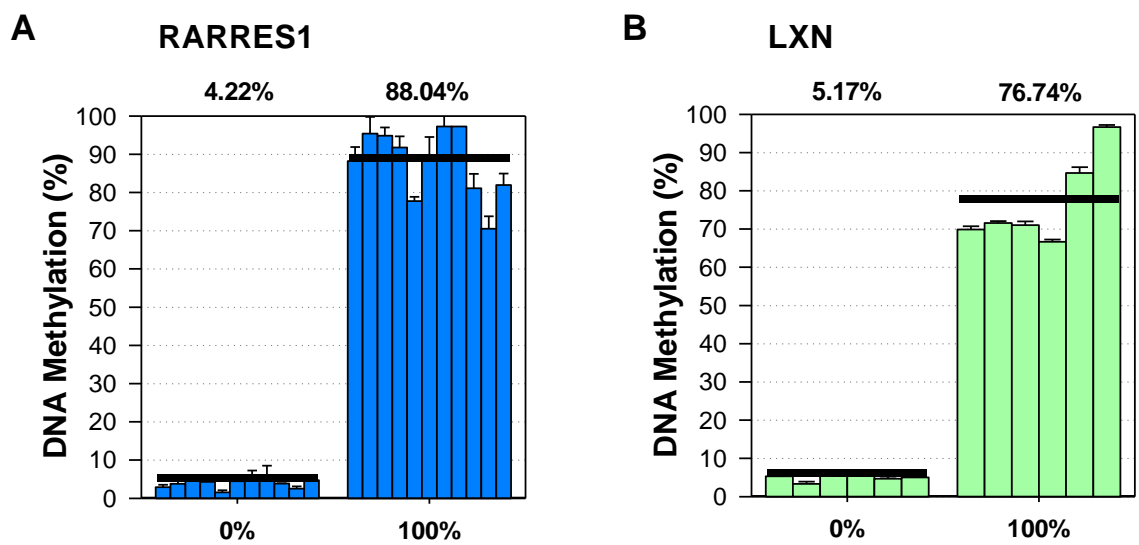
Figure 34. Pyrosequencing analysis of the CpG islands within the RARRES1 and LXN genes in 0% and 100% methylated control DNA.
(a) The percentage promoter methylation of RARRES1 and **(b)** LXN in 0% and 100% methylated control DNA. Bars = single CpG sites; black line = average of individual CpG sites; error bars expressed as standard deviation of n=3 technical replicates.
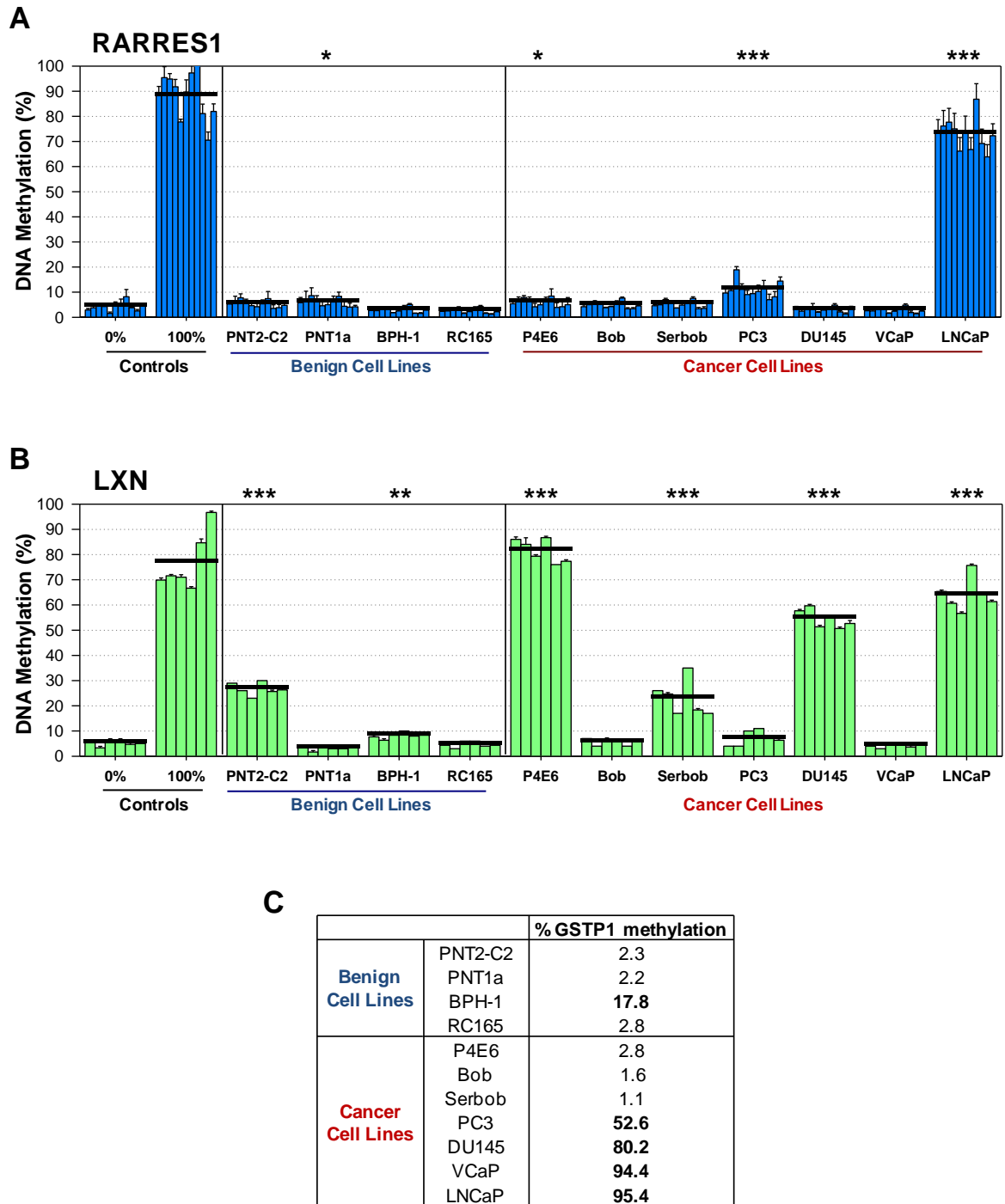
Figure 35. Pyrosequencing analysis of the CpG islands within the LXN and RARRES1 genes in prostate epithelial cell lines.
(a) The percentage promoter methylation of RARRES1 and **(b)** LXN in benign and cancer cell lines. Statistical significance values were measured by the Student's T-test (Unpaired, two-tailed; * $p<0.05$, ** $p<0.01$, *** $p<0.001$). Bars = single CpG sites; black line = average of individual CpG sites; error bars expressed as standard deviation of n=3 technical replicates. **(c)** The average percentage promoter methylation of a GSTP1 control gene in the same cell lines (experiment performed by Dr. Davide Pellacani).
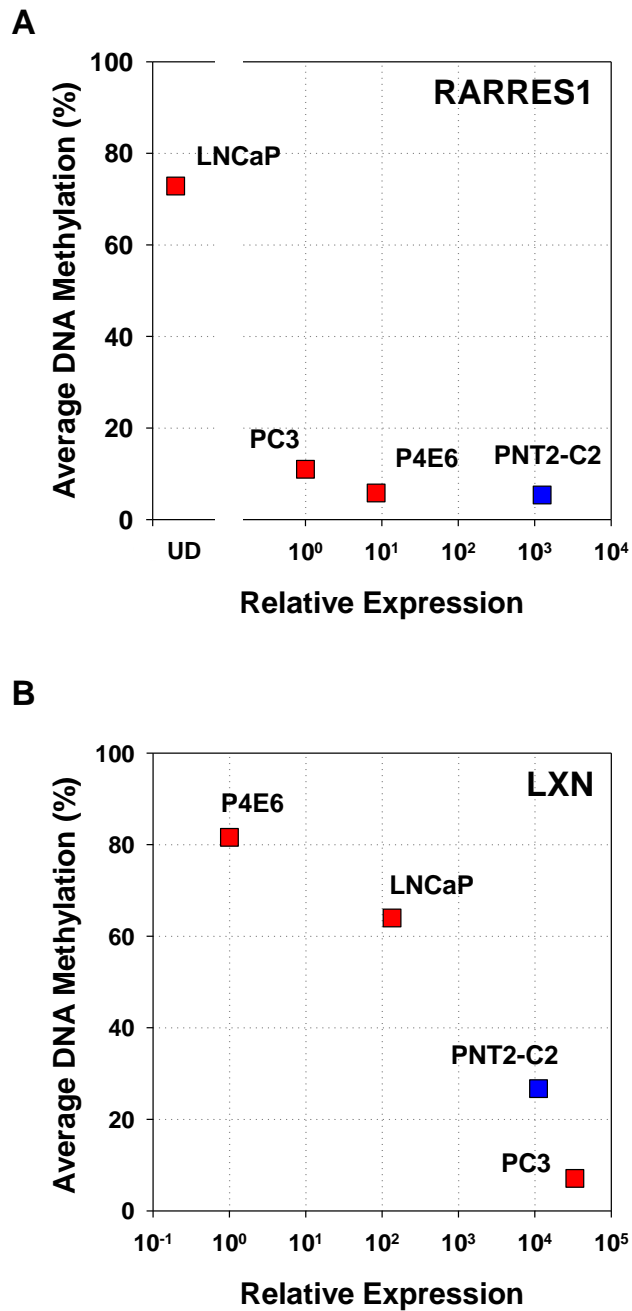
Figure 36. Correlation between expression and DNA methylation of RARRES1 and LXN in prostate epithelial cell lines.
(a) Dot plot showing the correlation between mRNA expression (X-axis) relative to a GAPDH control gene, analysed using qRT-PCR (see Figure 20) and average percentage of promoter DNA methylation (Y-axis), analysed by pyrosequencing (see Figure 35) of RARRES1 and **(b)** LXN, in benign (PNT2-C2) and cancer (P4E6, PC3 and LNCaP) cell lines. Expression plotted on a log10 scale to enable optimal visualisation; UD: expression undetectable after 40 cycles; n=3 technical replicates. The percentage promoter methylation was calculated as the average of 11 (RARRES1) and 6 (LXN) individual CpG sites.

3.5.2. RARRES1 and LXN show low levels of DNA methylation in primary prostate epithelial cultures

RARRES1 and LXN expression was shown to be regulated by DNA methylation in CaP epithelial cell lines. To determine whether RARRES1 and LXN were methylated in primary prostate epithelial cultures, pyrosequencing analysis of RARRES1 and LXN in primary BPH (n=3) and CaP (n=3) cultures was performed.

Low levels of DNA methylation within RARRES1 and LXN was seen in all BPH and CaP cultures analysed (less than 10%). Two out of three CaP cultures (PE671 and PE665) showed significant hypermethylation of RARRES1 compared to the 0% methylated control DNA. However, the average methylation was still below 10% (Figure 37a). None of the CaP tissues analysed showed significant hypermethylation of LXN (Figure 37b).

As the expression of RARRES1 and LXN was significantly lower in SC than TA and CB cells, it could be hypothesised that expression is repressed by DNA methylation in the SC. Analysis of the methylation of RARRES1 and LXN in whole population epithelial cultures would mask any hypermethylation present in the rare SC. Furthermore, as RARRES1 expression was also significantly repressed in CB cells from CaP cultures, compared to BPH cultures, RARRES1 may be hypermethylated in CB cells derived from CaP. Consequently, to investigate if RARRES1 and LXN were hypermethylated in enriched subpopulations from primary prostate epithelial cultures, pyrosequencing analysis was performed on SCs, TA and CB cells from BPH (n=2) and CaP (n=2) cultures.

There was no significant difference in methylation levels of RARRES1 (Figure 38a) or LXN (Figure 38b) in any subpopulation from any BPH or CaP sample. Furthermore, all average methylation levels were below 10%.

Taken together, this data demonstrates that RARRES1 and LXN possess very low levels of DNA methylation in whole population and enriched primary prostate epithelial cultures from BPH and CaP. This indicates that the regulation of RARRES1 and LXN expression within SCs, TA and CB subpopulations is not due to DNA methylation. It also suggests that the repression of RARRES1 expression in CB cells from CaP cultures is not due to DNA methylation.
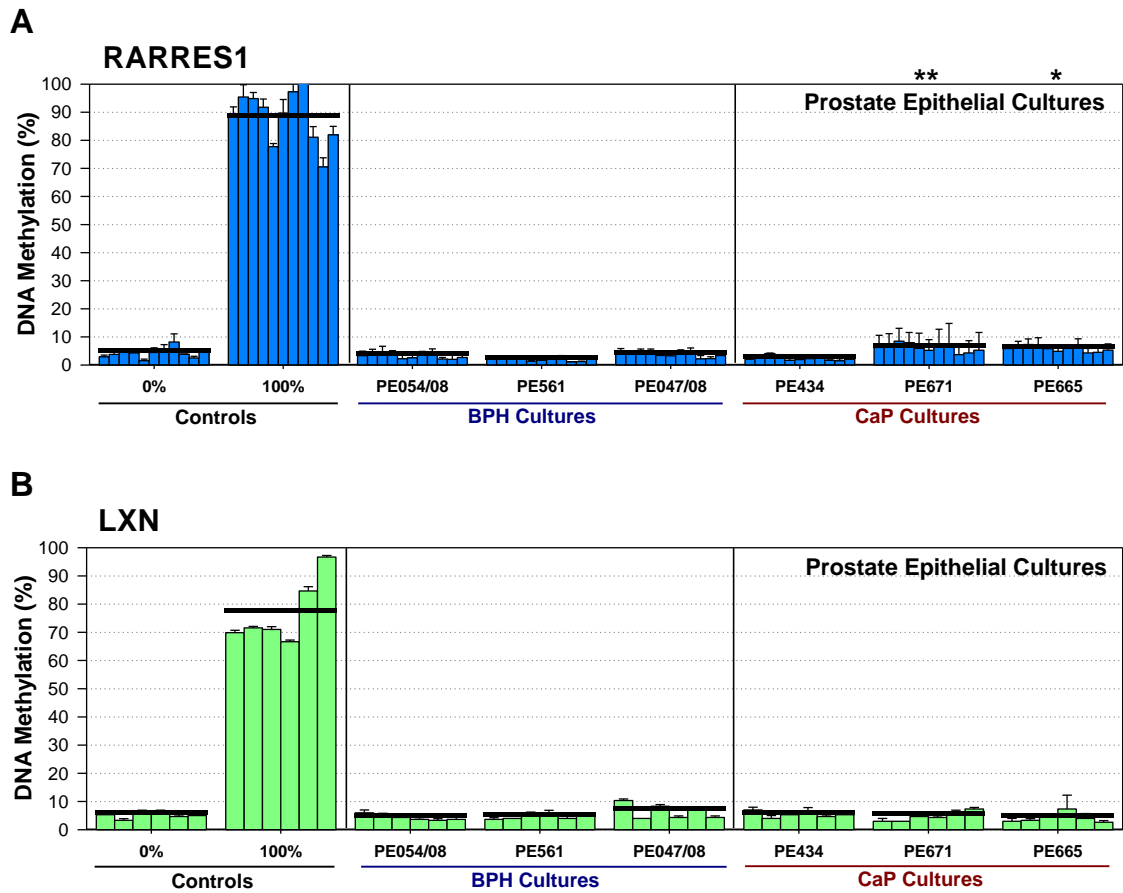
Figure 37. Pyrosequencing analysis of the CpG islands within the LXN and RARRES1 genes in primary prostate epithelial cultures.
(a) The percentage promoter methylation of RARRES1 and **(b)** LXN in primary prostate epithelial cultures derived from BPH (n=3) and CaP (n=3). Statistical significance values were measured by the Student's T-test (Unpaired, two-tailed; * $p<0.05$, ** $p<0.01$). Bars = single CpG sites; black line = average of individual CpG sites; error bars expressed as standard deviation of n=3 technical replicates.
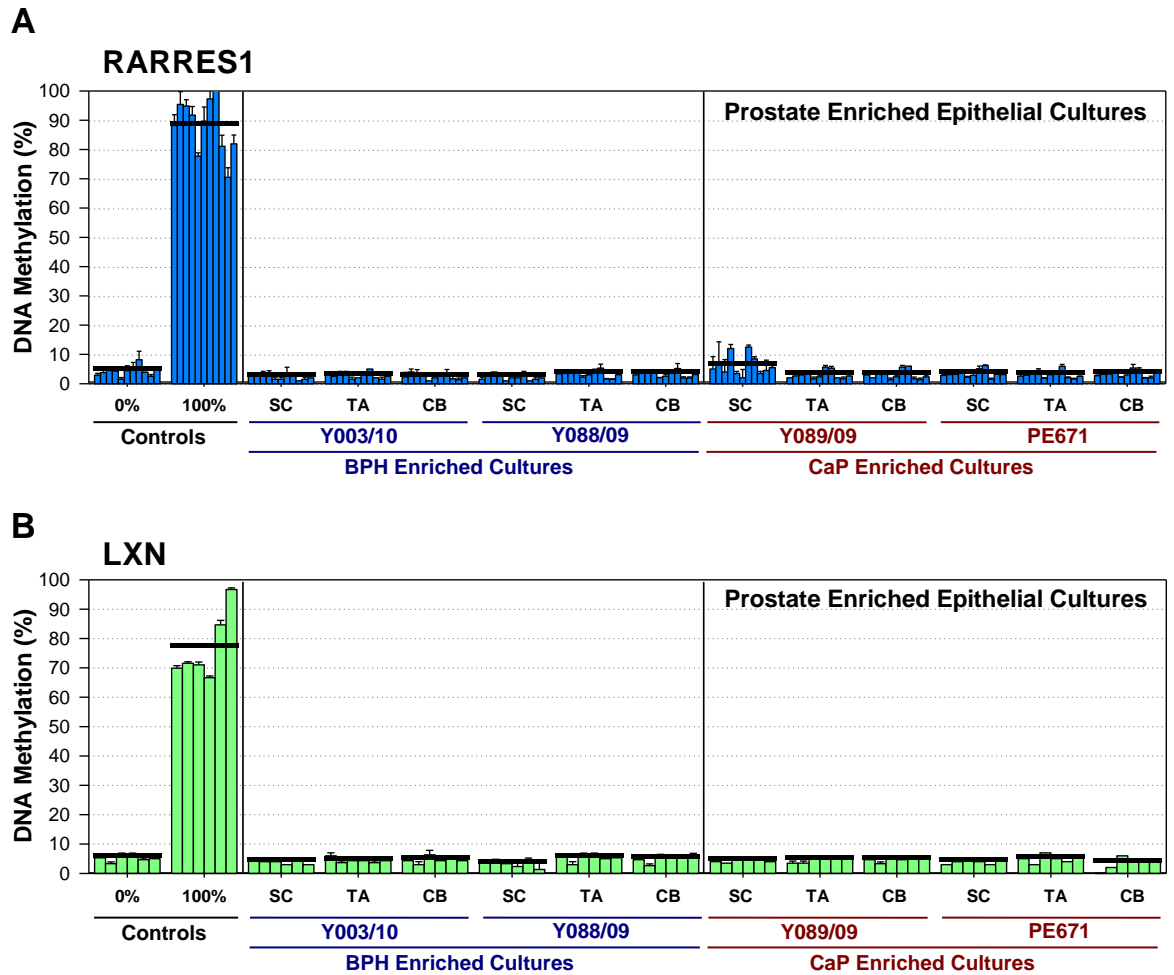
Figure 38. Pyrosequencing analysis of the CpG islands within the LXN and RARRES1 genes in primary prostate epithelial cultures.
(a) The percentage promoter methylation of RARRES1 and **(b)** LXN in enriched SC, TA and CB cell subpopulations of primary prostate epithelial cultures derived from BPH (n=2) and CaP (n=2). Bars = single CpG sites; black line = average of individual CpG sites; error bars expressed as standard deviation of n=3 technical replicates.

3.5.3. RARRES1 and LXN show low levels of DNA methylation in primary prostate tissues

RARRES1 and LXN were repressed by DNA methylation in malignant prostate epithelial cell lines. However, RARRES1 and LXN showed low levels of DNA methylation in primary prostate basal epithelial cultures. To determine whether RARRES1 and LXN are regulated by DNA methylation in primary prostate tissues from which the cultures were derived, pyrosequencing analysis was performed on primary BPH (n=3) and CaP (n=3) tissues. The gDNA derived from CaP tissue was commercially available high Gleason grade (grade 8 or 9) CaP gDNA obtained from Origene, which was reported to contain between 75 - 95% tumour tissue.

The results showed that low levels (less than 11%) of DNA methylation of RARRES1 (Figure 39a) and LXN (Figure 39b) was seen in all tissues analysed. Unexpectedly, RARRES1 was significantly hypermethylated compared to the 0% methylated control DNA in two out of three BPH tissues and LXN showed significant hypermethylation in one BPH tissue (although the average methylation remained low at less than 15%). However, none of the CaP tissues analysed showed significant hypermethylation of RARRES1 and LXN.

To confirm that the CaP tissue was indeed cancer, the average percentage methylation values of a GSTP1 control gene, in the same BPH (performed by Dr. Davide Pellacani) and CaP tissues, were analysed (Figure 39c). These results showed that GSTP1 was hypermethylated in all CaP tissues (66-73% methylation), but not in the BPH tissues, confirming that the tissues did contain a high proportion of CaP cells.

Taken together, these results show that RARRES1 and LXN possess very low levels of DNA methylation in primary prostate BPH and CaP tissues and so confirm that both genes are not regulated by DNA methylation in primary CaP.
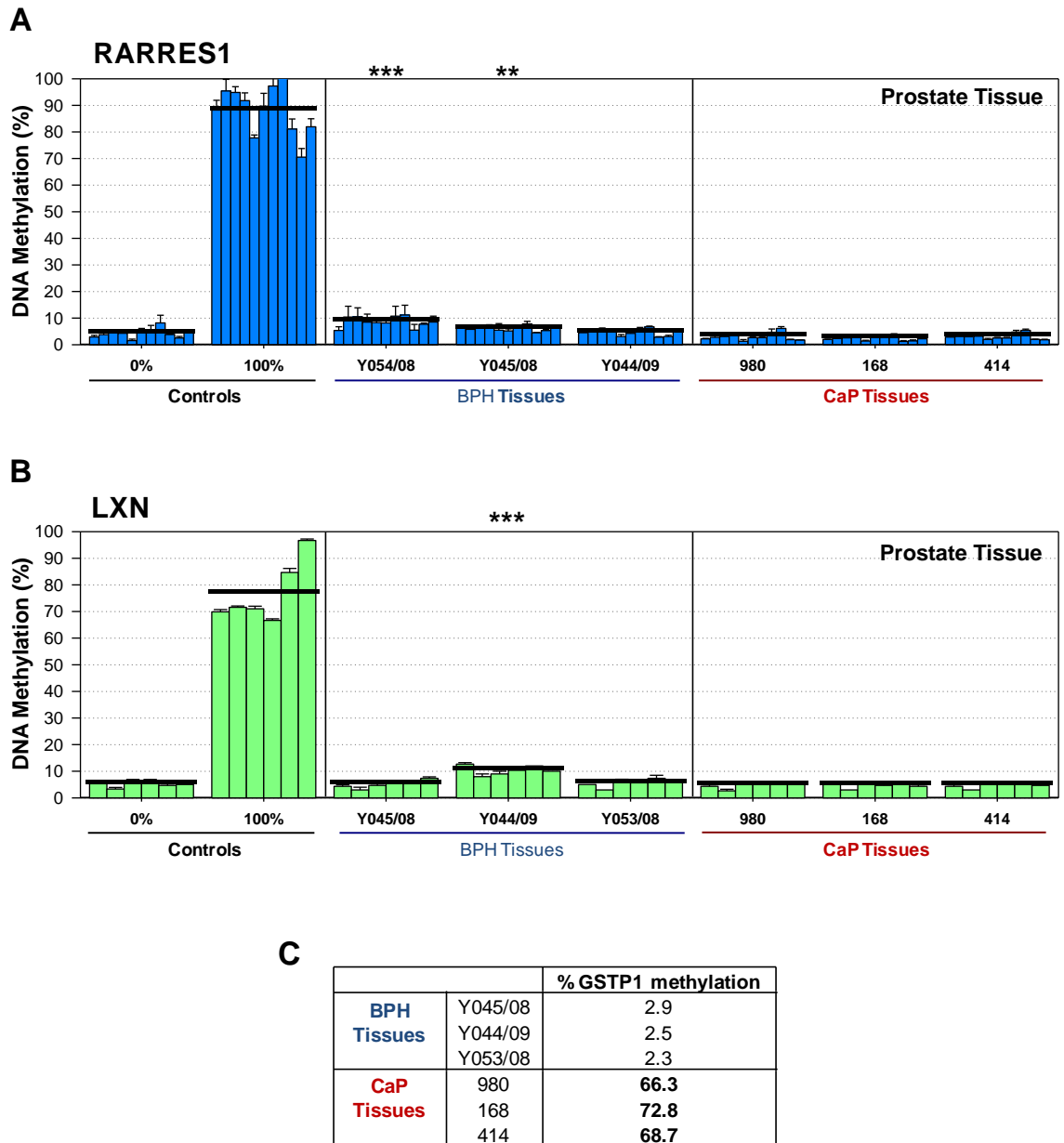
Figure 39. Pyrosequencing analysis of the CpG islands within the LXN and RARRES1 genes in primary prostate tissues.
(a) The percentage promoter methylation of RARRES1 and **(b)** LXN in primary prostate tissues derived from BPH (n=3) and CaP (n=3). DNA derived from BPH tissues was extracted from glass slides of pooled snap frozen tissue sections by Dr. Davide Pellacani. DNA derived from CaP tissues was commercial gDNA obtained from Origene. Statistical significance values were measured by the Student's T-test (Unpaired, two-tailed; ** p<0.01, *** p<0.001). Bars = single CpG sites; black line = average of individual CpG sites; error bars expressed as standard deviation of n=3 technical replicates. **(c)** The average percentage promoter methylation of a GSTP1 control gene in the same BPH (experiment performed by Dr. Davide Pellacani) and CaP tissues.

3.5.4. RARRES1 and LXN show low levels of DNA methylation in some prostate xenograft tissues

RARRES1 and LXN expression was shown to be regulated by DNA methylation in malignant prostate epithelial cell lines, but not in primary CaP tissue. To further confirm that RARRES1 and LXN are not methylated in primary CaP samples, pyrosequencing analysis of RARRES1 and LXN in CaP xenograft samples, established in $RAG2^{-/-}\gamma C^{-/-}$ mice, was performed. As these cells are tumourigenic in mice, they should contain a more homogeneous population of cancer cells compared to epithelial tissues, which can contain a portion of benign cells. As these xenografts could contain a proportion of mouse cells, methylation levels of RARRES1 (Figure 40a) and LXN (Figure 40b) were analysed in mouse STO fibroblast gDNA by pyrosequencing as a control. This analysis did not produce a pyrogram trace, confirming that the pyrosequencing primers used were human-specific, and will detect methylation in human cells only.

RARRES1 showed significantly hypermethylation in only one xenograft sample, the early passage (P.3) of Y042, though the average methylation was low at less than 10% (Figure 41a). No other xenograft, at any passage, showed significant hypermethylation of RARRES1.

LXN was significantly hypermethylated in both the Y019 and Y042 xenograft samples at low passage number (Figure 41b). In contrast to RARRES1, methylation of LXN increased significantly with serial passaging of the Y042 xenograft sample, to a maximum of 30% at passage 23. This suggests that, akin to what was seen in cell lines, serial passaging and immortalisation may increase the methylation of certain genes. As this trend to increase LXN methylation (3-fold) with increased passage of xenograft tumours is not seen with RARRES1, it would suggest that any hypermethylation seen is not due to general methylation of a large genomic area that contains both genes.

An independent experiment performed by Dr. Davide Pellacani showed that levels of GSTP1 methylation in the same xenograft samples at low passage were also very low (less than 4%) (Figure 41c).

Taken together, these results show that RARRES1 possesses very low levels of DNA methylation in primary xenograft tissues. In contrast, LXN is significantly hypermethylated in some primary xenograft tissues and the average methylation increases with increased passage of the xenograft.

A

RARRES1 – Mouse STO DNA

Sequence to analyse:

B
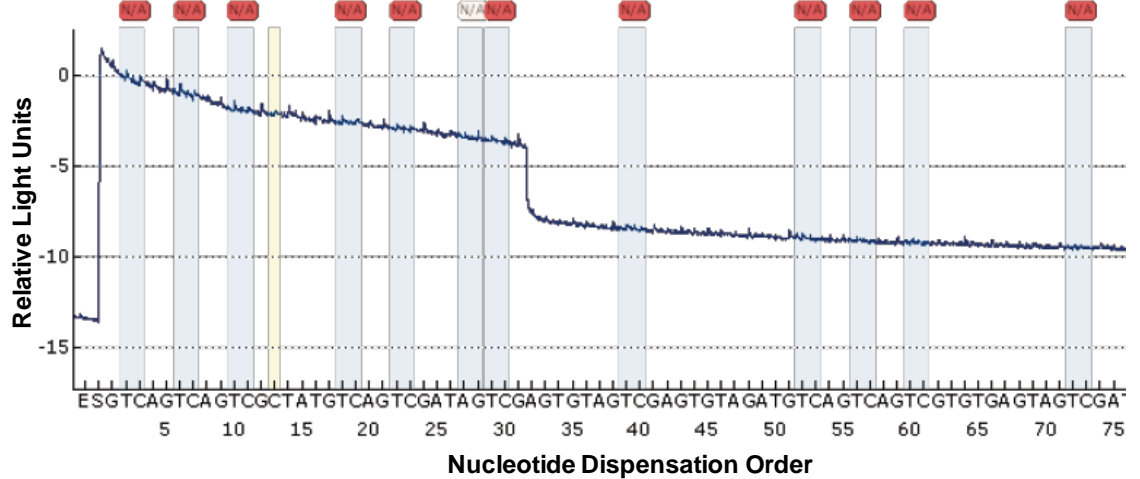
LXN – Mouse STO DNA

Sequence to analyse:
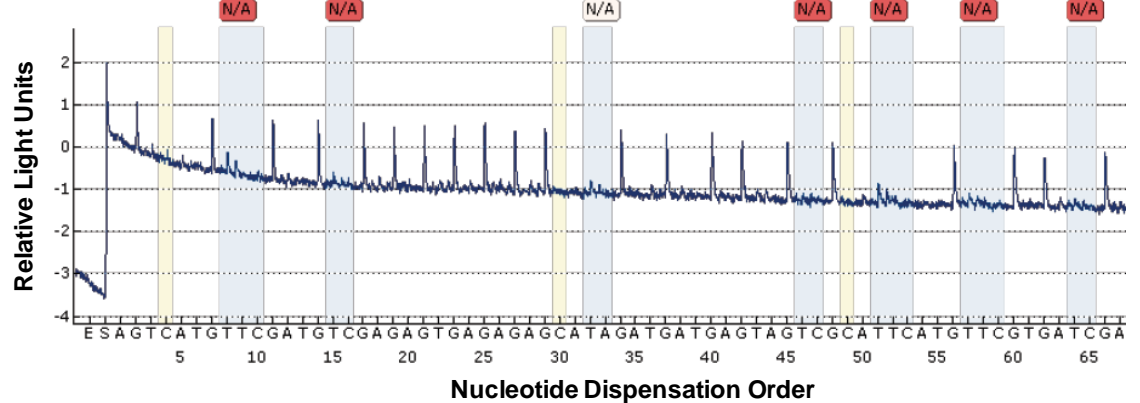
Figure 40. Pyrogram traces after pyrosequencing analysis of RARRES1 and LXN using mouse STO DNA.
Pyrosequencing pyrogram trace produced by the PyroMark Q24 software after analysis of DNA methylation of RARRES1 and LXN in mouse STO gDNA. The pyrograms confirm that each assay does not detect mouse gDNA and is human-specific.
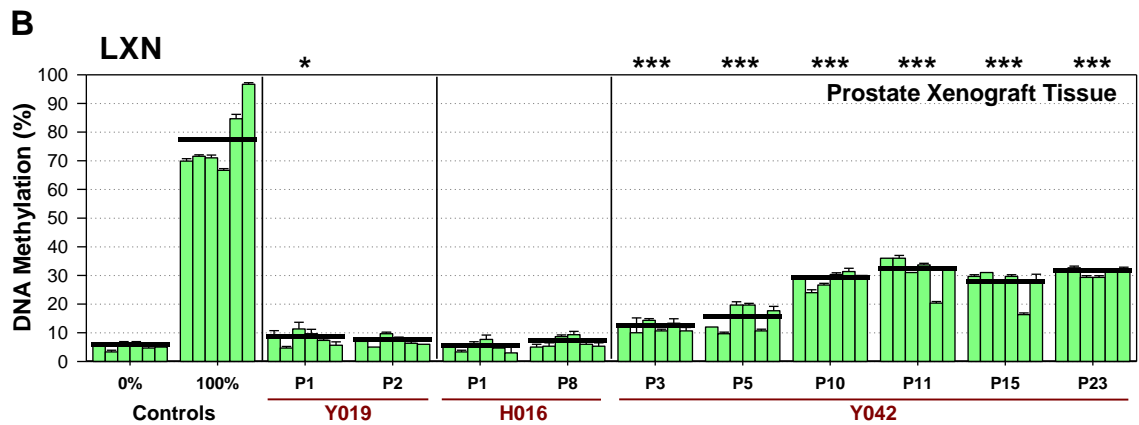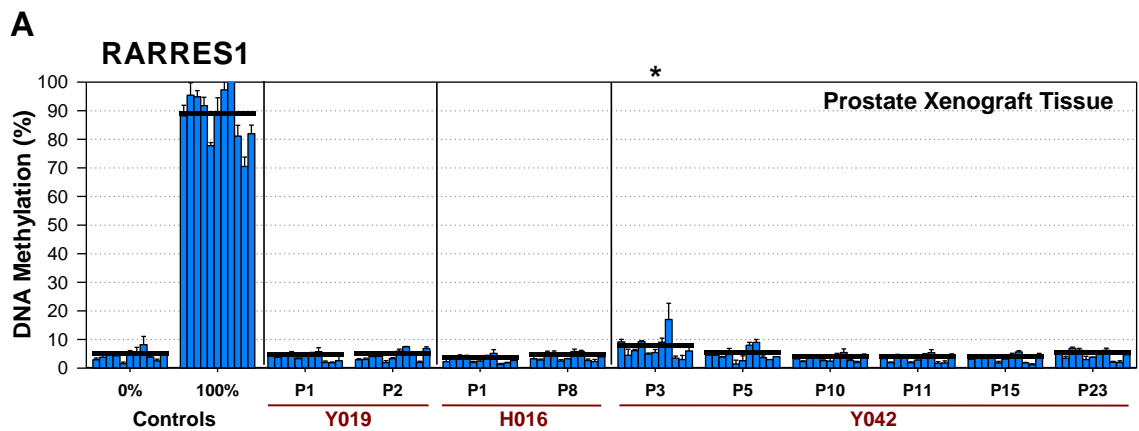
Figure 41. Pyrosequencing analysis of the CpG islands within the LXN and RARRES1 genes in primary prostate xenograft tissues.
(a) The percentage promoter methylation of RARRES1 and **(b)** LXN in CaP xenograft tissues generated in RAG2$^{-/-}$γC$^{-/-}$ mice, which were serially passaged *in vivo*. Various passage numbers of xenograft tissue were analysed. Statistical significance values were measured by the Student's T-test (Unpaired, two-tailed; ** p<0.01, *** p<0.001). Bars = single CpG sites; black line = average of individual CpG sites; error bars expressed as standard deviation of n=3 technical replicates. **(c)** The average percentage promoter methylation of a GSTP1 control gene in the same xenografts tissues (experiment performed by Dr. Davide Pellacani).

3.6. Regulation of RARRES1 and LXN by retinoic acid

3.6.1. RARRES1 and LXN expression is induced by retinoic acid in basal prostate epithelial cell lines

RARRES1 was initially identified as the most up-regulated gene in response to RA in skin raft cultures (Nagpal et al., 1996), so we investigated if RA has a role in controlling expression of both RARRES1 and LXN in prostate epithelial cells. We initially carried out bioinformatics analysis, using the JASPAR database, of a 5 kB region upstream of each of the RARRES1 and LXN transcription start sites (TSS) in order to find putative binding sites for RARs important in regulating expression. The consensus sequences used to identify RAREs are shown in Figure 42a. A schematic diagram detailing the RAREs present in the 5 kB upstream region shows that RARRES1 contains one RARE, 3632 bp (relative score: 0.802) upstream of the TSS, and LXN contains two RAREs, 2835 bp (relative score: 0.846) and 3402 bp (relative score: 0.819) upstream of the TSS (Figure 42b). In addition, RARRES1 contains two further RAREs, 7706 bp (relative score: 0.808) and 8833 bp (relative score: 0.830) downstream of the TSS (data not shown).

To investigate if RA is able to directly regulate expression of RARRES1 and LXN, a panel of prostate epithelial cell lines with basal (PNT1a, BPH-1, RC165 and Bob) and luminal characteristics (LNCaP) were treated with 500 nM atRA over a time course and RARRES1 and LXN mRNA expression was quantified. Both RARRES1 and LXN showed a time-dependent response to atRA in the majority of cell lines tested. Significant induction of RARRES1 expression was seen in three out of four basal cells, with the greatest increase in expression seen after treatment for 24 hours (PNT1a: 3.6-fold; BPH-1: 5.2-fold; RC165: 19.4-fold) (Figure 42c). The Bob cell line did not respond to atRA treatment. Expression of RARRES1 initially decreased in response to atRA in the luminal LNCaP cell line. However, a significant increase (3.5-fold) in expression was seen after 72 hours. Significant induction of LXN expression was seen in all four basal cell lines, with the greatest increase in expression seen after 24 hours treatment (PNT1a: 5.1-fold; BPH-1: 4.1-fold RC165: 35.8-fold; Bob: 2.6-fold) (Figure 42d). In contrast to RARRES1 expression, atRA treatment had no effect on LXN expression in the LNCaP cell line.

Taken together, these results show that the promoters of both RARRES1 and LXN contain RAREs and so could be directly regulated by RA. Moreover, atRA induces RARRES1 and LXN expression in basal epithelial cell lines, but not in the luminal LNCaP cell line.
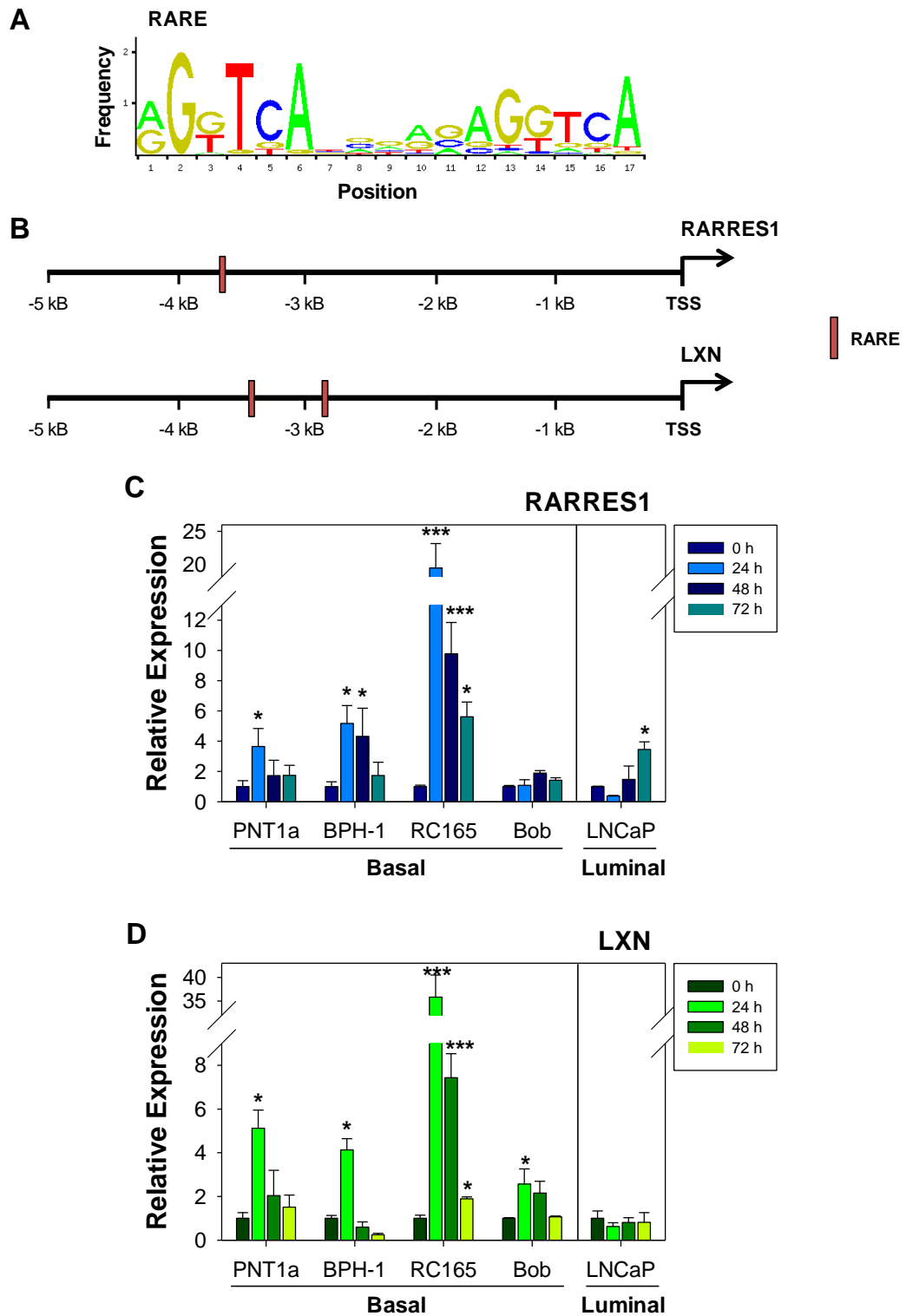
Figure 42. Analysis of RARRES1 and LXN expression after atRA treatment of prostate epithelial cell lines.
(**a**) Graphical representation of the consensus sequences used to determine RAREs in the RARRES1 and LXN promoters (taken from the JASPAR database website). **(b)** Depiction of RAREs found in a 5 kB portion of the RARRES1 and LXN promoters by bioinformatics analysis using the JASPAR database. **(c)** qRT-PCR expression data quantifying the expression of RARRES1 and **(d)** LXN, after treatment of basal (PNT2-C2, BPH-1, RC165 and Bob) and luminal (LNCaP) prostate cell lines with 500 nM atRA over a time course. Expression relative to an RPLPO control gene; n=3 technical replicates; error bars expressed as range of the mean. Statistical significance values were measured by the Student's t-test (Unpaired, two-tailed; * p<0.05, *** p<0.001).

3.6.2. RARRES1 and LXN expression is induced by retinoic acid in prostate epithelial cell cultures

RARRES1 and LXN mRNA levels were increased in basal prostate epithelial cell lines following atRA treatment. To examine whether RA also regulated expression of RARRES1 and LXN in the primary prostate basal epithelial cultures, a primary prostate CaP epithelial culture (PE519) was treated with increasing concentrations of atRA over a time course and RARRES1 and LXN mRNA expression was quantified by qRT-PCR.

Expression of RARRES1 (Figure 43a) and LXN (Figure 43b) after treatment increased in a dose and time-dependent manner, with an initial increase in RARRES1 expression seen after 24 hours (4-fold) and a further delayed increase seen after 96 hours (570-fold). The magnitude of LXN expression after treatment was similar to RARRES1 after 24 hours (4-fold), however, a smaller increase after 96 hours (185-fold) was seen. There was one inconsistency in the data after treatment with 10 nM atRA for 72 hours, the expression of RARRES1 and LXN appeared to decrease compared to 48 hours and increase again at 96 hours. This could be due to the cell media being changed for fresh media (without additional atRA being added) after 48 hours. However, the half-life of atRA is very short at 0.5-2 hours, so this is probably not the case. It is most probably an anomalous time point, as the inconsistency is seen in RARRES1 and LXN expression and with no other concentration of atRA. From this result, 100 nM atRA treatment for 72 hours was chosen as a suitable concentration and time point to use for subsequent experiments. This was because: (1) 100 nM atRA produced the greatest increase in expression at 72 hours and (2) the increase in expression was greater than at 24 and 48 hours.

While basal cell lines induced RARRES1 and LXN to a maximum level after 24 hours, the highest increase in RARRES1 and LXN expression was seen after 96 hours in primary cultures. In addition, the fold increase in expression was considerably higher in primary cultures than the fold changes seen in cell lines. This difference could be due to primary samples taking longer to respond to atRA and induce transcription. Alternatively, in primary samples, atRA may indirectly regulate transcription of RARRES1 and LXN by inducing the expression of different genes that are able to transactivate RARRES1 and LXN. These genes may not be induced by atRA, or may not regulate RARRES1 and LXN transcription in cell lines.

Whole population prostate basal epithelial cultures increased RARRES1 and LXN mRNA expression in response to atRA treatment. To investigate whether there was a difference in the induction of expression, within different subpopulations in the basal epithelial hierarchy, primary prostate BPH and CaP epithelial cultures enriched for SC, TA and CB cells were treated with 100 nM atRA for 72 hours and RARRES1 and LXN mRNA expression was quantified by qRT-PCR. The expression of each sample was normalised to the lowest expressor within each subpopulation (set at one). Subsequently, RARRES1 and LXN expression, with and without

atRA treatment, was compared, but not expression between cell subpopulations. Expression levels between SC, TA and CB populations were described in Section 3.2.2.

RARRES1 and LXN expression was induced upon atRA treatment in all enriched cultures. This induction in RARRES1 expression was significant in TA (300-fold) and CB (800-fold) cells derived from CaP (Figure 44c). In BPH samples, there was a consistent up-regulation in each subpopulation after treatment, however, the high variability seen in each cell population resulted in a non-significant increase (Figure 44a). The induction in LXN expression was significant in TA (50-fold) and CB (100-fold) cells derived from BPH (Figure 24b) and TA (40-fold) and CB (120-fold) cells derived from CaP (Figure 44d).

The general trend observed for both genes was that the induction of expression after atRA treatment increased with the differentiation status of the culture. The average induction of expression of RARRES1 in the atRA-treated SC population was lower than in the CB population, from both BPH (4-fold lower) and CaP (10-fold lower) cultures. Similary, the induction in expression of LXN in the atRA-treated SC population was 4-fold lower than in the CB population from CaP cultures. However, there was no difference in average induction of LXN expression between any of the subpopulations from atRA-treated BPH cultures; only a 1.4-fold lower induction in expression was observed in the SC compared to the CB population. This discrepancy was most probably due to the average expression of LXN in the atRA-treated BPH SC population being skewed to a higher expression, due to one anomalous point (Y048/10). Another point to note is that although the expression of RARRES1 and LXN in DMSO-treated SC, TA and CB cells was set at one in Figure 44, the starting values between the three populations were different as described in Figures 24 and 25.

Taken together, these results indicate that atRA induces RARRES1 and LXN expression in primary prostate basal epithelial cultures. Furthermore, atRA is able to induce RARRES1 and LXN to higher levels in the most differentiated CB subpopulation.
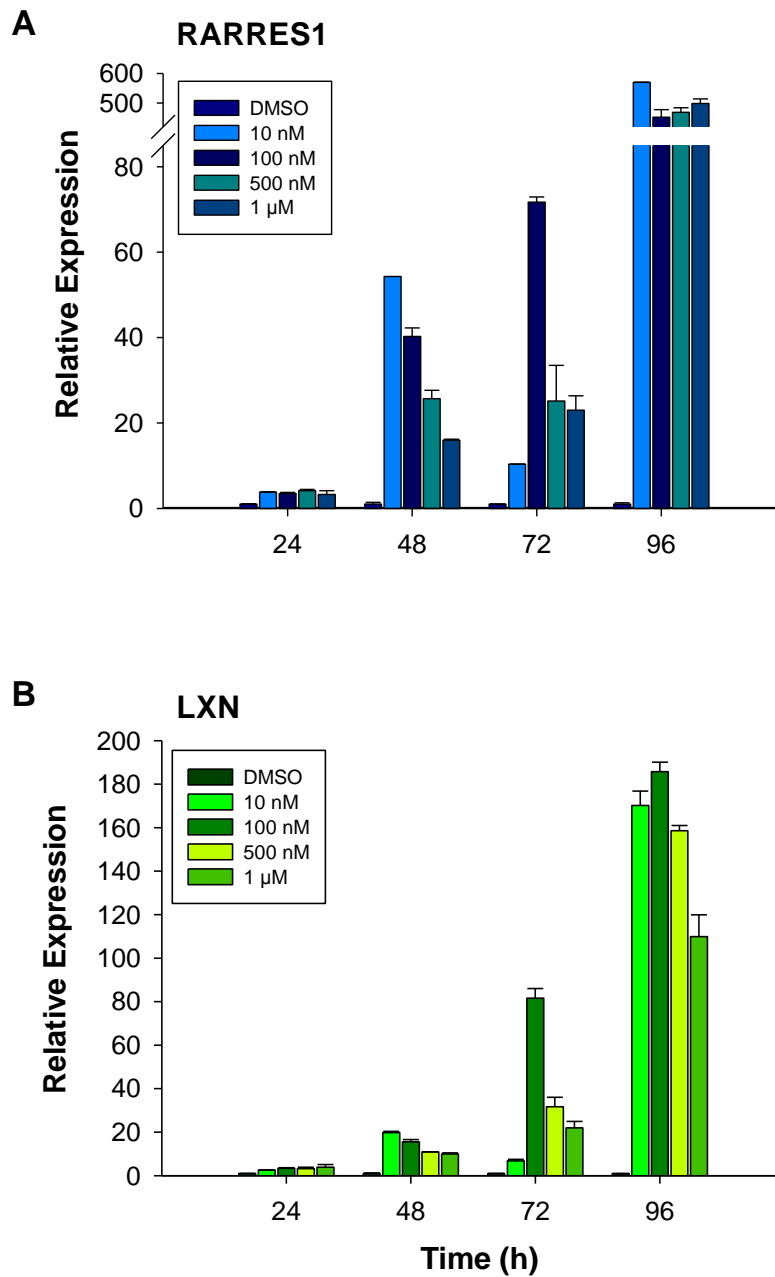
A **RARRES1**

B **LXN**

Figure 43. Analysis of RARRES1 and LXN expression after atRA treatment of a primary prostate BPH epithelial culture.
qRT-PCR expression data quantifying the relative expression of **(a)** RARRES1 and **(b)** LXN, after treatment of a primary CaP epithelial cell culture (PE519) with various concentrations of atRA over a time course. Expression relative to an RPLPO control gene; n=3 technical replicates; error bars expressed as range of the mean.
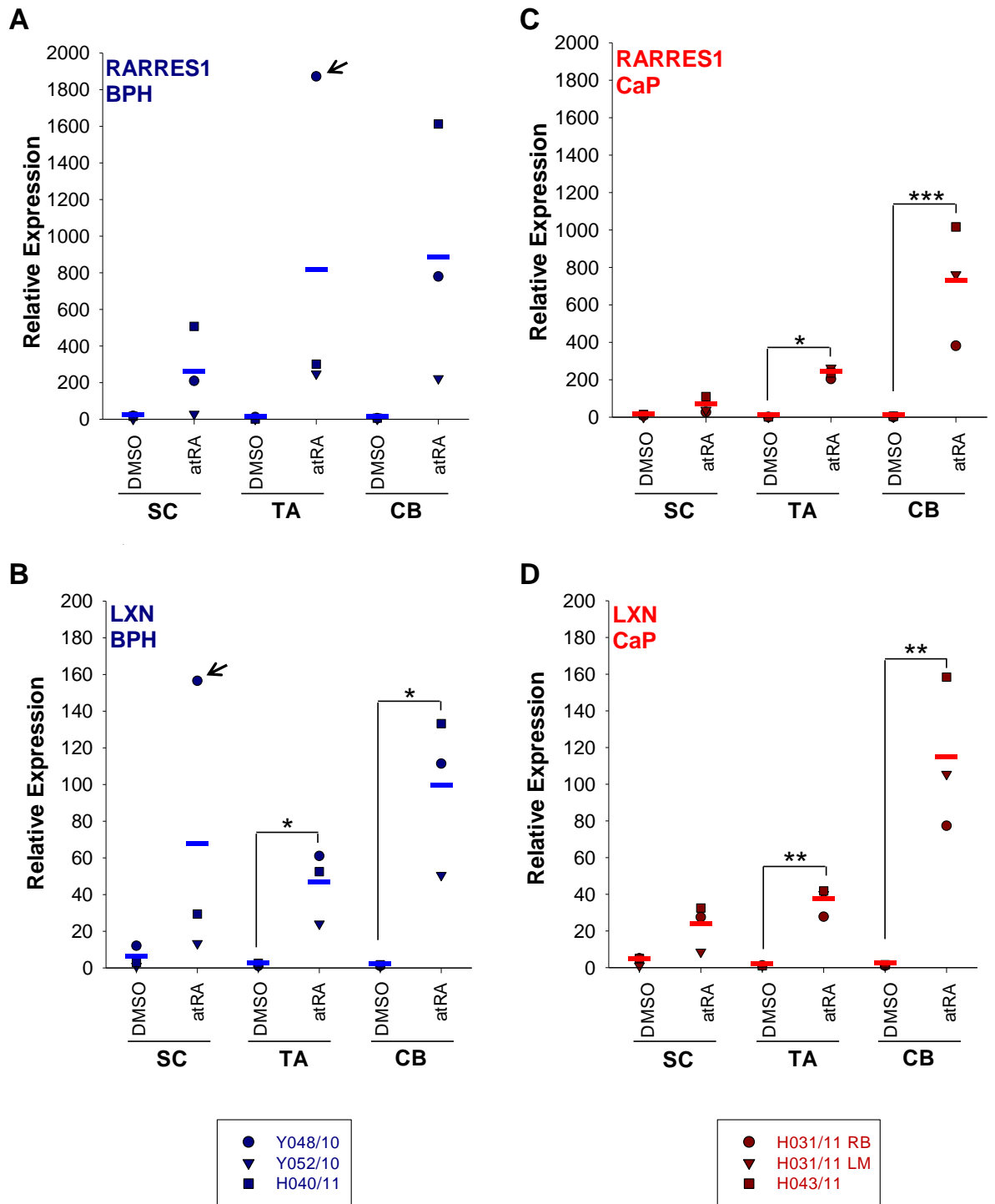
Figure 44. Analysis of RARRES1 and LXN expression in enriched primary prostate epithelial cultures after atRA treatment.
qRT-PCR expression data quantifying the relative expression of **(a, c)** RARRES1 and **(b, d)** LXN expression after treatment of primary epithelial cell cultures (enriched for SC, TA and CB cells) derived from BPH (n=3) or CaP (n=3) with 100 nM atRA for 72 hours. All expression values are relative to an RPLPO endogenous control. Within each subpopulation, expression of all DMSO-treated and atRA-treated samples was normalised to the DMSO-treated sample showing the lowest expression of RARRES1 or LXN (set at 1). Statistical significance values were measured by the Student's T-test (Unpaired, two-tailed; * P<0.05, ** P<0.01, *** P<0.001). Average expression denoted by a horizontal line (Blue: BPH; Red: CaP). Arrows indicate outliers.

3.6.3. Retinoic acid receptors are expressed and active in primary prostate epithelial cultures

Since atRA induced expression of RARRES1 and LXN in primary prostate epithelial cultures, it is probable that RARs are expressed and active within primary cultures. To determine whether RARs were expressed within the basal hierarchy, a primary CaP culture (H082/11 LA) was treated with 500 nM atRA for 24 hours, and immunofluorescence performed to detect RAR α, β and γ protein. Figure 45a shows that all three RAR isoforms were expressed; RAR α demonstrated predominantly nuclear expression, but RAR β and γ showed mainly cytoplasmic with some nuclear expression. RAR α and γ appeared to be expressed at different levels between cells, with high expression seen in some cells and considerably lower expression in others. In contrast, the expression of RAR β was homogenous between cells. Furthermore, after atRA treatment there was no difference in the localisation of any of the 3 RAR isoforms, RAR α remained in the nucleus and RAR β and γ stayed mostly in the cytoplasm. This is not an unexpected result, as it is known that RARs are within the nucleus and attached to DNA in the absence of RA (Bastien and Rochette-Egly, 2004).

To test the overall ability of primary prostate epithelial cultures to activate transcription following atRA treatment, a primary BPH (Y054/11) and CaP (H082/11 RA) culture was transfected with a luciferase reporter plasmid. The active regulatory elements in the plasmid were composed of a TATA box element and a tandem array of RAREs, which upon ligand-bound RAR binding, activated luciferase transcription. 24 hours after transfection with the plasmid, cells were treated with increasing concentrations of atRA, and luciferase activity measured after a further 24 hours. The primary BPH (Figure 45b) and CaP (Figure 45c) cultures were able to significantly activate luciferase expression following atRA treatment, to a maximum of 14.8-fold and 26.5-fold induction, respectively when treated with 1 μM atRA.

The decreased ability of SC subpopulation to induce RARRES1 and LXN expression after atRA treatment (Figure 44), suggests that there may be a differential reponse to atRA through differentiation in the prostate basal hierarchy. To examine if there was differential expression of RARs or intracellular lipid-binding proteins in SCs and CB cells (BPH and CaP results were pooled), Affymetrix gene-expression array data (Birnie et al., 2008) was re-examined (Figure 45d). These results show that all three isoforms of RARs were expressed at low levels, and that there was no difference in expression between the SCs and CB cells. Interestingly, RXR α was expressed at high levels, but no difference was seen between SC and CB subpopulations. However, the CRABP2 gene, encoding a protein that functions to transfer atRA to the nucleus, was over-expressed in the CB compared to the SC subpopulation. Taken together, these results show that RARs are expressed and transcriptionally active in primary prostate epithelial cultures. However, the differential induction in RARRES1 and LXN expression between SC and CB subpopulations may be due to differential expression of CRABP2.

A

B

C

CaP

Relative Luminescence Units

400
200

35
30
25
20
15
10
5
0

-    DMSO   250 nM   500 nM   1 µM   +

*

RARE plasmid
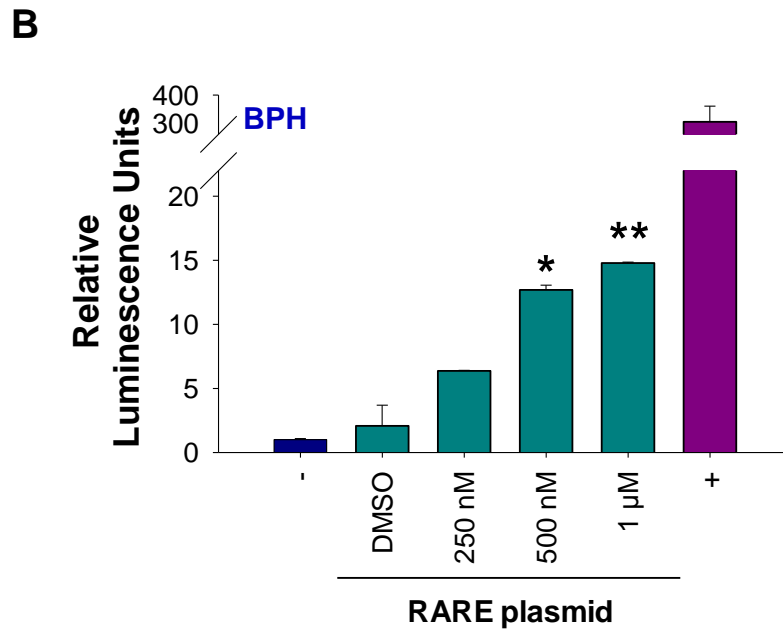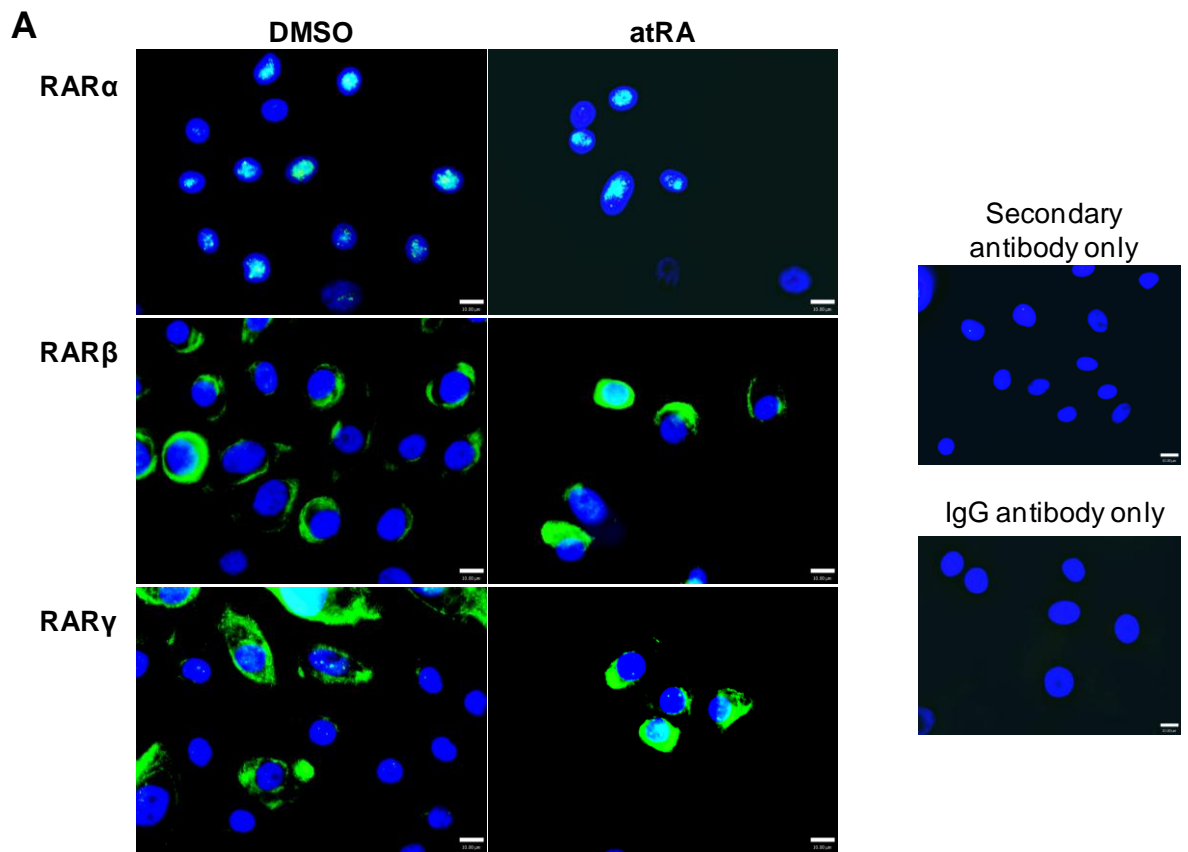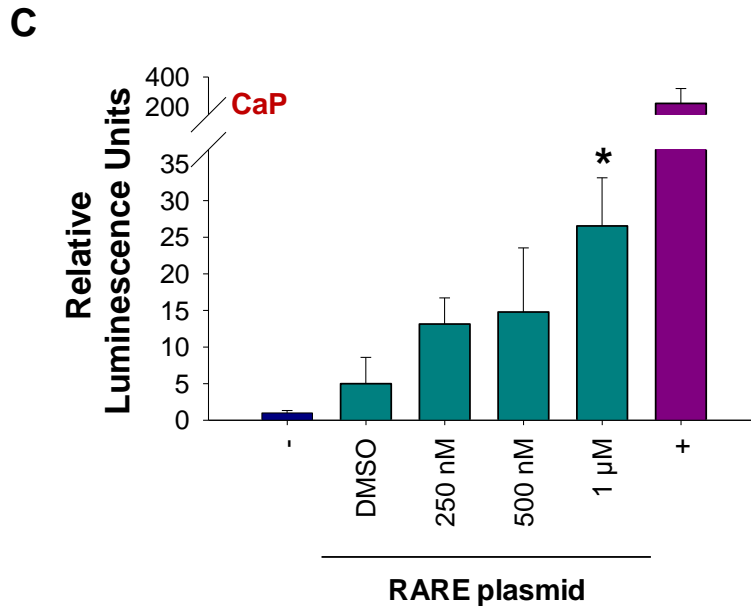
D

Gene Title	Gene Symbol	Mean Absolute Expression	
		Stem	Committed
retinoic acid receptor, alpha	RARA	99.01	95.63
retinoic acid receptor, beta	RARB	34.29	41.50
retinoic acid receptor, gamma	RARG	176.98	181.40
retinoid X receptor, alpha	**RXRA**	**890.34**	**894.31**
retinoid X receptor, beta	RXRB	292.07	238.95
cellular retinoic acid binding protein 2	**CRABP2**	**882.93**	**1164.12**

Figure 45. Analysis of expression and transcriptional activity of retinoic acid receptors in response to atRA in primary prostate epithelial cell cultures.
(a) RAR α, β and γ expression was detected by immunofluorescence in primary epithelial cultures derived from CaP (H082/11 LA), treated with 500 nM atRA for 24 hours or a DMSO control. Cells were counterstained with DAPI to enable nuclear visualisation. White scale bar represents 10 µm. **(b)** Luciferase activity in primary prostate epithelial cell cultures derived from BPH (Y054/11) and **(c)** CaP (H082/11 RA), transfected with a RARE reporter plasmid in response to increasing concentrations of atRA. Luciferase activity was normalised to the values of the cells transfected with a negative control plasmid (lacked RARE regulatory elements). Statistical significance with respect to DMSO control was measured by the Student's T-test (Unpaired, two-tailed; * $p<0.05$; ** $p<0.01$). **(d)** Affymetrix gene-expression array data showing mean gene expression values of RARs and intracellular lipid-binding proteins that bind RA in SCs and CB cells (BPH and CaP samples pooled together).

3.7. Homology of RARRES1 and LXN

3.7.1. RARRES1 and LXN share a conserved CPA4 binding domain

LXN has been described as the only known endogenous MCP inhibitor in humans. Moreover, the crystal structure of LXN in complex with human CPA4 has been solved, which describes an inhibitory loop from LXN that protrudes into the CPA4 active site (Pallares et al., 2005). To determine whether RARRES1 may also interact with CPA4, both RARRES1 (transcript 1 and 2) and LXN amino acid sequences were aligned, using the Clustal W method in the Lasergene MegAlign software (Figure 46a).

The alignment identified a 30% protein sequence similarity between RARRES1 and LXN, confirming that the two proteins are homologues. The only apparent difference between the two proteins was a lack of an N-terminal transmembrane domain in LXN that is present in both isoforms of RARRES1. Interestingly, the C-terminal CPA4-binding loop that is present in LXN was also present in isoform one of RARRES1. The five key amino acids required for the interaction between LXN and CPA4, were completely conserved in LXN from a number of different species (Figure 46b), highlighting their importance. Moreover, the same five amino acids from the CPA4 binding loop were 100% conserved in RARRES1 from a number of other species, including *H. Sapiens*. These results suggest that RARRES1 may also be able to interact with the carboxypeptidase CPA4.

A

RARRES1 transmembrane domain
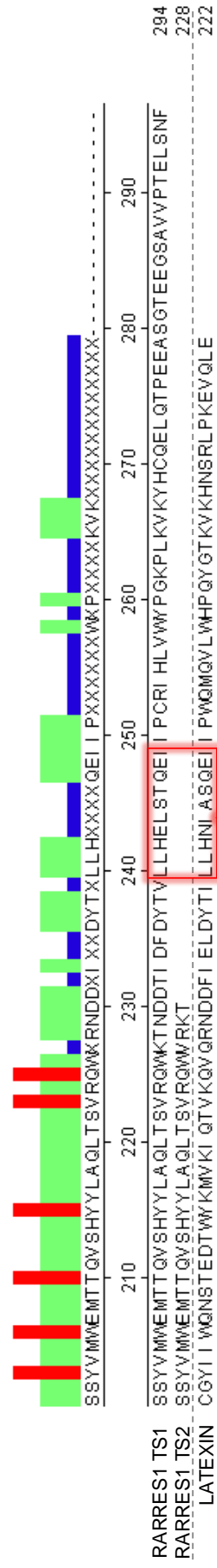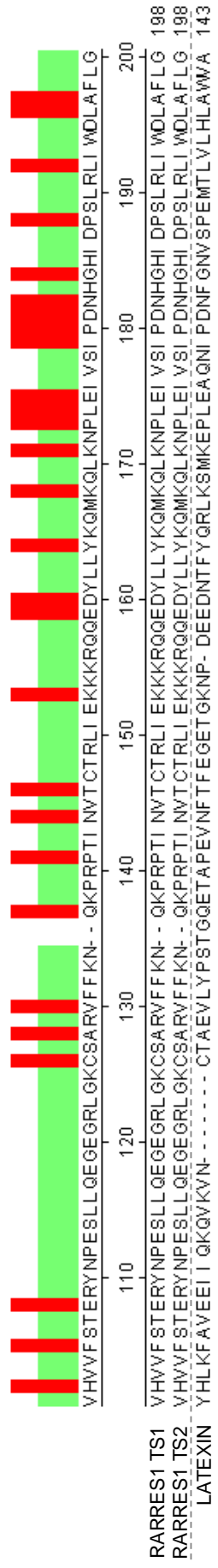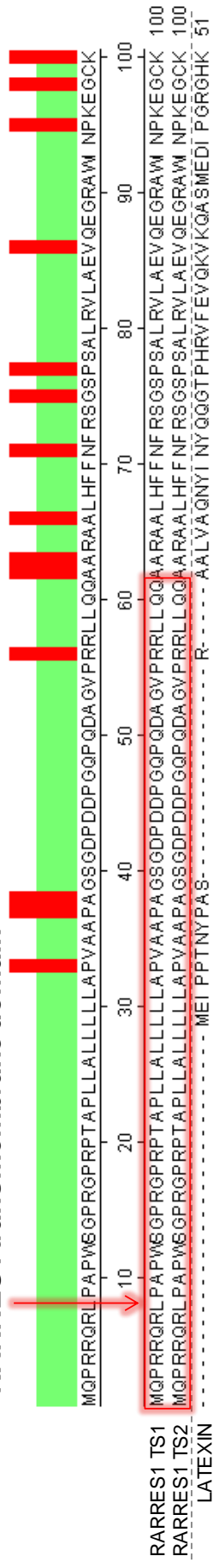
CPA4 binding domain
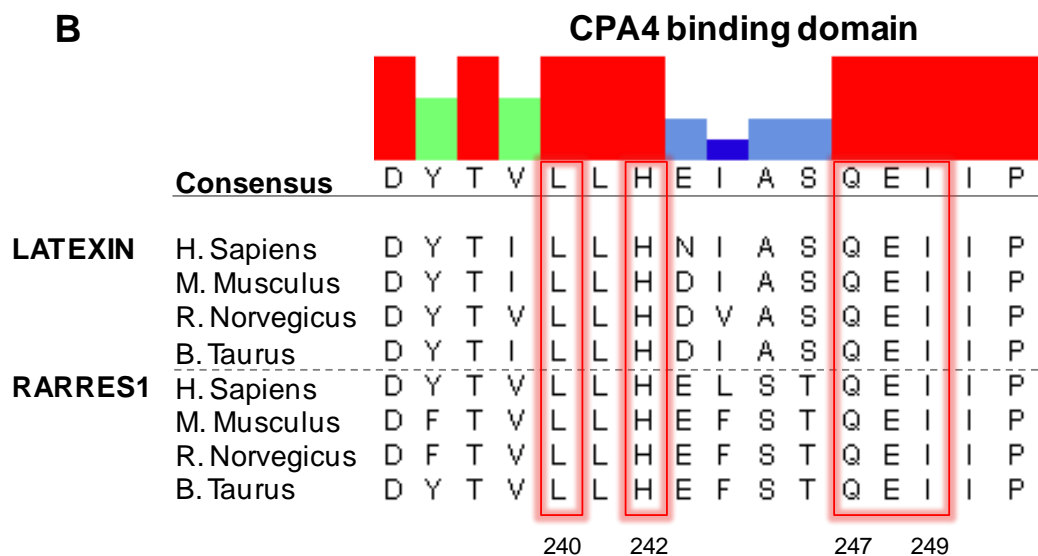
Figure 46. Amino acid sequence alignment of RARRES1 and LXN.
(a) Alignment of transcript 1 (TS1) and 2 (TS2) of RARRES1 and LXN aligned by the Clustal W method using the Lasergene MegAlign software. Highlighted by red boxes are the N-terminal transmembrane domain present in RARRES1 (1-61aa) and the CPA4 binding domain present in both RARRES1 TS1 and LXN (240-249aa; taken from (Pallares et al., 2005)). **(b)** Alignment of the CPA4 binding domain and surrounding amino acids (236-251aa) within RARRES1 and LXN from various species. Highlighted in red boxes are the key amino acids from LXN that are required to bind to CPA4 (240, 242, 247-249aa), which are fully conserved in RARRES1.

3.7.2. RARRES1 is located in the ER, and LXN is located in the nucleus of prostate epithelial cell lines

The cellular location of RARRES1 has been a matter of debate in the literature, with various groups speculating upon its location. Nagpal et al. (1996) initially suggested that RARRES1 was a transmembrane protein with a long extracellular region, due to the presence of a large hydrophobic patch at its N-terminus. More recently, based on the N-glycosylation status of RARRES1, it was proposed that the transmembrane protein faced the cytoplasm, enabling interaction with cytoplasmic proteins (Sahab et al., 2011). In contrast, little work has been done to identify the location of LXN.

Initially, and due to a lack of a specific antibody for RARRES1, haemagglutinin (HA)-tagged RARRES1 (RARRES1-HA) and LXN (LXN-HA) cDNA fusion expression vectors obtained from GeneCopoeia were transfected into PC3 and LNCaP cell lines to investigate their cellular location. Advantages for using epitope-tagged proteins includes: (1) the utilisation of well-characterised antibodies, (2) the antibody is specific to the tag so cross-reaction is avoided and (3) immunochemistry is possible for poorly immunogenic proteins (Jarvik and Telmer, 1998). Figure 47 shows that the HA-tagged expression vectors were transfected into cells effectively, with a transfection efficiency after 24 hours, of around 30% and 25% for RARRES1-HA in LNCaP and PC3 cells, respectively and 30% for LXN-HA in LNCaP cells. These preliminary experiments suggested that RARRES1 was located to the cytoplasm of cells and LXN was within the nucleus.

Following the commercialisation of a specific antibody to detect RARRES1, LNCaP cells were transfected with RARRES1-HA (Figure 47a) and LXN-HA (Figure 47e) and dual labelled with native antibody and a HA-tag antibody, which showed co-localisation of both epitope and native antibodies after transfection.

To determine the specific location of RARRES1, RARRES1-HA transfected LNCaP and PC3 cells were co-stained with anti-HA and cell compartmental marker antibodies and visualised using confocal microscopy. The results showed that RARRES1-HA did not co-localise with the plasma membrane marker α1-Na/K-ATPase (Figure 48b), but did co-stain with the ER marker, protein disulphide isomerase (PDI) (Figure 48c, d), suggesting that RARRES1 is located on the ER lumen membrane.

The cellular location of LXN was also visualised by confocal microscopy in LXN-HA transfected LNCaP cells, by co-staining with anti-LXN and anti-HA antibodies (Figure 48e). In contrast to RARRES1, immunofluorescence images showed that LXN-HA was located in a non-random pattern in the nucleus of LNCaP cells. To verify that the staining was genuinely nuclear and not due to artefacts, a stringent immunofluorescence procedure specifically for nuclear proteins was performed, using a 2% paraformaldehyde fixative and 0.2% TX-100, followed by 0.5% NP-40 to

permeabilise cells (Figure 48f). Despite LXN showing nuclear localisation, it did not contain a canonical nuclear localisation signal, as searched for using the PSORT tool (http://psort.nibb.ac.jp/form2.html).

To confirm that RARRES1 is not located in the plasma membrane of cells, a cellular fractionation technique was performed by Hannah Walker in the PC3 prostate epithelial cell line (Figure 49). RARRES1-HA transfection vectors were transfected into the PC3 cell line and cells were lysed and fractionated, using sodium carbonate and ultracentrifugation, after 24 hours. Western blotting was then utilised to visualise the expression of RARRES1-HA in the unbroken cells, wash or plasma membrane fractions. The results showed that RARRES1 was present in unbroken cells and the wash fraction after RARRES1-HA transfection, but not in mock (reagent only)-transfected cells. Importantly, RARRES1 expression was not detected in the plasma membrane fraction, which supported the result found by immunofluorescence. The control markers showed that each cell fraction was pure, with the plasma membrane marker α1-K/Na-ATPase being expressed only in the unbroken cell and plasma membrane fractions. The cytoplasmic β-actin marker was detected purely in the unbroken cell and wash fractions.

To confirm that the localisation of RARRES1 and LXN was the same in all cells and not just the representative cells in Figure 48, images of RARRES1-HA and LXN-HA expression were taken prior to zooming in (Figure 47). This confirmed that cytoplasmic (more specifically ER-located) and nuclear expression of RARRES1 and LXN, respectively, was not restricted to a small proportion of cells.

Taken together, RARRES1 and LXN are located in different cellular compartments in prostate epithelial cell lines. RARRES1 is not located on the plasma membrane, but is more probably located within the ER lumen membrane, whereas LXN is located within the nucleus.
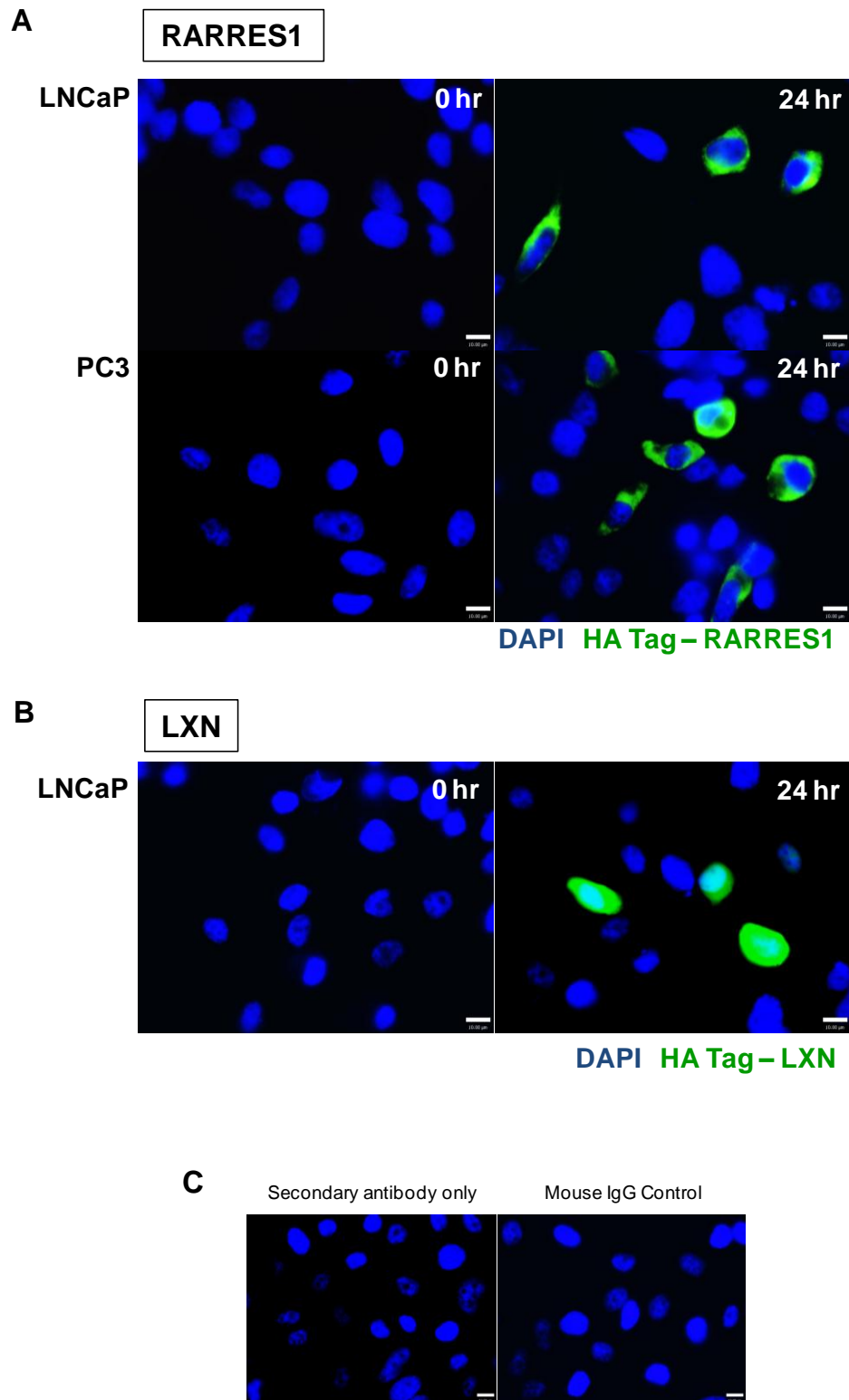
Figure 47. Immunofluorescence images of HA-tagged RARRES1 and LXN transfected into prostate epithelial cell lines.
(a) RARRES1 over-expression was detected by immunofluorescence in LNCaP and PC3 cells and **(b)** LXN over-expression in LNCaP cells using anti-HA tag antibodies at 0 hours or 24 hours after transfection. Cells were counterstained with DAPI to enable nuclear visualisation. White scale bar represents 10 μm. **(c)** Antibody controls using mouse IgG instead of primary antibody and secondary antibody only.

LNCaP   **LXN**

E DAPI | LXN | HA-tag (LXN) | Merge

10.00 μm

F DAPI | HA-tag (LXN) | LXN | Merge

10 μm

Rabbit + Mouse Secondary Antibody only   Rabbit + Mouse IgG Control Antibody

G
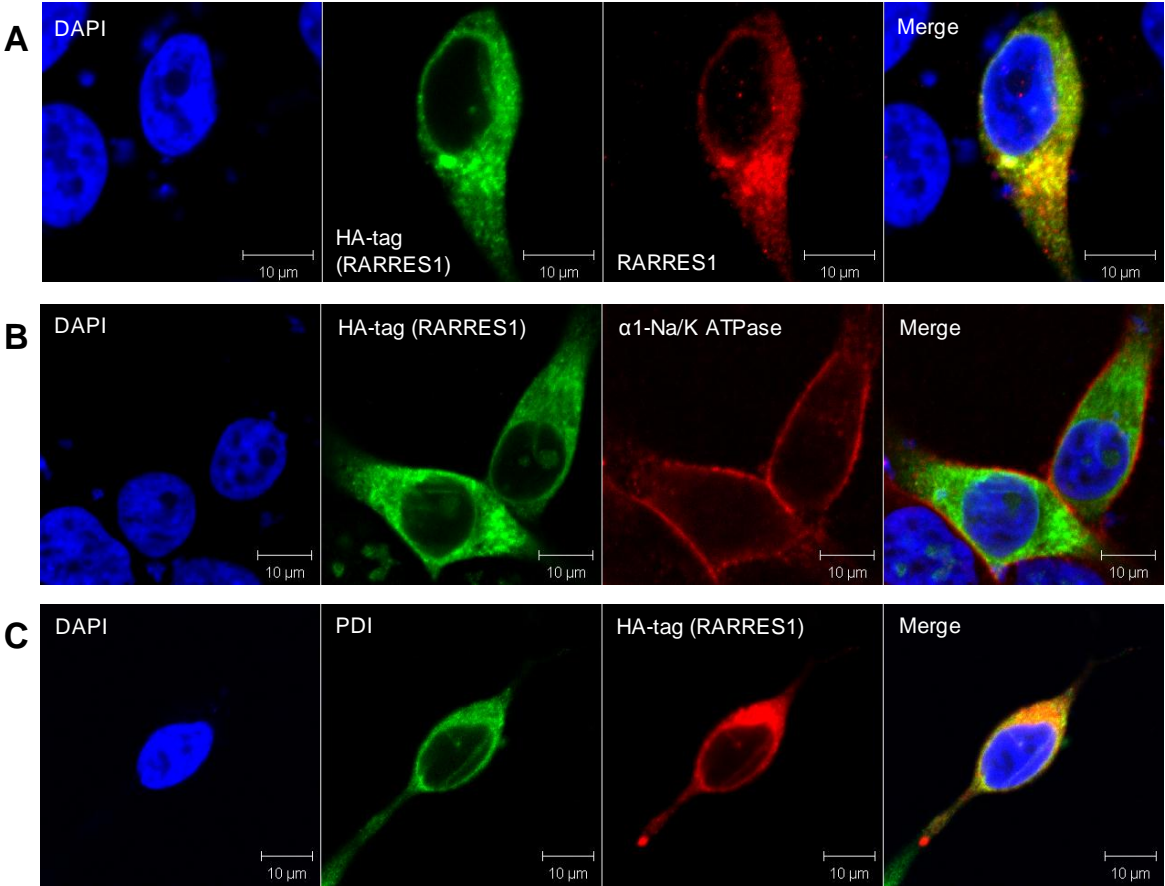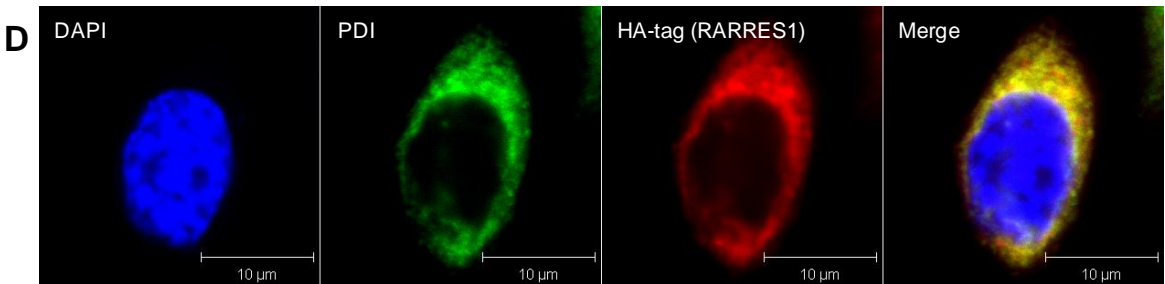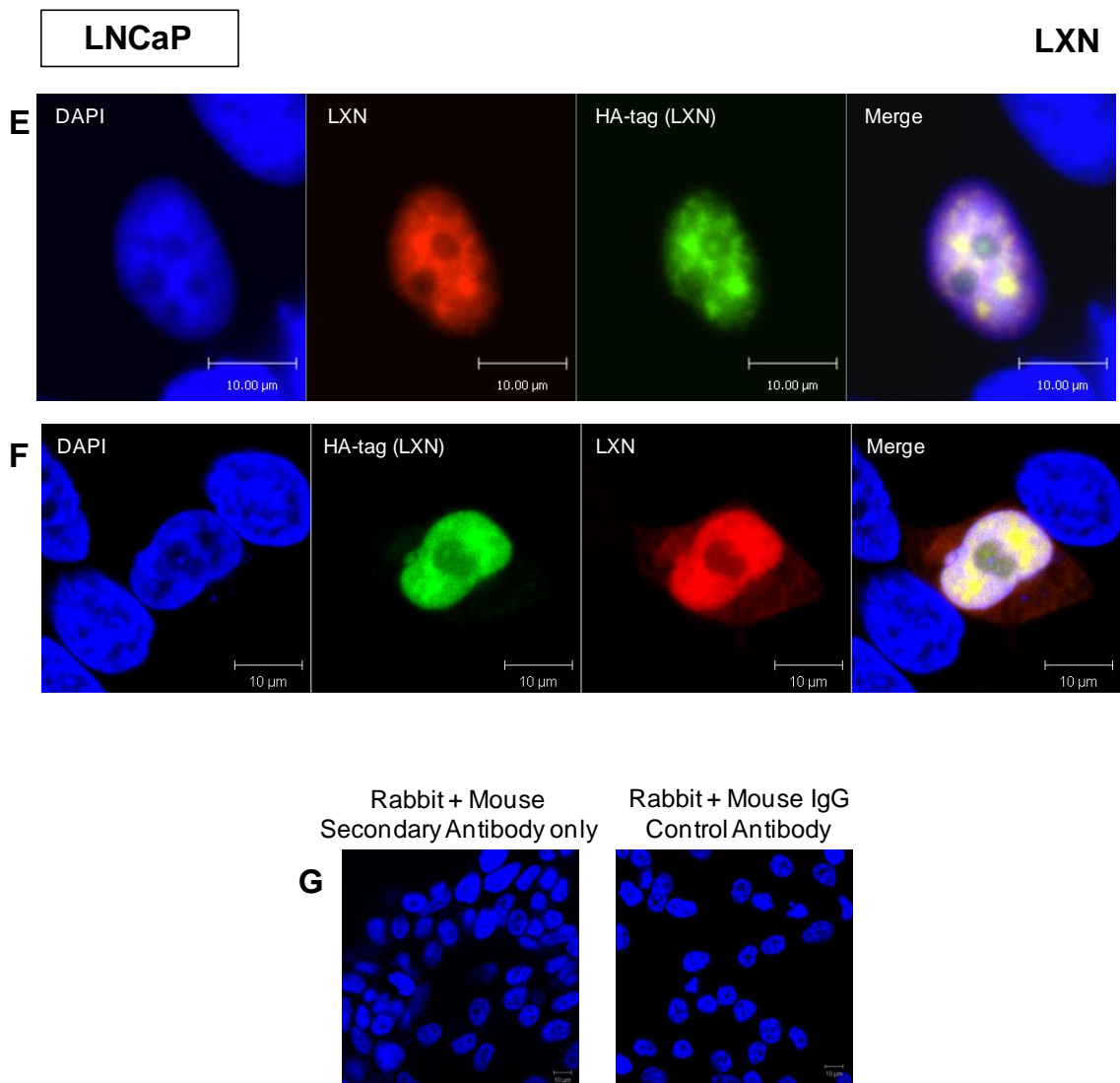
Figure 48. Immunofluorescence images of HA-tagged RARRES1 and LXN transfected into prostate epithelial cell lines.
Confocal Immunofluorescence images depicting the location of HA-tagged RARRES1 in LNCaP (a, b, c) and PC3 (d) cells and LXN in LNCaP (e, f) cells, 24 hours after transfection. Cells we co-stained with anti-HA tag and **(a)** anti-RARRES1, **(b)** anti-α1-Na/K-ATPase (plasma membrane marker), **(c, d)** anti-protein disulphide isomerise (PDI; ER marker), **(e)** anti-LXN antibodies or **(f)** anti-LXN antibodies after a more stringent nuclear fixation protocol: 2% paraformaldehyde fixative and 0.2% TX-100, followed by 0.5% NP-40 to permeabilise cells. Cells were counterstained with DAPI to enable nuclear visualisation. White scale bar represents 10 μm. **(g)** Antibody controls using rabbit or mouse IgG instead of primary antibody and secondary antibody only.
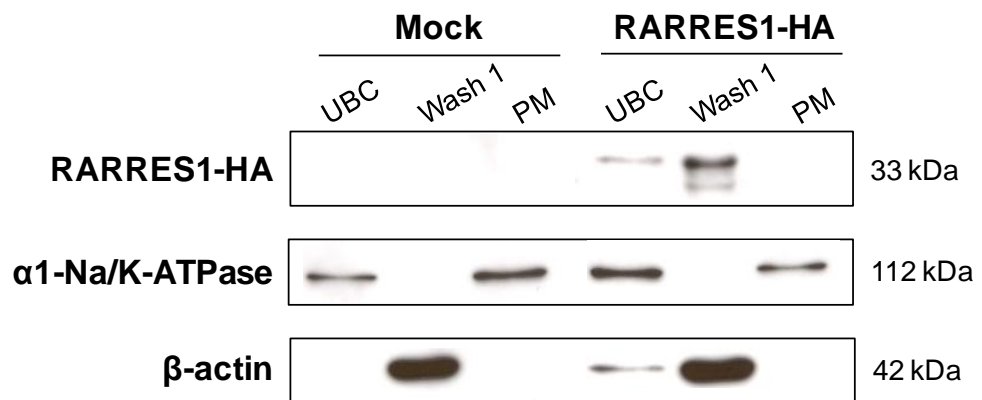
Figure 49. Cellular fractionation by western blotting of HA-tagged RARRES1 in the PC3 prostate epithelial cell line.
Western blot data showing protein levels of RARRES1-HA (33 kDa) in the unbroken cell fraction (UBC), wash fraction (Wash 1) and plasma membrane fraction (PM) of PC3 cells, transfected with HA-tagged RARRES1 or reagent-only control (Mock), for 24 hours prior to lysing the cells. Cells were fractionated using the sodium carbonate and ultracentrifugation method. Blots were probed with the plasma membrane marker α1-Na/K-ATPase (112 kDa) and cytoplasm marker β-actin (42 kDa) to ensure a pure plasma membrane population was obtained. This experiment was performed by Hannah Walker.

3.8. Function of RARRES1 and LXN in prostate epithelial cell lines

3.8.1. RARRES1 and LXN expression is modulated by siRNA and over-expression vectors in prostate epithelial cell lines

To assess the function of RARRES1 and LXN in the cell, knockdown and over-expression experiments were performed in prostate epithelial cell lines. SiRNA oligonucleotides targeted against RARRES1 and LXN were utilised to knockdown expression, as they: (1) minimise non-specific effects, (2) provide the ability to control the amount of siRNA more accurately than vector driven approaches and (3) are a fast and straightforward method to transiently knock down a gene. In all cases, expression knockdown was calculated relative to a non-specific scrambled siRNA negative control. 10 nM scrambled, RARRES1 and LXN siRNAs were transfected into the PNT1a cell line, derived from normal human prostate (as it expresses RARRES1 and LXN to high levels) and mRNA and protein were extracted over a time course.

RARRES1 mRNA was successfully knocked down by greater than 90%, 24 and 48 hours after transfection (Figure 50a). RARRES1 protein levels also suffered a significant knockdown, with the siRNA achieving a maximum reduction of 80% after 96 hours (Figure 50b). This delay in protein down-regulation is indicative of a long half-life of RARRES1. LXN mRNA (Figure 50c) and protein (Figure 50d) was successfully knocked down by almost 100% after 48, 72 and 96 hours. These results confirm that both siRNAs were able to reduce RARRES1 and LXN expression, to a point where changes in cell function could be measured.

Expression-ready, full-length ORF clones containing RARRES1 or LXN cDNA were utilised and transfected into cells for over-expression studies as they: (1) are expression and sequence verified clones, (2) are a cost-effective and time-effective method and (3) contain HA and/or GFP tags to monitor transfection and over-expression. In all cases, over-expression was relative to an empty vector negative control. Expression vectors were transfected into PNT1a and LNCaP cell lines and mRNA and protein expression quantified by qRT-PCR and western blotting, respectively. RARRES1 mRNA was over-expressed to higher levels after 24 hours (2,500-fold) than 48 hours (500-fold) in PNT1a cells (Figure 51a). However, in LNCaP cells RARRES1 mRNA was higher after 48 hours (9,000-fold) than 24 hours (5,000-fold) (Figure 51b). RARRES1 protein levels also saw a significant over-expression, with the greatest increase seen after 96 hours in both PNT1a (Figure 51e) and LNCaP (Figure 51f) cells. Similarly to RARRES1, LXN mRNA was over-expressed to higher levels after 24 hours (10,000-fold) than 48 hours (1,000-fold) in PNT1a cells (Figure 51c), but expressed at higher levels after 48 hours (4,500-fold) than 24 hours (2,500-fold) in LNCaP cells (Figure 51d). LXN protein levels also saw a significant over-expression, with the greatest increase seen after 96 hours in PNT1a cells (Figure 51g) and after 48 hours in LNCaP cells (Figure 51h). In PNT1a cells, RARRES1 and LXN mRNAs were rapidly over-expressed at 24 hours, but then partially down-regulated at 48 hours. This very transient expression appears to be a feature of this cell type, as

in LNCaP cells mRNA expression continued to increase at 48 hours and the overall increase in expression was of a higher magnitude in this cell line. Taken together, these results confirm that both expression vectors were able to increase RARRES1 and LXN expression, to a point where changes in cell function could be measured.
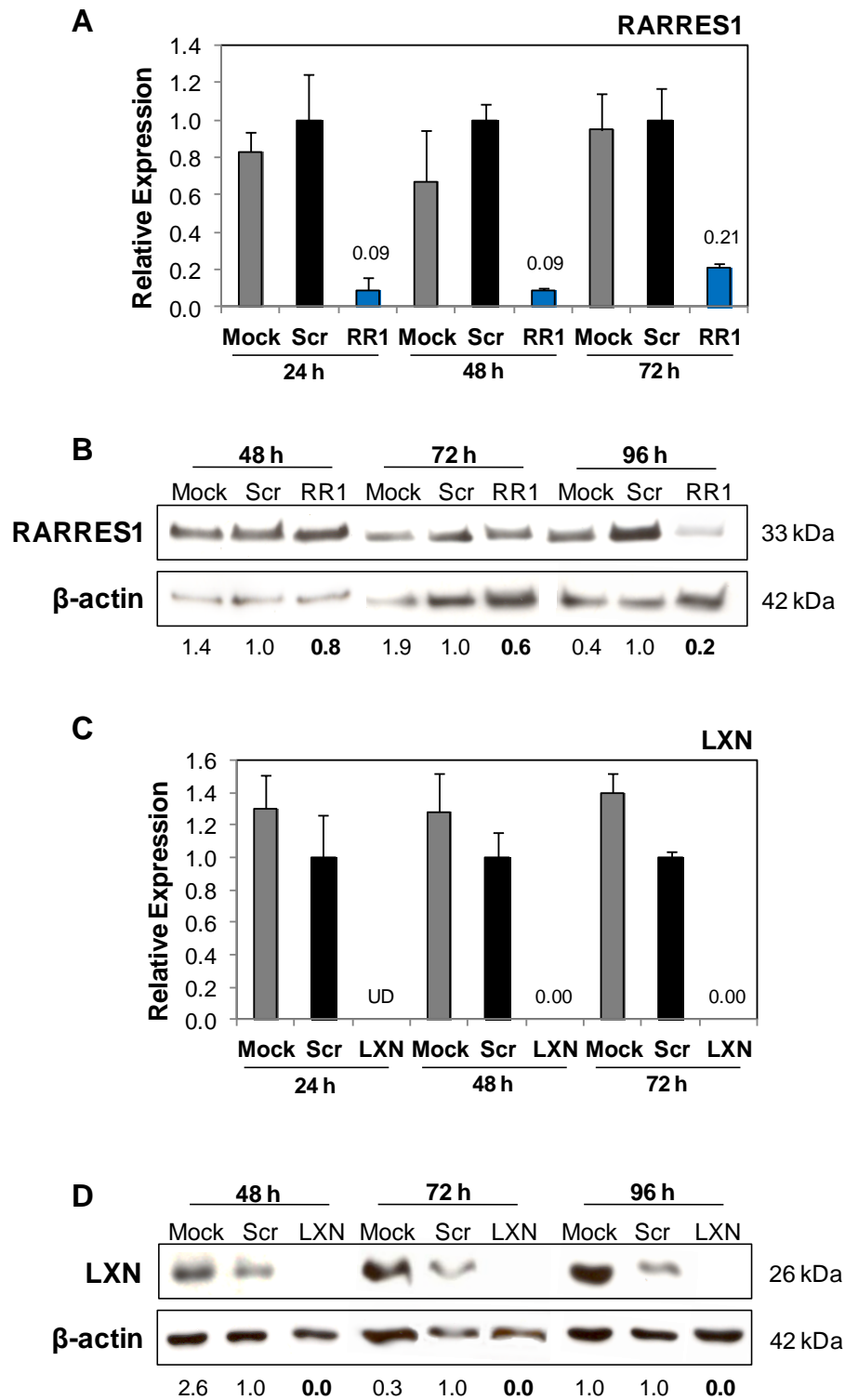
Figure 50. SiRNA knockdown of RARRES1 and LXN in the PNT1a epithelial cell line.
qRT-PCR data showing expression of **(a)** RARRES1 and **(b)** LXN relative to an 18S endogenous control gene over time in reagent-only (mock), 10 nM scrambled (scr), RARRES1 (RR1) or LXN siRNA (LXN) samples from PNT1a cells. All values are normalised to scr, which is set at 1 for each time point; UD: undetectable expression after 40 cycles; n=3 technical replicates; error bars expressed as range of the mean. Quantified western blot data showing protein levels of **(c)** RARRES1 (33 kDa) and **(d)** LXN (29 kDa) over time in mock, scr and RR1/LXN samples from PNT1a cells. Protein expression was quantified relative to a β-actin (42 kDa) loading control and relative to the scr control at each time point (set at 1; values below each blot).

E

		48 h			72 h			96 h		RARRES1 PNT1a
	Mock	Vect	RR1	Mock	Vect	RR1	Mock	Vect	RR1	
RARRES1-HA										33 kDa
β-actin										42 kDa
	0	0	**0.14**	0	0	**0.36**	0	0	**1.0**	

F

		48 h			72 h			96 h		RARRES1 LNCaP
	Mock	Vect	RR1	Mock	Vect	RR1	Mock	Vect	RR1	
RARRES1-HA										33 kDa
β-actin										42 kDa
	0	0	**0.63**	0	0	**0.49**	0	0	**1.0**	

G

		48 h			72 h			96 h		LXN PNT1a
	Mock	Vect	LXN	Mock	Vect	LXN	Mock	Vect	LXN	
LXN-HA										26 kDa
β-actin										42 kDa
	0	0	**0.51**	0	0	**0.73**	0	0	**1.0**	

H

		48 h			72 h			96 h		LXN LNCaP
	Mock	Vect	LXN	Mock	Vect	LXN	Mock	Vect	LXN	
LXN-HA										26 kDa
β-actin										42 kDa
	0	0	**1.0**	0	0	**0.86**	0	0	**0.52**	
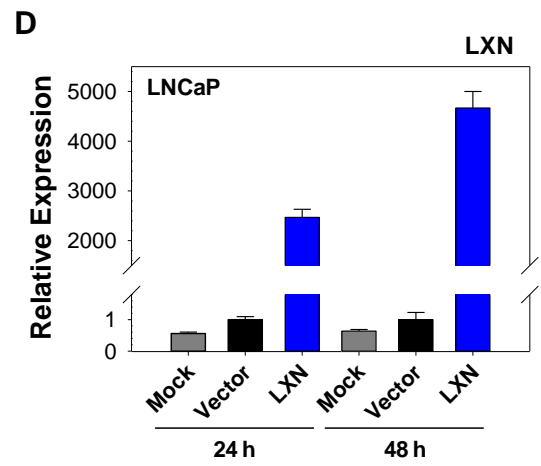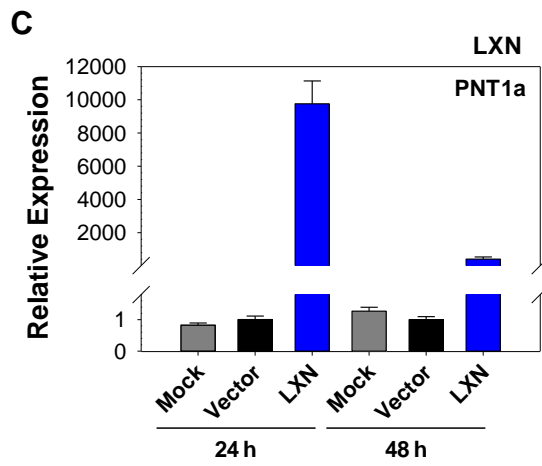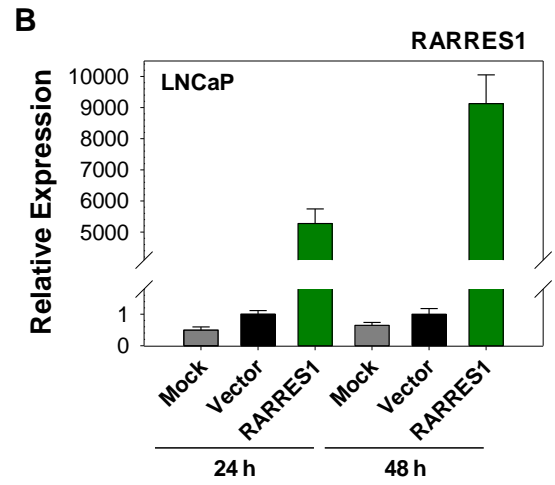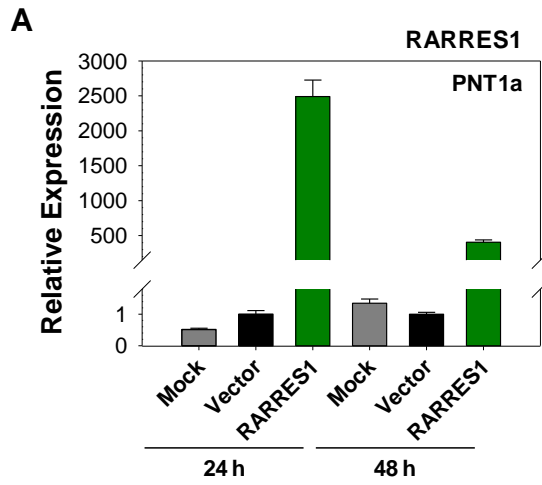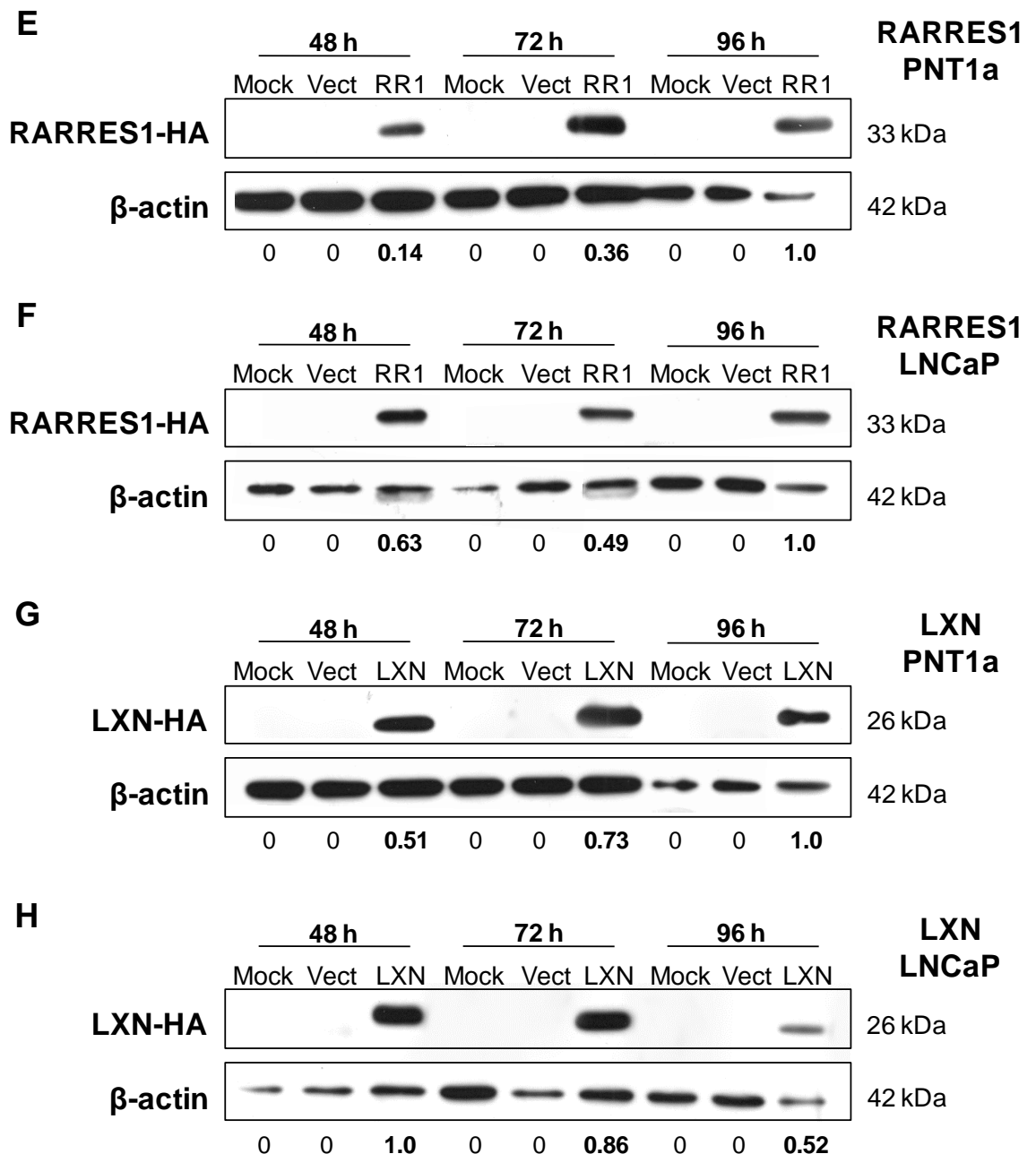
Figure 51. Over-expression of RARRES1 and LXN in the PNT1a and LNCaP epithelial cell lines.
qRT-PCR data showing expression of **(a, b)** RARRES1 and **(c, d)** LXN relative to a GAPDH endogenous control gene over time in PNT1a (a, c) and LNCaP (b, d) cells transfected with reagent-only (mock), empty vector (vect), RARRES1 (RR1) or LXN (LXN) vectors. All values are normalised to vect, which is set at 1 for each time point; n=3 technical replicates; error bars expressed as range of the mean. Quantified western blot data showing protein levels of **(e, f)** RARRES1 (33 kDa) and **(g, h)** LXN (29 kDa) over time, in PNT1a (e, g) and LNCaP (f, h) cells transfected with mock, vect, RR1 or LXN vectors. Protein expression was quantified relative to a β-actin (42 kDa) loading control and relative to the highest expressing sample (set at 1; values below each blot).

3.8.2. RARRES1 and LXN regulate the motility of prostate epithelial cell lines

It has been shown previously that RARRES1 expression affects tumour cell invasion in prostate cancer PC-3M cells (Jing et al., 2002) and nasopharyngeal carcinoma HK1-EBV cells (Kwok et al., 2009). To investigate the motility of prostate epithelial cells after modulating RARRES1 and LXN expression, wound healing assays were performed in the highly motile benign PNT1a cell line. This assay was utilised as it: (1) mimics, to some extent, cell migration *in vivo*, (2) is simple and (3) is inexpensive (Rodriguez et al., 2005).

Cells were transfected with 10 nM scrambled, RARRES1 and LXN siRNAs or empty vector control, RARRES1 and LXN expression vectors and grown to 90% confluency. After 54 hours a wound was created in the cell monolayer and migration into the wound was monitored over 18 hours. Images were taken 18 hours after wounding and the percentage of wound closure was calculated. The width of the wound at 0 hours and 18 hours was measured, the average (of 10 points) taken and the relative percentage wound closure at 18 hours with respect to 0 hours was calculated (Figure 52a).

After knock down of RARRES1, the extent of migration significantly (P<0.05) increased from 56% with the scrambled siRNA-treated cells, to 80% with RARRES1 siRNA-treated (Figure 52b, c). Conversely, the percentage closure decreased after LXN knockdown, from 56% in scrambled siRNA-treated cells, to 21% in LXN siRNA-treated cells. The reciprocal experiment was then performed; RARRES1 and LXN were over-expressed via the transfection of cDNA expression vectors into PNT1a cells (Figure 52d, e). Wound closure decreased from 68% in vector control-treated cells, to 51% after RARRES1 over-expression and significantly (P<0.05) increased to 88%, after LXN over-expression. These results suggest that the two proteins have opposite effects on cell motility, RARRES1 represses motility and LXN promotes cell motility.

One point to note is that cells were not serum-starved prior to creating the wound in these assays and the effect on cell motility could therefore be due to changes in cell proliferation. However, this is unlikely as it has previously been shown that RARRES1 over-expression has no effect on the PC-3M prostate cell line (Jing et al., 2002) and visually there was no difference in cell number in this experiment.

In summary, these wound healing assays show that RARRES1 represses cell motility, but LXN promotes the cell motility of prostate epithelial cell lines.

A

Grow monolayer of cells → Create wound with 1ml pipette tip → **18 hrs** → Take pictures of wound after 18hrs

Using Volocity software, measure average size of wound at 0 hours and 18 hours Calculate % wound closure

B

Knockdown

C

	Scrambled	RARRES1	LXN
0 hrs			
18 hrs			

D

Overexpression

E
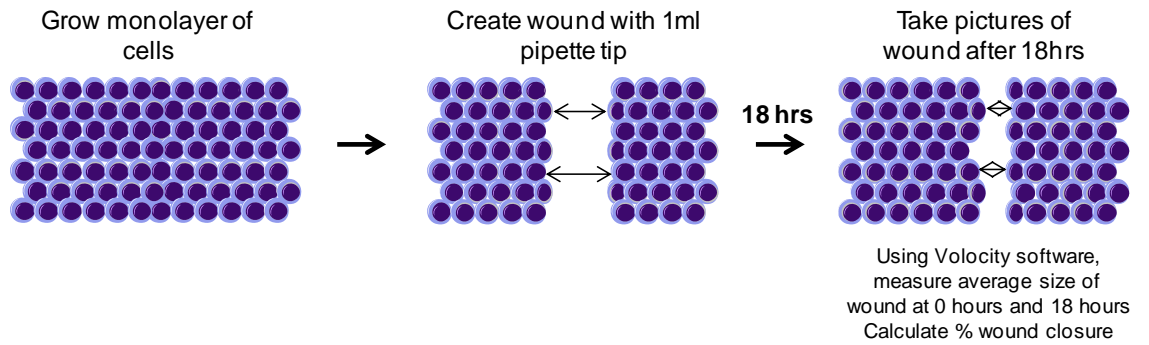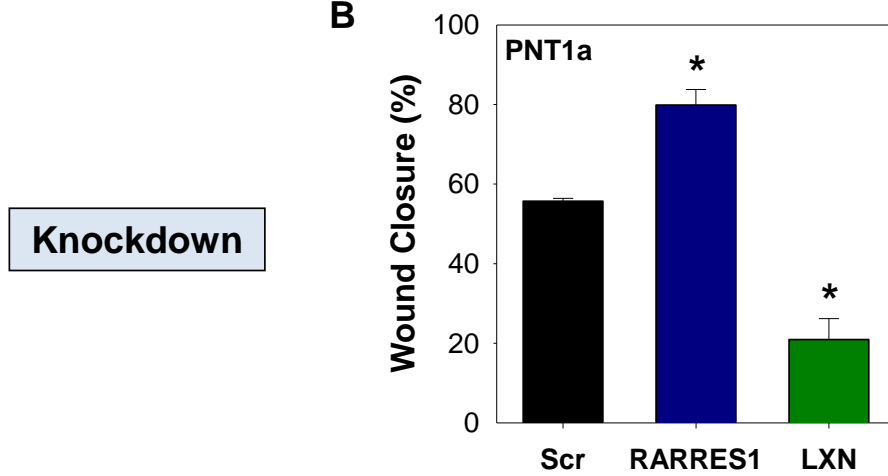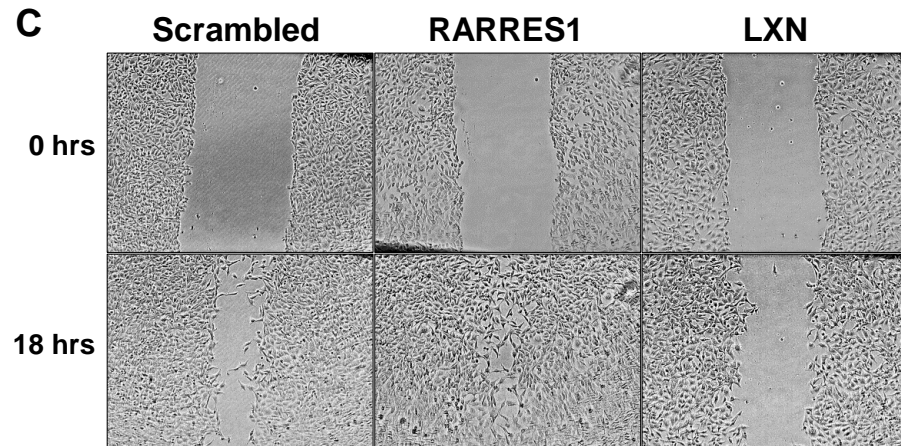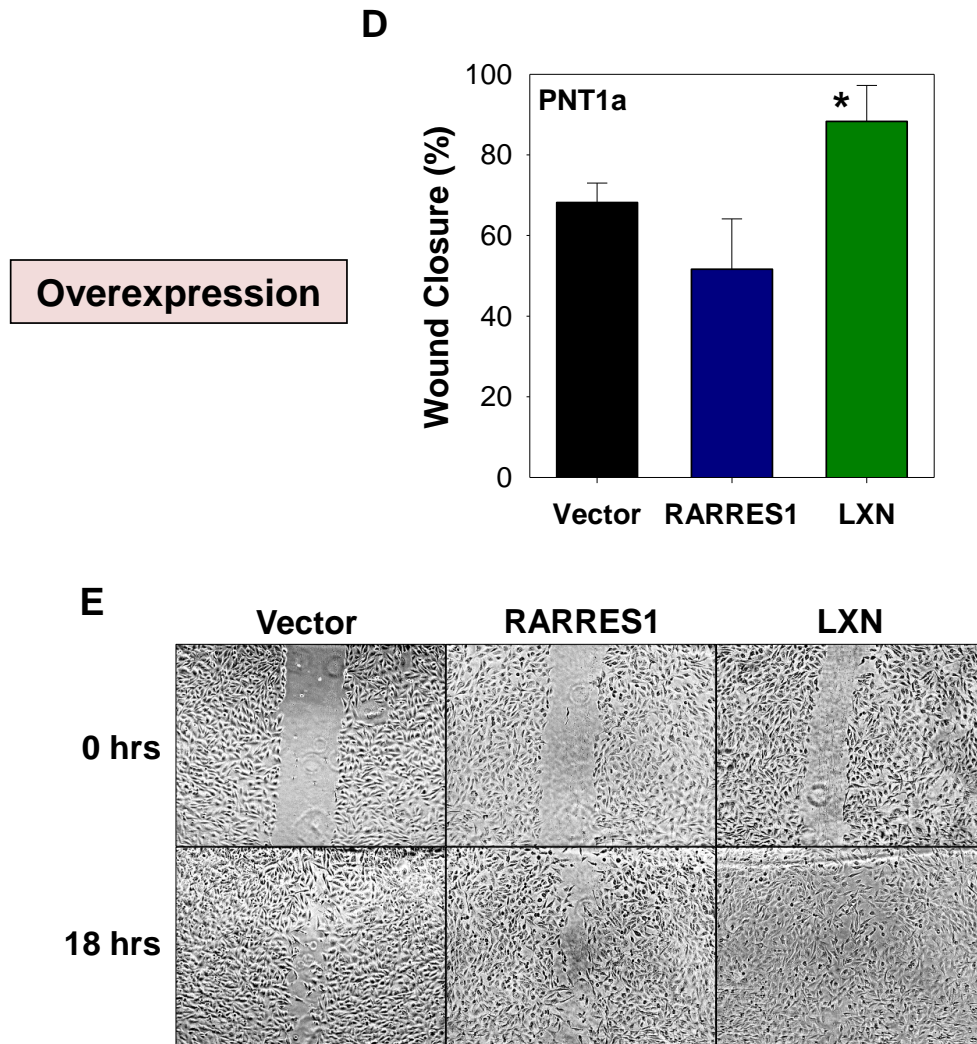
Figure 52. Wound healing assay after modulation of RARRES1 and LXN expression in the PNT1a epithelial cell line.
(a) Schematic of wound healing assay performed. **(b/c)** Representative images and wound healing assay data showing the motility of PNT1a cells transfected with 10 nM scrambled, RARRES1 and LXN siRNA or **(d/e)** empty vector, RARRES1-HA and LXN-HA transfection vectors, 72 hours after transfection and 18 hours after wounding with a 1 ml pipette tip. % wound closure was calculated by taking an average of the size of the wound after 18 hours, relative to the starting wound size (Error bars expressed at the standard deviation of n=3 biological replicates). Statistical significance values were measured by the Student's T-test (Unpaired, two-tailed; * $P<0.05$).

3.8.3. RARRES1 and LXN regulate the invasion of prostate epithelial cell lines

Experiments in Section 3.8.2 show that RARRES1 and LXN have opposite effects on the migration of prostate epithelial cell lines. It has also previously been shown that RARRES1 expression affects tumour cell invasion in CaP PC-3M cells (Jing et al., 2002) and nasopharyngeal carcinoma HK1-EBV cells (Kwok et al., 2009). To investigate the invasive capacity of cells after modulating RARRES1 and LXN expression, Matrigel invasion assays were performed in non-malignant PNT1a and malignant LNCaP prostate epithelial cell lines. PNT1a cells were transfected with 10 nM scrambled, RARRES1 and LXN siRNA and LNCaP cells were transfected with vector control, RARRES1 or LXN expression vectors for 24 hours prior to commencing the invasion assay, as described in Section 2.10.2. A highly invasive MDA-MB-231 breast cancer cell line and highly motile, but weakly invasive, PNT1a prostate epithelial cell line were used as positive and negative controls, respectively.

Results show that the invasion of relatively non-invasive PNT1a cells increased from 5% in the scrambled siRNA-treated cells, to 7% in RARRES1 siRNA-treated and 14% in LXN siRNA-treated cells (Figure 54a). After RARRES1 knockdown, there was a slight increase in the number of motile cells, but a more prominent increase in the number of invasive cells, from 5.8 in the scrambled siRNA-treated cells, to 9.2 cells per field (Figure 54b). In contrast, after LXN knockdown, there was a considerable decrease in the number of motile cells, from 72.5 in control treated, to 28.3 cells per field, but only a marginal increase in the number of invasive cells. Taken together, these data confirms the wound healing assay data, which showed that after RARRES1 and LXN knockdown, cell migration increased and decreased, respectively. RARRES1 knockdown increased invasion more than LXN knockdown, but due to the major effect of LXN on migration, overall relative invasion was higher after LXN siRNA treatment.

The reciprocal over-expression experiment was next performed in malignant LNCaP cells, which harbour the lowest expression of RARRES1 and LXN. Over-expression in the relatively non-invasive PNT1a cells would decrease their invasive potential even further, so this cell type was not used for this experiment. Results shows that the invasion of LNCaP cells decreased from 55.9% in vector-treated cells, to 45.8% after RARRES1 over-expression and 35.3% after LXN over-expression (Figure 54c). When looking at the raw data, there was an increase in the number of motile cells from 3.8 cells in the control cells, to 5.7 cells after RARRES1 over-expression and 7.9 cells per field after LXN over-expression (Figure 54d). Unexpectedly, there was also an increase in the number of invasive cells from 4.8 cells in the control cells, to 5.9 cells after RARRES1 over-expression and 6.3 cells per field after LXN over-expression. RARRES1 and LXN over-expression in the LNCaP cell line led to a greater increase in the migration of cells, compared to the invasion of cells, therefore resulting in a decrease in relative invasion. Taken together, the invasion assay results demonstrate that both RARRES1 and LXN function to suppress invasion in prostate epithelial cell lines. The result for RARRES1 is clear-

cut, a lack of expression increases the invasive capacity of cells. However, the effect that LXN has on invasion is predominantly due to its effect on cell motility.
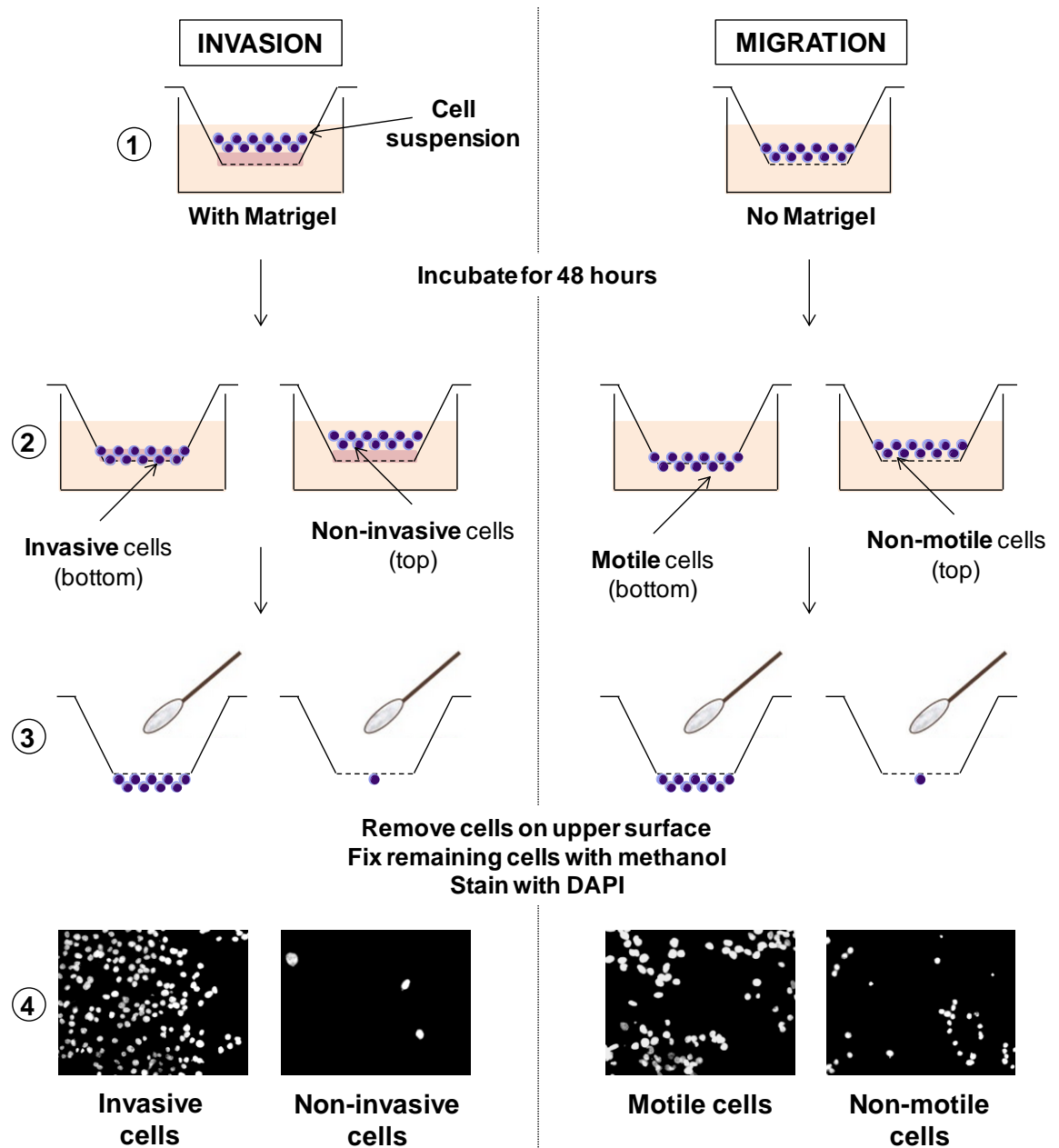
Figure 53. Schematic of Matrigel invasion assay.
1. Cell suspension placed in inserts coated with Matrigel. **2.** Invasive/Motile cells move through the porous insert (motile) or degrade the Matrigel (invasive). Non-motile/non-invasive cells remain in the upper chamber. **3.** Cells on the upper surface are removed. Cells on bottom surface are fixed with methanol and stained with DAPI. **4.** Cells are counted at 20 x magnification.

A
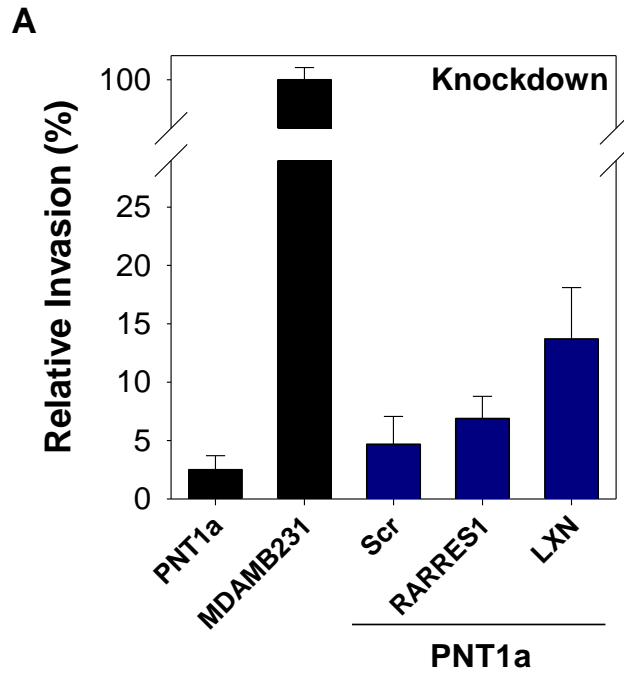
B

KNOCKDOWN		Average cells per field			
		No Matrigel Motility	With Matrigel Invasion	Invasion/Motility	Relative Invasion
-	PNT1a	77.5	3.3	0.043	**2.5%**
+	MDA-MB-231	48.3	83.0	1.72	**100.0%**
PNT1a	Scr	72.5	5.8	0.08	**4.7%**
	RARRES1	77.5	9.2	0.12	**6.9%**
	LXN	28.3	6.7	0.24	**13.7%**

C
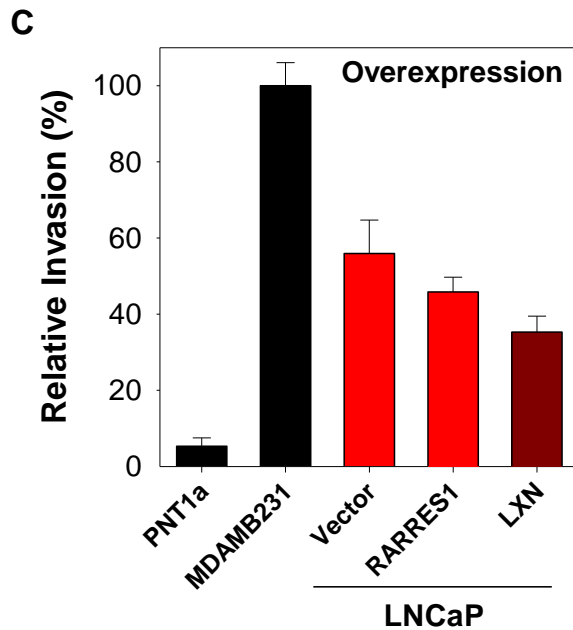
D

OVEREXPRESSION		Average cells per field			
		No Matrigel Motility	With Matrigel Invasion	Invasion/Motility	Relative Invasion
-	PNT1a	144.0	17.3	0.12	**5.3%**
+	MDA-MB-231	31.7	71.6	2.26	**100.0%**
LNCaP	Vector	3.8	4.8	1.26	**55.9%**
	RARRES1	5.7	5.9	1.04	**45.8%**
	LXN	7.9	6.3	0.80	**35.3%**

Figure 54. Matrigel invasion assay after modulation of RARRES1 and LXN expression in prostate epithelial cell lines.
(a, b) Matrigel invasion assay data showing the relative percentage of invasive PNT1a cells transfected with 10 nM scrambled (scr), RARRES1 and LXN siRNA (knockdown) or **(c, d)** LNCaP cells transfected with vector only, RARRES1-HA, and LXN-HA transfection vectors (over-expression). All data is 72 hours after transfection. **(b, d)** Raw data tables showing the average number of motile and invasive cells per field of view and the respective relative invasion percentages. The percentage of cells invading into Matrigel was measured in the presence of RPMI medium + 10% FCS as chemo-attractant, below the Matrigel. The benign PNT1a cell line and highly metastatic MDA-MB-231 cell line were used, as negative and positive controls for invasion. (Error bars expressed as standard deviation of n=3 technical replicates).

3.8.4. Knockdown of LXN in the metastatic PC3 cell line induces apoptosis

LXN expression is down regulated by DNA methylation in most malignant prostate epithelial cell lines. However, LXN is over-expressed in one of the most metastatic CaP cell lines, PC3. To determine the role of LXN in CaP metastasis and the PC3 cell line, expression of LXN was knocked down by siRNA. 10 nM scrambled and LXN siRNAs were transfected into the PC3 cell line and mRNA and protein were extracted over a time course.

LXN mRNA was knocked down by a maximum of 84%, 48 hours after transfection (Figure 55a). LXN protein levels also suffered a significant knockdown, with the siRNA achieving almost 100% reduction after 72 hours and 96 hours (Figure 55b). These results confirmed that LXN siRNAs were able to reduce LXN expression to a point where changes in cell function could be measured. After transfection of LXN siRNA into PC3 cells, unlike any other cell line tested, a phenotypic effect on the cells was visible. Considerably fewer cells were present after 72 hours onwards, compared to the scrambled-siRNA control and cells acquired an apoptotic phenotype (Figure 55c).

A flow cytometry-based apoptosis assay was performed to determine whether cell death was occurring by apoptosis. A FITC-labelled inhibitor of pan-caspase was used to stain activated caspases in the cell, and a dead cell stain, Sytox-blue, was used to detect dead cells. After siRNA treatment of PC3 cells for 96 hours, a 5% increase in the number of dead cells (from 3.3% with scr, to 8.0%) and a 15% increase in dying apoptotic cells (from 2.8% with scr to 17.5%), was observed (Figure 55d, e). These results show that LXN expression is crucial for the viability of PC3 cells, hence the need for these cells to over-express this gene.

A

B

C
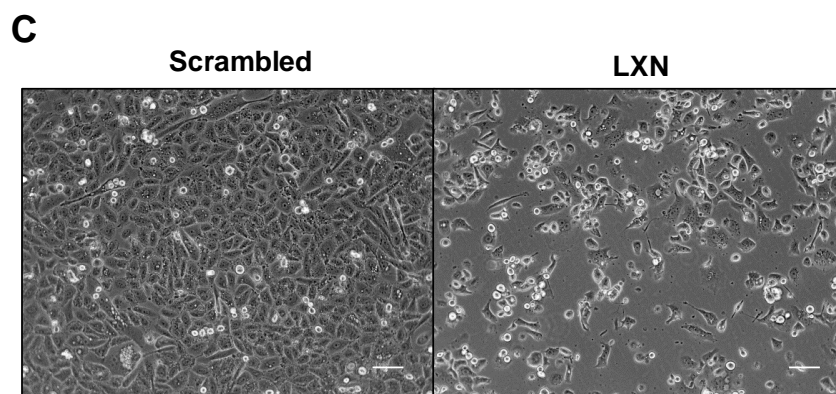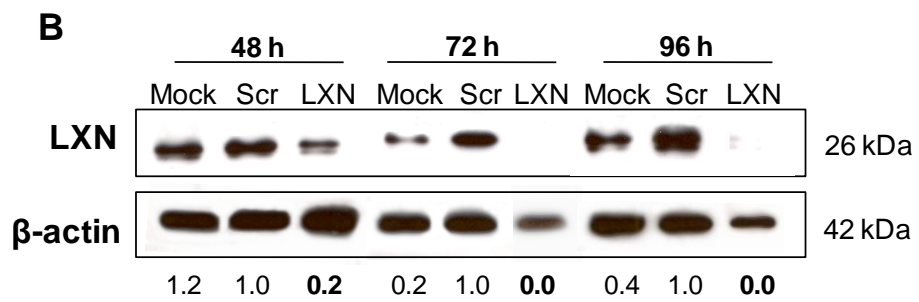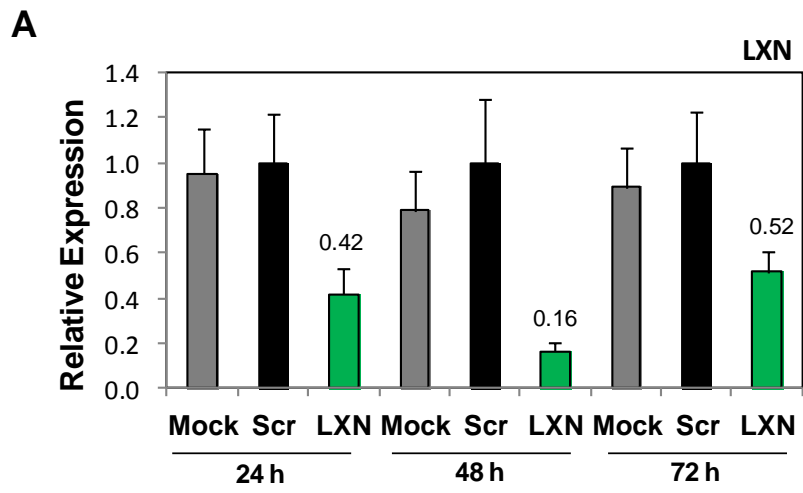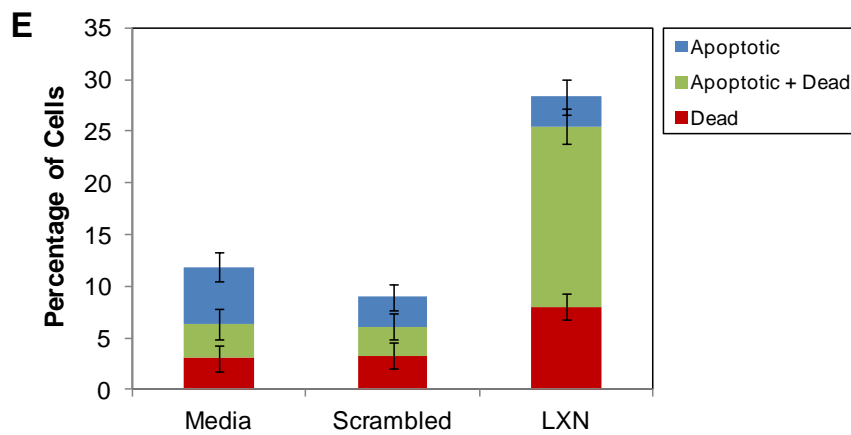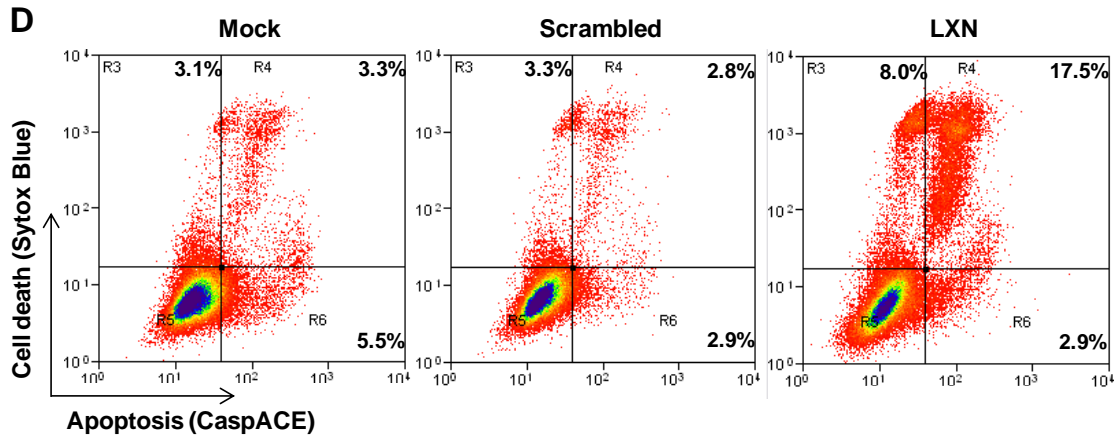
Figure 55. Apoptosis assay after siRNA knockdown of LXN in the PC3 prostate epithelial cell line.

(a) qRT-PCR data showing expression of LXN relative to an 18S endogenous control gene over time in reagent-only (mock), 10 nM scrambled (scr) and LXN siRNA (LXN) samples from PC3 cells. All values are normalised to scr, which is set at 1 for each time point (n=3 technical replicates; error bars expressed as range of the mean). **(b)** Quantified western blot data showing protein levels of LXN (29 kDa) over time in mock, scr and LXN samples from PC3 cells. Protein expression was quantified relative to a β-actin (42 kDa) loading control and relative to the scr control at each time point (set at 1; values below each blot). **(c)** Images at 20 x magnification of PC3 cells transfected with scrambled or LXN siRNA for 96 hours. **(d)** Representative images and **(e)** quantification of flow cytometry analysis (n=2 replicates) for apoptosis of PC3 cells transfected with transfection reagent only (mock), scrambled siRNA or LXN siRNA for 96 hours. Cells were dual-stained with a CaspACE-FITC apoptosis marker and Sytox Blue dead cell stain (Violet 1).

3.9. Function of RARRES1 and LXN in primary prostate epithelial cultures

3.9.1. RARRES1 and LXN expression is knocked down by siRNA in primary prostate epithelial cultures

RARRES1 and LXN affect the motility and invasion of epithelial cell lines. To determine the function of RARRES1 and LXN in primary prostate epithelial cell cultures, siRNAs against RARRES1 and LXN were utilised to knock-down expression. In all cases, expression knockdown was relative to a non-specific scrambled siRNA negative control. 50 nM scrambled, RARRES1 and LXN siRNAs were transfected into a primary prostate CaP (H131/11 RA) epithelial culture and mRNA and protein was extracted over a time course. RARRES1 and LXN were knocked down by siRNA instead of being over-expressed in prostate epithelial cultures as: (1) they are easier to transfect into typically difficult-to-transfect primary cells, (2) they have lower off-target effects and cytotoxicity and (3) RARRES1 and LXN expression is low in only a small proportion of cells, so knocking down expression in the remaining cells would result in a greater effect than over-expression, in a minority of cells.

RARRES1 mRNA was successfully knocked down to a maximum of 90%, 72 hours after transfection (Figure 56a). RARRES1 protein levels also suffered a significant knockdown, with the siRNA achieving almost 100% knockdown after 96 hours (Figure 56b). LXN mRNA was successfully knocked down to a maximum of 95%, 48 hours after transfection (Figure 56c). LXN protein levels also saw a significant knockdown, with the siRNA achieving almost 100% knockdown after 72 hours (Figure 56d). These results confirm that despite primary cells being notoriously difficult to transfect, both siRNAs are able to reduce RARRES1 and LXN expression to a point where changes in cell function could be measured. Furthermore, as seen in cell lines, only the full-length 33 kDa RARRES1 isoform was expressed and not the shorter variant.

To confirm that RARRES1 and LXN were also knocked down by siRNA in other primary cultures, mRNA expression levels of RARRES1 (Figure 56e) and LXN (Figure 56f) after siRNA transfection were measured by qRT-PCR, in a further three primary cultures. These results showed that RARRES1 and LXN mRNA was knocked down to levels greater than 60% in all samples after 24 hours. Protein knockdown was not analysed as mRNA and protein knockdown was shown to correlate in Figure 56a-d.

Results
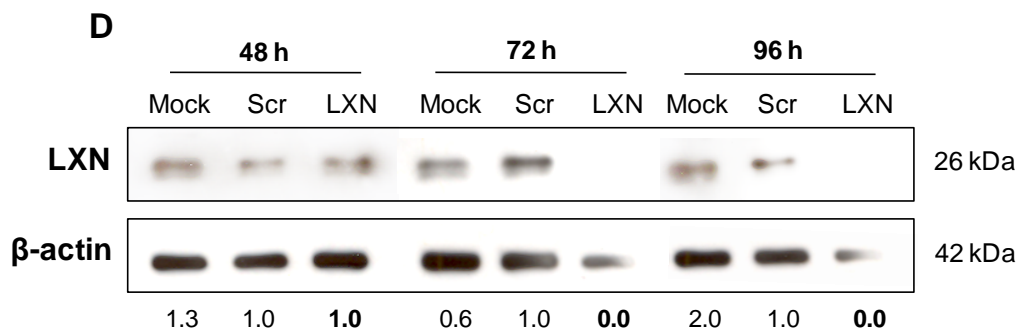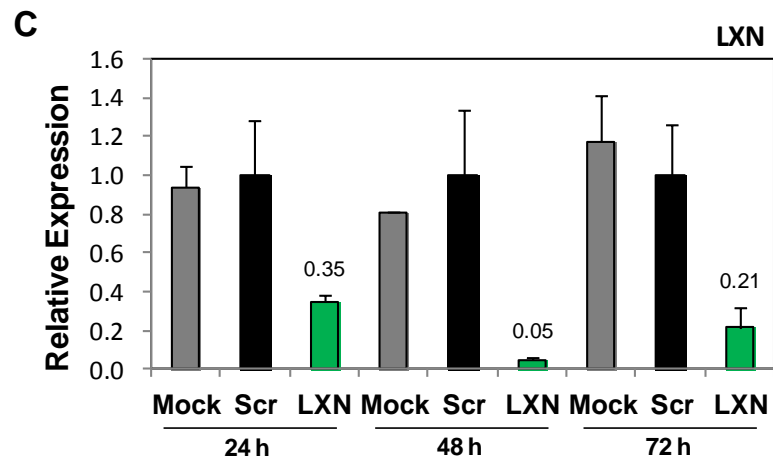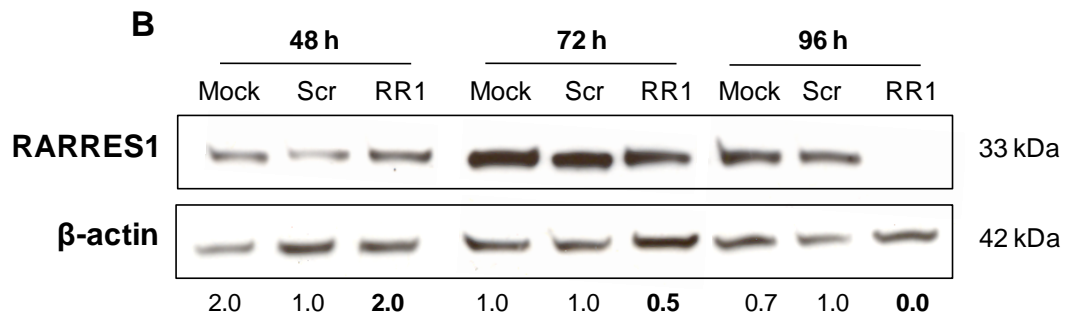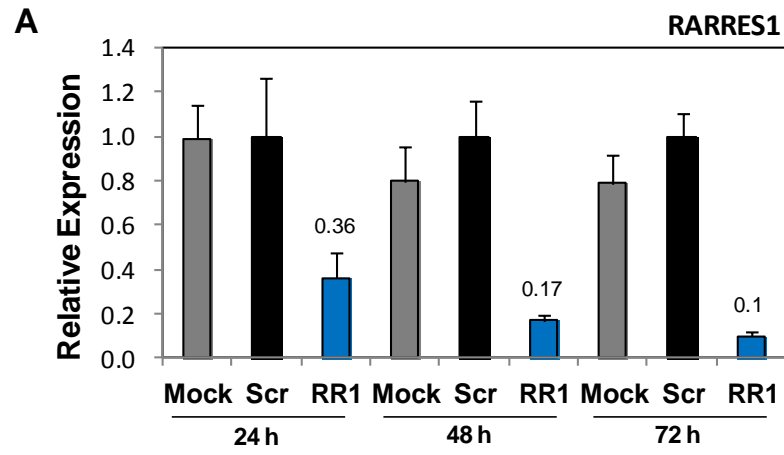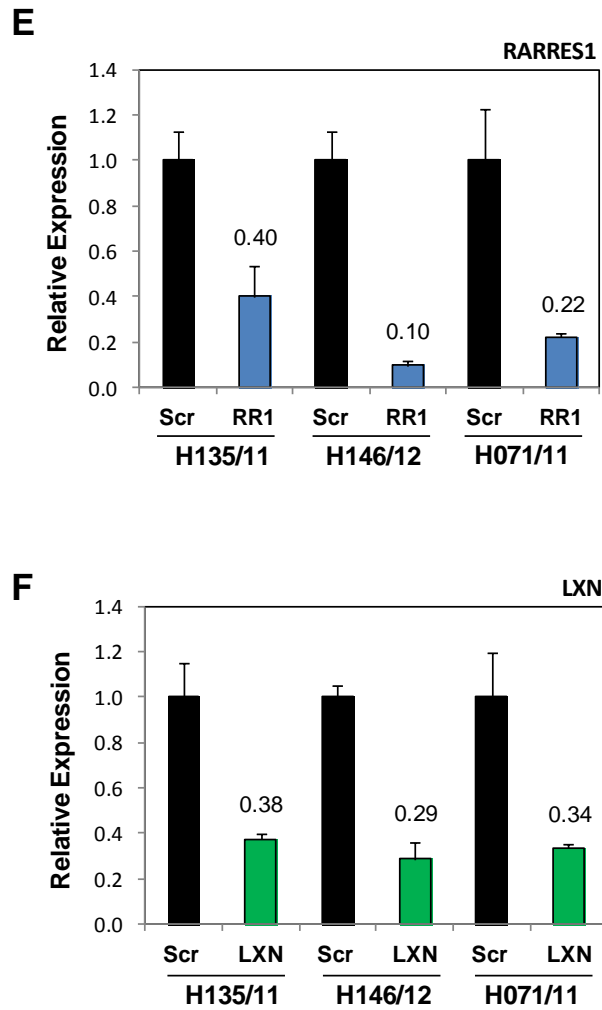
Figure 56. SiRNA knockdown of RARRES1 and LXN in primary prostate epithelial cultures.
qRT-PCR data showing expression of **(a)** RARRES1 and **(c)** LXN relative to an 18S endogenous control gene over time in reagent-only (mock), 50 nM scrambled siRNA (scr) and RARRES1 siRNA (RR1) or LXN siRNA (LXN) samples from H131/11 RA primary epithelial cells. All values are normalised to scr, which is set at 1 for each time point; n=3 technical replicates; error bars expressed as range of the mean. **(b)** Quantified western blot data showing protein levels of RARRES1 (33 kDa) and **(d)** LXN (29 kDa) over time in mock, scr and RR1/LXN samples from PEH131/11 RA primary epithelial cells. Protein expression was quantified relative to a β-actin (42 kDa) loading control and relative to the scr control at each time point (set at 1; values below each blot). **(e)** qRT-PCR data showing expression of RARRES1 and **(f)** LXN relative to an 18S endogenous control gene over time in scr, RR1 or LXN siRNA samples from PEH135/11, PEH146/12 and PEH071/11 primary epithelial cells, 24 hours after transfection.

3.9.2. RARRES1 and LXN do not regulate growth or proliferation of primary prostate epithelial cultures

Over-expression of RARRES1 in human adipose tissue-derived mesenchymal SCs inhibited cell proliferation, whereas knock-down of expression by siRNA promoted cell proliferation (Ohnishi et al., 2009). Similarly, knockdown of RARRES1 in nasopharyngeal carcinoma HK1 cells increased cell proliferation and over-expression decreased cell proliferation (Kwok et al., 2009). However, after over-expression of RARRES1 in the PC-3M prostate cell line, no difference in growth rate was seen (Jing et al., 2002). To determine if RARRES1 and LXN regulated proliferation of primary prostate epithelial cultures, viable cell counts, Ki67 expression and cell cycle analysis were performed.

Primary BPH (n=3) and CaP (n=5) epithelial cultures were initially transfected with 50 nM scrambled, RARRES1 or LXN siRNA or remained untransfected (media). At 2 day intervals, cells were trypsinised and viable cell number was analysed on the Vi-Cell cell viability analyser (Figure 57). Cells were grown without irradiated mouse STO feeder cells, which die 4-5 days after plating. Despite the lack of feeder cells, the majority of the BPH and CaP cultures showed exponential growth curves. Results show that there was no obvious effect on cell proliferation after RARRES1 and LXN knockdown. Knockdown of RARRES1 and LXN in CaP sample H131/11 RA seemed to almost double cell numbers after 8 days, suggesting that RARRES1 and LXN may indeed repress proliferation in this sample. However, this trend was not repeated in any other BPH or CaP sample. In fact, in the CaP samples H144/11 and H146/12 RB, RARRES1 and LXN knockdown appeared to marginally suppress cell number compared to the media and scrambled controls. Therefore, due to the variability between patient samples, it can be concluded that knockdown of RARRES1 and LXN does not affect cell proliferation.

To verify if RARRES1 and LXN resulted in an effect on cell proliferation, Ki67 expression was quantified in primary BPH (n=3) and CaP (n=4) epithelial cultures, after transfection with 50nM scrambled, RARRES1 or LXN siRNA for 96 hours. Results show that there was no significant difference in the average percentage of Ki67 positive cells after RARRES1 or LXN knockdown, in both BPH (Figure 58b) and CaP (Figure 58c) cultures.

Cell cycle analysis by flow cytometry was finally performed, to investigate if RARRES1 and LXN knockdown had an effect on the cell cycle. As previously, primary BPH (n=2) and CaP (n=1) epithelial cultures were transfected with 50 nM scrambled, RARRES1 or LXN siRNA or remained untransfected (media). After 96 hours, cells were trypsinised, fixed with ethanol and then propidium iodide was used to stain the DNA. The proportion of cells in G0/G1, S, or G2/M phases was quantified on the flow cytometer. Results show that the majority of cells in all samples resided in the G0/G1 phase, but no apparent differences were seen after RARRES1 and LXN knockdown (Figure 59). The H131/11 RA CaP culture showed a small decrease in the number of cells in G0/G1 phase and an increase in cells in S and G2/M phases after RARRES1 and LXN knockdown, suggesting that a lack of the two proteins was causing cells to re-enter the

cell cycle (Figure 59a). However, the opposite trend was seen in the H158/12 BPH sample (Figure 59c) and no difference was seen with the H159/11 BPH culture (Figure 59b). Taken together these results indicate that RARRES1 and LXN knockdown does not have an effect on the cell cycle.
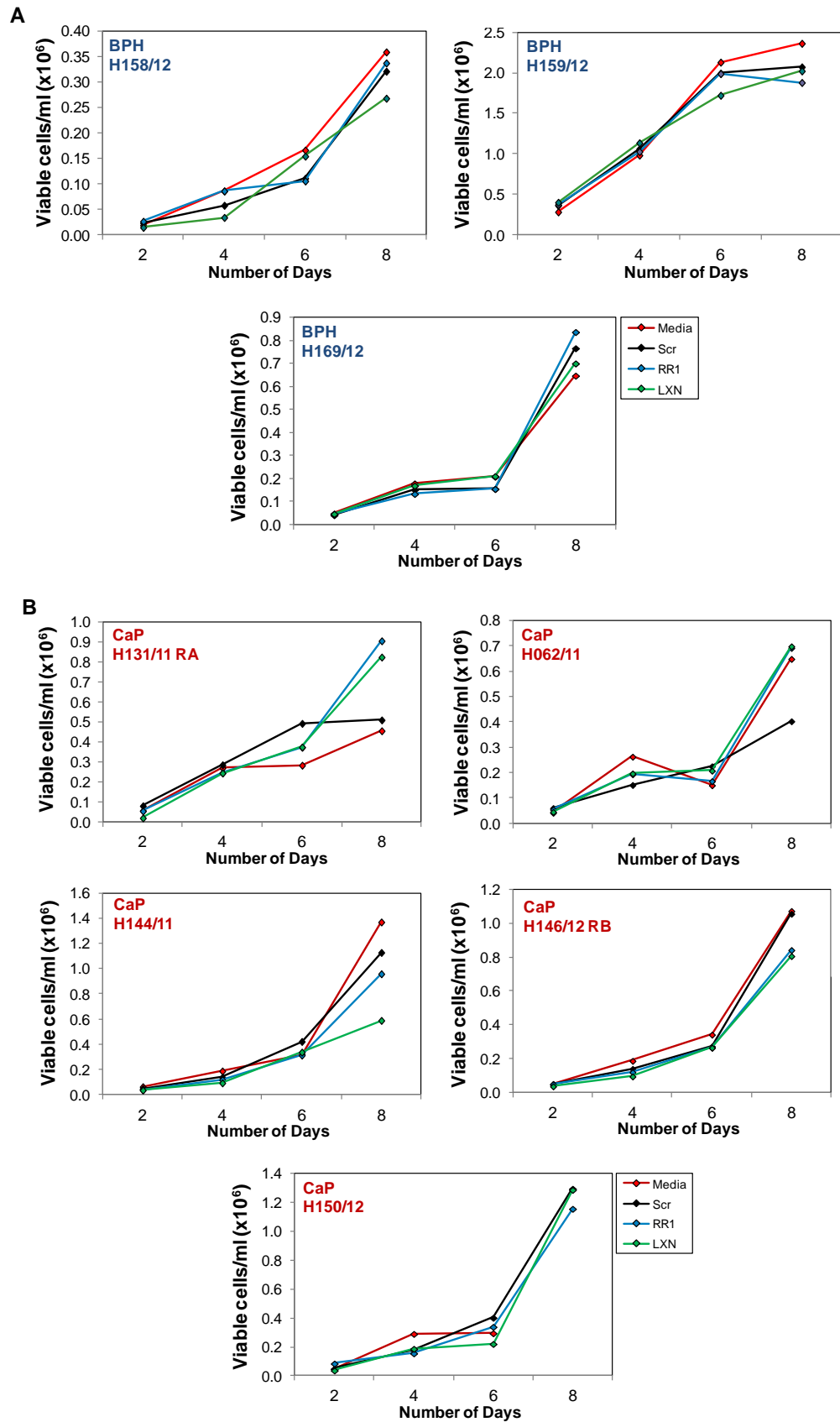
Figure 57. Viable cell count analysis of primary prostate epithelial cultures after siRNA knockdown of RARRES1 and LXN.
Viable cell counts of **(a)** primary BPH (n=3) and **(b)** CaP (n=5) epithelial cultures were performed at 2 day intervals after transfection with 50 nM scrambled (scr), RARRES1 (RR1) or LXN siRNA or untransfected (media) on the Vi-Cell cell viability analyser. Cells were grown in the absence of mouse feeder STO cells.
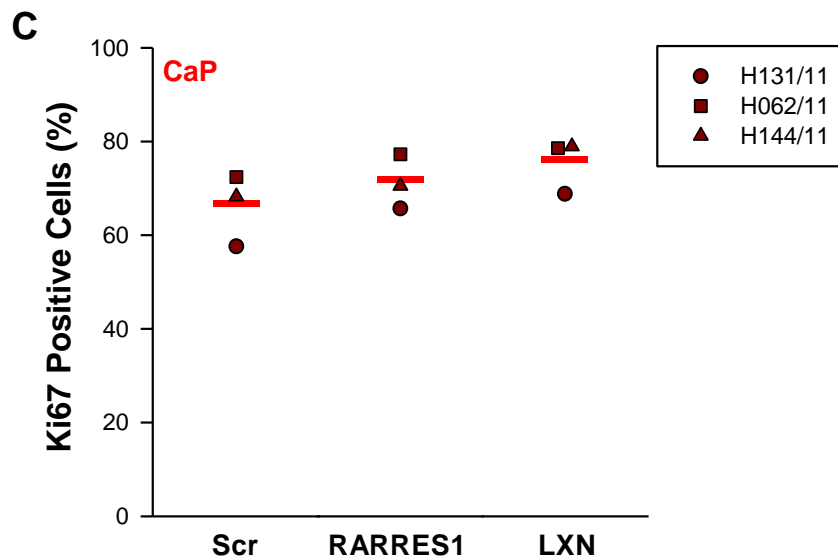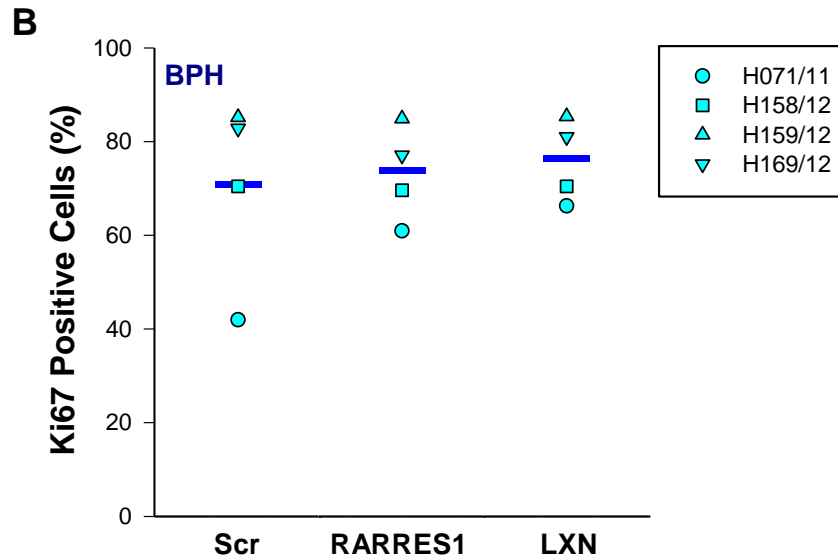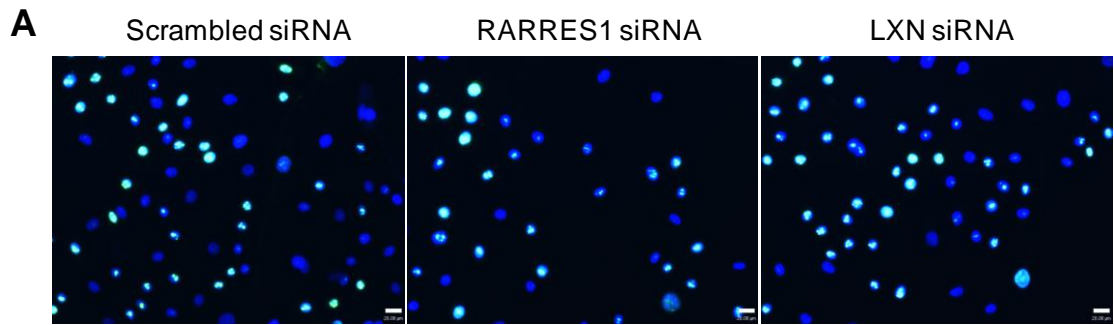
Figure 58. Analysis of Ki67 expression by immunofluorescence in primary prostate epithelial cultures after siRNA knockdown of RARRES1 and LXN.
(a) Representative 20 x immunofluorescence images of Ki67 staining of a primary prostate CaP (H131/11) epithelial culture after transfection with 50 nM scrambled, RARRES1 or LXN siRNA for 96 hours. **(b)** Quantification of Ki67 staining in primary BPH (n=3) and CaP (n=4) cultures after RARRES1 and **(c)** LXN knockdown. The average percentage of Ki67-positive cells was calculated from at least 10 fields of view. Cells were counterstained with DAPI to enable nuclear visualisation. White scale bar represents 20 μm.
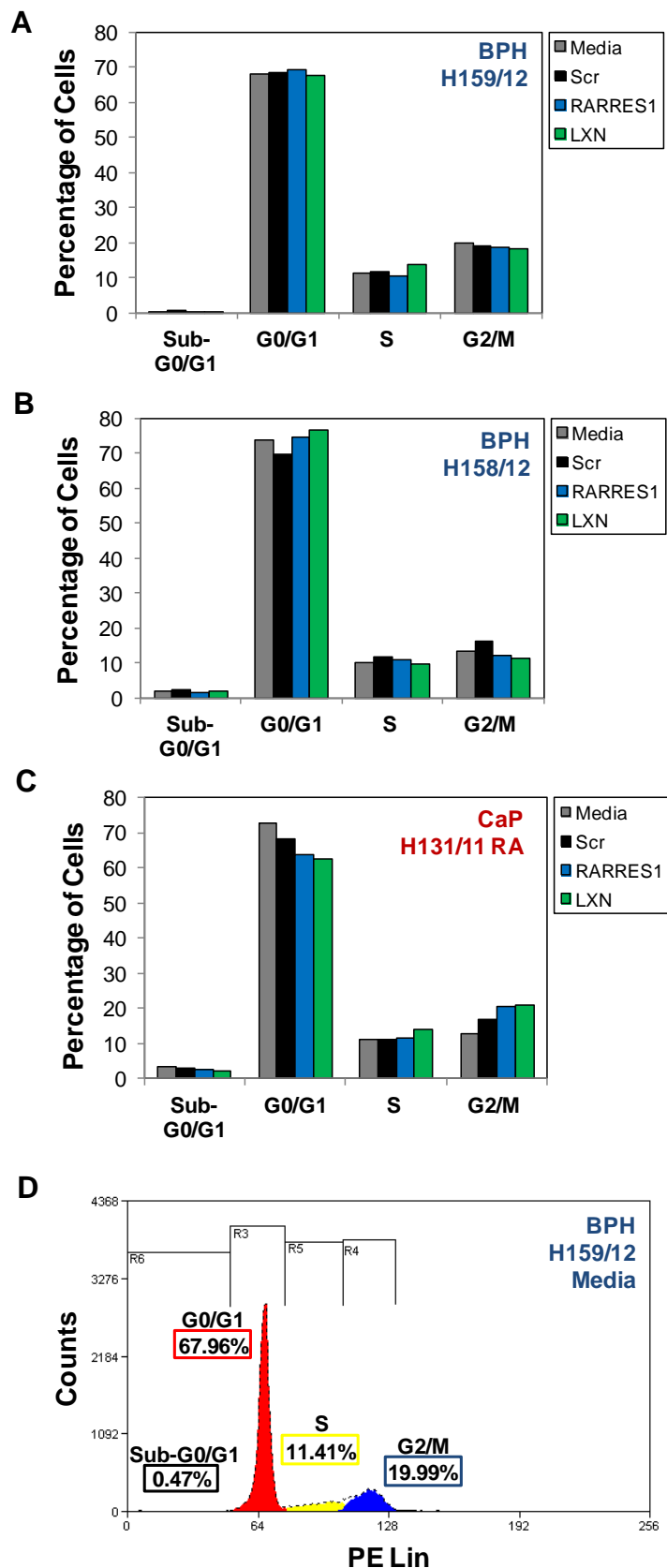
Figure 59. Flow cytometry cell cycle analysis of primary prostate epithelial cultures after siRNA knockdown of RARRES1 and LXN.
Cell cycle analysis by flow cytometry using propidium iodide staining (PE) of primary prostate **(a)** H159/12, **(b)** H158/12 BPH and **(c)** H131/11 CaP epithelial cultures, 96 hours after transfection with 50 nM scrambled, RARRES1 or LXN siRNA or untransfected (media). **(d)** Representative cell cycle profile.

3.9.3. RARRES1 and LXN knockdown increases the colony forming efficiency of primary prostate epithelial cultures

LXN was initially identified as a gene that negatively regulates HSC number (Liang et al., 2007). A lack of LXN expression has since been shown to enhance the colony forming efficiency of HSCs (Mitsunaga et al., 2011). Similarly, the over-expression of LXN in a gastric cancer cell line, MGC803, inhibited colony formation (Li et al., 2011). To determine if RARRES1 and LXN knockdown affects colony formation in primary prostate epithelial cultures, colony forming assays were performed.

Primary BPH (n=3) and CaP (n=4) epithelial cultures were initially transfected with 50 nM scrambled, RARRES1 or LXN siRNA or left untransfected (media only) for 96 hours. Colony forming assays were then performed to determine the recovery of the whole cell population measured by calculating the colony forming efficiency (CFE). Cells were plated at 100 cells per 6 well plate in triplicate, with irradiated mouse STO feeder cells. Cells were left for 7-14 days until colonies started to emerge, and then fixed with a crystal violet stain. The number of colonies containing at least 32 cells (5 cell doublings) were counted visually and the relative CFE calculated.

The results show that after RARRES1 knockdown, the average CFE of BPH cultures significantly increased from 0.81 with the scrambled siRNA, to 1.66 (Figure 60a) and CaP cultures significantly increased from 0.98 with the scrambled siRNA, to 1.65 (Figure 60b). Similarly, after LXN knockdown, the average CFE of BPH cultures significantly increased from 0.81 to 1.99 and CaP cultures significantly increased from 0.98 to 1.83, relative to scrambled siRNA.

Taken together, these results show that both RARRES1 and LXN expression significantly affects colony formation, with LXN knockdown increasing CFE to a greater extent than RARRES1 knockdown.
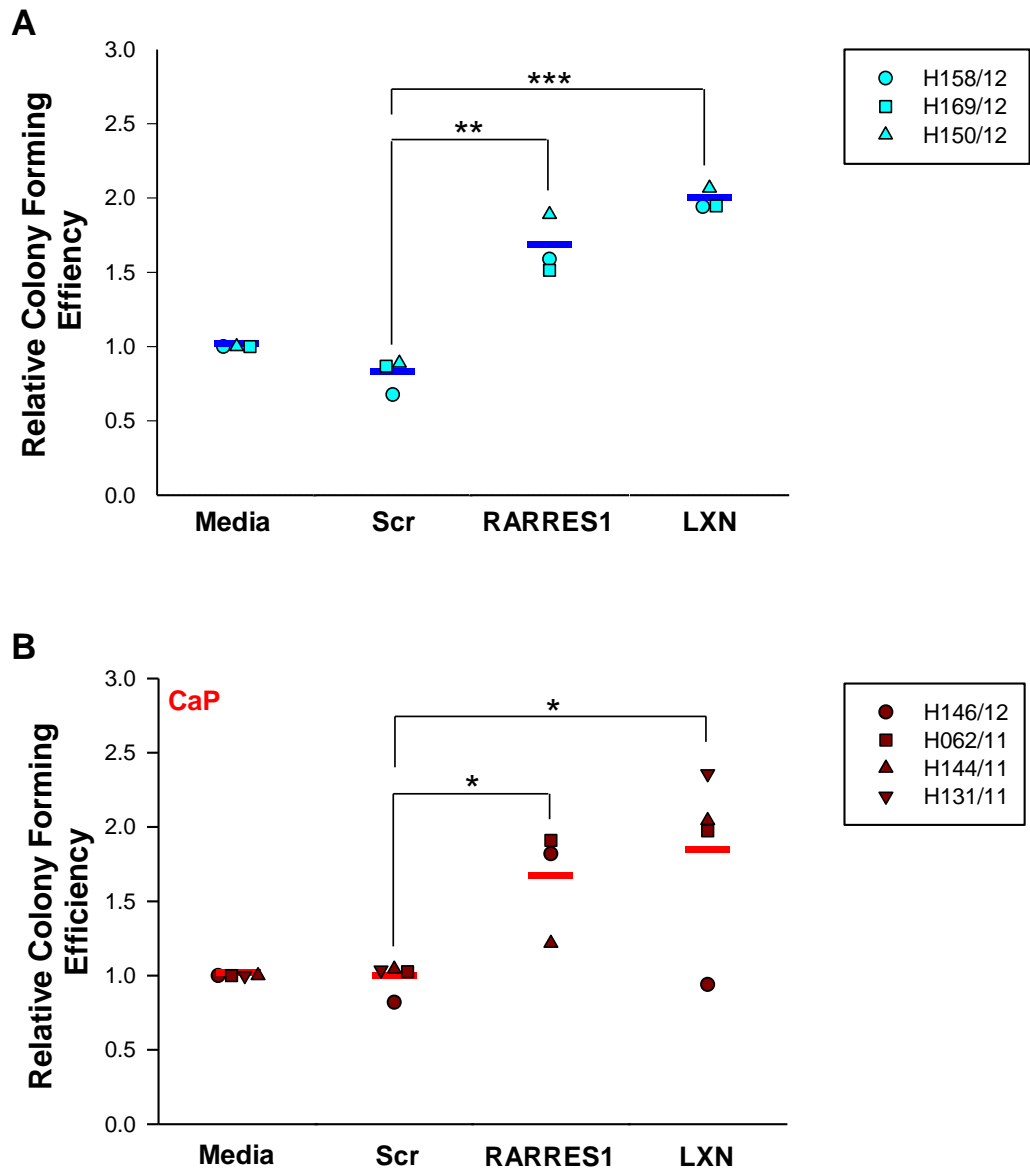
Figure 60. Colony forming assay analysis of primary prostate epithelial cultures after siRNA knockdown of RARRES1 and LXN.
(a) Colony forming assay recovery data after transfection of primary BPH (n=3) and **(b)** CaP (n=4) epithelial cultures with 50 nM scrambled, RARRES1 or LXN siRNA or untransfected (media) for 96 hours. Cells were plated at 100 cells per 6 well plate (n=3 replicates), with irradiated mouse STO feeder cells. Cells were left for 7-14 days until colonies started to emerge, and then fixed with a crystal violet stain. The number of colonies containing at least 32 cells (5 cell doublings) were counted visually and the relative CFE calculated by dividing the number of colonies by the number of cells plated. Relative CFE was calculated by setting the CFE for each media sample at 1. Statistical significance values were measured by the Student's T-test (Unpaired, two-tailed; * $P<0.05$, ** $P<0.01$, ***$P<0.001$).

3.9.4. RARRES1 and LXN knockdown does not affect the differentiation status of primary prostate epithelial cultures

RARRES1 and LXN are prostate SC-silenced genes, whose expression increases with differentiation and LXN negatively regulates HSC number (Liang et al., 2007). Consequently, after knockdown of RARRES1 and LXN in primary prostate epithelial cells, an expansion of undifferentiated SC and TA may be hypothesised to occur.

To determine if the differentiation status of primary prostate BPH (n=2) and CaP (n=1) epithelial cultures was affected by RARRES1 and LXN knockdown, the expression of a panel of differentiation surface markers was analysed by flow cytometry, 96 hours after transfection of cells with 50nM scrambled, RARRES1 or LXN siRNA. Basal surface markers analysed included the SC marker CD133, a subunit of the $\alpha_2\beta_1$-integrin subunit (CD49b) and the basal cell marker, CD44. As shown in Figure 61a, CD133 marks SCs only, but CD49b and CD44 are expressed on the majority of basal cells. The expression of the cell marker CD24, which marks a more intermediate/differentiated cell phenotype, was also analysed.

Results show that the number of CD24-positive cells in all samples was over 90% and there was no difference in the number of CD24-expressing cells, after RARRES1 and LXN knockdown (Figure 61b). In contrast, there was a slight decrease in the average median expression of CD24 on cells from 185, in scrambled siRNA-treated cells, to 146 after RARRES1 knockdown and 155 arbitrary units after LXN knockdown. The results also show that the number of CD133 positive cells in scrambled siRNA treated samples ranged from 0.01 - 0.05% (Figure 61e). There were over twice as many CD133-expressing cells after LXN knockdown, compared to the scrambled siRNA control in one sample (H071/11), but no change in any of the other samples, or after RARRES1 knockdown. There was also no difference in the median expression, or the number of CD44 (Figure 61c) and CD49b-expressing (Figure 61d) cells.

CK expression patterns were also determined in a number of primary prostate epithelial cultures, after RARRES1 and LXN knockdown, by immunofluorescence. As expected, the vast majority of cells within the basal cultures stained positive for the basal CK5 marker and very few cells expressed the differentiated CK 18 and 8 markers. No significant difference in expression of CK 5, 18 or 8 was observed between scrambled siRNA-treated cells and RARRES1 siRNA-treated cells, but there appeared to be a slight increase in CK 8 and 18 expression after LXN siRNA treatment, compared to the scrambled control (Figure 62).

Taken together, these results show that there is a slight decrease in CD24 expression, but no difference in CD133, CD44 or CD49b expression, after RARRES1 and LXN siRNA knockdown, suggesting that a lack of RARRES1 or LXN has a negligible effect on the differentiation status of primary prostate epithelial cultures.

A

Basal Layer   **Luminal Layer**

Stem   Transit Amplifying   Committed Basal   Secretory Luminal

CD133
CD49b
CD44
CD24
CK5
CK18
CK8
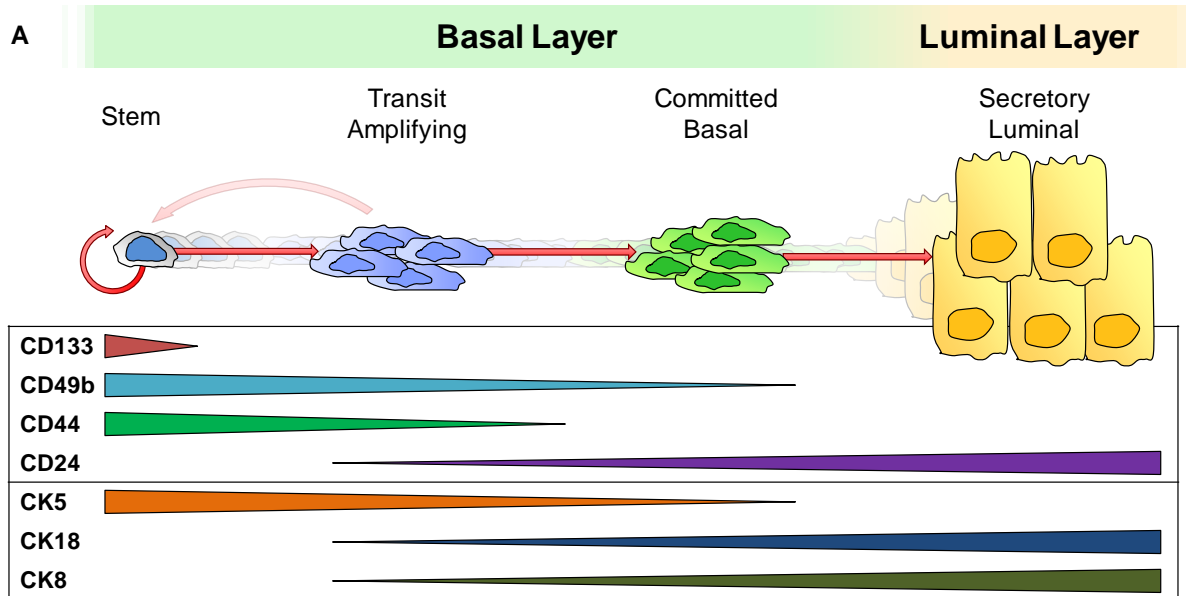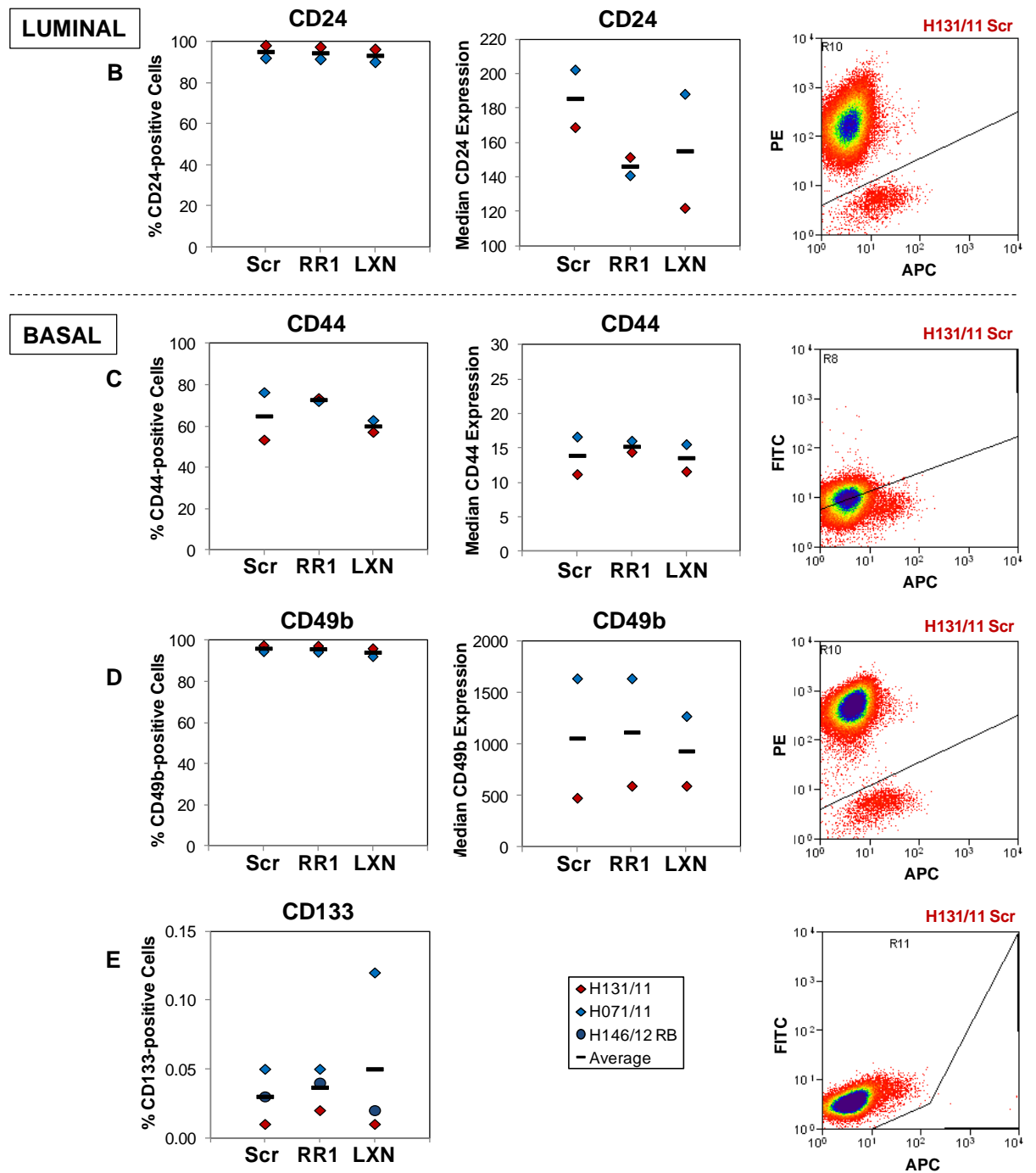
Figure 61. Analysis of the expression of differentiation markers in primary prostate epithelial cultures after siRNA knockdown of RARRES1 and LXN.
(a) Diagram depicting which cell types within the human prostate epithelium express the cell surface and cytokeratin markers analysed. Flow cytometry analysis data displaying the percentage of positive cells, median expression and representative flow cytometry diagram of luminal **(b)** CD24, basal **(c)** CD44, **(d)** CD49b and **(e)** CD133 cell surface markers, in primary prostate BPH (blue; n=2) and CaP (red; n=1) epithelial cells after transfection with 50 nM scrambled, RARRES1 or LXN siRNA for 96 hours.
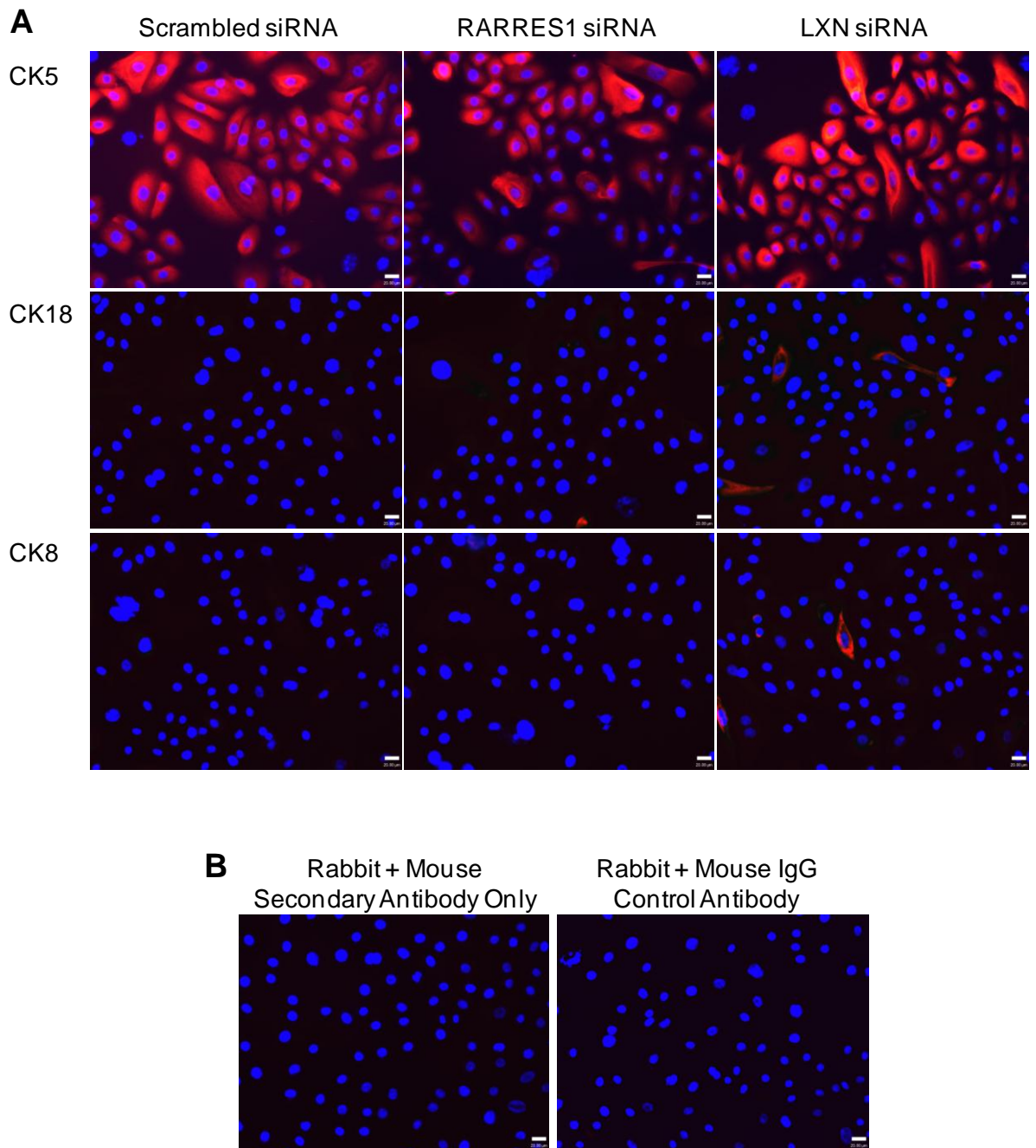
Figure 62. Analysis of the expression of cytokeratins in primary prostate epithelial cultures after siRNA knockdown of RARRES1 and LXN.
(a) Representative immunofluorescence images of CK 5, 18 and 8 staining of a primary CaP epithelial culture (H131/11), after transfection with 50 nM scrambled, RARRES1 or LXN siRNA for 96 hours. Cells were counterstained with DAPI to enable nuclear visualisation. White scale bar represents 20 μm. **(b)** Antibody controls using rabbit and mouse IgG instead of primary antibody and secondary antibody only.

3.9.5. RARRES1 and LXN knockdown regulates the invasion of primary prostate epithelial cultures

RARRES1 and LXN knockdown increases the invasion of prostate epithelial cell lines. To investigate the invasive capacity of primary cells after modulating RARRES1 and LXN expression, Matrigel invasion assays were performed in primary prostate BPH (n=4) and CaP (n=5) epithelial cultures.

Primary BPH and CaP cultures were transfected with 50 nM scrambled, RARRES1 or LXN siRNA or untransfected (media) for 24 hours prior to commencing the invasion assay. As in cell lines, invasive cells were defined as cells that were able to degrade Matrigel BM matrix, RPMI + 10% FCS was used as a chemo-attractant and cells were counted 72 hours after siRNA transfection. The MDA-MB-231 and PNT1a cell lines were used as positive and negative controls, respectively.

The results show that the average invasion of BPH primary epithelial cultures increased from 47% in scrambled siRNA-treated cells, to 77.6% after RARRES1 knockdown and 66.5% after LXN knockdown (Figure 63a). After both RARRES1 and LXN knockdown, there was a decrease in the number of motile cells in two out of four BPH samples, but an increase in two out of four BPH samples (Figure 63c). An increase in the number of invasive cells after RARRES1 knockdown occurred in all BPH samples analysed and in three out of four samples after LXN knockdown.

Similarly, the average invasion of CaP primary epithelial cultures increased from 58.4% in scrambled siRNA-treated cells, to 73.3% after RARRES1 knockdown and 80.3% after LXN knockdown (Figure 63b). After both RARRES1 and LXN knockdown, there was an increase in the number of motile cells in four out of five CaP samples tested. An increase in the number of invasive cells after RARRES1 knockdown was observed in all CaP samples analysed and in four out of five samples after LXN knockdown.

There was only a small difference in the average percentage invasion (7.7%) of primary prostate BPH (46.7%) and CaP (54.4%) epithelial cultures. This amount of invasion was higher than expected for non-invasive BPH cultures and a few reasons could account for this:

- Too high a cell number (2.5×10^5 cells) was placed in the insert at the start of the invasion assay.
- The BPH cultures analysed contained a proportion of invasive cancer cells.
- The concentration of Matrigel (750 µg/ml) was too low.

Firstly, if too many cells were used in the assay, the invasive cells would invade through the Matrigel layer and create 'tunnels' for the non-invasive cells to move through. If fewer cells were present, then less non-invasive cells would move through the 'tunnels'. To identify if too high a

cell number was the cause of the problem, 2.5 x 10^4 cells from one BPH sample (H189/12; identified by an asterisk) were applied to the cell inserts and the percentage invasion measured. The results show that the percentage invasion was 37.9% in the untransfected sample, which is comparable to that seen for the higher cell number samples, indicating that this may not the reason for the high levels of invasion seen in BPH cultures.

Secondly, if the tissue, initially diagnosed as BPH, was found to be CaP after pathology analysis, the invasive capacity would be expected to be higher. The pathology reports for all BPH samples analysed corroborated the BPH diagnosis for all tissues, confirming that this was not the reason for high invasion of BPH cultures.

Finally, if the concentration of Matrigel was too low, then even non-invasive BPH cells would be able to move through the Matrigel, leading to a false high result. Consequently, the percentage invasion would also be higher for invasive CaP cultures, unless the CaP cultures contained only a low percentage of CaP cells in them. The concentration of Matrigel was not varied, as this concentration is routinely used in the laboratory for invasion assays and BPH cultures have previously been published as lowly invasive using this method (Collins et al., 2005).

Reassuringly, the highest Gleason grade cancer (H135/11; Gleason 9) showed the highest levels of invasion in scrambled siRNA-treated cells (64%), indicating that it does contain a considerable proportion of cancer cells.

Taken together, these data shows that after RARRES1 and LXN knockdown the invasion of primary BPH epithelial cultures significantly increases. This corresponds with the data seen in cell lines and further confirms and proposes a metastasis function for RARRES1 and LXN, respectively.

A

BPH

B

CaP

Results
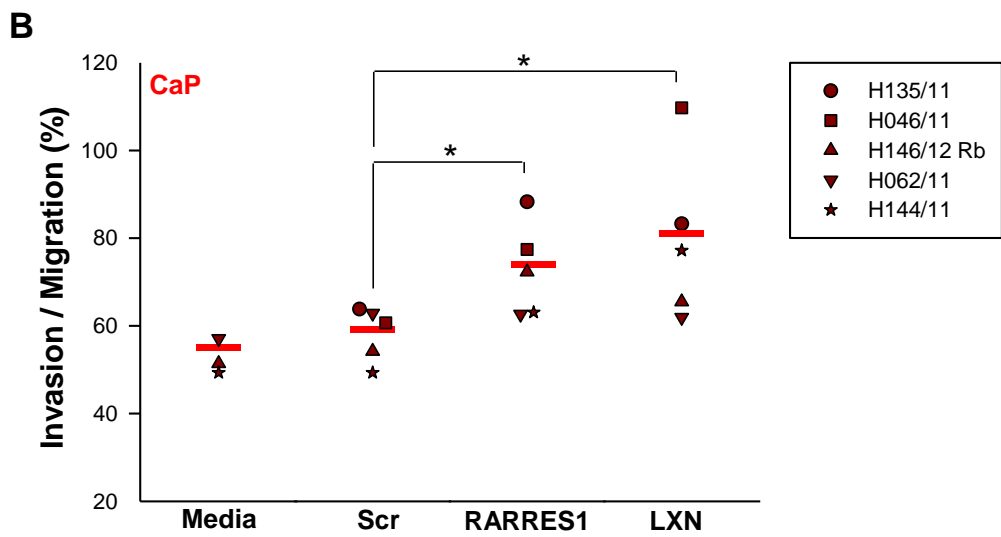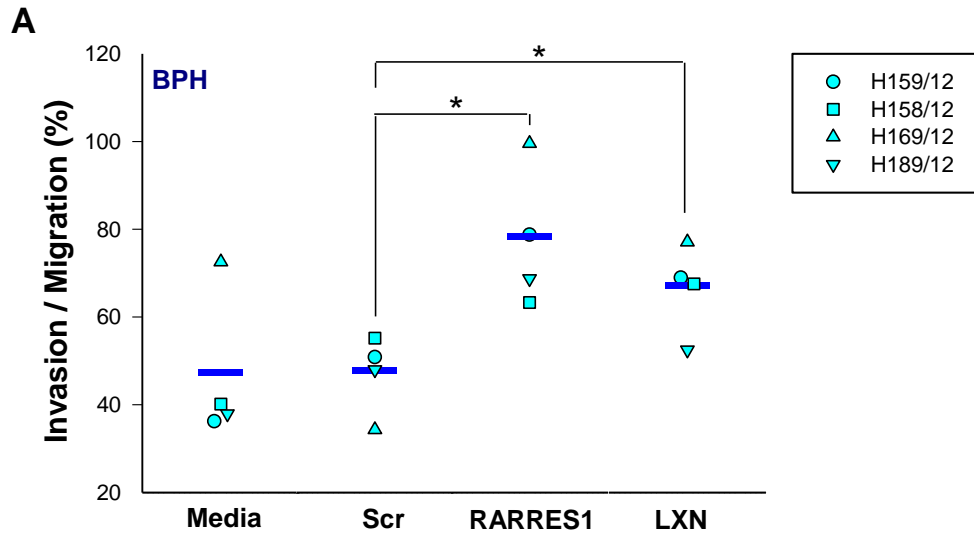
B

	KNOCKDOWN		Number of cells per field		
			No Matrigel	With Matrigel	
			Motility	Invasion	Invasion/Motility
BPH	H159/12	Media	99.3	36.0	36.2%
		Scr	182.8	92.7	50.7%
		RR1	127.1	100.4	79.0%
		LXN	123.3	85.1	69.0%
	H158/12	Media	88.2	35.4	40.2%
		Scr	167.6	92.3	55.1%
		RR1	168.6	106.3	63.0%
		LXN	151.0	101.9	67.5%
	H169/12	Scr	123.7	42.4	34.3%
		RR1	75.5	75.2	99.6%
		LXN	154.0	118.8	77.1%
	H189/12 *	Media	1.9	0.7	37.9%
		Scr	1.7	0.8	48.0%
		RR1	2.1	1.5	68.8%
		LXN	2.7	1.4	52.5%
Cancer	H135/11 Gleason 9	Scr	90.2	57.7	64.0%
		RR1	112.3	102.3	91.1%
		LXN	91.8	79.8	86.9%
	H146/12 Rb Gleason 8	Scr	93.9	51.6	54.9%
		RR1	89.0	64.3	72.3%
		LXN	91.4	59.9	65.5%
	H062/12 Gleason 7	Media	23.5	12.1	51.4%
		Scr	33.0	20.8	62.9%
		RR1	53.1	33.3	62.6%
		LXN	64.3	39.8	61.9%
	H144/12 Gleason 7	Media	78.1	44.6	57.1%
		Scr	104.1	51.3	49.3%
		RR1	106.8	67.3	63.1%
		LXN	104.6	80.8	77.2%
	H046/11 * Gleason 8	Media	3.7	2.0	54.5%
		Scr	2.3	1.4	60.7%
		RR1	2.6	2.0	77.4%
		LXN	6.0	6.6	109.7%

Figure 63. Matrigel invasion assay after siRNA knockdown of RARRES1 and LXN expression in primary prostate epithelial cultures.
(a) Matrigel invasion assay data showing the percentage invasion/migration of primary prostate BPH (n=4) and **(b)** CaP (n=5) epithelial cultures transfected with 50 nM scrambled, RARRES1 or LXN siRNA. All data is 72 hours after transfection. **(c)** Raw data table showing the average number of motile and invasive cells per field of view and the respective invasion/migration percentages. Values that are higher (red) and lower (blue) than the Scr control are shaded. The percentage of cells invading into Matrigel was measured in the presence of RPMI medium +10% FCS as chemo-attractant, below the Matrigel. The benign PNT1a cell line and highly metastatic MDA-MB-231 cell line were used as negative and positive controls for invasion (not shown), respectively. The samples marked with a * indicate experiments where 25,000 cells instead of 250,000 cells were plated per insert. Statistical significance values were measured by the Student's T-test (Unpaired, two-tailed; * P<0.05).

3.9.6. RARRES1 and LXN knockdown rescues the decrease in invasion of primary prostate epithelial cultures after retinoic acid treatment

RARRES1 and LXN knockdown increases the invasion of prostate epithelial cell lines and primary prostate epithelial cultures. RA induces the expression of RARRES1 and LXN in primary prostate epithelial cultures and so would be expected to decrease the invasion of these cells. To investigate the invasive capacity of primary cells after RA treatment and then siRNA knockdown of RARRES1 and LXN expression, Matrigel invasion assays were performed.

A primary BPH epithelial culture (H189/12) was treated with 100 nM atRA for 18 hours, before transfecting the cells with 50 nM scrambled, RARRES1 or LXN siRNA or left untransfected (media only) for a further 24 hours prior to commencing the invasion assay. As previously, invasive cells were defined as cells that were able to degrade Matrigel BM matrix, RPMI + 10% FCS was used as a chemo-attractant and cells were counted 72 hours after siRNA transfection. The MDA-MB-231 and PNT1a cell lines were used as positive and negative controls, respectively.

The results show that the average invasion of the BPH culture decreased from 40.5% with the DMSO vehicle control treatment, to 26.7% with atRA treatment (Figure 64a). AtRA-treatment decreased the number of motile cells from 1.9 to 1.6 and the number of invasive cells from 0.7 to 0.4, indicating that atRA has a combined effect on reducing the motility and invasion of primary cultures (Figure 64b).

As expected, after both RARRES1 and LXN knockdown, there was an increase in the average invasion of DMSO-treated cells from 51.3% with the scrambled siRNA, to 73.4% with RARRES1 siRNA and 56.1% with LXN siRNA.

Interestingly, after knockdown of RARRES1 and LXN expression in atRA-treated cells, there was a greater increase in average invasion, than after knockdown in DMSO-treated cells. Invasion increased to 94% in atRA-treated cells, compared to 73.4% in DMSO-treated cells after RARRES1 knockdown. However, this can be attributed to a decrease in the number of motile cells (from 2.1 to 1.7), rather than an increase in the number of invasive cells. Similarly, invasion increased to 65.5% in atRA-treated cells, compared to 56.1% in DMSO-treated cells, after LXN knockdown. Again, this is probably due to a decrease in the number of motile cells from 2.7 to 1.5, rather than an increase in invasive cells (which also decreases from 1.4 to 0.9).

This data suggests that atRA treatment decreases the invasion of primary prostate epithelial cultures, but subsequent knockdown of RARRES1 or LXN results in a rescue of invasion, to levels higher than those seen in DMSO-treated cells.

A
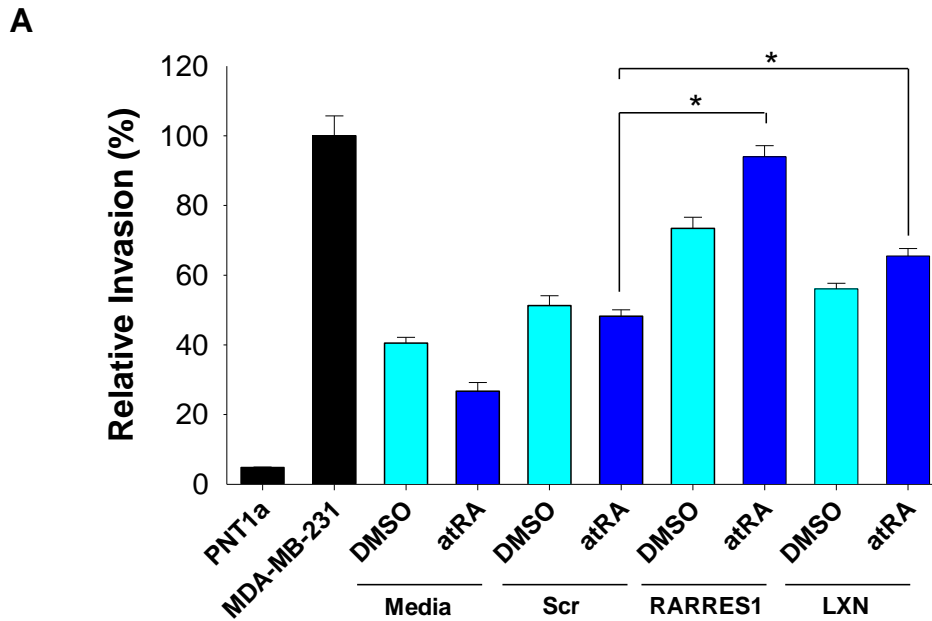
B

H189/12 BPH KNOCKDOWN		Nunber of cells per field			
		No Matrigel	With Matrigel		
		Motility	Invasion	Invasion/Motility	Relative Invasion
-	PNT1a	16.3	0.7	4.5%	**4.8%**
+	MDA-MB-231	34.1	31.9	93.6%	**100.0%**
DMSO	Media	1.9	0.7	37.9%	**40.5%**
	Scr	1.7	0.8	48.0%	**51.3%**
	RR1	2.1	1.5	68.8%	**73.4%**
	LXN	2.7	1.4	52.5%	**56.1%**
atRA	Media	1.6	0.4	25.0%	**26.7%**
	Scr	2.1	0.9	45.2%	**48.2%**
	RR1	1.7	1.5	88.0%	**94.0%**
	LXN	1.5	0.9	61.4%	**65.5%**

Figure 64. Matrigel invasion assay after atRA treatment followed by siRNA knockdown of RARRES1 and LXN expression in primary prostate epithelial cultures.
(a) Matrigel invasion assay data showing the relative percentage of invasive primary prostate BPH (H189/12) epithelial cells initially treated with 100 nM atRA for 18 hours, and then transfected with 50 nM scrambled, RARRES1 or LXN siRNA for a further 72 hours. **(b)** Raw data table showing the average number of motile and invasive cells per field of view, and the respective relative invasion percentages. The percentage of cells invading into Matrigel was measured in the presence of RPMI medium +10% FCS as chemo-attractant, below the Matrigel. The benign PNT1a cell line and highly metastatic MDA-MB-231 cell line were used as negative and positive controls for invasion. Statistical significance values were measured by the Student's T-test (Unpaired, two-tailed; * P<0.05).

4. DISCUSSION

The identification of phenotypic differences between undifferentiated SCs and their more differentiated counterparts is crucial for designing new SC-based therapeutics for CaP. Examination of expression profiles of genes differentially expressed between SCs and their differentiated counterparts (Birnie et al., 2008) identified an expression signature of genes, which were over-expressed in the SC compartment derived from CaP tissues, providing new therapeutic targets. However, there were also classes of genes whose expression was significantly down-regulated in the SC fraction, compared to more differentiated epithelial cells. For these genes, the restoration of their expression or function could act as a differentiation therapy and deplete the SC pool. Two highly homologous genes: RARRES1 and LXN were identified as two of the most significantly down-regulated genes in prostate SCs. RARRES1 and LXN were explored as potential tumour suppressor and differentiation-associated genes, whose expression, epigenetic regulation and function was investigated in detail in this study. The expression and epigenetic regulation of their potential interacting protein CPA4 was also analysed in the same cell models.

4.1. Expression patterns of RARRES1 and LXN

The publication of a seminal paper by Jing et al. (2002) initially suggested that RARRES1 may be a tumour suppressor gene that is involved in the malignant progression of CaP, due to its diminished expression in CaP cell lines and primary tissues. Since then, RARRES1 expression has been shown to be reduced in a number of human cancer cell lines and primary tissues (Youssef et al., 2004), primary colorectal adenocarcinoma (Wu et al., 2006), colon cancer cell lines (Wu et al., 2011) and breast cancer cell lines (Peng et al., 2012). More recently, LXN expression has been shown to be significantly reduced in human gastric carcinoma tissues (Li et al., 2011). Moreover, over-expression of LXN in the same tissues reduced tumour growth in mice, suggesting a tumour suppressor function for LXN. The findings in this present work showed that RARRES1 expression was indeed down-regulated in CaP cell lines, compared to benign cells and expression decreased with increased malignancy of the cell line (Section 3.1.1). Furthermore, it is the first data to show that LXN expression is also down-regulated in CaP cell lines, with the exception of the metastatic PC3 cells, where LXN was over-expressed. This confirmed a role for RARRES1 as a metastasis suppressor in CaP and suggested that LXN could also be involved in CaP progression.

We showed that all prostate epithelial cell lines analysed expressed the full-length RARRES1 protein isoform, but not the shorter variant. This was in contrast to a study by Wu et al. (2011), which showed that both isoforms of RARRES1 were expressed at higher levels in normal prostate tissue compared to a range of different normal tissues, including colon, lung and bone

marrow. Furthermore, the full-length isoform was expressed at higher levels than the shorter isoform in normal prostate tissues. However, Wu et al. (2011) used normal prostate tissue extracts composed of a combination of stromal and epithelial compartments, as opposed to a pure epithelial cell component examined in this study. This suggests that expression of the shorter form of RARRES1 may be expressed within prostate stromal cells, but epithelial cells express only the full-length RARRES1 isoform.

Analysis of gene expression profiles identified RARRES1 and LXN as two of the most significantly down-regulated genes in prostate SCs (Section 3.2.1). Further analysis of differential expression at the mRNA (Section 3.2.2) and protein (Section 3.2.3) levels confirmed that both RARRES1 and LXN expression was significantly lower in the SC fraction from BPH and LXN expression was also significantly reduced in the SC fraction from CaP samples. Interestingly, and following from both the CaP cell line expression data and previous literature data (Jing et al., 2002; Youssef et al., 2004), RARRES1 expression was considerably lower in SC, TA and CB subpopulations from CaP compared to BPH, which was statistically significant in the CB subpopulation. Furthermore, the most malignant CaP samples (Gleason grade 8 and 9, castrate-resistant) showed the lowest levels of expression of both RARRES1 and LXN. These results indicate that the expression of both genes is progressively lost with increased malignancy of the cancer and could be due to de-differentiation and increased invasiveness of the cancer as it becomes more aggressive.

The SC connection was not unexpected for LXN, as it has previously been described as a gene responsible for negatively regulating HSC number in mice (Liang et al., 2007). Surprisingly, a previous study showed that LXN was preferentially expressed in murine haematopoietic stem/progenitor cells, compared to more differentiated cells (Mitsunaga et al., 2011). Mitsunaga et al. (2011) suggested that LXN inhibited the self-renewal capacity of HSCs by maintaining the expression levels of molecules involved in their interaction with the bone marrow niche. These results seem incoherent for two reasons. Firstly, they do not determine the expression level of LXN in a pure HSC population, instead they conclude that the LXN-positive cells lie within a bone marrow mononuclear fraction, which may include haematopoietic stem/progenitor cells. However, immunohistochemical staining revealed that LXN-expressing cells resided close to the inner surface of bone, suggesting that they represented HSCs. Secondly, as HSCs have a considerable capacity for self-renewal (Orkin and Zon, 2008), it would be contradictory for LXN to be expressed at high levels within this cell population. LXN would be expected to be poorly expressed within the HSC population, as it is in prostate SCs in this study. Mitsunaga et al. (2011) may be looking at a cell-type more committed to differentiation than an HSC, such as a TA-equivalent cell, which expresses LXN at higher levels than SCs or CB cells in this study. RARRES1 has been shown to control the proliferation and differentiation of adult adipose-derived mesenchymal SCs (Ohnishi et al., 2009), which suggests that it may also be a putative SC controller. However, this is the first study to elucidate a connection between RARRES1 and prostate SC differentiation.

To further this analysis, it would be interesting to explore how the expression levels of RARRES1 and LXN in luminal cells derived from BPH and CaP tissues compare with basal cell expression at the RNA and protein level. As luminal cells constitute the majority of cells (>99%) in CaP following transformation (Grisanzio and Signoretti, 2008) and RARRES1 and LXN are putative tumour suppressor genes, it would be expected that expression would be low in luminal cells from CaP, due to repression by DNA methylation. In contrast, as RARRES1 expression correlates with the differentiation of normal colorectal (Wu et al., 2006) and prostate (Jing et al., 2002) tissues, RARRES1 would be expected to be expressed at higher levels in luminal cells compared to basal cells from normal prostate and BPH. This may be due to an increased activity of the RA pathway through differentiation, resulting in an enhanced expression of RA-responsive genes in more terminally differentiated luminal cells (Figure 66). Luminal cell lines have been shown to sustain atRA-dependent gene expression, to a higher extent than basal cell lines (Rivera-Gonzalez et al., 2012). Furthermore, CRABP2, which functions to deliver RA to nuclear RARs, was expressed at higher levels in the CB compared to the SC subpopulation of primary prostate cultures by Affymetrix gene-expression array analysis (see Section 4.4). This suggests that, although RAR expression does not increase through differentiation in the basal hierarchy, the increase in CRABP2 expression could account for the enhanced RARRES1 and LXN expression. Additionally, CRABP2 expression has been shown to be down-regulated in head and neck tumours (Calmon et al., 2009) and CaP (Okuducu et al., 2005) which could contribute to the repression of RARRES1 and LXN expression in cancer.

4.2. Expression and chromatin structure regulation of CPA4

The expression status of CPA4 was investigated in prostate epithelial cell lines (Section 3.1.2). The results showed that there was no defined pattern of CPA4 expression between benign prostate and CaP cell lines; CPA4 was ubiquitously expressed. Intriguingly, the LNCaP cell line showed low mRNA, but high protein expression of CPA4, which could be explained by CPA4 having an increased half-life, specifically in these cells, due to increased stabilisation or reduced degradation of the protein. CPA4 possesses a signal peptide sequence (Tanco et al., 2010), suggesting that the protein is targeted to the ER lumen and then either retained in the secretory pathway, targeted to lysosomes or secreted. In these prostate cell lines, CPA4 was predominantly expressed and secreted from cells in an inactive pro-form.

We explored chromatin regulation of CPA4 by initially treating a panel of benign and CaP cell lines and primary cultures with two HDACIs: TSA and NaBu. HDACIs function mainly by enzymatically inhibiting HDACs, which relaxes chromatin by inducing the acetylation of histones, leading to transcriptional activation of a small number of genes. Our results showed that CPA4 was significantly induced by both HDACIs in all benign prostate and CaP cell lines (Section 3.3.1) and primary BPH and CaP epithelial cultures (Section 3.3.2). NaBu induced

CPA4 expression to a greater extent than TSA in the most basal and non-malignant cell lines (PNT2-C2 and P4E6), whereas TSA had a larger effect on the more differentiated and malignant cell lines (PC3 and LNCaP). Similarly, in primary prostate basal epithelial cultures, CPA4 expression was induced to higher levels after NaBu treatment, than after TSA treatment. This suggests that there was a differentiation- or cancer-associated effect between the actions of NaBu and TSA. Although little is known about the mechanism of action of these HDACIs, it could be attributed to the fact that the pan-HDACI, TSA, targets class one, two and four HDACs with nanomolar potency compared to NaBu, which targets only class one HDACs (Schultz et al., 2004; Bieliauskas and Pflum, 2008). However, it has recently been reported that TSA has a greater specificity for cancer cells compared to normal cells (Chang et al., 2012), which corroborates our data in cell lines. However, TSA did not possess an enhanced specificity for primary CaP cells, suggesting that TSA may have a greater specificity for intermediate/luminal cancer cells rather than basal cells, which constitute the majority of cells in the PC3 and LNCaP cell lines. Furthermore, the fold change of CPA4 expression, after treatment of primary epithelial cultures, was low in comparison to the high magnitude of change seen in cell lines. This could be due to a higher concentration of HDACI being necessary to induce the same magnitude of expression of CPA4 in primary cultures. In contrast to CPA4, HDAC inhibition caused a reduction in the mRNA levels of RARRES1 and LXN in the majority of cells lines tested, suggesting that HDAC is not the primary repressive epigenetic mechanism for these two genes in prostate epithelial cell lines (Section 3.3.1).

As CPA4 expression was modified by chromatin remodelers, we sought to determine whether CPA4 was directly regulated by chromatin structure. ChIP analysis highlighted a correlation between expression status and active or inactive chromatin marks present on the CPA4 promoter. The cell line with the highest transcriptional activity of CPA4 (PNT2-C2) had an enrichment for an active euchromatin mark and the cell line that expressed the lowest levels of expression of CPA4 (LNCaP) had an enrichment for an inactive heterochromatin mark (Section 3.3.3). This is the first evidence to show that CPA4 is directly regulated by chromatin structure. A previous study initially identified CPA4, named CPA3 at that time, as a gene indirectly up-regulated by NaBu differentiation treatment of the PC3 CaP cell line (Huang et al., 1999). Huang et al. (1999) found that induction of CPA4 expression, by HDACIs, was blocked by the protein synthesis inhibitor cycloheximide, but induction of p21 was not. Furthermore, anti-sense expression of p21 inhibited induction of CPA4 by NaBu. This suggests that HDAC inhibition directly led to transactivation of the p21 gene, which mediated induction of CPA4 expression in PC3 cells. Our data, taken together with these studies, alludes to the fact that CPA4 can be regulated by chromatin structure directly, but HDAC inhibition in PC3 cells is able to induce CPA4 expression further, through an indirect mechanism involving p21.

4.3. Methylation of RARRES1 and LXN in the prostate

Examination of the promoter and gene body of both RARRES1 and LXN identified that both RARRES1 and LXN possessed potentially functional CpG islands (Section 3.5.1). Recent approaches enabling genome-wide studies (Weber et al., 2005; Harris et al., 2010; Huang et al., 2010) have emphasised that the location of CpG islands in relation to a gene, influences its effect on transcriptional control and methylation of a CpG island, located within the vicinity of the TSS blocks the initiation of transcription (Jones, 2012). Therefore, the location of the CpG islands at the 5' end of both genes suggests that DNA methylation within this region would interfere with initiation of transcription of RARRES1 and LXN. Consequently, pyrosequencing assays were created within a region that has previously described RARRES1 hypermethylation (Youssef et al., 2004; Zhang et al., 2004) and within the LXN CpG island.

Pyrosequencing analysis demonstrated that the expression of RARRES1 and LXN was significantly hypermethylated in CaP cell lines (Section 3.5.1), corroborating the literature (Youssef et al., 2004; Zhang et al., 2004; Ellinger et al., 2008; Kloth et al., 2012). Furthermore, both RARRES1 and LXN were, at least partially, independently regulated by DNA methylation in the PC3 cell line in particular. Moreover, high levels of DNA methylation of RARRES1 and LXN showed a positive correlation with low transcriptional activity. RARRES1 and LXN expression was restored in CaP cell lines upon treatment with a DNA demethylating agent, further supporting the conclusion that their expression correlates with DNA methylation (Section 3.4.1). However, CPA4 expression was not induced by the same DNA demethylating agent in CaP cell lines, suggesting that although CPA4 is regulated by chromatin structure, it is not regulated by DNA methylation.

Surprisingly, low levels of DNA methylation in the RARRES1 and LXN CpG islands were found in primary epithelial cultures (Section 3.5.2) and primary tissues (Section 3.5.3), derived from CaP patients. Similarly, CaP xenograft tissues showed low levels of DNA methylation of both genes, but levels of LXN methylation increased with increased passaging of the xenograft (Section 3.5.4). In addition, DNA demethylating treatment of primary CaP epithelial cultures showed that LXN was not regulated by DNA methylation, but RARRES1 was, in specific samples (Section 3.4.2). Our results are contrary to previously published data, which described RARRES1 as a gene hypermethylated in primary CaP (Figure 65). The first evidence that RARRES1 was hypermethylated in cancer used a COBRA method to show that, amongst other cancer cell lines, PC3 and LNCaP cells hypermethylated RARRES1 (Youssef et al., 2004), corroborating the data in this study. They also showed that 53% of human cancer tissues exhibited hypermethylation of RARRES1 within the same region analysed in this project. Further studies reported that 52% (Zhang et al., 2004) and 96% (Ellinger et al., 2008) of human CaP tissues hypermethylated RARRES1. More recently, a pyrosequencing assay identified RARRES1 and LXN as being hypermethylated in 60% and 29% of primary CaP tissues,

respectively (Kloth et al., 2012). The lack of hypermethylation seen here in primary tissues and epithelial cultures derived from CaP could be explained by:

(1) The techniques to quantify DNA methylation differed between this and previous studies:

Most of the initial studies, which found that a high proportion of human CaP hypermethylated RARRES1, used a methylation-specific PCR (MSP) technique. MSP is a sensitive method for the detection of low level methylation and can be sensitive to at least 0.1% methylated template (Herman et al., 1996), but it is prone to false positives (Aggerholm and Hokland, 2000; Rand et al., 2002). MSP has been made quantitative by the addition of fluorescent TaqMan probes, enabling real time detection (Eads et al., 2000), which is what was utilised by Erlanger et al. (2008). However, due to its quantitative nature and increased sensitivity (Derks et al., 2004), it may result in even more false positives. Hence the extremely high incidence of RARRES1 methylation (96%) found using this technique. The most recent study (Kloth et al., 2012) used the same pyrosequencing technique as utilised in this project to quantify methylation and this resulted in a lower occurrence of methylation (60%). Kloth et al. (2012) set the threshold for hypermethylation of RARRES1 in individual tissues at only 8.5%, however, this was higher than the average level of methylation of RARRES1 seen in the majority of samples tested in this study. Therefore, as a pyrosequencing technique has also found higher levels of DNA methylation of RARRES1 and LXN, it seems that the technique used here is not a good reason for the discrepancy.

(2) Hypermethylation of RARRES1 and LXN is established in luminal CaP cells:

The primary epithelial cultures used in this study are of an undifferentiated basal phenotype. Culturing of cells results in a loss of the differentiated luminal cells from tissues which constitute the majority of cells in CaP (>99%) (Grisanzio and Signoretti, 2008) and also means that primary epithelial cultures represent a very different model from the (mostly luminal) cancer cell line models (e.g. LNCaP and VCaP). Similarly, the xenograft tumours analysed in this study are largely of a basal/intermediate phenotype (Maitland et al., 2011a), resulting from either an amplification of undifferentiated basal cells or de-differentiation of luminal cells in the mouse. Consequently, if hypermethylation of RARRES1 and LXN is established during differentiation and is present only in the luminal cell fraction, this would mean that the basal cultures and xenograft tissues would possess only very low levels of methylation. The issue of whether RARRES1 and LXN silencing is a cause or consequence of DNA hypermethylation remains unknown and whether silencing or DNA methylation comes first, has long been a matter of debate in the field. In fact, genome-wide studies have shown that genes that are already silenced by PcG protein complexes are much more likely to be methylated in cancer (Ohm et al., 2007; Schlesinger et al., 2007; Widschwendter et al., 2007; Gal-Yam et al., 2008). These studies suggest that silencing of RARRES1 and LXN by a different epigenetic mechanism, such

as pre-marking by PcG complexes in basal cancer cells is a pre-requisite to DNA hypermethylation, established during differentiation in luminal cancer cells. It would be interesting to investigate whether other epigenetic mechanisms, such as PcG complexes, are responsible for the initial gene repression in basal cells.

Lack of DNA methylation in basal CaP cells is not restricted to these genes; it has been shown in our laboratory to be true also for GSTP1, one of the most hypermethylated genes in CaP. GSTP1 has been shown to be hypermethylated, but not expressed, only in CaP luminal cells, while it was expressed, but not hypermethylated, in BPH luminal cells and BPH or CaP derived basal cells (Pellacani et al., 2012). It would therefore be interesting to correlate expression and methylation of RARRES1 and LXN in luminal cells derived from both BPH and CaP. This is the most convincing explanation as to why DNA hypermethylation is not present in primary basal epithelial cultures, but does not explain why RARRES1 and LXN are not methylated in the primary CaP tissues analysed.

(3) The presence, in our primary cultures and tissues, of a heterogeneous mix of benign and cancerous cells:

We currently fractionate epithelial from stromal cells within a tissue sample and ensure that the cells derived from CaP tissue are cancer by removing core tissue biopsies from regions of the prostate with palpable tumours. In addition, the epithelial cultures contain a high proportion of cancerous cells as they: (1) express the TMPRSS2:ERG gene fusion (Birnie et al., 2008), (2) express high levels of active telomerase (Rane, unpublished), (3) have a higher invasive capacity compared to BPH cultures (Collins et al., 2005) and (4) express carcinogenesis-associated genes (Birnie et al., 2008). To gain a higher sensitivity during methylation analysis, the solution might be to find a way to analyse a more homogeneous population of cells. However, neither RARRES1 nor LXN were hypermethylated in primary CaP tissues purchased from Origene, which were certified Gleason grades 8 or 9, contained between 75-95% tumour tissue and significantly hypermethylated the GSTP1 gene. It is possible that the frequency of hypermethylation of RARRES1 and LXN is low and the three CaP samples analysed did not hypermethylate either gene. In fact, previous data showed that 60% and 29% of human CaP tissues hypermethylated RARRES1 and LXN, respectively, as detected by pyrosequencing (Kloth et al., 2012).

(4) DNA methylation of RARRES1 and LXN is present in a different CpG island:

Previous studies showed that hypermethylation of RARRES1 occurred within two different regions, encompassing each CpG island (proximal and distal regions) surrounding the RARRES1 promoter (Figure 65). A recent interesting paper has shown that in breast cancer, hypermethylation at the proximal, but not at the distal region of the RARRES1 promoter was necessary to exert a repression of expression (Peng et al., 2012). This concurs with the lack of

RARRES1 hypermethylation seen in primary CaP samples within the proximal region and confirms that it was correct to design the pyrosequencing assay within the proximal region. Primary breast cancer tissues displayed significant hypermethylation of RARRES1 at the distal site, but not at the proximal site and showed no significant reduction in RARRES1 expression. Conversely, breast cancer cell lines, which hypermethylated RARRES1 at both sites, also significantly repressed its expression. If this is also the case in the prostate, it is possible that hypermethylation is necessary within the proximal region to exert an effect on gene silencing. Moreover, previous studies which demonstrated hypermethylation of RARRES1 within the distal region did not correlate the hypermethylation with a repression of gene expression (Tokumaru et al., 2004; Ellinger et al., 2008; Kloth et al., 2012). Peng et al. (2012) also showed that the TF, CTCF, was important for inhibiting the spread of methylation from the distal site to the proximal and sustaining the RARRES1 promoter in a transcription-prone state. This is a plausible reason as to why RARRES1 is not hypermethylated in primary CaP and future work should involve quantifying the extent of DNA methylation within this distal region in our prostate cell models. Indeed the reason for the discrepancy could be a combination of all four factors.

The differentiation-associated properties of RARRES1 and LXN would suggest that tight regulation of their expression within the basal epithelial hierarchy is required. The data presented here shows that although the expression of RARRES1 and LXN was low in prostate SCs, DNA methylation was not responsible for repression of expression in enriched subpopulations of cells derived from basal primary cultures. Despite this, there have been a number of studies suggesting that induction of cell differentiation and cell fate determination in adult SCs are controlled by epigenetic changes in DNA methylation and chromatin structure (Hsieh and Gage, 2004; Tagoh et al., 2004; Fan et al., 2005; Roloff and Nuber, 2005; Xi and Xie, 2005). Areas of epigenetic regulation other than DNA methylation are increasingly being explored for their involvement in regulating the proliferation and differentiation of adult SC (Gangaraju and Lin, 2009). In particular in haematopoiesis, Chen et al. (2004) provided the first evidence that miRNAs are involved in the differentiation of an adult SC lineage. Since then, miRNAs have been shown to be involved in SC differentiation in a number of tissues including bone (Luzi et al., 2008; Mizuno et al., 2008), skin (Yi et al., 2008), brain (Silber et al., 2008) and prostate (Liu et al., 2011a). Subsequently, it would be interesting to investigate, in future work, whether miRNAs or chromatin structure play a role in controlling the expression of RARRES1 and LXN in prostate SCs and their differentiated counterparts.

A

RARRES1

Exon 1

This study

This study Seq

Zhang 2004 (1)

Zhang 2004 (2)

Youssef 2004 (3)

Youssef 2004 (3)

Youssef 2004 (3)

Youssef 2004 (4)

Tokumaru 2004 (5)

Ellinger 2008 (6)

Kloth 2012 (7)

Kloth 2012 Seq

CpG Island

CpG Island

Proximal Region

Distal Region
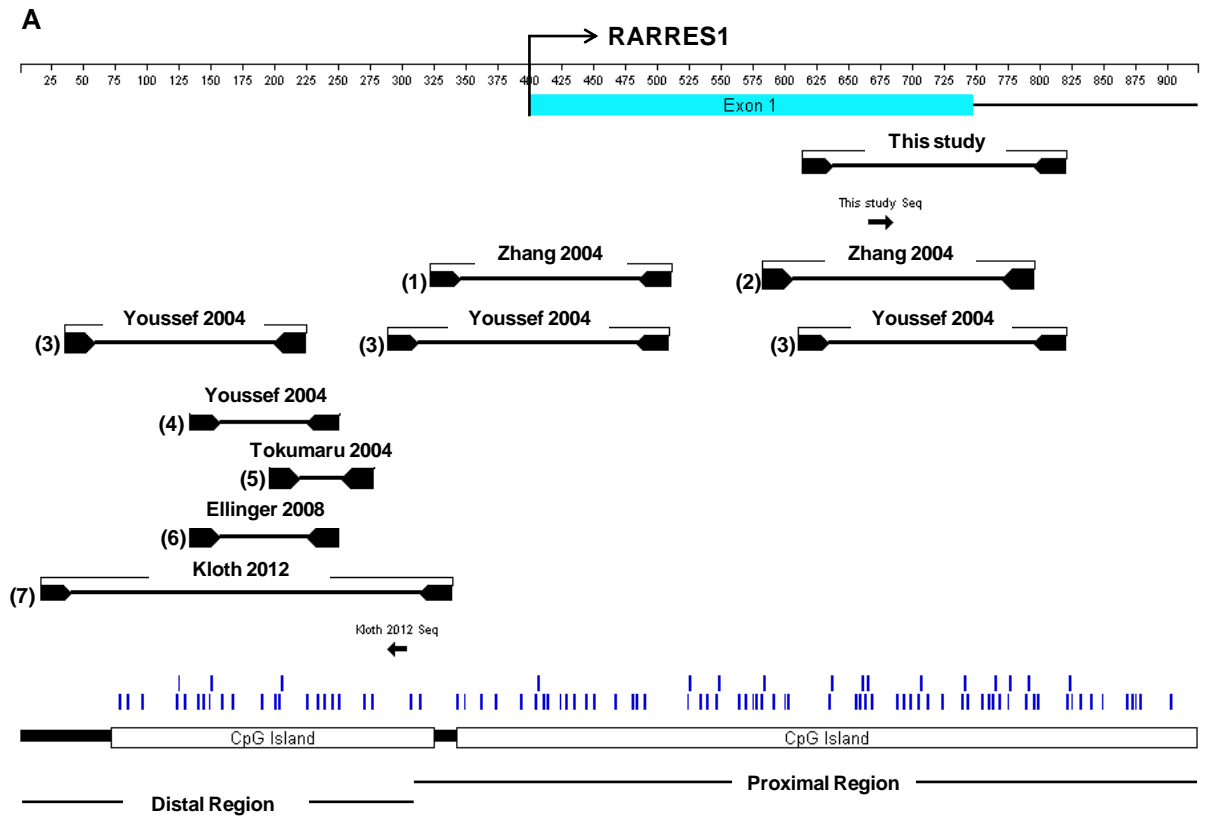
B

Frequency of RARRES1 hypermethylation	Technique	Reference	Threshold for hypermethylation
53% of 74 human cancer tissues	Methylation Specific PCR (**4**) COBRA (**3**)	(Youssef et al., 2004)	Positive result
53% of 50 human CaP tissues	Methylation Specific PCR (**2**) Bisulphite sequencing (**1**)	(Zhang et al., 2004)	Positive result
70% of 61 human CaP tissues	Quantitative real-time methylation specific PCR (**5**)	(Tokumaru et al., 2004)	Positive result
96% of 80 human CaP tissues	Quantitative Methylation Specific PCR (**6**)	(Ellinger et al., 2008)	Calculated using ROC analysis
60% of 86 human CaP tissues	Pyrosequencing (**7**)	(Kloth et al., 2012)	>8.5% (defined using ROC analysis)

Figure 65. Locations of primers used in different publications measuring RARRES1 methylation.
(a) Diagram depicting the relative locations of primer sets spanning both CpG islands used in a number of different studies to measure RARRES1 methylation by a range of different techniques. **(b)** Table showing the percentage hypermethylation of RARRES1 in each study.

4.4. Retinoic acid regulation of RARRES1 and LXN

The presence of RAREs upstream of the RARRES1 and LXN transcription start sites initially suggested a direct role for regulation of both genes by RA within the prostate (Section 3.6.1). Indeed, initial experiments showed that both RARRES1 and LXN were induced by atRA in basal prostate cell lines, but not in the luminal LNCaP cell line (Section 3.6.1). Previous studies have shown that the LNCaP cells can sustain atRA-dependent gene expression (Rivera-Gonzalez et al., 2012), so the lack of induction of RARRES1 and LXN in this cell line is more likely due to the much higher levels of DNA methylation of these genes in LNCaP cells. The RA ligand may be prevented from binding to the RARs and/or recruiting co-activators due to: (1) methylated CpG sites directly blocking binding, (2) the formation of heterochromatin associated with methylated DNA preventing access or (3) the binding of MBD proteins to methylated cytosines, which recruit HDAC proteins leading to a non-permissive chromatin state that prevents binding (Vaissiere et al., 2008). All cell lines were treated with one initial dose of 500 nM atRA at 0 hours, and media was not changed for the duration of the experiment. This, and the fact that atRA has a half-life of only 0.8 hours (Muindi et al., 1992) could account for the rapid induction of expression of RARRES1 and LXN at 24 hours and then decay in the majority of cell lines.

More importantly, after atRA treatment of primary prostate basal cultures and enrichment for SCs, TA and CB cells, the expression of both RARRES1 and LXN was significantly induced in each population (Section 3.6.2). Furthermore, the more differentiated TA and CB cells were more responsive to atRA and consequently induced RARRES1 and LXN expression to a greater magnitude than in the SC fraction. These results correlate with previous studies which showed that RA promoted SC differentiation in a range of different tissues, including human HSCs (Sammons et al., 2000; Luo et al., 2007), mouse embryonic SCs (Simandi et al., 2010), stem-like glioma cells (Campos et al., 2010), rabbit bone marrow-derived mesenchymal SCs (Su et al., 2010) and human breast cancer SCs (Ginestier et al., 2009). Conversely, inhibition of retinoid signalling pathways has been shown to induce the expansion of human HSCs (Chute et al., 2006).

Prostate SCs demonstrate high ALDH activity (van den Hoogen et al., 2010), suggesting that they possess the ability to convert vitamin A to RA. However, as our results show less induction of RARRES1 and LXN in the SC population, we hypothesise that the SC may be less responsive to atRA and the RA ligand produced acts in a paracrine signalling fashion by promoting RA-dependent expression in neighbouring differentiated cells, more than in the SC itself. In fact, there is data from the developing embryo suggesting that RA synthesised in one cell type can act on an adjacent cell type (Matt et al., 2005; Duester, 2008). Duester (2008) described the paracrine mechanism of RA signalling during early organogenesis, which could also be occurring within the prostate epithelium. ALDH[+] prostate SCs facilitate conversion of retinol to RA. RA is then released and taken up by surrounding CRABP2-expressing TA, CB

and luminal cells, which transfer RA to the nucleus and initiate gene transcription of RARRES1 and LXN (Figure 65).

Retinoids stimulate both prostate epithelial differentiation and growth (Peehl et al., 1993; Seo et al., 1997), while squamous metaplasia develops in RAR γ knockout mice (Lohnes et al., 1995) and pre-neoplastic lesions develop after RXR α inactivation in the prostatic epithelium (Huang et al., 2002). All these phenomena are consistent with an effect of RA on a tumour initiating cell or CSC. Depending on the stage of prostate development, RA can either positively (Vezina et al., 2008) or negatively affect prostate formation and gland development (Aboseif et al., 1997). Given the inhibitory effects on adult stem and amplifying cells, both RARRES1 and LXN could play a role in embryonic morphogenesis.

We showed that the RA pathway was expressed and active within primary prostate basal cultures (Section 3.6.3). Before and after atRA treatment, RAR α showed predominantly nuclear expression, but RAR β and γ were mainly cytoplasmic and displayed some nuclear expression. Their localisation presumably did not change after atRA treatment, since according to the present model, RARs are within the nucleus and bound to RAREs in the absence of RA ligand (Dilworth et al., 2000; Dilworth and Chambon, 2001; Bastien and Rochette-Egly, 2004). RAR α has previously been shown to be expressed within the nuclei of BPH and CaP epithelial cells, corroborating the RAR α expression pattern in this study (Gyftopoulos et al., 2000). Interestingly, RAR β and γ showed some cytoplasmic expression in these cells correlating with a previous study investigating the immunohistochemical (IHC) localisation of RARs in the human prostate, which found strong positivity of RAR γ in the cytoplasm of cells, with some nuclear staining and saw strong positivity of RAR α in both cytoplasm and nuclei (Richter et al., 2002). Richter et al. (2002) also found that RAR β expression was absent from carcinoma tissues but was present in basal cells from normal prostate, BPH and PIN tissues; however, this was predominantly nuclear expression. This suggests that although RAR β expression is lost in CaP (Nakayama et al., 2001; Zhang et al., 2004), basal cells derived from cancer tissues still retain RAR β expression. Using immunocytochemistry we found expression of RAR β in CaP basal cells, but due to Richter et al. (2002) using an IHC technique on tissue sections, the expression status in luminal cells possibly masked the positivity in the few basal cells seen in cancer. Although the same antibodies used by Richter et al. (2002) were used in this study, different techniques, patient samples and sample types were used. In addition, this study used epithelial cultures rather than tissue sections, so slightly contrasting results might be expected.

We concluded that the differential induction in RARRES1 and LXN expression between SC, TA and CB subpopulations may be due to differential expression of CRABP2, as no difference in the expression of RAR α, β and γ was observed. CRABP2 was expressed at higher levels in the CB compared to the SC subpopulation by Affymetrix gene-expression array analysis and functions to deliver RA from the cytosol to nuclear RARs (Figure 66) (Cornic et al., 1994; Dong et al., 1999; Noy, 2000; Sessler and Noy, 2005). A recent study has shown that induction of

differentiation of embryonic SC, by the removal of leukaemia inhibitory factor (LIF) or with retinoid treatment, greatly increases the expression of CRABP2 (Lane et al., 2008), supporting the hypothesis that CRABP2 expression increases through cell differentiation. Indeed, it would be important in future work to investigate the differential expression and function of CRABP2 within the basal prostate epithelial hierarchy and to determine whether the differentiation-specific induction of RARRES1 and LXN is due to CRABP2 expression and function.

Taken together, this data suggests that RA plays an important role in basal prostate cell differentiation by inducing the expression of these novel differentiation-associated, SC-silenced genes. It would now be important to identify which of the RARs bind directly to the promoters of RARRES1 and LXN to directly regulate transcriptional activity, by performing ChIP with and without atRA treatment. The hypothesis would be that RAR β and γ are responsible for regulating RARRES1, due to its expression being induced by a RAR β/γ-specific retinoid in skin keratinocytes (Nagpal et al., 1996). Here, RAR β and γ showed some nuclear expression but RAR α displayed predominantly nuclear expression, suggesting that in contrast to skin, in prostate basal cells RAR α is responsible for inducing RARRES1 and LXN expression.

BPH

RARRES1 and LXN Expression

Induction by Retinoic Acid

RA

Stem Cell

Transit Amplifying Cell

Committed Basal Cell

Luminal Cell

ALDH +++

CRABP2 +

RARαβγ +

CRABP2 ++

RARαβγ +

CRABP2 +++

RARαβγ +

CRABP2 ++++

RARαβγ +++

CaP

RARRES1 and LXN Expression

Induction by Retinoic Acid

DNA Methylation

RA

Stem Cell

Transit Amplifying Cell

Committed Basal Cell

Luminal Cell

ALDH +++

CRABP2 +

RARαβγ +

CRABP2 ++

RARαβγ +

CRABP2 +++

RARαβγ +

CRABP2 +

RARαγ +++

RARβ

Figure 66. Model predicting the role of retinoic acid in prostate epithelial differentiation.
ALDH-positive prostate SCs convert high quantities of retinol to RA, which act in a paracrine signalling fashion on neighbouring TA, CB and luminal cells (LC), to induce RA-dependent expression of RARRES1 and LXN. Levels of the RA binding protein CRABP2, increase through differentiation to a maximum in CB and LC, suggesting that this protein is a major factor in inducing high levels of RARRES1 and LXN expression in more differentiated cells. RARs are predicted to be expressed to high levels in LC. In contrast, in CaP tissue CRABP2 and RARβ are repressed by DNA methylation, which could contribute to the predicted repressed expression of RARRES1 and LXN.

4.5. Cellular localisation of RARRES1 and LXN

Determining the sub-cellular localisation of proteins, in particular of novel proteins, is important for understanding their molecular function. Sequence alignment performed in this study and other studies (Aagaard et al., 2005) showed that RARRES1 and LXN shared 30% amino acid sequence homology and differed predominantly by the lack of an N-terminal transmembrane domain present in RARRES1, but absent in LXN (Section 3.7.1). This predicted that although RARRES1 and LXN are homologous, their cellular localisation is potentially different. The intracellular localisation of RARRES1 has been speculated upon in the literature, although no study has convincingly shown its precise location. Sequence analysis initially predicted that RARRES1 was a transmembrane protein with a small N-terminal intracellular region, a single membrane-spanning hydrophobic region and a long C-terminal extracellular region (Jing et al., 2002). More recently, it was proposed that RARRES1 is a type III transmembrane protein purely based on its N-glycosylation status, with its long C-terminal domain now facing the cytoplasm (Sahab et al., 2011). The intracellular localisation of LXN in human cells is unknown, but an early study in rat mast cells indicated a cytoplasmic granular distribution that was not associated with lysosomal structures (Uratani et al., 2000).

In this study we provided undisputable evidence by two independent techniques: immunofluorescence (with native and epitope-tagged protein) and cellular fractionation, that RARRES1 is not a plasma membrane protein, as previously supposed, but resides within the ER (Section 3.7.2). This is also the first study to provide a localisation for LXN in human cells, which conversely resides predominantly within the nucleus. HA-tagged RARRES1 co-localised with the ER lumen marker, PDI, in both LNCaP and PC3 cells, but did not co-localise with the plasma membrane marker, α1-Na/K-ATPase. This result was further supported by a cellular fractionation assay, which showed that HA-tagged RARRES1 did not reside within the plasma membrane compartment in PC3 cells. Immunofluorescence was also performed with native protein in primary epithelial cultures, which showed the same cellular localisation of RARRES1 and LXN after staining. This confirmed that the epitope tagged protein did not interfere with native localisation of LXN and RARRES1. Electron microscopy was briefly performed to elucidate which side of the ER membrane RARRES1 was positioned, i.e. facing the cytoplasm or the lumen, but produced unsatisfactory results due to technical problems. The ER is the largest organelle with a plethora of functions associated with it (Lynes and Simmen, 2011), so identifying the function of RARRES1 within the ER would be complex.

A very recent paper has shown that RARRES1 is secreted by plexiform neurofibroma Schwann cells, but not by normal Schwann cells derived from non-neoplastic peripheral nerve (Chen et al., 2012). While Chen et al. (2012) detected intracellular RARRES1 at the correct molecular mass (33 kDa), the secreted RARRES1 protein was of a higher molecular mass (~110 kDa) and could not be detected by commercial RARRES1 antibodies, suggesting that it may be post-translationally modified, potentially by heparan sulphate modifications. Furthermore, only the C-

terminal domain of RARRES1 could be detected in conditioned media, suggesting that either RARRES1 is cleaved at the transmembrane domain in the secretory vesicle or an, as yet, undiscovered splice variant lacking a transmembrane domain is secreted. A possible secretory function for RARRES1 firmly supports a localisation for RARRES1 within the ER, possibly facing the lumen. In contrast, Chen et al. (2012) showed that the expression of RARRES1 increased in neoplastic Schwann cells compared to normal Schwann cells, suggesting that secretory RARRES1 may be tissue-specific. However, RARRES1 protein has also previously been detected in the conditioned media secretome of human alveolar adenocarcinoma A549 cells (Caccia et al., 2011), Hela cells, colorectal carcinoma (Colo205) cells and hepatocellular carcinoma (Hep3B) cells (Wu et al., 2010). It would be interesting in future experiments to investigate if a secreted form of RARRES1 is present in conditioned media from benign prostate epithelial cells.

Although LXN resides predominantly within the nucleus, we identified that it lacks a canonical nuclear localisation signal (NLS), suggesting that LXN is transported to the nucleus tethered to a protein complex or via the ER. In fact, only 62% of proteins localised to Cajal bodies and 41% of proteins concentrated at the nuclear periphery contain an NLS (Bickmore and Sutherland, 2002). In further work it would be interesting to identify the protein, or protein complex, that LXN interacts with, in order to further elucidate its function, by performing co-immunoprecipitation coupled with mass spectrometry. Similar to the ER, proteins within the nucleus have a multitude of functions associated with them.

4.6. RARRES1 and LXN as invasion suppressors

Progression of cancer is a multistep process where a defined set of events are common to cancer cells (Hahn and Weinberg, 2002; Hanahan and Weinberg, 2011). One hallmark of cancer progression is tumour invasion and metastasis, whereby through a series of discrete steps, tumour cells increase their migratory capacity and acquire an enhanced capacity to invade surrounding tissues resulting in metastasis. Contrasting results in epithelial cell lines showed that both RARRES1 and LXN had opposite effects on the migration of PNT1a cells (Section 3.8.2). As an invasion suppressor, the function of RARRES1 to suppress migration was expected. However, the function of LXN in promoting the migration of the same cells was unexpected.

To then determine the effect of RARRES1 and LXN on invasion, Matrigel invasion assays, based on the Boyden chamber assay, were performed (Section 3.8.3) (Albini et al., 1987). These results showed that RARRES1 functioned to suppress invasion in epithelial cell lines, but LXN predominantly effected migration of the same cells. One hypothesis for the contrasting results for the effect of RARRES1 and LXN in cell lines could be that in the stage of metastasis, where the cancer cell invades into the basement membrane, LXN and RARRES1 expression is

not needed (such as in metastatic LNCaP cells). However, for the migratory stage of metastasis, LXN expression may be needed. The over-expression of LXN at basal levels in the highly metastatic CaP cell line, PC3, may support this theory. A CaspACE assay was used as a highly sensitive and quantitative assay to measure caspase 3 activity (an early marker of apoptotic cell death) and after knock down of LXN in the PC3 cell line, we showed here that a significant proportion of the cells underwent apoptosis (Section 3.8.4). This result suggests that LXN expression is crucial for the viability of PC3 cells.

To determine if the effect of RARRES1 and LXN on migration and invasion was recapitulated in primary prostate cells, siRNA knockdown only was performed (Section 3.9.1). After siRNA knockdown of RARRES1 and LXN in primary epithelial cultures, a significant increase in the overall invasive capacity of both BPH and CaP cultures was observed (Section 3.9.5). There was a larger increase in invasion seen in BPH samples after suppression of RARRES1, compared to CaP samples, which could easily be attributed to the decreased expression levels of RARRES1 observed in CaP samples. Therefore, the effect of knocking down expression would be less significant than in BPH samples, where basal expression levels were higher. Unlike prostate cell lines, suppression of LXN in primary cultures did not result in an obvious effect on the number of migratory cells. This result suggests that, despite the cell line data, both RARRES1 and LXN function to suppress invasion of prostate epithelial cultures. This result exemplifies further the differences between cell line and primary cell models and reiterates the importance of confirming every result seen in cell lines in a primary cell model.

Indeed, these results corroborate previous studies, which showed that low levels of RARRES1 increased the invasion of CaP PC-3M cells and nasopharyngeal and breast cancer cell lines (Jing et al., 2002; Kwok et al., 2009; Peng et al., 2012). However, this is the only study to show that RARRES1 suppresses invasion in primary cancer epithelial cells. Moreover, it is the first study to show that LXN also functions as an invasion suppressor. Future studies should involve determining how RARRES1 and LXN suppress the invasive capacity of prostate epithelial cells.

Inhibition of ECM peptidases or other proteinases is the most likely explanation for the function of RARRES1 and LXN, as both genes have been shown to possess carboxypeptidase domains in this study (Section 3.7.1). Due to the ER-location of RARRES1, it could function to sequester cell adhesion molecules within the cell. As LXN is predominantly nuclear it could function to regulate or be regulated by TFs. No effect on cell growth, proliferation, cell cycle or apoptosis was seen after siRNA knockdown of RARRES1 or LXN (Section 3.9.2), suggesting that they do not modulate cell cycle and proliferation regulators, or pro-apoptotic proteins.

The role of RARRES1 and LXN in invasion and also as SC-silenced genes, suggests a function for them in the EMT. Recent studies have demonstrated that EMT plays a critical role in tumour metastasis and invasion (Thiery, 2002) and is linked with SC differentiation (Mani et al., 2008; Santisteban et al., 2009). Consequently, it would be interesting to determine if after repression

of RARRES1 and LXN expression, markers for EMT, such as a loss of E-cadherin and gain of N-cadherin and vimentin expression is seen.

4.7. Effect of retinoic acid on invasion

We showed that RA treatment of a primary BPH epithelial culture also resulted in a reduction of the invasive capacity of the culture, in a similar manner to over-expression of RARRES1 (Section 3.9.6). These results correlate with a number of studies, which have shown that retinoids have a well-recognised role in suppressing tumour growth and metastasis *in vivo* and inhibiting invasion *in vitro* (Lotan, 1991)*.* One of the first studies, which stated that RA suppresses cancer cell invasion *in vitro,* was performed in rat mammary adenocarcinoma cells (Nakajima et al., 1989). More recently, RA has been shown to suppress invasion in a number of prostate models in addition to human neuroblastoma cell lines (Messi et al., 2008) and thyroid carcinoma cell lines (Lan et al., 2009). AtRA-treated DU145 cells (Webber and Waghray, 1995) and 13-*cis*-RA-treated LNCaP cells (Dahiya et al., 1994) had a reduced ability to invade Matrigel compared to controls. RA treatment of DU145 cells also reduced urokinase-type plasminogen activator (uPA) activity (Waghray and Webber, 1995) and reduced uPA-mediated degradation of fibronectin and laminin (Webber and Waghray, 1995). Similarly, in an invasive rat prostate adenocarcinoma model, atRA inhibited invasion but also inhibited MMP2, MMP 9, α-, β-, and γ- catenin expression (Nwankwo, 2002).

The effect of atRA treatment on invasion is presumable due to a shift in the cultures to a more differentiated and therefore less invasive phenotype. In fact, studies in breast cancer have shown that the most primitive CD44^{+}CD24^{-} breast CSC displayed an enhanced invasive capacity (Sheridan et al., 2006). Furthermore, it has recently been shown that a small population of CSCs are critical for the initiation of metastatic growth at a secondary site (Malanchi et al., 2012). For future work it would be interesting to determine if atRA treatment suppresses the invasion of a highly invasive CaP culture to an even greater extent.

4.8. Function of RARRES1 and LXN in differentiation

As RARRES1 and LXN expression is low in prostate SCs and increasingly up-regulated through differentiation, it would be predicted that after siRNA knockdown of both proteins, there would be an expansion of the undifferentiated cell pool (SC and TA cells) in primary prostate cultures. In this study we show that there was a marginal decrease in CD24 expression after suppression of both RARRES1 and LXN, but no difference in the number of CD24-positive cells or any basal cell surface marker after 96 hours treatment (Section 3.9.4). Surprisingly, there was a slight increase in luminal CK 8 and 18 expression after LXN siRNA treatment, compared to the scrambled control in representative images, however, this was minimal. Therefore, it can be

concluded that, based on cell marker expression, knockdown of RARRES1 and LXN did not affect the proportion of SCs versus differentiated cells within primary prostate cultures. However, it could be that 96 hours is too early a time point to see an increase in any basal cell marker. The results here show that the primary prostate cultures derived from human prostate tissue are predominantly of a basal to intermediate phenotype: around 65% of cells expressed CD44 (albeit at low levels), 95% of cells expressed CD49b to relatively high levels, 95% of cells expressed CD24 at intermediate levels and 0.03% of cells constituted a rare population of CD133-positive cells. In addition, the vast majority of cells stained positive for the basal CK 5 marker but very few cells expressed the luminal CK 8 and CK 18 cell markers. These results are concordant with previously published data, which showed that the cultures under the same conditions expressed $\alpha_2\beta_1$-integrin (CD49b) and CK 5, did not express CK 18 (Collins et al., 2001) but possessed a rare subset of CD133-expressing cells (Richardson et al., 2004).

Knockdown of RARRES1 and LXN expression also did not result in a change in the growth or proliferation of primary prostate cultures up to 8 days after treatment, as measured by cell viability counts, Ki67 staining and cell cycle analysis (Section 3.9.2). The results clearly showed that each culture displayed an exponential growth curve and the Ki67 expression data suggested that the majority of cells were proliferative and in cycle. Furthermore, the cell cycle analysis data showed that the majority of cells were in G0/G1 phases, with only a minority of cells in S-phase and G2/M phase.

To investigate the effect of RARRES1 and LXN on SC function, *in vitro* colony forming assays (CFA) were performed. Interestingly, after both RARRES1 and LXN suppression there was a significant increase in the CFE of both BPH and CaP primary prostate cultures (Section 3.9.3). The increase in CFE for RARRES1 is concordant with published data, which showed that RARRES1 over-expression in endometrial tumour cells and colon cancer cell lines resulted in suppression of colony forming ability (Takai and Jones, 2002). It was also found that RARRES1 plays a role in controlling the proliferation and differentiation of adult adipose-derived mesenchymal SCs (Ohnishi et al., 2009). Similarly, LXN-deficient HSCs have been shown to possess an enhanced colony forming ability (Mitsunaga et al., 2011) and modulation of LXN expression in gastric carcinoma cell lines affected colony forming ability in a similar manner (Li et al., 2011). The CFA is a technique to measure the self-renewal, proliferative capacity and potential of the SC to initiate colony growth. Therefore, this study is the first to show RARRES1 and LXN both suppress the self-renewal and proliferative potential of prostate SCs when expressed, which explains why their expression is low in the SC population. As there is no change in the proportion of cell types or proliferative properties of the cultures after suppression of RARRES1 or LXN, this result suggests that the more differentiated cells (TA and CB cells) within the cultures that usually possess a low CFE (Collins et al., 2005) acquire an enhanced CFE after loss of RARRES1 and LXN expression.

4.9. Mechanism of RARRES1 and LXN action

The precise mechanism of action of the two closely related genes RARRES1 and LXN has proven elusive. LXN has been described as the only known endogenous carboxypeptidase inhibitor and has been shown to inhibit the proteolytic activity of CPA in the rat (Normant et al., 1995). Furthermore, the crystal structure of LXN in complex with CPA4 has been solved, which showed that the protein interaction involves few contacts and inhibition is mainly caused by a C-terminal inhibitory loop (Pallares et al., 2005). Therefore, we performed amino acid sequence alignment of RARRES1 and LXN and identified that this inhibitory loop, which is conserved in LXN between species, is also present and highly conserved in RARRES1, suggesting that it too is able to interact with CPA4 (Section 3.7.1). Moreover, the five key amino acids required for the interaction of LXN with CPA4 were 100% conserved in both LXN and RARRES1 and between species. This suggests that both proteins may primarily function as carboxypeptidase inhibitors. Interestingly, only the full-length RARRES1 protein isoform but not the shorter variant possesses the CPA4 binding site. This raises the question, how would RARRES1 without a CPA4 binding site function, if not through CPA4? Perhaps it interacts with a different protein through a different domain. However, the results here show that all prostate epithelial cell lines and primary prostate cultures tested express only the full-length protein isoform. The ability of LXN and/or RARRES1 to function by binding to and inhibiting CPA4 sounds plausible when considering the function of this peptidase. The CPA4 gene is located in a putative CaP aggressiveness locus on chromosome 7q32 (Witte et al., 2000) and a non-synonymous coding single-nucleotide polymorphism (G303C) on the CPA4 gene was found to be associated with an increased risk of aggressive disease in younger men (Ross et al., 2009). Furthermore, a recent publication by Tanco et al. (2010) identified that the substrate specificity of CPA4 included chromogranin A and neurotensin, which have recognised roles in CaP progression (Kadmon et al., 1991; Sehgal et al., 1994) and differentiation (Swift et al., 2010).

Taking the localisation data into account, it is possible that ER-located RARRES1 could form a complex with the secreted CPA4 protein in prostate cells, whereas it would be less likely for nuclear LXN to form a complex with CPA4, due to compartmentalisation. To determine if RARRES1 and LXN were able to interact with CPA4 in the cell, co-immunoprecipitation analysis was performed on transfected HA-tagged RARRES1 and LXN by a technician in our laboratory (Hannah Walker; data not shown). The results showed that neither LXN nor RARRES1 was pulled down with CPA4 in LNCaP cells, confirming that neither LXN nor RARRES1 form a complex with CPA4 in these cells. However, a lack of interaction could be attributed to the HA-tag on RARRES1 and LXN inhibiting a possible interaction, or the co-immunoprecipitation method not working correctly. To ensure the co-immunoprecipitation method was working effectively, a well-recognised protein interaction could be used as a positive control, such as the β-catenin/APC protein complex or more importantly, the RARRES1/AGBL2 protein interaction.

To determine if RARRES1 and LXN do interact with a carboxypeptidase through their CPA4-interacting domain, future experiments could involve mutating either one or two of the most important amino acids in the inhibitory loop, i.e. glutamine (247, Q) or glutamic acid (248, E). If, after over-expression of mutated RARRES1 and LXN in prostate epithelial cell lines, there is no effect on invasion or motility, it can be presumed that both proteins function through this interaction domain. To test whether the differing sub-cellular localisations of RARRES1 and LXN account for their contrasting functions in cell lines, deletion of the N-terminal transmembrane domain in RARRES1 could be performed. If after removal of this domain, RARRES1 relocates and acts in a similar manner to LXN, it could be concluded that the differing localisation patterns account for the contrasting effects on motility of the two homologs in the PNT1a cell line, possibly by interacting with different proteins or protein complexes.

Sahab et al. (2011) recently showed that RARRES1 is able to interact with a cytosolic carboxypeptidase AGBL2 in the HEK 293 cell line. AGBL2 functions to regulate the tyrosination cycle by removing the C-terminal tyrosine of α-tubulin, which is important for microtubule function (Konishi and Setou, 2009). Detyrosinated α-tubulin is a more stable form of tubulin that is resistant to depolymerisation (Khawaja et al., 1988). It accumulates in cancer cells during tumour progression in nude mice (Lafanechere et al., 1998) and is frequently found in breast cancer (Mialhe et al., 2001). Moreover, a role for detyrosinated tubulin in SC differentiation, EMT and tumour invasion has been suggested (Whipple et al., 2010). Taking the localisation data into account, ER-located RARRES1 could potentially be able to bind AGBL2 if its long terminal C-terminal domain was facing the cytoplasm, but it is unlikely that nuclear LXN would, due to compartmentalisation. A loss of RARRES1 expression in the SC compartment and in cancer progression suggests there would be an increase in the amount of detyrosinated tubulin, which could account for the increased incidence in tumour invasion, EMT and SC differentiation (Figure 67).
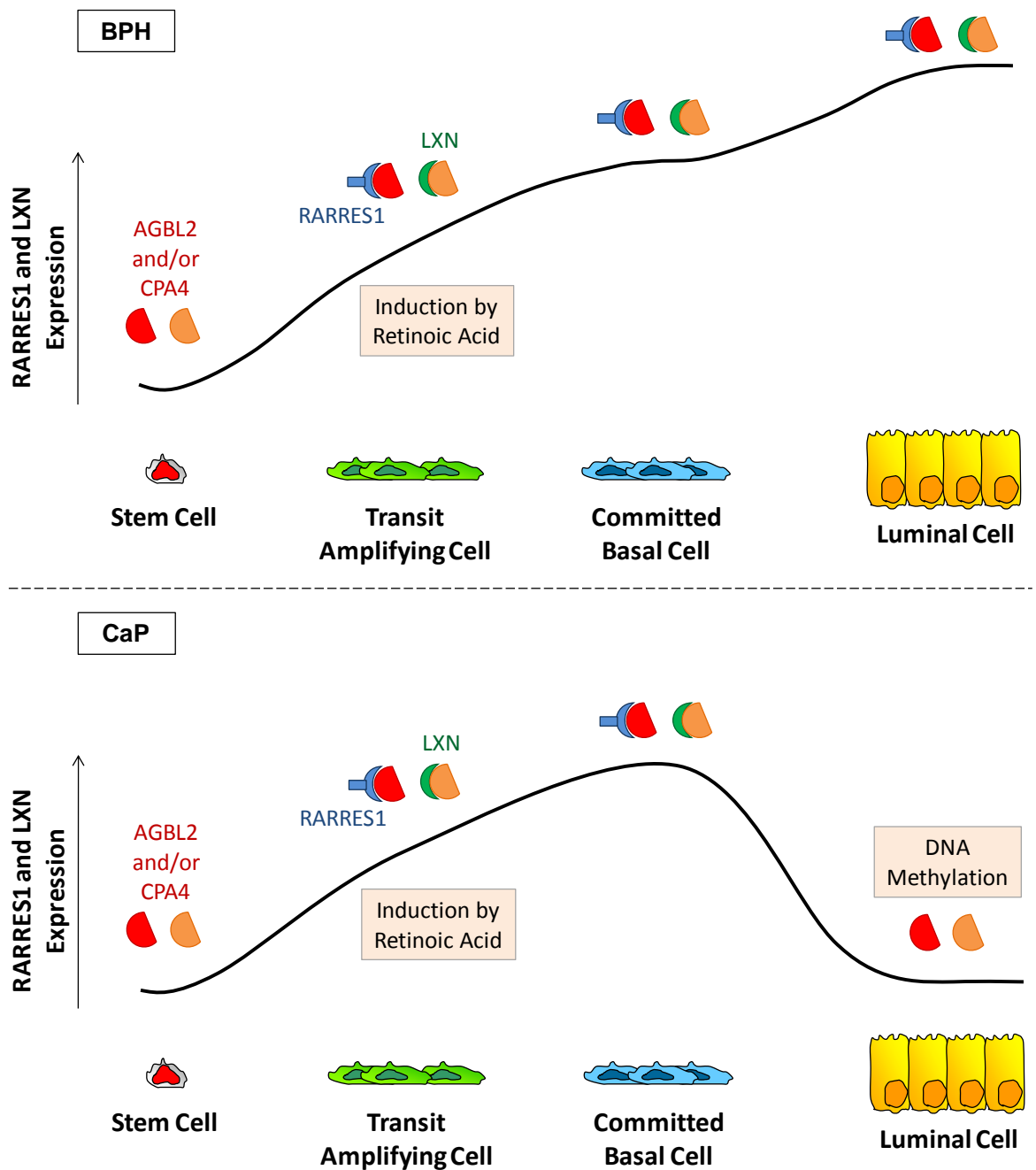
Figure 67. Model predicting the expression and function of RARRES1 and LXN within the prostate epithelial hierarchy.
RARRES1 and LXN expression is low in prostate SCs due to reduced RA activity or unknown epigenetic mechanisms, such as miRNA repression. Expression of both genes increases through differentiation, potentially due to an induction of RA activity, to a maximum in CB from CaP. Expression of RARRES1 and LXN is then predicted to be repressed by DNA methylation through further differentiation into LC, but in BPH, RARRES1 and LXN expression is predicted to increase further. Where RARRES1 is expressed, it is predicted to interact with AGBL2 and control the extent of tyrosinated tubulin, whereas LXN is predicted to interact with a different peptidase. In the absence of RARRES1, AGBL2 is active causing an increased amount of detyrosinated tubulin, which may contribute to EMT, SC differentiation and tumour invasion.

4.10. Differentiation therapy

The heterogeneity of CaP is reflected in its response to current treatments and the CSC hypothesis states that to cure CaP, elimination of the rare CSC is essential (Reya et al., 2001). Given the quiescent, long-lived nature of SCs and their protection by location in the 'SC niche', targeting this extremely rare population of cells is not a straightforward task. The key to eradicating the CSC lies in identifying the phenotypic differences between malignant SCs and the bulk of differentiated cells in the prostate. New therapeutic strategies would be required, which may include overcoming the mechanisms of SC resistance or SC differentiation therapy.

Differentiation therapy describes the process of inducing a quiescent SC to cycle and differentiate into amplifying progeny, which would ultimately obliterate the resistant SC pool. There have been a number of studies suggesting that SCs differentiate to TA, which further differentiate to CB and luminal cells within the prostate epithelial hierarchy (Isaacs and Coffey, 1989; Frame et al., 2010). Consequently, differentiation therapy should function to increase the number of TA and CB cells, rather than increase luminal cell number.

The dangers associated with targeting stemness are an important consideration to take into account when identifying new differentiation therapies. Elimination of normal prostate SCs could be tolerated, in the same way that removal of the prostate gland via radical prostatectomy is. However, untargeted inhibition of non-tissue specific stemness pathways, such as Wnt and Notch (Reya et al., 2001) could have undesired consequences in other tissues. Indeed, a recent study showed that progressive disruption of Notch1 in mice caused widespread vascular tumours, predominantly in the liver, which resulted in massive haemorrhages after extended periods of exposure, consistent with an effect on SCs (Liu et al., 2011b). There must be selectivity in targeting differentiation therapies towards a specific tissue or eradicating, specifically, CSCs. If a treatment is targeted towards the tissue in which the tumour resides, depending on the tissue, it can non-selectively eradicate both CSCs and normal SCs. This would suffice for CaP, but for tissues where normal SCs are an essential component, an alternative therapy that is selective only for CSC would be necessary. The major advantage of this is that it could potentially be used on a tissue-wide scale. A further factor to consider when designing differentiation therapies is the timing of treatments. In theory, removing the resistant and renewing part of the tumour with a single differentiation therapy should eradicate the tumour. However, targeting this rare SC population among the bulk of differentiated cells would prove difficult. Future differentiation therapies should be administered in combination with current therapeutics, which target the differentiated bulk of the tumour. It would be sensible to initially treat patients with current therapeutics to unmask the rare SC population, which could then be eradicated with differentiation therapy. Administering both therapeutics at the same time could increase potential cytotoxicity effects and weaken the response. Administering differentiation therapy first and then current therapeutics would pose the same problem as treating with the single differentiation therapy.

The results in this study show, that after inhibition of the SC-associated genes, RARRES1 and LXN in primary prostate epithelial cells, there is a highly significant increase in their colony forming ability and invasive capacity. Therefore, after over-expression of either gene in primary prostate cultures, it would be expected that there should be a decrease in colony forming ability and invasion, consistent with a differentiation effect on the SC population. In fact, after over-expression of RARRES1 and LXN in prostate epithelial cell lines, a decrease in invasion is seen. Consequently, a possible differentiation therapy could be transfection of prostate-specific RARRES1 and LXN lentiviral expression vectors into the prostate tumour. However, this would be technically very challenging and an easier alternative could be administration of RA, which should effectively increase RARRES1 and LXN expression and promote differentiation of the SC compartment.

4.11. Conclusions

This work has provided evidence that RARRES1 and LXN are two highly homologous genes, whose expression and regulation are closely related. Despite this, they reside in contrasting cellular locations but function similarly to suppress invasion and colony formation in primary prostate epithelial cultures. We have shown that RARRES1 and LXN are similarly repressed by DNA methylation in CaP epithelial cell lines, but are not in primary CaP epithelial cultures and tissues. Both RARRES1 and LXN were also identified as genes whose expression was down-regulated in prostate SCs, but was induced upon atRA treatment of basal primary cultures and cell lines. These new findings will lead to a better understanding of how SC-silenced genes are regulated and function in both normal prostate and CaP differentiation. Elucidating the protein networks that allow these highly similar genes to function will provide further insight into the complex regulation of SC differentiation, as well as invasion and metastasis in CaP.

This study also highlights the importance of RA in controlling gene expression patterns within individual sub-populations. The identification of RARRES1 and LXN as novel RA-induced, SC-associated genes has alluded to the significance of RA control of differentiation within the prostate epithelium. The majority of research on CaP, to date, has focussed on AR and androgens, despite the knowledge that basal cells, in particular SC, are independent of androgen signalling. Consequently, the results from this study show that focus should be moved to the involvement of RA in differentiation and CaP.

Furthermore, the identification that two SC-silenced genes, which also function as invasion suppressors, adds weight to the CSC hypothesis and that the SC is the ultimate controller of metastasis. Work should now be focussed on determining whether transfection of RARRES1 and LXN lentiviral expression vectors are able to reduce clonogenic ability and diminish the SC pool in primary prostate cultures. This would determine whether re-administration of RARRES1 and LXN would be a valid differentiation strategy for the treatment, and potentially eradication, of CaP.

APPENDICES

Appendix 1: Maps of vector plasmids

pReceiver-M45 (GeneCopoeia)

pReceiver-M45
RARRES1
7728 bp
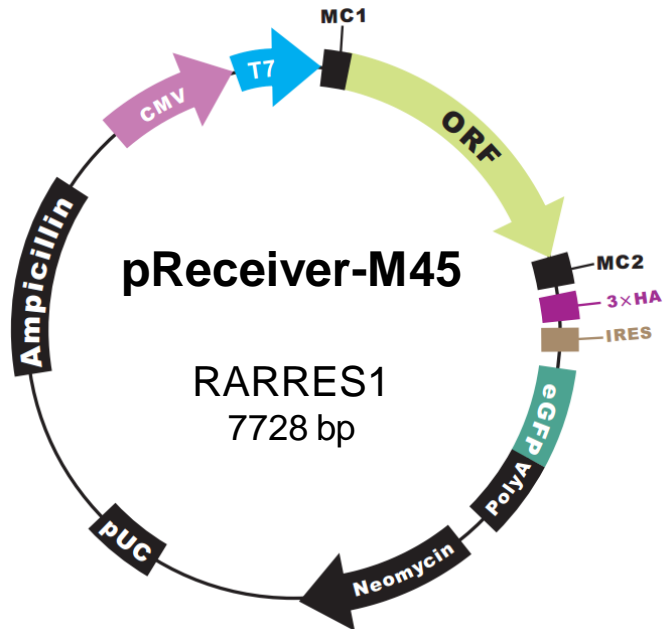
pReceiver-M06 (GeneCopoeia)

pReceiver-M06

Control vector with eGFP
6617 bp

pReceiver-M06

LXN
6564 bp
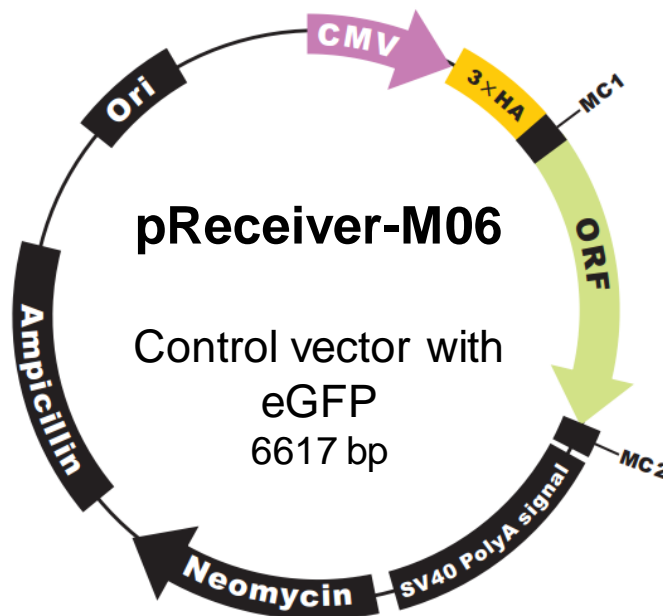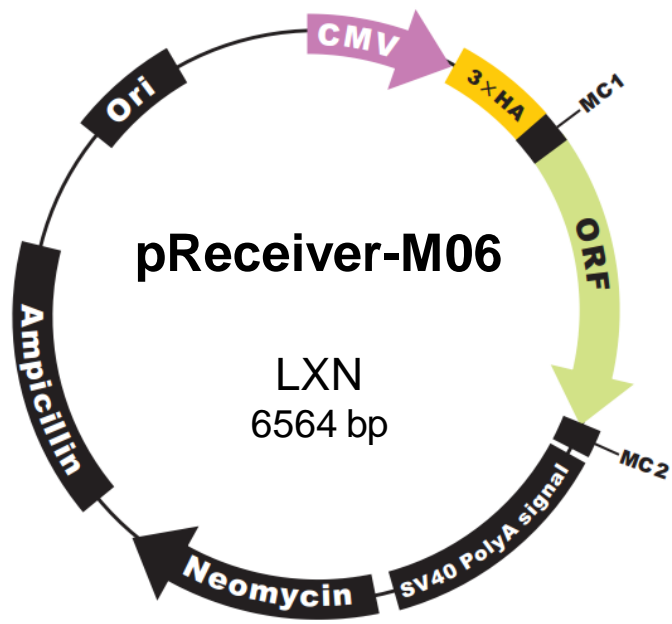
Appendix 2: PCR primer sequences

Primer Name	Primer Sequence (5' to 3')	Purpose
ChIP 1 Forward	GCT GGG TGA AGG CAA AGA CA	ChIP for CPA4
ChIP 1 Reverse	CCA GGA AGG GCA GTT AGA GG	
ChIP 2 Forward	TGG GAT TAC AGG CGT GAG C	
ChIP 2 Reverse	CAG TCT GGG ATG ATA GGA AAG TT	
ChIP 3 Forward	CTA AGC CAG CCT GAG CAA AGA T	
ChIP 3 Reverse	CAA AGG TGG GGA TGA GGA AC	
ChIP 4 Forward	TGG GAG AGG CAT TGG TAG	
ChIP 4 Reverse	CCC CGG GGA GTC AGT CAT A	
ChIP 5 Forward	CAA ATC CAT TCT CAC GCC ATA GTA	
ChIP 5 Reverse	CTT CAG CAG CCA ATC CAG AG	
ChIP 6 Forward	CCG CAA TGT CCT CCC TCC TTT CAG	
ChIP 6 Reverse	GGC GGG GTT TCT CTA TGT TGG TCA	
ChIP 7 Forward	GAG TTT GGG CTG GGT CCG AGA TG	
ChIP 7 Reverse	GCC AAG CTA CAG AGG TCA ACA AA	
ChIP 8 Forward	CTT GCC GAG GTC AGG GAA CGA T	
ChIP 8 Reverse	TGG AGG TCA GCG GGT AAC T	
RARRES1 Pyro Forward	AGT TTT AGG ATG TTG GGG TTT	Pyrosequencing for RARRES1
RARRES1 Pyro Reverse Biotin	TAC CCA AAT ATC ACC TCC CAA	
RARRES1 Pyro Sequencing	GGA GTT TTA TTT TTT TAA TT	
LXN Nested PCR Forward	GTT GGT GTT TGA TAA GTA TGT T	Pyrosequencing for LXN
LXN Nested PCR Reverse	CCC CTA CTA AAC TCA CCT CCA T	
LXN Pyro Forward	GAT GTA GGG AGT TTG GGT TTA AAT AG	
LXN Pyro Reverse Biotin	CCA ATA AAC AAT AAC TTC AAA ACT T	
LXN Pyro Sequencing	GGG AGT TTG GGT TTA AAT A	
GSTP1 Pyro Forward	GGG GAG GGA TTA TTT TTA TAA G	Pyrosequencing for GSTP1
GSTP1 Pyro Reverse Biotin	AAT TAA CCC CAT ACT AAA AAC TCT	
GSTP1 Pyro Sequence	GGA TTA TTT TTA TAA GGT	

Appendix 3: Patient primary epithelial sample details

Patient ID	Pathology	Gleason grade	Age	Operation
PE109/06	BPH	-	70	TURP
PE561	BPH	-	72	TURP
Y082/06	BPH/TCC	-	73	Cystectomy
Y045/08	BPH	-	77	TURP
PE047/08	BPH	-	67	TURP
(PE)Y054/08	BPH	-	66	TURP
Y023/09	BPH	-	88	TURP
Y029/09	BPH	-	91	TURP
Y030/09	BPH	-	70	TURP
Y044/09	BPH	-	75	TURP
Y088/09	BPH	-	71	TURP
Y003/10	BPH	-	74	TURP
Y030/10	BPH	-	67	TURP
H040/10	BPH	-	-	TURP
Y040/10	BPH	-	67	TURP
Y048/10	BPH	-	70	TURP
Y052/10	BPH	-	72	TURP
Y059/10	BPH	-	60	TURP
Y061/10	BPH	-	81	TURP
H040/11	BPH	-	-	TURP
Y054/11	BPH	-	76	TURP
H071/11	BPH	-	-	TURP
H094/11	BPH	-	56	TURP
H150/12	BPH	-	65	LRP
H158/12	BPH	-	64	TURP
H159/12	BPH	-	62	TURP
H169/12	BPH	-	71	TURP
H189/12	BPH	-	51	TURP
PE025	Cancer	4+4	68	Radical
PE107	Cancer	3+3	68	Radical
PE434	Cancer	8 / 9	59	Radical
PE519	Cancer	3+3	79	Cystectomy
PE531	Cancer	4+5	57	Radical
PE665	Cancer	3+4	53	Radical
PE667	Cancer	3+3	47	Radical

PE671	Cancer	3+4	62	Radical
Y089/09	Cancer	CRPC	85	TURP
H016/09	Cancer	7	-	Radical
Y021/09	Cancer	CRPC (4+5)	67	TURP
Y091/09	Cancer	CRPC	81	TURP
H031/11 RB/LM	Cancer	7	-	Radical
H043/11	Cancer	7	-	ORP
H046/11	Cancer	3+5	-	LRP
H062/11	Cancer	-	67	LRP
H082/11 RA/LA	Cancer	-	53	ORP
H103/11	Cancer	-	55	LRP
H131/11 RA/RB/LM	Cancer	-	70	LRP
H135/11	Cancer	9	56	TURP
H144/11	Cancer	7	66	ORP
H146/12 RB	Cancer	7	57	LRP
H150/12	Cancer	6	65	LRP

ABBREVIATIONS

µg	Microgram
µl	Microlitre
µM	Micromolar
µm	Micrometre
^{103}Pd	Palladium radioisotope
^{125}I	Iodine radioisotope
18S	18 Svedberg units ribosomal RNA
^{192}Ir	Iridium radioisotope
5-Aza-dC	5-Aza-2'-deoxycytidine
5caC	5-carboxylcytosine
5fC	5-formylcytosine
5hmC	5-hydroxymethylcytosine
5mC	5-methylcytosine
ADP	Adenosine diphosphate
ADT	Androgen deprivation therapy
AGBL2	ATP/GTP binding protein-like 2
ALDH	Aldehyde dehydrogenase
APC	Allophycocyanin
AR	Androgen receptor
ATCC	American type culture collection
AtRA	All-*trans* retinoic acid
AZ	Anterior zone
Aza	5-Aza-2'-deoxycytidine
B. Taurus	Bos Taurus
BCA	Bicinchoninic acid
BM	Basement membrane
BMP	Bone morphogenetic protein
bp	Base pairs
BPH	Benign prostatic hyperplasia
BSA	Bovine serum albumin
CAGE	Cancer/testis antigen gene
CaP	Prostate cancer
CARM-1	Coactivator-associated arginine methyltransferase 1
CB	Committed basal
CD	Cluster of differentiation
cDNA	Complimentary DNA
CFA	Colony forming ability
CFE	Colony forming efficiency
ChIP	Chromatin immunoprecipitation

CK	Cytokeratin
Cl	Chloride
Cm	Centimetre
Cm^2	Centimetre squared
C-MET	C-Mesenchymal epithelial transition factor
CO$_2$	Carbon dioxide
COBRA	Combined bisulphite restriction analysis
Comm	Committed basal
COPG2IT1	Coatomer protein complex, subunit gamma 2, imprinted transcript 1
CPA	Carboxypeptidase
CpG	Cytosine-phosphate-guanine
CRABP	Cellular retinoic acid binding proteins
CRBP	Cellular retinol binding protein
CRIP1	Cysteine-rich protein 1
CRPC	Castrate resistant prostate cancer
CRU	Cancer research unit
CSC	Cancer stem cell
C$_T$	Threshold cycle
CTC	Circulating tumour cell
CXCR4	Chemokine (C-X-C motif) receptor 4
CYP17	Cytochrome P450, family 17
CYP1B1	Cytochrome P450, family 1, subfamily B, polypeptide 1
CZ	Central zone
D10	DMEM + 10% FCS
DAPI	4',6-diamidino-2-phenylindole
ddH$_2$0	Double distilled water
DEPC	Diethylpyrocarbonate
dH$_2$O	Distilled water
DHT	Dihydrotestosterone
DMEM	Dulbecco's modified eagle medium
DMSO	Dimethyl sulfoxide
DNA	Deoxyribonucleic acid
DNMT	DNA methyltransferase
dNTPS	Deoxyribonucleotide triphosphate
DR	Direct repeat
DTT	Dithiothreitol
E.Coli	Escherichia coli
ECACC	European collection of cell cultures
ECI	Endogenous carboxypeptidase inhibitor
ECL	Enhanced chemiluminescence
ECM	Extracellular matrix

EDTA	Ethylenediaminetetraacetic acid
EEF1A1	Eukaryotic translation elongation factor 1 alpha 1
EGF	Epidermal growth factor
eGFP	Enhanced green fluorescent protein
EMBOSS	European molecular biology open software suite
EMT	Epithelial-to-mesenchymal transition
ER	Endoplasmic reticulum
ERG	V-ets erythroblastosis virus E26 oncogene homolog
ES	Embryonic stem
EtOH	Ethanol
EZH2	Enhancer of Zeste homolog 2
FCS	Fetal calf serum
FDA	Food and Drug Administration
FGF	Fibroblast growth factor
FITC	Fluorescein isothiocyanate
FS	Forward scatter
g	Gram
G0	G zero phase
G1	Gap 1 phase
G2/M	Gap 2 phase/mitosis
GAPDH	Glyceraldehyde 3-phosphate dehydrogenase
gDNA	Genomic DNA
GFP	Green fluorescent protein
GNRH	Gonadotrophin-releasing hormone
GSTP1	Glutathione S-transferase Pi 1
G$_Y$	Gray
H. Sapiens	Homo Sapiens
H3	Histone 3
H3K4	Histone 3 lysine 4
H3K4Me2	Di-methylated histone 3 at lysine 4
H3K9	Histone 3 lysine 9
H3K27	Histone 3 lysine 27
H3K27Me3	Tri-methylated histone 3 at lysine 27
H3K36	Histone 3 lysine 36
H3K79	Histone 3 lysine 79
H4K20	Histone 4 lysine 20
H7	Ham's F-12 medium + 7% FCS
HA	Haemagglutinin
HAT	Histone acetyl transferase
HCl	Hydrogen chloride
HDAC	Histone deacetylase

HMT	Histone methyltransferases
HNSCC	Head and neck squamous cell carcinoma
HOX	Homeobox
HPLC	High-performance liquid chromatography
HPRT1	Hypoxanthine phosphoribosyltransferase 1
HPSE	Heparanase
HRP	Horseradish peroxidase
HSC	Haematopoietic stem cell
HUWE1	HECT, UBA and WWE domain containing 1, E3 ubiquitin protein ligase
IgG	Immunoglobulin G
IHC	Immunohistochemistry
IP	Immunoprecipitation
ITS-G	Insulin, transferrin, selenium solution
kB	Kilobase
KCl	Potassium chloride
kDa	Kilo Dalton
Ki67 (MKI67)	Antigen identified by monoclonal antibody Ki-67
KSFM	Keratinocyte serum free medium
LA	Left apex
LB	Left base
LB	Lysogeny broth
LHRH	Luteinizing-releasing hormone
LiCl	Lithium chloride
LIF	Leukaemia inhibitory factor
Lin	Linear
LOH	Loss of heterozygosity
LRP	Laparoscopic radical prostatectomy
LSD1	Amine oxidase (flavin containing) domain 2
LXN	Latexin
M. Musculus	Mus musculus
MACS	Magnetic-activated cell sorting
MAPK	Mitogen-activated protein kinase
MBD	Methyl-CpG-binding domain protein
MCP	Metallocarboxypeptidase
MDR1	Multidrug resistance protein 1
MEST	Mesoderm specific transcript homolog
MESTIT1	MEST intronic transcript 1, antisense RNA
MET	Mesenchymal-to-epithelial transition
MgCl$_2$	Magnesium chloride
MGMT	O-6-methylguanine-DNA methyltransferase

Min	Minute
MiRNA	Micro RNA
ml	Millilitre
mM	Millimolar
mm	millimetre
MMP	Matrix metallopeptidase
MOPS	3-(N-morpholino)propanesulfonic acid
mRNA	Messenger RNA
MSP	Methylation specific PCR
Mw	Molecular weight
NaBu	Sodium butyrate
NaCl	Sodium chloride
NaOH	Sodium hydroxide
NCOR	Nuclear receptor corepressor
NE	Neuroendocrine
ng	Nanogram
NKX3.1	NK3 transcription factor related, locus 1
NLS	Nuclear localisation signal
nM	Nanomolar
NP-40	Tergitol-type NP-40
ORF	Open reading frame
ORP	Open radical prostatectomy
P16INK4A	Cyclin-dependent kinase inhibitor 2A (CDKN2A)
P21	Cyclin-dependent kinase inhibitor 1A
P27KIP	Cyclin-dependent kinase inhibitor 1B(CDKN1B)
P160	MYB binding protein
P300-CBP	E1a-binding protein p300-CREB binding protein
P53	Tumour protein 53
P63	Tumour protein 63
PAGE	Polyacrylamide gel electrophoresis
PAP	Prostatic acid phosphatase
PBS	Phosphate-buffered saline
PcG	Polycomb complex
PCR	Polymerase chain reaction
PDI	Protein disulphide isomerase
PE	Phycoerythrin
PI	Propidium iodide
PI3K	Phosphoinositide 3-kinase
PIC	Protein inhibitor cocktail
PIN	Prostatic intraepithelial neoplasia
PIPES	Piperazine-N,N′-bis(2-ethanesulfonic acid)

PLAU	Urokinase-type plasminogen activator	
PM	Plasma membrane	
PPIA	Peptidylprolyl isomerise A	
PSA	Prostate-specific antigen	
PSAPb	PSA-probasin	
PTEN	Phosphatase and tensin homolog	
PTGS2	Prostaglandin-endoperoxide synthase 2	
Pyro	Pyrosequencing	
PZ	Peripheral zone	
qPCR	Quantitative PCR	
qRT-PCR	Quantitative real-time PCR	
R. Norvegicus	Rattus Norvegicus	
R1	Region 1	
R10	RPMI + 10% FCS	
R1881	Metribolone	
R2	Region 2	
R3	Region 3	
R5	RPMI + 5% FCS	
RA	Retinoic acid	
Radical	Radical prostatectomy	
Rag2	Recombination activating gene 2	
RALDH	Retinaldehyde dehydrogenase type 2	
RAR	Retinoic acid receptor	
RARE	Retinoic acid response element	
RARRES1	Retinoic acid receptor responder 1	
RARα	RAR alpha	
RARβ	RAR beta	
RARγ	RAR gamma	
RASSF1α	Ras association domain-containing protein 1	
RB	Right base	
RHO	Rhodopsin	
RISC	RNA-induced silencing complex	
RNA	Ribonucleic acid	
ROC	Receiver operator characteristic	
ROCK	Rho-associated, coiled-coil containing protein kinase	
RoDH	Retinol dehydrogenase	
RPLP0	Ribosomal protein, large, P0	
RPM	Revolutions per minute	
RPMI	Roswell Park Memorial Institute medium	
RR1	RARRES1	
RT	Room temperature	

RXR	Retinoid X receptor
S100P	S100 calcium binding protein P
SC	Stem cell
SCM	Stem cell medium
Scr	Scrambled siRNA
SDS	Sodium dodecyl sulphate
siRNA	Small interfering RNA
SIRT	Sirtuin
SMRT	Silencing mediator for retinoic and thyroid receptors
SOC	Super optimal broth
SRC	V-src sarcoma (Schmidt-Ruppin A-2) viral oncogene homolog
SS	Side scatter
Stem	Stem cell
SV40	Simian vacuolating virus 40 Tag
T25	25 cm^2 tissue culture flask
T75	75 cm^2 tissue culture flask
TA	Transit-amplifying cell
TAE	Tris base, acetic acid and EDTA buffer
Taq	Thermus aquaticus
TBS	Tris-buffered saline
TBST	Tris-buffered saline with Tween-20
TCC	Transitional cell carcinoma
TCI	Tissue carboxypeptidase inhibitor
TE	Tris EDTA buffer
TET	Tet methylcytosine dioxygenase
TF	Transcription factor
Tie2	Endothelium-specific receptor tyrosine kinase 2
TIG1	Tazarotene induced gene 1
TIMP3	TIMP metallopeptidase inhibitor 3
TMPRSS2	Transmembrane protease, serine 2
TPT1	Tumour protein, translationally-controlled 1
tRNA	Transfer ribonucleic acid
TS	Transcript
TSA	Trichostatin A
TSE	Tris, sucrose, EDTA buffer
TSS	Transcription start site
TURP	Transurethral resection of the prostate
TX-100	Triton X-100
TZ	Transitional zone
U/mg	Units per milligram
U/ml	Units per millilitre

UBC	Unbroken cells
UD	Undetected
UK	United Kingdom
uPa	Urokinase-type plasminogen activator
V	Volts
v/v	Volume per volume
VAD	Vitamin A deficiency
Vect	Vector
w/v	Weight per volume
WNT	Wingless-type MMTV integration site family
YWHAZ	Tyrosine 3-monooxygenase /tryptophan 5-monooxygenase activation protein, zeta polypeptide
ZEB	Zinc finger E-box binding homeobox
α1-Na/K-ATPase	Alpha 1 sodium-potassium adenosine triphosphate
β-2m	Beta-2 microglobulin
β-actin	Beta actin
γ-actin	Gamma actin

REFERENCES

- **Office for National Statistics Mortality Statistics**. Deaths registered in 2010, England and Wales. London: National Statistics; 2011.
  http://www.ons.gov.uk/ons/rel/vsob1/mortality-statistics--deaths-registered-in-England-and-Wales--series-dr-/index.html
  Accessed 13-09-2012
- **General Register Office for Scotland**. 2010 Deaths Time Series Data: Deaths in Scotland in 2010.
  http://www.gro-scotland.gov.uk/statistics/theme/vital-events/deaths/time-series.html
  Accessed 13-09-2012
- **Northern Ireland Statistics and Research Agency**.
  http://www.nisra.gov.uk/demography/default.asp14.htm
  Accessed 13-09-2012
- **Cancer Research UK.** Prostate Cancer 2010. UK prostate cancer statistics.
  http://info.cancerresearchuk.org/cancerstats/types/prostate/incidence/.
  Accessed 13-08-2012.
- **National cancer institute.**
  http://www.cancer.gov/dictionary?cdrid=44373
  Accessed 04-09-2012

1. **Aagaard, A., Listwan, P., Cowieson, N., Huber, T., Ravasi, T., Wells, C.A., Flanagan, J.U., Kellie, S., Hume, D.A., Kobe, B. and Martin, J.L.**, 2005. An inflammatory role for the mammalian carboxypeptidase inhibitor latexin: relationship to cystatins and the tumor suppressor TIG1, *Structure*. 13, 309-317.

2. **Abate-Shen, C. and Shen, M.M.**, 2000. Molecular genetics of prostate cancer, *Genes Dev*. 14, 2410-2434.

3. **Aboseif, S.R., Dahiya, R., Narayan, P. and Cunha, G.R.**, 1997. Effect of retinoic acid on prostatic development, *Prostate*. 31, 161-167.

4. **Abrahamsson, P.A., Falkmer, S., Falt, K. and Grimelius, L.**, 1989. The course of neuroendocrine differentiation in prostatic carcinomas. An immunohistochemical study testing chromogranin A as an "endocrine marker", *Pathol Res Pract*. 185, 373-380.

5. **Aggerholm, A. and Hokland, P.**, 2000. DAP-kinase CpG island methylation in acute myeloid leukemia: methodology versus biology?, *Blood*. 95, 2997-2999.

6. **Ahlgren, G., Pedersen, K., Lundberg, S., Aus, G., Hugosson, J. and Abrahamsson, P.A.**, 2000. Regressive changes and neuroendocrine differentiation in prostate cancer after neoadjuvant hormonal treatment, *Prostate*. 42, 274-279.

7. **Al-Hajj, M., Wicha, M.S., Benito-Hernandez, A., Morrison, S.J. and Clarke, M.F.**, 2003. Prospective identification of tumorigenic breast cancer cells, *Proc Natl Acad Sci U S A*. 100, 3983-3988.

8. **Al-Mehdi, A.B., Tozawa, K., Fisher, A.B., Shientag, L., Lee, A. and Muschel, R.J.**, 2000. Intravascular origin of metastasis from the proliferation of endothelium-attached tumor cells: a new model for metastasis, *Nat Med*. 6, 100-102.

9. **Alam, T.N., O'Hare, M.J., Laczko, I., Freeman, A., Al-Beidh, F., Masters, J.R. and Hudson, D.L.**, 2004. Differential expression of CD44 during human prostate epithelial cell differentiation, *J Histochem Cytochem*. 52, 1083-1090.

10. **Albini, A., Iwamoto, Y., Kleinman, H.K., Martin, G.R., Aaronson, S.A., Kozlowski, J.M. and McEwan, R.N.**, 1987. A rapid in vitro assay for quantitating the invasive potential of tumor cells, *Cancer Res*. 47, 3239-3245.

11. **Alcaraz, A., Takahashi, S., Brown, J.A., Herath, J.F., Bergstralh, E.J., Larson-Keller, J.J., Lieber, M.M. and Jenkins, R.B.**, 1994. Aneuploidy and aneusomy of chromosome 7 detected by fluorescence in situ hybridization are markers of poor prognosis in prostate cancer, *Cancer Res*. 54, 3998-4002.

12. **Anderton, J.A., Lindsey, J.C., Lusher, M.E., Gilbertson, R.J., Bailey, S., Ellison, D.W. and Clifford, S.C.**, 2008. Global analysis of the medulloblastoma epigenome identifies disease-subgroup-specific inactivation of COL1A2, *Neuro Oncol*. 10, 981-994.

13. **Ansel, K.M., Lee, D.U. and Rao, A.**, 2003. An epigenetic view of helper T cell differentiation, *Nat Immunol*. 4, 616-623.

14. **Arimatsu, Y.**, 1994. Latexin: a molecular marker for regional specification in the neocortex, *Neurosci Res*. 20, 131-135.

15. **Astrom, A., Pettersson, U., Chambon, P. and Voorhees, J.J.**, 1994. Retinoic acid induction of human cellular retinoic acid-binding protein-II gene transcription is mediated by retinoic acid receptor-retinoid X receptor heterodimers bound to one far upstream retinoic acid-responsive element with 5-base pair spacing, *J Biol Chem*. 269, 22334-22339.

16. **Attard, G., Rizzo, S., Ledaki, I., Clark, J., Reid, A.H., Thompson, A., Khoo, V., de Bono, J.S., Cooper, C.S. and Hudson, D.L.**, 2009. A novel, spontaneously immortalized, human prostate cancer cell line, Bob, offers a unique model for pre-clinical prostate cancer studies, *Prostate*. 69, 1507-1520.

17. **Aumuller, G.**, 1983. Morphologic and endocrine aspects of prostatic function, *Prostate*. 4, 195-214.

18. **Aumuller, G.**, 1991. Postnatal development of the prostate, *Bull Assoc Anat (Nancy)*. 75, 39-42.

19. **Bachmann, I.M., Halvorsen, O.J., Collett, K., Stefansson, I.M., Straume, O., Haukaas, S.A., Salvesen, H.B., Otte, A.P. and Akslen, L.A.**, 2006. EZH2 expression is associated with high proliferation rate and aggressive tumor subgroups in cutaneous melanoma and cancers of the endometrium, prostate, and breast, *J Clin Oncol*. 24, 268-273.

20. **Bailar, J.C., 3rd and Byar, D.P.**, 1970. Estrogen treatment for cancer of the prostate. Early results with 3 doses of diethylstilbestrol and placebo, *Cancer*. 26, 257-261.

21. **Bandyk, M.G., Zhao, L., Troncoso, P., Pisters, L.L., Palmer, J.L., von Eschenbach, A.C., Chung, L.W. and Liang, J.C.**, 1994. Trisomy 7: a potential cytogenetic marker of human prostate cancer progression, *Genes Chromosomes Cancer*. 9, 19-27.

22. **Bao, S., Wu, Q., McLendon, R.E., Hao, Y., Shi, Q., Hjelmeland, A.B., Dewhirst, M.W., Bigner, D.D. and Rich, J.N.**, 2006. Glioma stem cells promote radioresistance by preferential activation of the DNA damage response, *Nature*. 444, 756-760.

23. **Barrallo-Gimeno, A. and Nieto, M.A.**, 2005. The Snail genes as inducers of cell movement and survival: implications in development and cancer, *Development*. 132, 3151-3161.

24. **Bastien, J. and Rochette-Egly, C.**, 2004. Nuclear retinoid receptors and the transcription of retinoid-target genes, *Gene*. 328, 1-16.

25. **Baum, C.M., Weissman, I.L., Tsukamoto, A.S., Buckle, A.M. and Peault, B.**, 1992. Isolation of a candidate human hematopoietic stem-cell population, *Proc Natl Acad Sci U S A*. 89, 2804-2808.

26. **Baylin, S.B. and Jones, P.A.**, 2011. A decade of exploring the cancer epigenome - biological and translational implications, *Nat Rev Cancer*. 11, 726-734.

27. **Bedford, M.T. and van Helden, P.D.**, 1987. Hypomethylation of DNA in pathological conditions of the human prostate, *Cancer Res*. 47, 5274-5276.

28. **Beke, L., Nuytten, M., Van Eynde, A., Beullens, M. and Bollen, M.**, 2007. The gene encoding the prostatic tumor suppressor PSP94 is a target for repression by the Polycomb group protein EZH2, *Oncogene*. 26, 4590-4595.

29. **Beltran, H., Beer, T.M., Carducci, M.A., de Bono, J., Gleave, M., Hussain, M., Kelly, W.K., Saad, F., Sternberg, C., Tagawa, S.T. and Tannock, I.F.**, 2011. New therapies for castration-resistant prostate cancer: efficacy and safety, *Eur Urol*. 60, 279-290.

30. **Bentley, L., Nakabayashi, K., Monk, D., Beechey, C., Peters, J., Birjandi, Z., Khayat, F.E., Patel, M., Preece, M.A., Stanier, P., Scherer, S.W. and Moore, G.E.**, 2003. The imprinted region on human chromosome 7q32 extends to the carboxypeptidase A gene cluster: an imprinted candidate for Silver-Russell syndrome, *J Med Genet*. 40, 249-256.

31. **Berman, D.M., Desai, N., Wang, X., Karhadkar, S.S., Reynon, M., Abate-Shen, C., Beachy, P.A. and Shen, M.M.**, 2004. Roles for Hedgehog signaling in androgen production and prostate ductal morphogenesis, *Dev Biol*. 267, 387-398.

32. **Bernstein, B.E., Mikkelsen, T.S., Xie, X., Kamal, M., Huebert, D.J., Cuff, J., Fry, B., Meissner, A., Wernig, M., Plath, K., Jaenisch, R., Wagschal, A., Feil, R., Schreiber, S.L. and Lander, E.S.**, 2006. A bivalent chromatin structure marks key developmental genes in embryonic stem cells, *Cell*. 125, 315-326.

33. **Berry, P.A., Maitland, N.J. and Collins, A.T.**, 2008. Androgen receptor signalling in prostate: effects of stromal factors on normal and cancer stem cells, *Mol Cell Endocrinol*. 288, 30-37.

34. **Berthon, P., Cussenot, O., Hopwood, L., Leduc, A. and Maitland, N.**, 1995. Functional expression of sv40 in normal human prostatic epithelial and fibroblastic cells - differentiation pattern of nontumorigenic cell-lines, *Int J Oncol*. 6, 333-343.

35. **Bickmore, W.A. and Sutherland, H.G.**, 2002. Addressing protein localization within the nucleus, *EMBO J*. 21, 1248-1254.

36. **Bieliauskas, A.V. and Pflum, M.K.**, 2008. Isoform-selective histone deacetylase inhibitors, *Chem Soc Rev*. 37, 1402-1413.

37. **Bill-Axelson, A., Holmberg, L., Ruutu, M., Haggman, M., Andersson, S.O., Bratell, S., Spangberg, A., Busch, C., Nordling, S., Garmo, H., Palmgren, J., Adami, H.O., Norlen, B.J. and Johansson, J.E.**, 2005. Radical prostatectomy versus watchful waiting in early prostate cancer, *N Engl J Med*. 352, 1977-1984.

38. **Bird, A.**, 2002. DNA methylation patterns and epigenetic memory, *Genes Dev*. 16, 6-21.

39. **Bird, A.P.**, 1986. CpG-rich islands and the function of DNA methylation, *Nature*. 321, 209-213.

40. **Birnie, R., Bryce, S.D., Roome, C., Dussupt, V., Droop, A., Lang, S.H., Berry, P.A., Hyde, C.F., Lewis, J.L., Stower, M.J., Maitland, N.J. and Collins, A.T.**, 2008. Gene expression profiling of human prostate cancer stem cells reveals a pro-inflammatory phenotype and the importance of extracellular matrix interactions, *Genome Biol*. 9, R83.

41. **Blackwood, J.K., Williamson, S.C., Greaves, L.C., Wilson, L., Rigas, A.C., Sandher, R., Pickard, R.S., Robson, C.N., Turnbull, D.M., Taylor, R.W. and Heer, R.**, 2011. In situ lineage tracking of human prostatic epithelial stem cell fate reveals a common clonal origin for basal and luminal cells, *J Pathol*. 225, 181-188.

42. **Bohrer, M.H. and Schmoll, J.**, 1993. [Immunohistochemical and morphometric studies on neuroendocrine differentiation of prostate carcinomas], *Verh Dtsch Ges Pathol*. 77, 107-110.

43. **Bonkhoff, H. and Remberger, K.**, 1993. Widespread distribution of nuclear androgen receptors in the basal cell layer of the normal and hyperplastic human prostate, *Virchows Arch A Pathol Anat Histopathol*. 422, 35-38.

44. **Bonkhoff, H. and Remberger, K.**, 1996. Differentiation pathways and histogenetic aspects of normal and abnormal prostatic growth: a stem cell model, *Prostate*. 28, 98-106.

45. **Bonkhoff, H., Stein, U. and Remberger, K.**, 1994. The proliferative function of basal cells in the normal and hyperplastic human prostate, *Prostate*. 24, 114-118.

46. **Bonkhoff, H., Stein, U. and Remberger, K.**, 1995. Endocrine-paracrine cell types in the prostate and prostatic adenocarcinoma are postmitotic cells, *Hum Pathol*. 26, 167-170.

47. **Bonkhoff, H., Wernert, N., Dhom, G. and Remberger, K.**, 1991. Relation of endocrine-paracrine cells to cell proliferation in normal, hyperplastic, and neoplastic human prostate, *Prostate*. 19, 91-98.

48. **Bonnet, D. and Dick, J.E.**, 1997. Human acute myeloid leukemia is organized as a hierarchy that originates from a primitive hematopoietic cell, *Nat Med*. 3, 730-737.

49. **Bookstein, R., Rio, P., Madreperla, S.A., Hong, F., Allred, C., Grizzle, W.E. and Lee, W.H.**, 1990. Promoter deletion and loss of retinoblastoma gene expression in human prostate carcinoma, *Proc Natl Acad Sci U S A*. 87, 7762-7766.

50. **Bostwick, D.G., Liu, L., Brawer, M.K. and Qian, J.**, 2004. High-grade prostatic intraepithelial neoplasia, *Rev Urol*. 6, 171-179.

51. **Branco, M.R., Ficz, G. and Reik, W.**, 2012. Uncovering the role of 5-hydroxymethylcytosine in the epigenome, *Nat Rev Genet*. 13, 7-13.

52. **Brawer, M.K.**, 1999. Prostate-specific antigen: current status, *CA Cancer J Clin*. 49, 264-281.

53. **Brown, M.D., Gilmore, P.E., Hart, C.A., Samuel, J.D., Ramani, V.A., George, N.J. and Clarke, N.W.**, 2007. Characterization of benign and malignant prostate epithelial Hoechst 33342 side populations, *Prostate*. 67, 1384-1396.

54. **Bruce, W.R. and Van Der Gaag, H.**, 1963. A Quantitative Assay for the Number of Murine Lymphoma Cells Capable of Proliferation in Vivo, *Nature*. 199, 79-80.

55. **Brunschwig, C.S.a.A.**, 1961. Quantitative studies of autotransplantation of human cancer, *Cancer*. 14, 461-563.

56. **Bubendorf, L., Schopfer, A., Wagner, U., Sauter, G., Moch, H., Willi, N., Gasser, T.C. and Mihatsch, M.J.**, 2000. Metastatic patterns of prostate cancer: an autopsy study of 1,589 patients, *Hum Pathol*. 31, 578-583.

57. **Budhu, A.S. and Noy, N.**, 2002. Direct channeling of retinoic acid between cellular retinoic acid-binding protein II and retinoic acid receptor sensitizes mammary carcinoma cells to retinoic acid-induced growth arrest, *Mol Cell Biol*. 22, 2632-2641.

58. **Bui, M. and Reiter, R.E.**, 1998. Stem cell genes in androgen-independent prostate cancer, *Cancer Metastasis Rev*. 17, 391-399.

59. **Burger, P.E., Gupta, R., Xiong, X., Ontiveros, C.S., Salm, S.N., Moscatelli, D. and Wilson, E.L.**, 2009. High aldehyde dehydrogenase activity: a novel functional marker of murine prostate stem/progenitor cells, *Stem Cells*. 27, 2220-2228.

60. **Caccia, D., Zanetti Domingues, L., Micciche, F., De Bortoli, M., Carniti, C., Mondellini, P. and Bongarzone, I.**, 2011. Secretome compartment is a valuable source of biomarkers for cancer-relevant pathways, *J Proteome Res*. 10, 4196-4207.

61. **Calin, G.A. and Croce, C.M.**, 2006. MicroRNA signatures in human cancers, *Nat Rev Cancer*. 6, 857-866.

62. **Calmon, M.F., Rodrigues, R.V., Kaneto, C.M., Moura, R.P., Silva, S.D., Mota, L.D., Pinheiro, D.G., Torres, C., de Carvalho, A.F., Cury, P.M., Nunes, F.D., Nishimoto, I.N., Soares, F.A., da Silva, A.M., Kowalski, L.P., Brentani, H., Zanelli, C.F., Silva, W.A., Jr., Rahal, P., Tajara, E.H., Carraro, D.M., Camargo, A.A. and Valentini, S.R.**, 2009. Epigenetic silencing of CRABP2 and MX1 in head and neck tumors, *Neoplasia*. 11, 1329-1339.

63. **Campos, B., Wan, F., Farhadi, M., Ernst, A., Zeppernick, F., Tagscherer, K.E., Ahmadi, R., Lohr, J., Dictus, C., Gdynia, G., Combs, S.E., Goidts, V., Helmke, B.M., Eckstein, V., Roth, W., Beckhove, P., Lichter, P., Unterberg, A., Radlwimmer, B. and Herold-Mende, C.**, 2010. Differentiation therapy exerts antitumor effects on stem-like glioma cells, *Clin Cancer Res.* 16, 2715-2728.

64. **Cao, R., Wang, L., Wang, H., Xia, L., Erdjument-Bromage, H., Tempst, P., Jones, R.S. and Zhang, Y.**, 2002. Role of histone H3 lysine 27 methylation in Polycomb-group silencing, *Science.* 298, 1039-1043.

65. **Catalona, W.J., Carvalhal, G.F., Mager, D.E. and Smith, D.S.**, 1999. Potency, continence and complication rates in 1,870 consecutive radical retropubic prostatectomies, *J Urol.* 162, 433-438.

66. **Catalona, W.J., Partin, A.W., Slawin, K.M., Brawer, M.K., Flanigan, R.C., Patel, A., Richie, J.P., deKernion, J.B., Walsh, P.C., Scardino, P.T., Lange, P.H., Subong, E.N., Parson, R.E., Gasior, G.H., Loveland, K.G. and Southwick, P.C.**, 1998. Use of the percentage of free prostate-specific antigen to enhance differentiation of prostate cancer from benign prostatic disease: a prospective multicenter clinical trial, *JAMA.* 279, 1542-1547.

67. **Chang, J., Varghese, D.S., Gillam, M.C., Peyton, M., Modi, B., Schiltz, R.L., Girard, L. and Martinez, E.D.**, 2012. Differential response of cancer cells to HDAC inhibitors trichostatin A and depsipeptide, *Br J Cancer.* 106, 116-125.

68. **Chaudhary, P.M. and Roninson, I.B.**, 1991. Expression and activity of P-glycoprotein, a multidrug efflux pump, in human hematopoietic stem cells, *Cell.* 66, 85-94.

69. **Chen, C.Z., Li, L., Lodish, H.F. and Bartel, D.P.**, 2004. MicroRNAs modulate hematopoietic lineage differentiation, *Science.* 303, 83-86.

70. **Chen, H., Tu, S.W. and Hsieh, J.T.**, 2005. Down-regulation of human DAB2IP gene expression mediated by polycomb Ezh2 complex and histone deacetylase in prostate cancer, *J Biol Chem.* 280, 22437-22444.

71. **Chen, H.L., Seol, H., Brown, K.J., Gordish-Dressman, H., Hill, A., Gallo, V., Packer, R. and Hathout, Y.**, 2012. Secretome Survey of Human Plexiform Neurofibroma Derived Schwann Cells Reveals a Secreted form of the RARRES1 Protein, *Int J Mol Sci.* 13, 9380-9399.

72. **Cheville, J.C. and Bostwick, D.G.**, 1995. Postatrophic hyperplasia of the prostate. A histologic mimic of prostatic adenocarcinoma, *Am J Surg Pathol.* 19, 1068-1076.

73. **Chiou, S.H., Kao, C.L., Chen, Y.W., Chien, C.S., Hung, S.C., Lo, J.F., Chen, Y.J., Ku, H.H., Hsu, M.T. and Wong, T.T.**, 2008. Identification of CD133-positive radioresistant cells in atypical teratoid/rhabdoid tumor, *PLoS One.* 3, e2090.

74. **Cho, B., Lee, H., Jeong, S., Bang, Y.J., Lee, H.J., Hwang, K.S., Kim, H.Y., Lee, Y.S., Kang, G.H. and Jeoung, D.I.**, 2003. Promoter hypomethylation of a novel cancer/testis antigen gene CAGE is correlated with its aberrant expression and is seen in premalignant stage of gastric carcinoma, *Biochem Biophys Res Commun.* 307, 52-63.

75. **Chute, J.P., Muramoto, G.G., Whitesides, J., Colvin, M., Safi, R., Chao, N.J. and McDonnell, D.P.**, 2006. Inhibition of aldehyde dehydrogenase and retinoid signaling induces the expansion of human hematopoietic stem cells, *Proc Natl Acad Sci U S A*. 103, 11707-11712.

76. **Collins, A.T., Berry, P.A., Hyde, C., Stower, M.J. and Maitland, N.J.**, 2005. Prospective identification of tumorigenic prostate cancer stem cells, *Cancer Res*. 65, 10946-10951.

77. **Collins, A.T., Habib, F.K., Maitland, N.J. and Neal, D.E.**, 2001. Identification and isolation of human prostate epithelial stem cells based on alpha(2)beta(1)-integrin expression, *J Cell Sci*. 114, 3865-3872.

78. **Collins, A.T. and Maitland, N.J.**, 2006. Prostate cancer stem cells, *Eur J Cancer*. 42, 1213-1218.

79. **Cooney, K.A., Wetzel, J.C., Consolino, C.M. and Wojno, K.J.**, 1996. Identification and characterization of proximal 6q deletions in prostate cancer, *Cancer Res*. 56, 4150-4153.

80. **Coppola, V., De Maria, R. and Bonci, D.**, 2010. MicroRNAs and prostate cancer, *Endocr Relat Cancer*. 17, F1-17.

81. **Cornic, M., Delva, L., Castaigne, S., Lefebvre, P., Balitrand, N., Degos, L. and Chomienne, C.**, 1994. In vitro all-trans retinoic acid (ATRA) sensitivity and cellular retinoic acid binding protein (CRABP) levels in relapse leukemic cells after remission induction by ATRA in acute promyelocytic leukemia, *Leukemia*. 8, 914-917.

82. **Croce, C.M. and Calin, G.A.**, 2005. miRNAs, cancer, and stem cell division, *Cell*. 122, 6-7.

83. **Cui, K., Zang, C., Roh, T.Y., Schones, D.E., Childs, R.W., Peng, W. and Zhao, K.**, 2009. Chromatin signatures in multipotent human hematopoietic stem cells indicate the fate of bivalent genes during differentiation, *Cell Stem Cell*. 4, 80-93.

84. **Cunha, G.R., Donjacour, A.A., Cooke, P.S., Mee, S., Bigsby, R.M., Higgins, S.J. and Sugimura, Y.**, 1987. The endocrinology and developmental biology of the prostate, *Endocr Rev*. 8, 338-362.

85. **Cunningham, J.M., Shan, A., Wick, M.J., McDonnell, S.K., Schaid, D.J., Tester, D.J., Qian, J., Takahashi, S., Jenkins, R.B., Bostwick, D.G. and Thibodeau, S.N.**, 1996. Allelic imbalance and microsatellite instability in prostatic adenocarcinoma, *Cancer Res*. 56, 4475-4482.

86. **Curtis, K.M., Gomez, L.A., Rios, C., Garbayo, E., Raval, A.P., Perez-Pinzon, M.A. and Schiller, P.C.**, 2010. EF1alpha and RPL13a represent normalization genes suitable for RT-qPCR analysis of bone marrow derived mesenchymal stem cells, *BMC Mol Biol*. 11, 61.

87. **Dahiya, R., Park, H.D., Cusick, J., Vessella, R.L., Fournier, G. and Narayan, P.**, 1994. Inhibition of tumorigenic potential and prostate-specific antigen expression in LNCaP human prostate cancer cell line by 13-cis-retinoic acid, *Int J Cancer*. 59, 126-132.

88. **Davidson, D., Bostwick, D.G., Qian, J., Wollan, P.C., Oesterling, J.E., Rudders, R.A., Siroky, M. and Stilmant, M.**, 1995. Prostatic intraepithelial neoplasia is a risk factor for adenocarcinoma: predictive accuracy in needle biopsies, *J Urol*. 154, 1295-1299.

89. **Dawson, M.A. and Kouzarides, T.**, 2012. Cancer epigenetics: from mechanism to therapy, *Cell*. 150, 12-27.

90. **de Bono, J.S., Logothetis, C.J., Molina, A., Fizazi, K., North, S., Chu, L., Chi, K.N., Jones, R.J., Goodman, O.B., Jr., Saad, F., Staffurth, J.N., Mainwaring, P., Harland, S., Flaig, T.W., Hutson, T.E., Cheng, T., Patterson, H., Hainsworth, J.D., Ryan, C.J., Sternberg, C.N., Ellard, S.L., Flechon, A., Saleh, M., Scholz, M., Efstathiou, E., Zivi, A., Bianchini, D., Loriot, Y., Chieffo, N., Kheoh, T., Haqq, C.M. and Scher, H.I.**, 2011. Abiraterone and increased survival in metastatic prostate cancer, *N Engl J Med*. 364, 1995-2005.

91. **De Marzo, A.M., Marchi, V.L., Epstein, J.I. and Nelson, W.G.**, 1999. Proliferative inflammatory atrophy of the prostate: implications for prostatic carcinogenesis, *Am J Pathol*. 155, 1985-1992.

92. **De Marzo, A.M., Meeker, A.K., Epstein, J.I. and Coffey, D.S.**, 1998. Prostate stem cell compartments: expression of the cell cycle inhibitor p27Kip1 in normal, hyperplastic, and neoplastic cells, *Am J Pathol*. 153, 911-919.

93. **Dehm, S.M., Schmidt, L.J., Heemers, H.V., Vessella, R.L. and Tindall, D.J.**, 2008. Splicing of a novel androgen receptor exon generates a constitutively active androgen receptor that mediates prostate cancer therapy resistance, *Cancer Res*. 68, 5469-5477.

94. **Delva, L., Bastie, J.N., Rochette-Egly, C., Kraiba, R., Balitrand, N., Despouy, G., Chambon, P. and Chomienne, C.**, 1999. Physical and functional interactions between cellular retinoic acid binding protein II and the retinoic acid-dependent nuclear complex, *Mol Cell Biol*. 19, 7158-7167.

95. **Denmeade, S.R. and Isaacs, J.T.**, 2002. A history of prostate cancer treatment, *Nat Rev Cancer*. 2, 389-396.

96. **Derks, S., Lentjes, M.H., Hellebrekers, D.M., de Bruine, A.P., Herman, J.G. and van Engeland, M.**, 2004. Methylation-specific PCR unraveled, *Cell Oncol*. 26, 291-299.

97. **Despouy, G., Bastie, J.N., Deshaies, S., Balitrand, N., Mazharian, A., Rochette-Egly, C., Chomienne, C. and Delva, L.**, 2003. Cyclin D3 is a cofactor of retinoic acid receptors, modulating their activity in the presence of cellular retinoic acid-binding protein II, *J Biol Chem*. 278, 6355-6362.

98. **Dilworth, F.J. and Chambon, P.**, 2001. Nuclear receptors coordinate the activities of chromatin remodeling complexes and coactivators to facilitate initiation of transcription, *Oncogene*. 20, 3047-3054.

99. **Dilworth, F.J., Fromental-Ramain, C., Yamamoto, K. and Chambon, P.**, 2000. ATP-driven chromatin remodeling activity and histone acetyltransferases act sequentially during transactivation by RAR/RXR In vitro, *Mol Cell*. 6, 1049-1058.

100. **Donato, L.J. and Noy, N.**, 2005. Suppression of mammary carcinoma growth by retinoic acid: proapoptotic genes are targets for retinoic acid receptor and cellular retinoic acid-binding protein II signaling, *Cancer Res.* 65, 8193-8199.

101. **Dong, D., Ruuska, S.E., Levinthal, D.J. and Noy, N.**, 1999. Distinct roles for cellular retinoic acid-binding proteins I and II in regulating signaling by retinoic acid, *J Biol Chem.* 274, 23695-23698.

102. **Donovan, M., Olofsson, B., Gustafson, A.L., Dencker, L. and Eriksson, U.**, 1995. The cellular retinoic acid binding proteins, *J Steroid Biochem Mol Biol.* 53, 459-465.

103. **Dubbink, H.J., Verkaik, N.S., Faber, P.W., Trapman, J., Schroder, F.H. and Romijn, J.C.**, 1996. Tissue specific and androgen-regulated expression of human prostate-specific transglutaminase, *Biochem J.* 315 (Pt 3), 901-908.

104. **Duchesne, G.**, 2011. Localised prostate cancer - current treatment options, *Aust Fam Physician.* 40, 768-771.

105. **Duester, G.**, 2008. Retinoic acid synthesis and signaling during early organogenesis, *Cell.* 134, 921-931.

106. **Durand, B., Saunders, M., Leroy, P., Leid, M. and Chambon, P.**, 1992. All-trans and 9-cis retinoic acid induction of CRABPII transcription is mediated by RAR-RXR heterodimers bound to DR1 and DR2 repeated motifs, *Cell.* 71, 73-85.

107. **Eads, C.A., Danenberg, K.D., Kawakami, K., Saltz, L.B., Blake, C., Shibata, D., Danenberg, P.V. and Laird, P.W.**, 2000. MethyLight: a high-throughput assay to measure DNA methylation, *Nucleic Acids Res.* 28, E32.

108. **Egea, P.F., Rochel, N., Birck, C., Vachette, P., Timmins, P.A. and Moras, D.**, 2001. Effects of ligand binding on the association properties and conformation in solution of retinoic acid receptors RXR and RAR, *J Mol Biol.* 307, 557-576.

109. **El-Alfy, M., Pelletier, G., Hermo, L.S. and Labrie, F.**, 2000. Unique features of the basal cells of human prostate epithelium, *Microsc Res Tech.* 51, 436-446.

110. **Ellinger, J., Bastian, P.J., Jurgan, T., Biermann, K., Kahl, P., Heukamp, L.C., Wernert, N., Muller, S.C. and von Ruecker, A.**, 2008. CpG island hypermethylation at multiple gene sites in diagnosis and prognosis of prostate cancer, *Urology.* 71, 161-167.

111. **Elo, J.P., Kvist, L., Leinonen, K., Isomaa, V., Henttu, P., Lukkarinen, O. and Vihko, P.**, 1995. Mutated human androgen receptor gene detected in a prostatic cancer patient is also activated by estradiol, *J Clin Endocrinol Metab.* 80, 3494-3500.

112. **English, H.F., Santen, R.J. and Isaacs, J.T.**, 1987. Response of glandular versus basal rat ventral prostatic epithelial cells to androgen withdrawal and replacement, *Prostate.* 11, 229-242.

113. **Epping, M.T. and Bernards, R.**, 2009. Molecular basis of the anti-cancer effects of histone deacetylase inhibitors, *Int J Biochem Cell Biol.* 41, 16-20.

114. **Epstein, J.I.**, 2000. Gleason score 2-4 adenocarcinoma of the prostate on needle biopsy: a diagnosis that should not be made, *Am J Surg Pathol.* 24, 477-478.

115. **Epstein, J.I.**, 2010. An update of the Gleason grading system, *J Urol.* 183, 433-440.

116. **Eramo, A., Lotti, F., Sette, G., Pilozzi, E., Biffoni, M., Di Virgilio, A., Conticello, C., Ruco, L., Peschle, C. and De Maria, R.**, 2008. Identification and expansion of the tumorigenic lung cancer stem cell population, *Cell Death Differ*. 15, 504-514.

117. **Esquela-Kerscher, A. and Slack, F.J.**, 2006. Oncomirs - microRNAs with a role in cancer, *Nat Rev Cancer*. 6, 259-269.

118. **Evans, G.S. and Chandler, J.A.**, 1987. Cell proliferation studies in the rat prostate: II. The effects of castration and androgen-induced regeneration upon basal and secretory cell proliferation, *Prostate*. 11, 339-351.

119. **Fan, G., Martinowich, K., Chin, M.H., He, F., Fouse, S.D., Hutnick, L., Hattori, D., Ge, W., Shen, Y., Wu, H., ten Hoeve, J., Shuai, K. and Sun, Y.E.**, 2005. DNA methylation controls the timing of astrogliogenesis through regulation of JAK-STAT signaling, *Development*. 132, 3345-3356.

120. **Fang, D., Nguyen, T.K., Leishear, K., Finko, R., Kulp, A.N., Hotz, S., Van Belle, P.A., Xu, X., Elder, D.E. and Herlyn, M.**, 2005. A tumorigenic subpopulation with stem cell properties in melanomas, *Cancer Res*. 65, 9328-9337.

121. **Feinberg, A.P., Ohlsson, R. and Henikoff, S.**, 2006. The epigenetic progenitor origin of human cancer, *Nat Rev Genet*. 7, 21-33.

122. **Feinberg, A.P. and Vogelstein, B.**, 1983. Hypomethylation distinguishes genes of some human cancers from their normal counterparts, *Nature*. 301, 89-92.

123. **Feng, D., Peng, C., Li, C., Zhou, Y., Li, M., Ling, B., Wei, H. and Tian, Z.**, 2009. Identification and characterization of cancer stem-like cells from primary carcinoma of the cervix uteri, *Oncol Rep*. 22, 1129-1134.

124. **Ferrero Doria, R., Perez Flores, D., Terrer Artes, C., Guzman Martinez-Valls, P.L., Morga Egea, J.P., Tomas Ros, M., Rico Galiano, J.L., Sempere Gutierrez, A. and Fontana Compiano, L.O.**, 1997. [Impact of prostatic benign hyperplasia and prostatic inflammation on the increase of prostate specific antigen levels], *Actas Urol Esp*. 21, 100-104.

125. **Fink, T., Lund, P., Pilgaard, L., Rasmussen, J.G., Duroux, M. and Zachar, V.**, 2008. Instability of standard PCR reference genes in adipose-derived stem cells during propagation, differentiation and hypoxic exposure, *BMC Mol Biol*. 9, 98.

126. **Frame, F.M., Hager, S., Pellacani, D., Stower, M.J., Walker, H.F., Burns, J.E., Collins, A.T. and Maitland, N.J.**, 2010. Development and limitations of lentivirus vectors as tools for tracking differentiation in prostate epithelial cells, *Exp Cell Res*. 316, 3161-3171.

127. **Franks, L.M.**, 1954. Atrophy and hyperplasia in the prostate proper, *J Pathol Bacteriol*. 68, 617-621.

128. **Friedl, P. and Wolf, K.**, 2003. Tumour-cell invasion and migration: diversity and escape mechanisms, *Nat Rev Cancer*. 3, 362-374.

129. **Gaisa, N.T., Graham, T.A., McDonald, S.A., Poulsom, R., Heidenreich, A., Jakse, G., Knuechel, R. and Wright, N.A.**, 2011. Clonal architecture of human prostatic epithelium in benign and malignant conditions, *J Pathol*. 225, 172-180.

130. **Gal-Yam, E.N., Egger, G., Iniguez, L., Holster, H., Einarsson, S., Zhang, X., Lin, J.C., Liang, G., Jones, P.A. and Tanay, A.**, 2008. Frequent switching of Polycomb repressive marks and DNA hypermethylation in the PC3 prostate cancer cell line, *Proc Natl Acad Sci U S A*. 105, 12979-12984.

131. **Gangaraju, V.K. and Lin, H.**, 2009. MicroRNAs: key regulators of stem cells, *Nat Rev Mol Cell Biol*. 10, 116-125.

132. **Gao, H., Ouyang, X., Banach-Petrosky, W.A., Gerald, W.L., Shen, M.M. and Abate-Shen, C.**, 2006a. Combinatorial activities of Akt and B-Raf/Erk signaling in a mouse model of androgen-independent prostate cancer, *Proc Natl Acad Sci U S A*. 103, 14477-14482.

133. **Gao, H., Ouyang, X., Banach-Petrosky, W.A., Shen, M.M. and Abate-Shen, C.**, 2006b. Emergence of androgen independence at early stages of prostate cancer progression in Nkx3.1; Pten mice, *Cancer Res*. 66, 7929-7933.

134. **Gardiner-Garden, M. and Frommer, M.**, 1987. CpG islands in vertebrate genomes, *J Mol Biol*. 196, 261-282.

135. **Garzon, R., Calin, G.A. and Croce, C.M.**, 2009. MicroRNAs in Cancer, *Annu Rev Med*. 60, 167-179.

136. **Gaudet, F., Hodgson, J.G., Eden, A., Jackson-Grusby, L., Dausman, J., Gray, J.W., Leonhardt, H. and Jaenisch, R.**, 2003. Induction of tumors in mice by genomic hypomethylation, *Science*. 300, 489-492.

137. **Ghosh, S., Yates, A.J., Fruhwald, M.C., Miecznikowski, J.C., Plass, C. and Smiraglia, D.**, 2010. Tissue specific DNA methylation of CpG islands in normal human adult somatic tissues distinguishes neural from non-neural tissues, *Epigenetics*. 5, 527-538.

138. **Ghossein, R.A., Scher, H.I., Gerald, W.L., Kelly, W.K., Curley, T., Amsterdam, A., Zhang, Z.F. and Rosai, J.**, 1995. Detection of circulating tumor cells in patients with localized and metastatic prostatic carcinoma: clinical implications, *J Clin Oncol*. 13, 1195-1200.

139. **Giguere, V., Lyn, S., Yip, P., Siu, C.H. and Amin, S.**, 1990. Molecular cloning of cDNA encoding a second cellular retinoic acid-binding protein, *Proc Natl Acad Sci U S A*. 87, 6233-6237.

140. **Ginestier, C., Wicinski, J., Cervera, N., Monville, F., Finetti, P., Bertucci, F., Wicha, M.S., Birnbaum, D. and Charafe-Jauffret, E.**, 2009. Retinoid signaling regulates breast cancer stem cell differentiation, *Cell Cycle*. 8, 3297-3302.

141. **Gingrich, J.R., Barrios, R.J., Morton, R.A., Boyce, B.F., DeMayo, F.J., Finegold, M.J., Angelopoulou, R., Rosen, J.M. and Greenberg, N.M.**, 1996. Metastatic prostate cancer in a transgenic mouse, *Cancer Res*. 56, 4096-4102.

142. **Glass, C.K. and Rosenfeld, M.G.**, 2000. The coregulator exchange in transcriptional functions of nuclear receptors, *Genes Dev*. 14, 121-141.

143. **Gleason, D.F.**, 1966. Classification of prostatic carcinomas, *Cancer Chemother Rep*. 50, 125-128.

144. **Gleason, D.F.**, 1992. Histologic grading of prostate cancer: a perspective, *Hum Pathol*. 23, 273-279.

145. **Glinsky, G.V.**, 2008. "Stemness" genomics law governs clinical behavior of human cancer: implications for decision making in disease management, *J Clin Oncol*. 26, 2846-2853.

146. **Gokden, N., Roehl, K.A., Catalona, W.J. and Humphrey, P.A.**, 2005. High-grade prostatic intraepithelial neoplasia in needle biopsy as risk factor for detection of adenocarcinoma: current level of risk in screening population, *Urology*. 65, 538-542.

147. **Goldstein, A.S., Huang, J., Guo, C., Garraway, I.P. and Witte, O.N.**, 2010. Identification of a cell of origin for human prostate cancer, *Science*. 329, 568-571.

148. **Greenberg, N.M., DeMayo, F., Finegold, M.J., Medina, D., Tilley, W.D., Aspinall, J.O., Cunha, G.R., Donjacour, A.A., Matusik, R.J. and Rosen, J.M.**, 1995. Prostate cancer in a transgenic mouse, *Proc Natl Acad Sci U S A*. 92, 3439-3443.

149. **Gregory, C.W., Hamil, K.G., Kim, D., Hall, S.H., Pretlow, T.G., Mohler, J.L. and French, F.S.**, 1998. Androgen receptor expression in androgen-independent prostate cancer is associated with increased expression of androgen-regulated genes, *Cancer Res*. 58, 5718-5724.

150. **Grewal, S.I. and Jia, S.**, 2007. Heterochromatin revisited, *Nat Rev Genet*. 8, 35-46.

151. **Grisanzio, C. and Signoretti, S.**, 2008. p63 in prostate biology and pathology, *J Cell Biochem*. 103, 1354-1368.

152. **Grivennikov, S.I., Greten, F.R. and Karin, M.**, 2010. Immunity, inflammation, and cancer, *Cell*. 140, 883-899.

153. **Guo, Z., Yang, X., Sun, F., Jiang, R., Linn, D.E., Chen, H., Kong, X., Melamed, J., Tepper, C.G., Kung, H.J., Brodie, A.M., Edwards, J. and Qiu, Y.**, 2009. A novel androgen receptor splice variant is up-regulated during prostate cancer progression and promotes androgen depletion-resistant growth, *Cancer Res*. 69, 2305-2313.

154. **Gupta, G.P. and Massague, J.**, 2006. Cancer metastasis: building a framework, *Cell*. 127, 679-695.

155. **Gupta, P.B., Onder, T.T., Jiang, G., Tao, K., Kuperwasser, C., Weinberg, R.A. and Lander, E.S.**, 2009. Identification of selective inhibitors of cancer stem cells by high-throughput screening, *Cell*. 138, 645-659.

156. **Gyftopoulos, K., Sotiropoulou, G., Varakis, I. and Barbalias, G.A.**, 2000. Cellular distribution of retinoic acid receptor-alpha in benign hyperplastic and malignant human prostates: comparison with androgen, estrogen and progesterone receptor status, *Eur Urol*. 38, 323-330.

157. **Haaf, T.**, 1995. The effects of 5-azacytidine and 5-azadeoxycytidine on chromosome structure and function: implications for methylation-associated cellular processes, *Pharmacol Ther*. 65, 19-46.

158. **Hahn, W.C. and Weinberg, R.A.**, 2002. Modelling the molecular circuitry of cancer, *Nat Rev Cancer*. 2, 331-341.

159. **Halkidou, K., Gaughan, L., Cook, S., Leung, H.Y., Neal, D.E. and Robson, C.N.**, 2004. Upregulation and nuclear recruitment of HDAC1 in hormone refractory prostate cancer, *Prostate*. 59, 177-189.

160. **Hall, J.A., Maitland, N.J., Stower, M. and Lang, S.H.**, 2002. Primary prostate stromal cells modulate the morphology and migration of primary prostate epithelial cells in type 1 collagen gels, *Cancer Res*. 62, 58-62.

161. **Hamburger, A.W. and Salmon, S.E.**, 1977. Primary bioassay of human tumor stem cells, *Science*. 197, 461-463.

162. **Hanahan, D. and Weinberg, R.A.**, 2011. Hallmarks of cancer: the next generation, *Cell*. 144, 646-674.

163. **Harris, R.A., Wang, T., Coarfa, C., Nagarajan, R.P., Hong, C., Downey, S.L., Johnson, B.E., Fouse, S.D., Delaney, A., Zhao, Y., Olshen, A., Ballinger, T., Zhou, X., Forsberg, K.J., Gu, J., Echipare, L., O'Geen, H., Lister, R., Pelizzola, M., Xi, Y., Epstein, C.B., Bernstein, B.E., Hawkins, R.D., Ren, B., Chung, W.Y., Gu, H., Bock, C., Gnirke, A., Zhang, M.Q., Haussler, D., Ecker, J.R., Li, W., Farnham, P.J., Waterland, R.A., Meissner, A., Marra, M.A., Hirst, M., Milosavljevic, A. and Costello, J.F.**, 2010. Comparison of sequencing-based methods to profile DNA methylation and identification of monoallelic epigenetic modifications, *Nat Biotechnol*. 28, 1097-1105.

164. **Harrison, D.E. and Lerner, C.P.**, 1991. Most primitive hematopoietic stem cells are stimulated to cycle rapidly after treatment with 5-fluorouracil, *Blood*. 78, 1237-1240.

165. **Hayward, S.W., Dahiya, R., Cunha, G.R., Bartek, J., Deshpande, N. and Narayan, P.**, 1995. Establishment and characterization of an immortalized but non-transformed human prostate epithelial cell line: BPH-1, *In Vitro Cell Dev Biol Anim*. 31, 14-24.

166. **He, X., Marchionni, L., Hansel, D.E., Yu, W., Sood, A., Yang, J., Parmigiani, G., Matsui, W. and Berman, D.M.**, 2009. Differentiation of a highly tumorigenic basal cell compartment in urothelial carcinoma, *Stem Cells*. 27, 1487-1495.

167. **He, Y.F., Li, B.Z., Li, Z., Liu, P., Wang, Y., Tang, Q., Ding, J., Jia, Y., Chen, Z., Li, L., Sun, Y., Li, X., Dai, Q., Song, C.X., Zhang, K., He, C. and Xu, G.L.**, 2011. Tet-mediated formation of 5-carboxylcytosine and its excision by TDG in mammalian DNA, *Science*. 333, 1303-1307.

168. **Hebbard, L., Cecena, G., Golas, J., Sawada, J., Ellies, L.G., Charbono, A., Williams, R., Jimenez, R.E., Wankell, M., Arndt, K.T., DeJoy, S.Q., Rollins, R.A., Diesl, V., Follettie, M., Chen, L., Rosfjord, E., Cardiff, R.D., Komatsu, M., Boschelli, F. and Oshima, R.G.**, 2011. Control of mammary tumor differentiation by SKI-606 (bosutinib), *Oncogene*. 30, 301-312.

169. **Heinlein, C.A. and Chang, C.**, 2004. Androgen receptor in prostate cancer, *Endocr Rev*. 25, 276-308.

170. **Henrique, R., Jeronimo, C., Teixeira, M.R., Hoque, M.O., Carvalho, A.L., Pais, I., Ribeiro, F.R., Oliveira, J., Lopes, C. and Sidransky, D.**, 2006. Epigenetic

heterogeneity of high-grade prostatic intraepithelial neoplasia: clues for clonal progression in prostate carcinogenesis, *Mol Cancer Res*. 4, 1-8.

171. **Herman, J.G., Graff, J.R., Myohanen, S., Nelkin, B.D. and Baylin, S.B.**, 1996. Methylation-specific PCR: a novel PCR assay for methylation status of CpG islands, *Proc Natl Acad Sci U S A*. 93, 9821-9826.

172. **Hermann, P.C., Huber, S.L., Herrler, T., Aicher, A., Ellwart, J.W., Guba, M., Bruns, C.J. and Heeschen, C.**, 2007. Distinct populations of cancer stem cells determine tumor growth and metastatic activity in human pancreatic cancer, *Cell Stem Cell*. 1, 313-323.

173. **Holliday, R. and Pugh, J.E.**, 1975. DNA modification mechanisms and gene activity during development, *Science*. 187, 226-232.

174. **Horoszewicz, J.S., Leong, S.S., Chu, T.M., Wajsman, Z.L., Friedman, M., Papsidero, L., Kim, U., Chai, L.S., Kakati, S., Arya, S.K. and Sandberg, A.A.**, 1980. The LNCaP cell line--a new model for studies on human prostatic carcinoma, *Prog Clin Biol Res*. 37, 115-132.

175. **Hsieh, J. and Gage, F.H.**, 2004. Epigenetic control of neural stem cell fate, *Curr Opin Genet Dev*. 14, 461-469.

176. **Hu, R., Dunn, T.A., Wei, S., Isharwal, S., Veltri, R.W., Humphreys, E., Han, M., Partin, A.W., Vessella, R.L., Isaacs, W.B., Bova, G.S. and Luo, J.**, 2009. Ligand-independent androgen receptor variants derived from splicing of cryptic exons signify hormone-refractory prostate cancer, *Cancer Res*. 69, 16-22.

177. **Huang, H., Reed, C.P., Zhang, J.S., Shridhar, V., Wang, L. and Smith, D.I.**, 1999. Carboxypeptidase A3 (CPA3): a novel gene highly induced by histone deacetylase inhibitors during differentiation of prostate epithelial cancer cells, *Cancer Res*. 59, 2981-2988.

178. **Huang, J., Bi, Y., Zhu, G.H., He, Y., Su, Y., He, B.C., Wang, Y., Kang, Q., Chen, L., Zuo, G.W., Luo, Q., Shi, Q., Zhang, B.Q., Huang, A., Zhou, L., Feng, T., Luu, H.H., Haydon, R.C., He, T.C. and Tang, N.**, 2009. Retinoic acid signalling induces the differentiation of mouse fetal liver-derived hepatic progenitor cells, *Liver Int*. 29, 1569-1581.

179. **Huang, J., Powell, W.C., Khodavirdi, A.C., Wu, J., Makita, T., Cardiff, R.D., Cohen, M.B., Sucov, H.M. and Roy-Burman, P.**, 2002. Prostatic intraepithelial neoplasia in mice with conditional disruption of the retinoid X receptor alpha allele in the prostate epithelium, *Cancer Res*. 62, 4812-4819.

180. **Huang, J., Yao, J.L., di Sant'Agnese, P.A., Yang, Q., Bourne, P.A. and Na, Y.**, 2006. Immunohistochemical characterization of neuroendocrine cells in prostate cancer, *Prostate*. 66, 1399-1406.

181. **Huang, L., Pu, Y., Alam, S., Birch, L. and Prins, G.S.**, 2004. Estrogenic regulation of signaling pathways and homeobox genes during rat prostate development, *J Androl*. 25, 330-337.

182. **Huang, Y., Pastor, W.A., Shen, Y., Tahiliani, M., Liu, D.R. and Rao, A.**, 2010. The behaviour of 5-hydroxymethylcytosine in bisulfite sequencing, *PLoS One*. 5, e8888.

183. **Hudson, D.L., Guy, A.T., Fry, P., O'Hare, M.J., Watt, F.M. and Masters, J.R.**, 2001. Epithelial cell differentiation pathways in the human prostate: identification of intermediate phenotypes by keratin expression, *J Histochem Cytochem*. 49, 271-278.

184. **Hudson, D.L., O'Hare, M., Watt, F.M. and Masters, J.R.**, 2000. Proliferative heterogeneity in the human prostate: evidence for epithelial stem cells, *Lab Invest*. 80, 1243-1250.

185. **Hudson, M.A., Bahnson, R.R. and Catalona, W.J.**, 1989. Clinical use of prostate specific antigen in patients with prostate cancer, *J Urol*. 142, 1011-1017.

186. **Huggins, C., Stevens, R.E. and Hodges, C.V.**, 1941. Studies On Prostatic Cancer. II. The Effects Of Castration On Advanced Carcinoma Of The Prostate Gland, *Archives of Surgery*. 43, 209-223.

187. **Hurt, E.M., Kawasaki, B.T., Klarmann, G.J., Thomas, S.B. and Farrar, W.L.**, 2008. CD44+ CD24(-) prostate cells are early cancer progenitor/stem cells that provide a model for patients with poor prognosis, *Br J Cancer*. 98, 756-765.

188. **Igel, T.C., Knight, M.K., Young, P.R., Wehle, M.J., Petrou, S.P., Broderick, G.A., Marino, R. and Parra, R.O.**, 2001. Systematic transperineal ultrasound guided template biopsy of the prostate in patients at high risk, *J Urol*. 165, 1575-1579.

189. **Isaacs, J.T. and Coffey, D.S.**, 1989. Etiology and disease process of benign prostatic hyperplasia, *Prostate Suppl*. 2, 33-50.

190. **Ito, S., Shen, L., Dai, Q., Wu, S.C., Collins, L.B., Swenberg, J.A., He, C. and Zhang, Y.**, 2011a. Tet proteins can convert 5-methylcytosine to 5-formylcytosine and 5-carboxylcytosine, *Science*. 333, 1300-1303.

191. **Ito, T., Williams-Nate, Y., Iwai, M., Tsuboi, Y., Hagiyama, M., Ito, A., Sakurai-Yageta, M. and Murakami, Y.**, 2011b. Transcriptional regulation of the CADM1 gene by retinoic acid during the neural differentiation of murine embryonal carcinoma P19 cells, *Genes Cells*. 16, 791-802.

192. **Iversen, P., Tyrrell, C.J., Kaisary, A.V., Anderson, J.B., Van Poppel, H., Tammela, T.L., Chamberlain, M., Carroll, K. and Melezinek, I.**, 2000. Bicalutamide monotherapy compared with castration in patients with nonmetastatic locally advanced prostate cancer: 6.3 years of followup, *J Urol*. 164, 1579-1582.

193. **Izadpanah, R., Kaushal, D., Kriedt, C., Tsien, F., Patel, B., Dufour, J. and Bunnell, B.A.**, 2008. Long-term in vitro expansion alters the biology of adult mesenchymal stem cells, *Cancer Res*. 68, 4229-4238.

194. **Jaenisch, R. and Bird, A.**, 2003. Epigenetic regulation of gene expression: how the genome integrates intrinsic and environmental signals, *Nat Genet*. 33 Suppl, 245-254.

195. **Jarvik, J.W. and Telmer, C.A.**, 1998. Epitope tagging, *Annu Rev Genet*. 32, 601-618.

196. **Jenuwein, T. and Allis, C.D.**, 2001. Translating the histone code, *Science*. 293, 1074-1080.

197. **Jeronimo, C., Bastian, P.J., Bjartell, A., Carbone, G.M., Catto, J.W., Clark, S.J., Henrique, R., Nelson, W.G. and Shariat, S.F.**, 2011. Epigenetics in prostate cancer: biologic and clinical relevance, *Eur Urol*. 60, 753-766.

198. **Jiborn, T., Bjartell, A. and Abrahamsson, P.A.**, 1998. Neuroendocrine differentiation in prostatic carcinoma during hormonal treatment, *Urology*. 51, 585-589.

199. **Jin, M., Ishida, M., Katoh-Fukui, Y., Tsuchiya, R., Higashinakagawa, T., Ikegami, S. and Arimatsu, Y.**, 2006. Reduced pain sensitivity in mice lacking latexin, an inhibitor of metallocarboxypeptidases, *Brain Res*. 1075, 117-121.

200. **Jing, C., El-Ghany, M.A., Beesley, C., Foster, C.S., Rudland, P.S., Smith, P. and Ke, Y.**, 2002. Tazarotene-induced gene 1 (TIG1) expression in prostate carcinomas and its relationship to tumorigenicity, *J Natl Cancer Inst*. 94, 482-490.

201. **Jones, P.A.**, 2012. Functions of DNA methylation: islands, start sites, gene bodies and beyond, *Nat Rev Genet*. 13, 484-492.

202. **Jones, P.A. and Baylin, S.B.**, 2007. The epigenomics of cancer, *Cell*. 128, 683-692.

203. **Jones, P.A. and Liang, G.**, 2009. Rethinking how DNA methylation patterns are maintained, *Nat Rev Genet*. 10, 805-811.

204. **Jones, P.A. and Taylor, S.M.**, 1980. Cellular differentiation, cytidine analogs and DNA methylation, *Cell*. 20, 85-93.

205. **Jones, P.A., Wolkowicz, M.J., Rideout, W.M., 3rd, Gonzales, F.A., Marziasz, C.M., Coetzee, G.A. and Tapscott, S.J.**, 1990. De novo methylation of the MyoD1 CpG island during the establishment of immortal cell lines, *Proc Natl Acad Sci U S A*. 87, 6117-6121.

206. **Kadmon, D., Thompson, T.C., Lynch, G.R. and Scardino, P.T.**, 1991. Elevated plasma chromogranin-A concentrations in prostatic carcinoma, *J Urol*. 146, 358-361.

207. **Kadouchi, I., Sakamoto, K., Tangjiao, L., Murakami, T., Kobayashi, E., Hoshino, Y. and Yamaguchi, A.**, 2009. Latexin is involved in bone morphogenetic protein-2-induced chondrocyte differentiation, *Biochem Biophys Res Commun*. 378, 600-604.

208. **Kahl, P., Gullotti, L., Heukamp, L.C., Wolf, S., Friedrichs, N., Vorreuther, R., Solleder, G., Bastian, P.J., Ellinger, J., Metzger, E., Schule, R. and Buettner, R.**, 2006. Androgen receptor coactivators lysine-specific histone demethylase 1 and four and a half LIM domain protein 2 predict risk of prostate cancer recurrence, *Cancer Res*. 66, 11341-11347.

209. **Kaighn, M.E., Narayan, K.S., Ohnuki, Y., Lechner, J.F. and Jones, L.W.**, 1979. Establishment and characterization of a human prostatic carcinoma cell line (PC-3), *Invest Urol*. 17, 16-23.

210. **Kang, G.H., Lee, S., Lee, H.J. and Hwang, K.S.**, 2004. Aberrant CpG island hypermethylation of multiple genes in prostate cancer and prostatic intraepithelial neoplasia, *J Pathol*. 202, 233-240.

211. **Karakida, T., Yui, R., Suzuki, T., Fukae, M. and Oida, S.**, 2011. Retinoic acid receptor gamma-dependent signaling cooperates with BMP2 to induce osteoblastic differentiation of C2C12 cells, *Connect Tissue Res*. 52, 365-372.

212. **Karhadkar, S.S., Bova, G.S., Abdallah, N., Dhara, S., Gardner, D., Maitra, A., Isaacs, J.T., Berman, D.M. and Beachy, P.A.**, 2004. Hedgehog signalling in prostate regeneration, neoplasia and metastasis, *Nature*. 431, 707-712.

213. **Kasper, S., Sheppard, P.C., Yan, Y., Pettigrew, N., Borowsky, A.D., Prins, G.S., Dodd, J.G., Duckworth, M.L. and Matusik, R.J.**, 1998. Development, progression, and androgen-dependence of prostate tumors in probasin-large T antigen transgenic mice: a model for prostate cancer, *Lab Invest*. 78, 319-333.

214. **Kastner, P., Mark, M., Ghyselinck, N., Krezel, W., Dupe, V., Grondona, J.M. and Chambon, P.**, 1997. Genetic evidence that the retinoid signal is transduced by heterodimeric RXR/RAR functional units during mouse development, *Development*. 124, 313-326.

215. **Kawai, J., Hirose, K., Fushiki, S., Hirotsune, S., Ozawa, N., Hara, A., Hayashizaki, Y. and Watanabe, S.**, 1994. Comparison of DNA methylation patterns among mouse cell lines by restriction landmark genomic scanning, *Mol Cell Biol*. 14, 7421-7427.

216. **Kayashima, T., Yamasaki, K., Yamada, T., Sakai, H., Miwa, N., Ohta, T., Yoshiura, K., Matsumoto, N., Nakane, Y., Kanetake, H., Ishino, F., Niikawa, N. and Kishino, T.**, 2003. The novel imprinted carboxypeptidase A4 gene (CPA4) in the 7q32 imprinting domain, *Hum Genet*. 112, 220-226.

217. **Kellokumpu-Lehtinen, P., Santti, R. and Pelliniemi, L.J.**, 1979. Early cytodifferentiation of human prostatic urethra and Leydig cells, *Anat Rec*. 194, 429-443.

218. **Kellokumpu-Lehtinen, P., Santti, R.S. and Pelliniemi, L.J.**, 1981. Development of human fetal prostate in culture, *Urol Res*. 9, 89-98.

219. **Kelly, K. and Yin, J.J.**, 2008. Prostate cancer and metastasis initiating stem cells, *Cell Res*. 18, 528-537.

220. **Khawaja, S., Gundersen, G.G. and Bulinski, J.C.**, 1988. Enhanced stability of microtubules enriched in detyrosinated tubulin is not a direct function of detyrosination level, *J Cell Biol*. 106, 141-149.

221. **Kim, M., Turnquist, H., Jackson, J., Sgagias, M., Yan, Y., Gong, M., Dean, M., Sharp, J.G. and Cowan, K.**, 2002. The multidrug resistance transporter ABCG2 (breast cancer resistance protein 1) effluxes Hoechst 33342 and is overexpressed in hematopoietic stem cells, *Clin Cancer Res*. 8, 22-28.

222. **Kito, H., Suzuki, H., Ichikawa, T., Sekita, N., Kamiya, N., Akakura, K., Igarashi, T., Nakayama, T., Watanabe, M., Harigaya, K. and Ito, H.**, 2001. Hypermethylation of the CD44 gene is associated with progression and metastasis of human prostate cancer, *Prostate*. 49, 110-115.

223. **Klose, R.J. and Bird, A.P.**, 2006. Genomic DNA methylation: the mark and its mediators, *Trends Biochem Sci*. 31, 89-97.

224. **Kloth, M., Goering, W., Ribarska, T., Arsov, C., Sorensen, K.D. and Schulz, W.A.**, 2012. The SNP rs6441224 influences transcriptional activity and prognostically relevant hypermethylation of RARRES1 in prostate cancer, *Int J Cancer*. 131, E897-904.

225. **Klymkowsky, M.W. and Savagner, P.**, 2009. Epithelial-mesenchymal transition: a cancer researcher's conceptual friend and foe, *Am J Pathol*. 174, 1588-1593.

226. **Koivisto, P., Kononen, J., Palmberg, C., Tammela, T., Hyytinen, E., Isola, J., Trapman, J., Cleutjens, K., Noordzij, A., Visakorpi, T. and Kallioniemi, O.P.**, 1997. Androgen receptor gene amplification: a possible molecular mechanism for androgen deprivation therapy failure in prostate cancer, *Cancer Res*. 57, 314-319.

227. **Kong, D., Banerjee, S., Ahmad, A., Li, Y., Wang, Z., Sethi, S. and Sarkar, F.H.**, 2010. Epithelial to mesenchymal transition is mechanistically linked with stem cell signatures in prostate cancer cells, *PLoS One*. 5, e12445.

228. **Konishi, Y. and Setou, M.**, 2009. Tubulin tyrosination navigates the kinesin-1 motor domain to axons, *Nat Neurosci*. 12, 559-567.

229. **Korenchuk, S., Lehr, J.E., L, M.C., Lee, Y.G., Whitney, S., Vessella, R., Lin, D.L. and Pienta, K.J.**, 2001. VCaP, a cell-based model system of human prostate cancer, *In Vivo*. 15, 163-168.

230. **Korsten, H., Ziel-van der Made, A., Ma, X., van der Kwast, T. and Trapman, J.**, 2009. Accumulating progenitor cells in the luminal epithelial cell layer are candidate tumor initiating cells in a Pten knockout mouse prostate cancer model, *PLoS One*. 4, e5662.

231. **Kramer, G. and Marberger, M.**, 2006. Could inflammation be a key component in the progression of benign prostatic hyperplasia?, *Curr Opin Urol*. 16, 25-29.

232. **Kramer, G., Mitteregger, D. and Marberger, M.**, 2007. Is benign prostatic hyperplasia (BPH) an immune inflammatory disease?, *Eur Urol*. 51, 1202-1216.

233. **Krieger, J.N.**, 2004. Classification, epidemiology and implications of chronic prostatitis in North America, Europe and Asia, *Minerva Urol Nefrol*. 56, 99-107.

234. **Kronz, J.D., Allan, C.H., Shaikh, A.A. and Epstein, J.I.**, 2001. Predicting cancer following a diagnosis of high-grade prostatic intraepithelial neoplasia on needle biopsy: data on men with more than one follow-up biopsy, *Am J Surg Pathol*. 25, 1079-1085.

235. **Kwok, W.K., Pang, J.C., Lo, K.W. and Ng, H.K.**, 2009. Role of the RARRES1 gene in nasopharyngeal carcinoma, *Cancer Genet Cytogenet*. 194, 58-64.

236. **Kwong, J., Lo, K.W., Chow, L.S., Chan, F.L., To, K.F. and Huang, D.P.**, 2005. Silencing of the retinoid response gene TIG1 by promoter hypermethylation in nasopharyngeal carcinoma, *Int J Cancer*. 113, 386-392.

237. **Kyprianou, N. and Isaacs, J.T.**, 1988. Activation of programmed cell death in the rat ventral prostate after castration, *Endocrinology*. 122, 552-562.

238. **Labrie, F., Dupont, A., Cusan, L., Gomez, J., Emond, J. and Monfette, G.**, 1990. Combination therapy with flutamide and medical (LHRH agonist) or surgical castration in advanced prostate cancer: 7-year clinical experience, *J Steroid Biochem Mol Biol*. 37, 943-950.

239. **Lafanechere, L., Courtay-Cahen, C., Kawakami, T., Jacrot, M., Rudiger, M., Wehland, J., Job, D. and Margolis, R.L.**, 1998. Suppression of tubulin tyrosine ligase during tumor growth, *J Cell Sci*. 111 (Pt 2), 171-181.

240. **Lan, L., Cui, D., Luo, Y., Shi, B.Y., Deng, L.L., Zhang, G.Y. and Wang, H.**, 2009. Inhibitory effects of retinoic acid on invasiveness of human thyroid carcinoma cell lines in vitro, *J Endocrinol Invest*. 32, 731-738.

241. **Lane, M.A., Xu, J., Wilen, E.W., Sylvester, R., Derguini, F. and Gudas, L.J.**, 2008. LIF removal increases CRABPI and CRABPII transcripts in embryonic stem cells cultured in retinol or 4-oxoretinol, *Mol Cell Endocrinol*. 280, 63-74.

242. **Lang, S.H., Stark, M., Collins, A., Paul, A.B., Stower, M.J. and Maitland, N.J.**, 2001. Experimental prostate epithelial morphogenesis in response to stroma and three-dimensional matrigel culture, *Cell Growth Differ*. 12, 631-640.

243. **Langer, J.E., Rovner, E.S., Coleman, B.G., Yin, D., Arger, P.H., Malkowicz, S.B., Nisenbaum, H.L., Rowling, S.E., Tomaszewski, J.E., Wein, A.J. and Jacobs, J.E.**, 1996. Strategy for repeat biopsy of patients with prostatic intraepithelial neoplasia detected by prostate needle biopsy, *J Urol*. 155, 228-231.

244. **Latil, A., Baron, J.C., Cussenot, O., Fournier, G., Soussi, T., Boccon-Gibod, L., Le Duc, A., Rouesse, J. and Lidereau, R.**, 1994. Genetic alterations in localized prostate cancer: identification of a common region of deletion on chromosome arm 18q, *Genes Chromosomes Cancer*. 11, 119-125.

245. **Latil, A., Cussenot, O., Fournier, G., Driouch, K. and Lidereau, R.**, 1997. Loss of heterozygosity at chromosome 16q in prostate adenocarcinoma: identification of three independent regions, *Cancer Res*. 57, 1058-1062.

246. **Lee, J., Kotliarova, S., Kotliarov, Y., Li, A., Su, Q., Donin, N.M., Pastorino, S., Purow, B.W., Christopher, N., Zhang, W., Park, J.K. and Fine, H.A.**, 2006. Tumor stem cells derived from glioblastomas cultured in bFGF and EGF more closely mirror the phenotype and genotype of primary tumors than do serum-cultured cell lines, *Cancer Cell*. 9, 391-403.

247. **Lee, K.L. and Peehl, D.M.**, 2004. Molecular and cellular pathogenesis of benign prostatic hyperplasia, *J Urol*. 172, 1784-1791.

248. **Lee, W.H., Morton, R.A., Epstein, J.I., Brooks, J.D., Campbell, P.A., Bova, G.S., Hsieh, W.S., Isaacs, W.B. and Nelson, W.G.**, 1994. Cytidine methylation of regulatory sequences near the pi-class glutathione S-transferase gene accompanies human prostatic carcinogenesis, *Proc Natl Acad Sci U S A*. 91, 11733-11737.

249. **Leid, M., Kastner, P. and Chambon, P.**, 1992. Multiplicity generates diversity in the retinoic acid signalling pathways, *Trends Biochem Sci*. 17, 427-433.

250. **Leong, K.G. and Gao, W.Q.**, 2008. The Notch pathway in prostate development and cancer, *Differentiation*. 76, 699-716.

251. **Leong, K.G., Wang, B.E., Johnson, L. and Gao, W.Q.**, 2008. Generation of a prostate from a single adult stem cell, *Nature*. 456, 804-808.

252. **Lewis, E.B.**, 1978. A gene complex controlling segmentation in Drosophila, *Nature*. 276, 565-570.

253. **Li, C., Heidt, D.G., Dalerba, P., Burant, C.F., Zhang, L., Adsay, V., Wicha, M., Clarke, M.F. and Simeone, D.M.**, 2007. Identification of pancreatic cancer stem cells, *Cancer Res*. 67, 1030-1037.

254. **Li, E., Bestor, T.H. and Jaenisch, R.**, 1992. Targeted mutation of the DNA methyltransferase gene results in embryonic lethality, *Cell*. 69, 915-926.

255. **Li, J., Yen, C., Liaw, D., Podsypanina, K., Bose, S., Wang, S.I., Puc, J., Miliaresis, C., Rodgers, L., McCombie, R., Bigner, S.H., Giovanella, B.C., Ittmann, M., Tycko, B., Hibshoosh, H., Wigler, M.H. and Parsons, R.**, 1997. PTEN, a putative protein tyrosine phosphatase gene mutated in human brain, breast, and prostate cancer, *Science*. 275, 1943-1947.

256. **Li, X., Wang, X., He, K., Ma, Y., Su, N., He, H., Stolc, V., Tongprasit, W., Jin, W., Jiang, J., Terzaghi, W., Li, S. and Deng, X.W.**, 2008. High-resolution mapping of epigenetic modifications of the rice genome uncovers interplay between DNA methylation, histone methylation, and gene expression, *Plant Cell*. 20, 259-276.

257. **Li, Y., Basang, Z., Ding, H., Lu, Z., Ning, T., Wei, H., Cai, H. and Ke, Y.**, 2011. Latexin expression is downregulated in human gastric carcinomas and exhibits tumor suppressor potential, *BMC Cancer*. 11, 121.

258. **Liang, Y., Jansen, M., Aronow, B., Geiger, H. and Van Zant, G.**, 2007. The quantitative trait gene latexin influences the size of the hematopoietic stem cell population in mice, *Nat Genet*. 39, 178-188.

259. **Liang, Y. and Van Zant, G.**, 2008. Aging stem cells, latexin, and longevity, *Exp Cell Res*. 314, 1962-1972.

260. **Liao, C.P., Adisetiyo, H., Liang, M. and Roy-Burman, P.**, 2010. Cancer-associated fibroblasts enhance the gland-forming capability of prostate cancer stem cells, *Cancer Res*. 70, 7294-7303.

261. **Lilja, H.**, 1985. A kallikrein-like serine protease in prostatic fluid cleaves the predominant seminal vesicle protein, *J Clin Invest*. 76, 1899-1903.

262. **Lilja, H., Ulmert, D. and Vickers, A.J.**, 2008. Prostate-specific antigen and prostate cancer: prediction, detection and monitoring, *Nat Rev Cancer*. 8, 268-278.

263. **Linja, M.J., Savinainen, K.J., Saramaki, O.R., Tammela, T.L., Vessella, R.L. and Visakorpi, T.**, 2001. Amplification and overexpression of androgen receptor gene in hormone-refractory prostate cancer, *Cancer Res*. 61, 3550-3555.

264. **Liu, A.Y., True, L.D., LaTray, L., Nelson, P.S., Ellis, W.J., Vessella, R.L., Lange, P.H., Hood, L. and van den Engh, G.**, 1997. Cell-cell interaction in prostate gene regulation and cytodifferentiation, *Proc Natl Acad Sci U S A*. 94, 10705-10710.

265. **Liu, C., Kelnar, K., Liu, B., Chen, X., Calhoun-Davis, T., Li, H., Patrawala, L., Yan, H., Jeter, C., Honorio, S., Wiggins, J.F., Bader, A.G., Fagin, R., Brown, D. and Tang, D.G.**, 2011a. The microRNA miR-34a inhibits prostate cancer stem cells and metastasis by directly repressing CD44, *Nat Med*. 17, 211-215.

266.	**Liu, G., Yuan, X., Zeng, Z., Tunici, P., Ng, H., Abdulkadir, I.R., Lu, L., Irvin, D., Black, K.L. and Yu, J.S.**, 2006a. Analysis of gene expression and chemoresistance of CD133+ cancer stem cells in glioblastoma, *Mol Cancer*. 5, 67.

267.	**Liu, L., Yoon, J.H., Dammann, R. and Pfeifer, G.P.**, 2002. Frequent hypermethylation of the RASSF1A gene in prostate cancer, *Oncogene*. 21, 6835-6840.

268.	**Liu, Q., Yu, L., Gao, J., Fu, Q., Zhang, J., Zhang, P., Chen, J. and Zhao, S.**, 2000. Cloning, tissue expression pattern and genomic organization of latexin, a human homologue of rat carboxypeptidase A inhibitor, *Mol Biol Rep*. 27, 241-246.

269.	**Liu, S., Dontu, G., Mantle, I.D., Patel, S., Ahn, N.S., Jackson, K.W., Suri, P. and Wicha, M.S.**, 2006b. Hedgehog signaling and Bmi-1 regulate self-renewal of normal and malignant human mammary stem cells, *Cancer Res*. 66, 6063-6071.

270.	**Liu, Z., Turkoz, A., Jackson, E.N., Corbo, J.C., Engelbach, J.A., Garbow, J.R., Piwnica-Worms, D.R. and Kopan, R.**, 2011b. Notch1 loss of heterozygosity causes vascular tumors and lethal hemorrhage in mice, *J Clin Invest*. 121, 800-808.

271.	**Lohnes, D., Mark, M., Mendelsohn, C., Dolle, P., Decimo, D., LeMeur, M., Dierich, A., Gorry, P. and Chambon, P.**, 1995. Developmental roles of the retinoic acid receptors, *J Steroid Biochem Mol Biol*. 53, 475-486.

272.	**Lotan, R.**, 1991. Retinoids as modulators of tumor cells invasion and metastasis, *Semin Cancer Biol*. 2, 197-208.

273.	**Lou, W., Krill, D., Dhir, R., Becich, M.J., Dong, J.T., Frierson, H.F., Jr., Isaacs, W.B., Isaacs, J.T. and Gao, A.C.**, 1999. Methylation of the CD44 metastasis suppressor gene in human prostate cancer, *Cancer Res*. 59, 2329-2331.

274.	**Lu, W., Tinsley, H.N., Keeton, A., Qu, Z., Piazza, G.A. and Li, Y.**, 2009. Suppression of Wnt/beta-catenin signaling inhibits prostate cancer cell proliferation, *Eur J Pharmacol*. 602, 8-14.

275.	**Lukacs, R.U., Memarzadeh, S., Wu, H. and Witte, O.N.**, 2010. Bmi-1 is a crucial regulator of prostate stem cell self-renewal and malignant transformation, *Cell Stem Cell*. 7, 682-693.

276.	**Luo, P., Wang, A., Payne, K.J., Peng, H., Wang, J.G., Parrish, Y.K., Rogerio, J.W., Triche, T.J., He, Q. and Wu, L.**, 2007. Intrinsic retinoic acid receptor alpha-cyclin-dependent kinase-activating kinase signaling involves coordination of the restricted proliferation and granulocytic differentiation of human hematopoietic stem cells, *Stem Cells*. 25, 2628-2637.

277.	**Luzi, E., Marini, F., Sala, S.C., Tognarini, I., Galli, G. and Brandi, M.L.**, 2008. Osteogenic differentiation of human adipose tissue-derived stem cells is modulated by the miR-26a targeting of the SMAD1 transcription factor, *J Bone Miner Res*. 23, 287-295.

278.	**Lynes, E.M. and Simmen, T.**, 2011. Urban planning of the endoplasmic reticulum (ER): how diverse mechanisms segregate the many functions of the ER, *Biochim Biophys Acta*. 1813, 1893-1905.

279. **Ma, S., Chan, K.W., Hu, L., Lee, T.K., Wo, J.Y., Ng, I.O., Zheng, B.J. and Guan, X.Y.**, 2007. Identification and characterization of tumorigenic liver cancer stem/progenitor cells, *Gastroenterology*. 132, 2542-2556.

280. **Ma, S., Lee, T.K., Zheng, B.J., Chan, K.W. and Guan, X.Y.**, 2008. CD133+ HCC cancer stem cells confer chemoresistance by preferential expression of the Akt/PKB survival pathway, *Oncogene*. 27, 1749-1758.

281. **Ma, X., Ziel-van der Made, A.C., Autar, B., van der Korput, H.A., Vermeij, M., van Duijn, P., Cleutjens, K.B., de Krijger, R., Krimpenfort, P., Berns, A., van der Kwast, T.H. and Trapman, J.**, 2005. Targeted biallelic inactivation of Pten in the mouse prostate leads to prostate cancer accompanied by increased epithelial cell proliferation but not by reduced apoptosis, *Cancer Res*. 65, 5730-5739.

282. **Macintosh, C.A., Stower, M., Reid, N. and Maitland, N.J.**, 1998. Precise microdissection of human prostate cancers reveals genotypic heterogeneity, *Cancer Res*. 58, 23-28.

283. **Maden, M.**, 2002. Retinoid signalling in the development of the central nervous system, *Nat Rev Neurosci*. 3, 843-853.

284. **Maitland, N.J., Frame, F.M., Polson, E.S., Lewis, J.L. and Collins, A.T.**, 2011a. Prostate cancer stem cells: do they have a basal or luminal phenotype?, *Horm Cancer*. 2, 47-61.

285. **Maitland, N.J., Frame, F.M., Polson, E.S., Lewis, J.L. and Collins, A.T.**, 2011b. Prostate Cancer Stem Cells: Do They Have a Basal or Luminal Phenotype? , *Hormones and Cancer*. 2, 47-61.

286. **Maitland, N.J., Macintosh, C.A., Hall, J., Sharrard, M., Quinn, G. and Lang, S.**, 2001. In vitro models to study cellular differentiation and function in human prostate cancers, *Radiat Res*. 155, 133-142.

287. **Malanchi, I., Santamaria-Martinez, A., Susanto, E., Peng, H., Lehr, H.A., Delaloye, J.F. and Huelsken, J.**, 2012. Interactions between cancer stem cells and their niche govern metastatic colonization, *Nature*. 481, 85-89.

288. **Mani, S.A., Guo, W., Liao, M.J., Eaton, E.N., Ayyanan, A., Zhou, A.Y., Brooks, M., Reinhard, F., Zhang, C.C., Shipitsin, M., Campbell, L.L., Polyak, K., Brisken, C., Yang, J. and Weinberg, R.A.**, 2008. The epithelial-mesenchymal transition generates cells with properties of stem cells, *Cell*. 133, 704-715.

289. **Marques, R.B., van Weerden, W.M., Erkens-Schulze, S., de Ridder, C.M., Bangma, C.H., Trapman, J. and Jenster, G.**, 2006. The human PC346 xenograft and cell line panel: a model system for prostate cancer progression, *Eur Urol*. 49, 245-257.

290. **Marshall, J.R., Tangen, C.M., Sakr, W.A., Wood, D.P., Jr., Berry, D.L., Klein, E.A., Lippman, S.M., Parnes, H.L., Alberts, D.S., Jarrard, D.F., Lee, W.R., Gaziano, J.M., Crawford, E.D., Ely, B., Ray, M., Davis, W., Minasian, L.M. and Thompson, I.M., Jr.**, 2011. Phase III trial of selenium to prevent prostate cancer in men with high-grade prostatic intraepithelial neoplasia: SWOG S9917, *Cancer Prev Res (Phila)*. 4, 1761-1769.

291. **Maruyama, R., Toyooka, S., Toyooka, K.O., Virmani, A.K., Zochbauer-Muller, S., Farinas, A.J., Minna, J.D., McConnell, J., Frenkel, E.P. and Gazdar, A.F.**, 2002. Aberrant promoter methylation profile of prostate cancers and its relationship to clinicopathological features, *Clin Cancer Res*. 8, 514-519.

292. **Matsui, W., Huff, C.A., Wang, Q., Malehorn, M.T., Barber, J., Tanhehco, Y., Smith, B.D., Civin, C.I. and Jones, R.J.**, 2004. Characterization of clonogenic multiple myeloma cells, *Blood*. 103, 2332-2336.

293. **Matt, N., Dupe, V., Garnier, J.M., Dennefeld, C., Chambon, P., Mark, M. and Ghyselinck, N.B.**, 2005. Retinoic acid-dependent eye morphogenesis is orchestrated by neural crest cells, *Development*. 132, 4789-4800.

294. **McKenna, N.J. and O'Malley, B.W.**, 2002. Combinatorial control of gene expression by nuclear receptors and coregulators, *Cell*. 108, 465-474.

295. **McNeal, J.E.**, 1981. The zonal anatomy of the prostate, *Prostate*. 2, 35-49.

296. **Meissner, A., Mikkelsen, T.S., Gu, H., Wernig, M., Hanna, J., Sivachenko, A., Zhang, X., Bernstein, B.E., Nusbaum, C., Jaffe, D.B., Gnirke, A., Jaenisch, R. and Lander, E.S.**, 2008. Genome-scale DNA methylation maps of pluripotent and differentiated cells, *Nature*. 454, 766-770.

297. **Melton, C., Judson, R.L. and Blelloch, R.**, 2010. Opposing microRNA families regulate self-renewal in mouse embryonic stem cells, *Nature*. 463, 621-626.

298. **Messi, E., Florian, M.C., Caccia, C., Zanisi, M. and Maggi, R.**, 2008. Retinoic acid reduces human neuroblastoma cell migration and invasiveness: effects on DCX, LIS1, neurofilaments-68 and vimentin expression, *BMC Cancer*. 8, 30.

299. **Metzger, E., Wissmann, M., Yin, N., Muller, J.M., Schneider, R., Peters, A.H., Gunther, T., Buettner, R. and Schule, R.**, 2005. LSD1 demethylates repressive histone marks to promote androgen-receptor-dependent transcription, *Nature*. 437, 436-439.

300. **Mialhe, A., Lafanechere, L., Treilleux, I., Peloux, N., Dumontet, C., Bremond, A., Panh, M.H., Payan, R., Wehland, J., Margolis, R.L. and Job, D.**, 2001. Tubulin detyrosination is a frequent occurrence in breast cancers of poor prognosis, *Cancer Res*. 61, 5024-5027.

301. **Miki, J., Furusato, B., Li, H., Gu, Y., Takahashi, H., Egawa, S., Sesterhenn, I.A., McLeod, D.G., Srivastava, S. and Rhim, J.S.**, 2007. Identification of putative stem cell markers, CD133 and CXCR4, in hTERT-immortalized primary nonmalignant and malignant tumor-derived human prostate epithelial cell lines and in prostate cancer specimens, *Cancer Res*. 67, 3153-3161.

302. **Miller, S.J., Lavker, R.M. and Sun, T.-T.**, 2005a. Interpreting epithelial cancer biology in the context of stem cells: tumor properties and therapeutic implications, *Biochim Biophys Acta*. 1756, 25-52.

303. **Miller, S.J., Lavker, R.M. and Sun, T.T.**, 2005b. Interpreting epithelial cancer biology in the context of stem cells: tumor properties and therapeutic implications, *Biochim Biophys Acta*. 1756, 25-52.

304. **Minucci, S. and Pelicci, P.G.**, 2006. Histone deacetylase inhibitors and the promise of epigenetic (and more) treatments for cancer, *Nat Rev Cancer*. 6, 38-51.

305. **Mitsunaga, K., Kikuchi, J., Wada, T. and Furukawa, Y.**, 2011. Latexin regulates the abundance of multiple cellular proteins in hematopoietic stem cells., *Journal of cellular physiology.*

306. **Mizuiri, H., Yoshida, K., Toge, T., Oue, N., Aung, P.P., Noguchi, T. and Yasui, W.**, 2005. DNA methylation of genes linked to retinoid signaling in squamous cell carcinoma of the esophagus: DNA methylation of CRBP1 and TIG1 is associated with tumor stage, *Cancer Sci*. 96, 571-577.

307. **Mizuno, Y., Yagi, K., Tokuzawa, Y., Kanesaki-Yatsuka, Y., Suda, T., Katagiri, T., Fukuda, T., Maruyama, M., Okuda, A., Amemiya, T., Kondoh, Y., Tashiro, H. and Okazaki, Y.**, 2008. miR-125b inhibits osteoblastic differentiation by down-regulation of cell proliferation, *Biochem Biophys Res Commun*. 368, 267-272.

308. **Molofsky, A.V., Pardal, R., Iwashita, T., Park, I.K., Clarke, M.F. and Morrison, S.J.**, 2003. Bmi-1 dependence distinguishes neural stem cell self-renewal from progenitor proliferation, *Nature*. 425, 962-967.

309. **Moore, K.A. and Lemischka, I.R.**, 2006. Stem cells and their niches, *Science*. 311, 1880-1885.

310. **Morel, A.P., Lievre, M., Thomas, C., Hinkal, G., Ansieau, S. and Puisieux, A.**, 2008. Generation of breast cancer stem cells through epithelial-mesenchymal transition, *PLoS One*. 3, e2888.

311. **Morote, J., Trilla, E., Esquena, S., Serrallach, F., Abascal, J.M., Munoz, A., Id M'Hammed, Y. and de Torres, I.M.**, 2002. The percentage of free prostatic-specific antigen is also useful in men with normal digital rectal examination and serum prostatic-specific antigen between 10.1 and 20 ng/ml, *Eur Urol*. 42, 333-337.

312. **Morrison, S.J. and Kimble, J.**, 2006. Asymmetric and symmetric stem-cell divisions in development and cancer, *Nature*. 441, 1068-1074.

313. **Moskaluk, C.A., Duray, P.H., Cowan, K.H., Linehan, M. and Merino, M.J.**, 1997. Immunohistochemical expression of pi-class glutathione S-transferase is down-regulated in adenocarcinoma of the prostate, *Cancer*. 79, 1595-1599.

314. **Muindi, J.R., Frankel, S.R., Huselton, C., DeGrazia, F., Garland, W.A., Young, C.W. and Warrell, R.P., Jr.**, 1992. Clinical pharmacology of oral all-trans retinoic acid in patients with acute promyelocytic leukemia, *Cancer Res*. 52, 2138-2142.

315. **Murant, S.J., Rolley, N., Phillips, S.M., Stower, M. and Maitland, N.J.**, 2000. Allelic imbalance within the E-cadherin gene is an infrequent event in prostate carcinogenesis, *Genes Chromosomes Cancer*. 27, 104-109.

316. **Muthusamy, V., Duraisamy, S., Bradbury, C.M., Hobbs, C., Curley, D.P., Nelson, B. and Bosenberg, M.**, 2006. Epigenetic silencing of novel tumor suppressors in malignant melanoma, *Cancer Res*. 66, 11187-11193.

317. **Nagle, R.B., Ahmann, F.R., McDaniel, K.M., Paquin, M.L., Clark, V.A. and Celniker, A.**, 1987. Cytokeratin characterization of human prostatic carcinoma and its derived cell lines, *Cancer Res*. 47, 281-286.

318. **Nagpal, S., Patel, S., Asano, A.T., Johnson, A.T., Duvic, M. and Chandraratna, R.A.**, 1996. Tazarotene-induced gene 1 (TIG1), a novel retinoic acid receptor-responsive gene in skin, *J Invest Dermatol*. 106, 269-274.

319. **Nagrath, S., Sequist, L.V., Maheswaran, S., Bell, D.W., Irimia, D., Ulkus, L., Smith, M.R., Kwak, E.L., Digumarthy, S., Muzikansky, A., Ryan, P., Balis, U.J., Tompkins, R.G., Haber, D.A. and Toner, M.**, 2007. Isolation of rare circulating tumour cells in cancer patients by microchip technology, *Nature*. 450, 1235-1239.

320. **Nakajima, M., Lotan, D., Baig, M.M., Carralero, R.M., Wood, W.R., Hendrix, M.J. and Lotan, R.**, 1989. Inhibition by retinoic acid of type IV collagenolysis and invasion through reconstituted basement membrane by metastatic rat mammary adenocarcinoma cells, *Cancer Res*. 49, 1698-1706.

321. **Nakayama, M., Bennett, C.J., Hicks, J.L., Epstein, J.I., Platz, E.A., Nelson, W.G. and De Marzo, A.M.**, 2003. Hypermethylation of the human glutathione S-transferase-pi gene (GSTP1) CpG island is present in a subset of proliferative inflammatory atrophy lesions but not in normal or hyperplastic epithelium of the prostate: a detailed study using laser-capture microdissection, *Am J Pathol*. 163, 923-933.

322. **Nakayama, M., Gonzalgo, M.L., Yegnasubramanian, S., Lin, X., De Marzo, A.M. and Nelson, W.G.**, 2004. GSTP1 CpG island hypermethylation as a molecular biomarker for prostate cancer, *J Cell Biochem*. 91, 540-552.

323. **Nakayama, T., Watanabe, M., Yamanaka, M., Hirokawa, Y., Suzuki, H., Ito, H., Yatani, R. and Shiraishi, T.**, 2001. The role of epigenetic modifications in retinoic acid receptor beta2 gene expression in human prostate cancers, *Lab Invest*. 81, 1049-1057.

324. **Nan, X., Campoy, F.J. and Bird, A.**, 1997. MeCP2 is a transcriptional repressor with abundant binding sites in genomic chromatin, *Cell*. 88, 471-481.

325. **Nan, X., Ng, H.H., Johnson, C.A., Laherty, C.D., Turner, B.M., Eisenman, R.N. and Bird, A.**, 1998. Transcriptional repression by the methyl-CpG-binding protein MeCP2 involves a histone deacetylase complex, *Nature*. 393, 386-389.

326. **Nickel, J.C.**, 2008. Inflammation and benign prostatic hyperplasia, *Urol Clin North Am*. 35, 109-115; vii.

327. **Normant, E., Martres, M.P., Schwartz, J.C. and Gros, C.**, 1995. Purification, cDNA cloning, functional expression, and characterization of a 26-kDa endogenous mammalian carboxypeptidase inhibitor, *Proc Natl Acad Sci U S A*. 92, 12225-12229.

328. **Noy, N.**, 2000. Retinoid-binding proteins: mediators of retinoid action, *Biochem J*. 348 Pt 3, 481-495.

329. **Nwankwo, J.O.**, 2002. Anti-metastatic activities of all-trans retinoic acid, indole-3-carbinol and (+)-catechin in Dunning rat invasive prostate adenocarcinoma cells, *Anticancer Res*. 22, 4129-4135.

330. **Ogishima, T., Shiina, H., Breault, J.E., Tabatabai, L., Bassett, W.W., Enokida, H., Li, L.C., Kawakami, T., Urakami, S., Ribeiro-Filho, L.A., Terashima, M., Fujime, M., Igawa, M. and Dahiya, R.**, 2005. Increased heparanase expression is caused by promoter hypomethylation and up-regulation of transcriptional factor early growth response-1 in human prostate cancer, *Clin Cancer Res*. 11, 1028-1036.

331. **Ohm, J.E., McGarvey, K.M., Yu, X., Cheng, L., Schuebel, K.E., Cope, L., Mohammad, H.P., Chen, W., Daniel, V.C., Yu, W., Berman, D.M., Jenuwein, T., Pruitt, K., Sharkis, S.J., Watkins, D.N., Herman, J.G. and Baylin, S.B.**, 2007. A stem cell-like chromatin pattern may predispose tumor suppressor genes to DNA hypermethylation and heritable silencing, *Nat Genet*. 39, 237-242.

332. **Ohnishi, S., Okabe, K., Obata, H., Otani, K., Ishikane, S., Ogino, H., Kitamura, S. and Nagaya, N.**, 2009. Involvement of tazarotene-induced gene 1 in proliferation and differentiation of human adipose tissue-derived mesenchymal stem cells, *Cell Prolif*. 42, 309-316.

333. **Okano, M., Bell, D.W., Haber, D.A. and Li, E.**, 1999. DNA methyltransferases Dnmt3a and Dnmt3b are essential for de novo methylation and mammalian development, *Cell*. 99, 247-257.

334. **Okuducu, A.F., Janzen, V., Ko, Y., Hahne, J.C., Lu, H., Ma, Z.L., Albers, P., Sahin, A., Wellmann, A., Scheinert, P. and Wernert, N.**, 2005. Cellular retinoic acid-binding protein 2 is down-regulated in prostate cancer, *Int J Oncol*. 27, 1273-1282.

335. **Oldridge, E.E., Pellacani, D., Collins, A.T. and Maitland, N.J.**, 2012. Prostate cancer stem cells: Are they androgen-responsive?, *Mol Cell Endocrinol*. 360, 14-24.

336. **Orkin, S.H. and Zon, L.I.**, 2008. Hematopoiesis: an evolving paradigm for stem cell biology, *Cell*. 132, 631-644.

337. **Pakneshan, P., Xing, R.H. and Rabbani, S.A.**, 2003. Methylation status of uPA promoter as a molecular mechanism regulating prostate cancer invasion and growth in vitro and in vivo, *FASEB J*. 17, 1081-1088.

338. **Pallares, I., Berenguer, C., Aviles, F.X., Vendrell, J. and Ventura, S.**, 2007. Self-assembly of human latexin into amyloid-like oligomers, *BMC Struct Biol*. 7, 75.

339. **Pallares, I., Bonet, R., Garcia-Castellanos, R., Ventura, S., Aviles, F.X., Vendrell, J. and Gomis-Ruth, F.X.**, 2005. Structure of human carboxypeptidase A4 with its endogenous protein inhibitor, latexin, *Proc Natl Acad Sci U S A*. 102, 3978-3983.

340. **Park, I.K., Qian, D., Kiel, M., Becker, M.W., Pihalja, M., Weissman, I.L., Morrison, S.J. and Clarke, M.F.**, 2003. Bmi-1 is required for maintenance of adult self-renewing haematopoietic stem cells, *Nature*. 423, 302-305.

341. **Park, S., Shinohara, K., Grossfeld, G.D. and Carroll, P.R.**, 2001. Prostate cancer detection in men with prior high grade prostatic intraepithelial neoplasia or atypical prostate biopsy, *J Urol*. 165, 1409-1414.

342. **Patra, S.K., Patra, A. and Dahiya, R.**, 2001. Histone deacetylase and DNA methyltransferase in human prostate cancer, *Biochem Biophys Res Commun*. 287, 705-713.

343. **Peehl, D.M., Wong, S.T. and Stamey, T.A.**, 1993. Vitamin A regulates proliferation and differentiation of human prostatic epithelial cells, *Prostate*. 23, 69-78.

344. **Peeling, W.B.**, 1989. Phase III studies to compare goserelin (Zoladex) with orchiectomy and with diethylstilbestrol in treatment of prostatic carcinoma, *Urology*. 33, 45-52.

345. **Pellacani, D., Kestoras, D., Droop, A.P., Wilson, K.M., Polson, E.S., Hager, S., Frame, F.M., Berry, P.A., Stower, M.J., Simms, M.S., Mann, V.M., Collins, A.T. and Maitland, N.J.**, 2012. DNA hypermethylation in prostate cancer is a consequence of aberrant epithelial differentiation. , *Manuscript in preparation.* .

346. **Peng, Z., Shen, R., Li, Y.W., Teng, K.Y., Shapiro, C.L. and Lin, H.J.**, 2012. Epigenetic repression of RARRES1 is mediated by methylation of a proximal promoter and a loss of CTCF binding, *PLoS One*. 7, e36891.

347. **Penn, N.W., Suwalski, R., O'Riley, C., Bojanowski, K. and Yura, R.**, 1972. The presence of 5-hydroxymethylcytosine in animal deoxyribonucleic acid, *Biochem J*. 126, 781-790.

348. **Pham, P.V., Phan, N.L., Nguyen, N.T., Truong, N.H., Duong, T.T., Le, D.V., Truong, K.D. and Phan, N.K.**, 2011. Differentiation of breast cancer stem cells by knockdown of CD44: promising differentiation therapy, *J Transl Med*. 9, 209.

349. **Phillips, T.M., McBride, W.H. and Pajonk, F.**, 2006. The response of CD24(-/low)/CD44+ breast cancer-initiating cells to radiation, *J Natl Cancer Inst*. 98, 1777-1785.

350. **Piccirillo, S.G., Reynolds, B.A., Zanetti, N., Lamorte, G., Binda, E., Broggi, G., Brem, H., Olivi, A., Dimeco, F. and Vescovi, A.L.**, 2006. Bone morphogenetic proteins inhibit the tumorigenic potential of human brain tumour-initiating cells, *Nature*. 444, 761-765.

351. **Placer, J. and Morote, J.**, 2011. [Usefulness of prostatic specific antigen (PSA) for diagnosis and staging of patients with prostate cancer], *Arch Esp Urol*. 64, 659-680.

352. **Polyak, K. and Weinberg, R.A.**, 2009. Transitions between epithelial and mesenchymal states: acquisition of malignant and stem cell traits, *Nat Rev Cancer*. 9, 265-273.

353. **Prince, M.E., Sivanandan, R., Kaczorowski, A., Wolf, G.T., Kaplan, M.J., Dalerba, P., Weissman, I.L., Clarke, M.F. and Ailles, L.E.**, 2007. Identification of a subpopulation of cells with cancer stem cell properties in head and neck squamous cell carcinoma, *Proc Natl Acad Sci U S A*. 104, 973-978.

354. **Prins, G.S. and Putz, O.**, 2008. Molecular signaling pathways that regulate prostate gland development, *Differentiation*. 76, 641-659.

355. **Psaila, B. and Lyden, D.**, 2009. The metastatic niche: adapting the foreign soil, *Nat Rev Cancer*. 9, 285-293.

356. **Quinn, M. and Babb, P.**, 2002. Patterns and trends in prostate cancer incidence, survival, prevalence and mortality. Part I: international comparisons, *BJU Int*. 90, 162-173.

357. **Rajasekhar, V.K., Studer, L., Gerald, W., Socci, N.D. and Scher, H.I.**, 2011. Tumour-initiating stem-like cells in human prostate cancer exhibit increased NF-kappaB signalling, *Nat Commun*. 2, 162.

358. **Rand, K., Qu, W., Ho, T., Clark, S.J. and Molloy, P.**, 2002. Conversion-specific detection of DNA methylation using real-time polymerase chain reaction (ConLight-MSP) to avoid false positives, *Methods*. 27, 114-120.

359. **Raviv, G., Janssen, T., Zlotta, A.R., Louis, L., Descamps, F., Verhest, A. and Schulman, C.C.**, 1996. [High-grade intraepithelial prostatic neoplasms: diagnosis and association with prostate cancer], *Acta Urol Belg*. 64, 11-15.

360. **Reya, T., Morrison, S.J., Clarke, M.F. and Weissman, I.L.**, 2001. Stem cells, cancer, and cancer stem cells, *Nature*. 414, 105-111.

361. **Ricci-Vitiani, L., Lombardi, D.G., Pilozzi, E., Biffoni, M., Todaro, M., Peschle, C. and De Maria, R.**, 2007. Identification and expansion of human colon-cancer-initiating cells, *Nature*. 445, 111-115.

362. **Richardson, G.D., Robson, C.N., Lang, S.H., Neal, D.E., Maitland, N.J. and Collins, A.T.**, 2004. CD133, a novel marker for human prostatic epithelial stem cells, *J Cell Sci*. 117, 3539-3545.

363. **Richter, F., Joyce, A., Fromowitz, F., Wang, S., Watson, J., Watson, R., Irwin, R.J., Jr. and Huang, H.F.**, 2002. Immunohistochemical localization of the retinoic Acid receptors in human prostate, *J Androl*. 23, 830-838.

364. **Riggs, A.D.**, 1975. X inactivation, differentiation, and DNA methylation, *Cytogenet Cell Genet*. 14, 9-25.

365. **Risbridger, G.P., Davis, I.D., Birrell, S.N. and Tilley, W.D.**, 2010. Breast and prostate cancer: more similar than different, *Nat Rev Cancer*. 10, 205-212.

366. **Rittmaster, R.S.**, 1994. Finasteride, *N Engl J Med*. 330, 120-125.

367. **Rivera-Gonzalez, G.C., Droop, A.P., Rippon, H.J., Tiemann, K., Pellacani, D., Georgopoulos, L.J. and Maitland, N.J.**, 2012. Retinoic acid and androgen receptors combine to achieve tissue specific control of human prostatic transglutaminase expression: a novel regulatory network with broader significance, *Nucleic Acids Res*. 40, 4825-4840.

368. **Robinson, E.J., Neal, D.E. and Collins, A.T.**, 1998. Basal cells are progenitors of luminal cells in primary cultures of differentiating human prostatic epithelium, *Prostate*. 37, 149-160.

369. **Rodriguez, L.G., Wu, X. and Guan, J.L.**, 2005. Wound-healing assay, *Methods Mol Biol*. 294, 23-29.

370. **Roloff, T.C. and Nuber, U.A.**, 2005. Chromatin, epigenetics and stem cells, *Eur J Cell Biol*. 84, 123-135.

371. **Ross, P.L., Cheng, I., Liu, X., Cicek, M.S., Carroll, P.R., Casey, G. and Witte, J.S.**, 2009. Carboxypeptidase 4 gene variants and early-onset intermediate-to-high risk prostate cancer, *BMC Cancer*. 9, 69.

372. **Roth, S.Y., Denu, J.M. and Allis, C.D.**, 2001. Histone acetyltransferases, *Annu Rev Biochem*. 70, 81-120.

373. **Roy-Burman, P., Wu, H., Powell, W.C., Hagenkord, J. and Cohen, M.B.**, 2004. Genetically defined mouse models that mimic natural aspects of human prostate cancer development, *Endocr Relat Cancer*. 11, 225-254.

374. **Rumpold, H., Heinrich, E., Untergasser, G., Hermann, M., Pfister, G., Plas, E. and Berger, P.**, 2002. Neuroendocrine differentiation of human prostatic primary epithelial cells in vitro, *Prostate*. 53, 101-108.

375. **Ruska, K.M., Sauvageot, J. and Epstein, J.I.**, 1998. Histology and cellular kinetics of prostatic atrophy, *Am J Surg Pathol*. 22, 1073-1077.

376. **Rutella, S., Bonanno, G., Procoli, A., Mariotti, A., Corallo, M., Prisco, M.G., Eramo, A., Napoletano, C., Gallo, D., Perillo, A., Nuti, M., Pierelli, L., Testa, U., Scambia, G. and Ferrandina, G.**, 2009. Cells with characteristics of cancer stem/progenitor cells express the CD133 antigen in human endometrial tumors, *Clin Cancer Res*. 15, 4299-4311.

377. **Sabbath, K.D. and Griffin, J.D.**, 1985. Clonogenic cells in acute myeloblastic leukaemia, *Scand J Haematol*. 35, 251-256.

378. **Sahab, Z.J., Hall, M.D., Me Sung, Y., Dakshanamurthy, S., Ji, Y., Kumar, D. and Byers, S.W.**, 2011. Tumor suppressor RARRES1 interacts with cytoplasmic carboxypeptidase AGBL2 to regulate the alpha-tubulin tyrosination cycle, *Cancer Res*. 71, 1219-1228.

379. **Sakr, W.A., Haas, G.P., Cassin, B.F., Pontes, J.E. and Crissman, J.D.**, 1993. The frequency of carcinoma and intraepithelial neoplasia of the prostate in young male patients, *J Urol*. 150, 379-385.

380. **Sammons, J., Ahmed, N., Khokher, M.A. and Hassan, H.T.**, 2000. Mechanisms mediating the inhibitory effect of all-trans retinoic acid on primitive hematopoietic stem cells in human long-term bone marrow culture, *Stem Cells*. 18, 214-219.

381. **Sanchez, P., Hernandez, A.M., Stecca, B., Kahler, A.J., DeGueme, A.M., Barrett, A., Beyna, M., Datta, M.W., Datta, S. and Ruiz i Altaba, A.**, 2004. Inhibition of prostate cancer proliferation by interference with SONIC HEDGEHOG-GLI1 signaling, *Proc Natl Acad Sci U S A*. 101, 12561-12566.

382. **Santisteban, M., Reiman, J.M., Asiedu, M.K., Behrens, M.D., Nassar, A., Kalli, K.R., Haluska, P., Ingle, J.N., Hartmann, L.C., Manjili, M.H., Radisky, D.C., Ferrone, S. and Knutson, K.L.**, 2009. Immune-induced epithelial to mesenchymal transition in vivo generates breast cancer stem cells, *Cancer Res*. 69, 2887-2895.

383. **Saric, T., Brkanac, Z., Troyer, D.A., Padalecki, S.S., Sarosdy, M., Williams, K., Abadesco, L., Leach, R.J. and O'Connell, P.**, 1999. Genetic pattern of prostate cancer progression, *Int J Cancer*. 81, 219-224.

384. **Savagner, P., Kusewitt, D.F., Carver, E.A., Magnino, F., Choi, C., Gridley, T. and Hudson, L.G.**, 2005. Developmental transcription factor slug is required for effective re-epithelialization by adult keratinocytes, *J Cell Physiol*. 202, 858-866.

385. **Schatton, T., Murphy, G.F., Frank, N.Y., Yamaura, K., Waaga-Gasser, A.M., Gasser, M., Zhan, Q., Jordan, S., Duncan, L.M., Weishaupt, C., Fuhlbrigge, R.C., Kupper, T.S., Sayegh, M.H. and Frank, M.H.**, 2008. Identification of cells initiating human melanomas, *Nature*. 451, 345-349.

386. **Schauer, I.G. and Rowley, D.R.**, 2011. The functional role of reactive stroma in benign prostatic hyperplasia, *Differentiation*. 82, 200-210.

387. **Schlesinger, C., Bostwick, D.G. and Iczkowski, K.A.**, 2005. High-grade prostatic intraepithelial neoplasia and atypical small acinar proliferation: predictive value for cancer in current practice, *Am J Surg Pathol*. 29, 1201-1207.

388. **Schlesinger, Y., Straussman, R., Keshet, I., Farkash, S., Hecht, M., Zimmerman, J., Eden, E., Yakhini, Z., Ben-Shushan, E., Reubinoff, B.E., Bergman, Y., Simon, I. and Cedar, H.**, 2007. Polycomb-mediated methylation on Lys27 of histone H3 pre-marks genes for de novo methylation in cancer, *Nat Genet*. 39, 232-236.

389. **Schmittgen, T.D. and Livak, K.J.**, 2008. Analyzing real-time PCR data by the comparative C(T) method, *Nat Protoc*. 3, 1101-1108.

390. **Schroder, F.H. and Blom, J.H.**, 1989. Natural history of benign prostatic hyperplasia (BPH), *Prostate Suppl*. 2, 17-22.

391. **Schuettengruber, B., Chourrout, D., Vervoort, M., Leblanc, B. and Cavalli, G.**, 2007. Genome regulation by polycomb and trithorax proteins, *Cell*. 128, 735-745.

392. **Schultz, B.E., Misialek, S., Wu, J., Tang, J., Conn, M.T., Tahilramani, R. and Wong, L.**, 2004. Kinetics and comparative reactivity of human class I and class IIb histone deacetylases, *Biochemistry*. 43, 11083-11091.

393. **Schulz, W.A., Elo, J.P., Florl, A.R., Pennanen, S., Santourlidis, S., Engers, R., Buchardt, M., Seifert, H.H. and Visakorpi, T.**, 2002. Genomewide DNA hypomethylation is associated with alterations on chromosome 8 in prostate carcinoma, *Genes Chromosomes Cancer*. 35, 58-65.

394. **Sciarra, A., Mariotti, G., Salciccia, S., Autran Gomez, A., Monti, S., Toscano, V. and Di Silverio, F.**, 2008. Prostate growth and inflammation, *J Steroid Biochem Mol Biol*. 108, 254-260.

395. **Scoumanne, A. and Chen, X.**, 2007. The lysine-specific demethylase 1 is required for cell proliferation in both p53-dependent and -independent manners, *J Biol Chem*. 282, 15471-15475.

396. **Sehgal, I., Powers, S., Huntley, B., Powis, G., Pittelkow, M. and Maihle, N.J.**, 1994. Neurotensin is an autocrine trophic factor stimulated by androgen withdrawal in human prostate cancer, *Proc Natl Acad Sci U S A*. 91, 4673-4677.

397. **Sen, G.L., Reuter, J.A., Webster, D.E., Zhu, L. and Khavari, P.A.**, 2010. DNMT1 maintains progenitor function in self-renewing somatic tissue, *Nature*. 463, 563-567.

398. **Seo, R., McGuire, M., Chung, M. and Bushman, W.**, 1997. Inhibition of prostate ductal morphogenesis by retinoic acid, *J Urol*. 158, 931-935.

399. **Seruga, B. and Tannock, I.F.**, 2011. Chemotherapy-based treatment for castration-resistant prostate cancer, *J Clin Oncol*. 29, 3686-3694.

400. **Sessler, R.J. and Noy, N.**, 2005. A ligand-activated nuclear localization signal in cellular retinoic acid binding protein-II, *Mol Cell*. 18, 343-353.

401. **Sharma, S.V., Lee, D.Y., Li, B., Quinlan, M.P., Takahashi, F., Maheswaran, S., McDermott, U., Azizian, N., Zou, L., Fischbach, M.A., Wong, K.K., Brandstetter, K., Wittner, B., Ramaswamy, S., Classon, M. and Settleman, J.**, 2010. A chromatin-mediated reversible drug-tolerant state in cancer cell subpopulations, *Cell*. 141, 69-80.

402. **Shen, M.M. and Abate-Shen, C.**, 2010. Molecular genetics of prostate cancer: new prospects for old challenges, *Genes Dev*. 24, 1967-2000.

403. **Shepherd, D., Keetch, D.W., Humphrey, P.A., Smith, D.S. and Stahl, D.**, 1996. Repeat biopsy strategy in men with isolated prostatic intraepithelial neoplasia on prostate needle biopsy, *J Urol*. 156, 460-462; discussion 462-463.

404. **Sheridan, C., Kishimoto, H., Fuchs, R.K., Mehrotra, S., Bhat-Nakshatri, P., Turner, C.H., Goulet, R., Jr., Badve, S. and Nakshatri, H.**, 2006. CD44+/CD24- breast cancer cells exhibit enhanced invasive properties: an early step necessary for metastasis, *Breast Cancer Res*. 8, R59.

405. **Sherwood, E.R., Theyer, G., Steiner, G., Berg, L.A., Kozlowski, J.M. and Lee, C.**, 1991. Differential expression of specific cytokeratin polypeptides in the basal and luminal epithelia of the human prostate, *Prostate*. 18, 303-314.

406. **Shimono, Y., Zabala, M., Cho, R.W., Lobo, N., Dalerba, P., Qian, D., Diehn, M., Liu, H., Panula, S.P., Chiao, E., Dirbas, F.M., Somlo, G., Pera, R.A., Lao, K. and Clarke, M.F.**, 2009. Downregulation of miRNA-200c links breast cancer stem cells with normal stem cells, *Cell*. 138, 592-603.

407. **Shridhar, P.**, 1979. The lymphatics of the prostate gland and their role in the spread of prostatic carcinoma, *Ann R Coll Surg Engl*. 61, 114-122.

408. **Shukla, V., Vaissiere, T. and Herceg, Z.**, 2008. Histone acetylation and chromatin signature in stem cell identity and cancer, *Mutat Res*. 637, 1-15.

409. **Shultz, L.D., Schweitzer, P.A., Christianson, S.W., Gott, B., Schweitzer, I.B., Tennent, B., McKenna, S., Mobraaten, L., Rajan, T.V., Greiner, D.L. and et al.**, 1995. Multiple defects in innate and adaptive immunologic function in NOD/LtSz-scid mice, *J Immunol*. 154, 180-191.

410. **Signoretti, S., Waltregny, D., Dilks, J., Isaac, B., Lin, D., Garraway, L., Yang, A., Montironi, R., McKeon, F. and Loda, M.**, 2000. p63 is a prostate basal cell marker and is required for prostate development, *Am J Pathol*. 157, 1769-1775.

411. **Silber, J., Lim, D.A., Petritsch, C., Persson, A.I., Maunakea, A.K., Yu, M., Vandenberg, S.R., Ginzinger, D.G., James, C.D., Costello, J.F., Bergers, G., Weiss, W.A., Alvarez-Buylla, A. and Hodgson, J.G.**, 2008. miR-124 and miR-137 inhibit proliferation of glioblastoma multiforme cells and induce differentiation of brain tumor stem cells, *BMC Med*. 6, 14.

412. **Simandi, Z., Balint, B.L., Poliska, S., Ruhl, R. and Nagy, L.**, 2010. Activation of retinoic acid receptor signaling coordinates lineage commitment of spontaneously

differentiating mouse embryonic stem cells in embryoid bodies, *FEBS Lett*. 584, 3123-3130.

413. **Singh, S.K., Clarke, I.D., Terasaki, M., Bonn, V.E., Hawkins, C., Squire, J. and Dirks, P.B.**, 2003. Identification of a cancer stem cell in human brain tumors, *Cancer Res*. 63, 5821-5828.

414. **Singh, S.K., Hawkins, C., Clarke, I.D., Squire, J.A., Bayani, J., Hide, T., Henkelman, R.M., Cusimano, M.D. and Dirks, P.B.**, 2004. Identification of human brain tumour initiating cells, *Nature*. 432, 396-401.

415. **Smith, M.R., Biggar, S. and Hussain, M.**, 1995. Prostate-specific antigen messenger RNA is expressed in non-prostate cells: implications for detection of micrometastases, *Cancer Res*. 55, 2640-2644.

416. **Son, M.S., Kang, M.J., Park, H.C., Chi, S.G. and Kim, Y.H.**, 2009. Expression and mutation analysis of TIG1 (tazarotene-induced gene 1) in human gastric cancer, *Oncol Res*. 17, 571-580.

417. **Stanford, J.L. and Ostrander, E.A.**, 2001. Familial prostate cancer, *Epidemiol Rev*. 23, 19-23.

418. **Stone, K.R., Mickey, D.D., Wunderli, H., Mickey, G.H. and Paulson, D.F.**, 1978. Isolation of a human prostate carcinoma cell line (DU 145), *Int J Cancer*. 21, 274-281.

419. **Stott, S.L., Hsu, C.H., Tsukrov, D.I., Yu, M., Miyamoto, D.T., Waltman, B.A., Rothenberg, S.M., Shah, A.M., Smas, M.E., Korir, G.K., Floyd, F.P., Jr., Gilman, A.J., Lord, J.B., Winokur, D., Springer, S., Irimia, D., Nagrath, S., Sequist, L.V., Lee, R.J., Isselbacher, K.J., Maheswaran, S., Haber, D.A. and Toner, M.**, 2010. Isolation of circulating tumor cells using a microvortex-generating herringbone-chip, *Proc Natl Acad Sci U S A*. 107, 18392-18397.

420. **Struhl, G.**, 1981. A gene product required for correct initiation of segmental determination in Drosophila, *Nature*. 293, 36-41.

421. **Su, Z.Y., Li, Y., Zhao, X.L. and Zhang, M.**, 2010. All-trans retinoic acid promotes smooth muscle cell differentiation of rabbit bone marrow-derived mesenchymal stem cells, *J Zhejiang Univ Sci B*. 11, 489-496.

422. **Swift, S.L., Burns, J.E. and Maitland, N.J.**, 2010. Altered expression of neurotensin receptors is associated with the differentiation state of prostate cancer, *Cancer Res*. 70, 347-356.

423. **Tagoh, H., Melnik, S., Lefevre, P., Chong, S., Riggs, A.D. and Bonifer, C.**, 2004. Dynamic reorganization of chromatin structure and selective DNA demethylation prior to stable enhancer complex formation during differentiation of primary hematopoietic cells in vitro, *Blood*. 103, 2950-2955.

424. **Tahiliani, M., Koh, K.P., Shen, Y., Pastor, W.A., Bandukwala, H., Brudno, Y., Agarwal, S., Iyer, L.M., Liu, D.R., Aravind, L. and Rao, A.**, 2009. Conversion of 5-methylcytosine to 5-hydroxymethylcytosine in mammalian DNA by MLL partner TET1, *Science*. 324, 930-935.

425. **Takahashi, S., Shan, A.L., Ritland, S.R., Delacey, K.A., Bostwick, D.G., Lieber, M.M., Thibodeau, S.N. and Jenkins, R.B.**, 1995. Frequent loss of heterozygosity at 7q31.1 in primary prostate cancer is associated with tumor aggressiveness and progression, *Cancer Res.* 55, 4114-4119.

426. **Takai, D. and Jones, P.A.**, 2002. Comprehensive analysis of CpG islands in human chromosomes 21 and 22, *Proc Natl Acad Sci U S A.* 99, 3740-3745.

427. **Takai, N., Kawamata, N., Walsh, C.S., Gery, S., Desmond, J.C., Whittaker, S., Said, J.W., Popoviciu, L.M., Jones, P.A., Miyakawa, I. and Koeffler, H.P.**, 2005. Discovery of epigenetically masked tumor suppressor genes in endometrial cancer, *Mol Cancer Res.* 3, 261-269.

428. **Tamura, G., So, K., Miyoshi, H., Honda, T., Nishizuka, S. and Motoyama, T.**, 2009. Quantitative assessment of gene methylation in neoplastic and non-neoplastic gastric epithelia using methylation-specific DNA microarray, *Pathol Int.* 59, 895-899.

429. **Tanco, S., Zhang, X., Morano, C., Aviles, F.X., Lorenzo, J. and Fricker, L.D.**, 2010. Characterization of the substrate specificity of human carboxypeptidase A4 and implications for a role in extracellular peptide processing, *J Biol Chem.* 285, 18385-18396.

430. **Taplin, M.E., Rajeshkumar, B., Halabi, S., Werner, C.P., Woda, B.A., Picus, J., Stadler, W., Hayes, D.F., Kantoff, P.W., Vogelzang, N.J. and Small, E.J.**, 2003. Androgen receptor mutations in androgen-independent prostate cancer: Cancer and Leukemia Group B Study 9663, *J Clin Oncol.* 21, 2673-2678.

431. **Thiery, J.P.**, 2002. Epithelial-mesenchymal transitions in tumour progression, *Nat Rev Cancer.* 2, 442-454.

432. **Thiery, J.P., Acloque, H., Huang, R.Y. and Nieto, M.A.**, 2009. Epithelial-mesenchymal transitions in development and disease, *Cell.* 139, 871-890.

433. **Thompson, I.M., Chi, C., Ankerst, D.P., Goodman, P.J., Tangen, C.M., Lippman, S.M., Lucia, M.S., Parnes, H.L. and Coltman, C.A., Jr.**, 2006. Effect of finasteride on the sensitivity of PSA for detecting prostate cancer, *J Natl Cancer Inst.* 98, 1128-1133.

434. **Thompson, I.M., Pauler, D.K., Goodman, P.J., Tangen, C.M., Lucia, M.S., Parnes, H.L., Minasian, L.M., Ford, L.G., Lippman, S.M., Crawford, E.D., Crowley, J.J. and Coltman, C.A., Jr.**, 2004. Prevalence of prostate cancer among men with a prostate-specific antigen level < or =4.0 ng per milliliter, *N Engl J Med.* 350, 2239-2246.

435. **Tokizane, T., Shiina, H., Igawa, M., Enokida, H., Urakami, S., Kawakami, T., Ogishima, T., Okino, S.T., Li, L.C., Tanaka, Y., Nonomura, N., Okuyama, A. and Dahiya, R.**, 2005. Cytochrome P450 1B1 is overexpressed and regulated by hypomethylation in prostate cancer, *Clin Cancer Res.* 11, 5793-5801.

436. **Tokumaru, Y., Harden, S.V., Sun, D.I., Yamashita, K., Epstein, J.I. and Sidransky, D.**, 2004. Optimal use of a panel of methylation markers with GSTP1 hypermethylation in the diagnosis of prostate adenocarcinoma, *Clin Cancer Res.* 10, 5518-5522.

437. **Tost, J. and Gut, I.G.**, 2007. DNA methylation analysis by pyrosequencing, *Nat Protoc.* 2, 2265-2275.

438. **Tsihlias, J., Kapusta, L.R., DeBoer, G., Morava-Protzner, I., Zbieranowski, I., Bhattacharya, N., Catzavelos, G.C., Klotz, L.H. and Slingerland, J.M.**, 1998. Loss of cyclin-dependent kinase inhibitor p27Kip1 is a novel prognostic factor in localized human prostate adenocarcinoma, *Cancer Res.* 58, 542-548.

439. **Tsujimura, A., Koikawa, Y., Salm, S., Takao, T., Coetzee, S., Moscatelli, D., Shapiro, E., Lepor, H., Sun, T.T. and Wilson, E.L.**, 2002. Proximal location of mouse prostate epithelial stem cells: a model of prostatic homeostasis, *J Cell Biol.* 157, 1257-1265.

440. **Uratani, Y., Takiguchi-Hayashi, K., Miyasaka, N., Sato, M., Jin, M. and Arimatsu, Y.**, 2000. Latexin, a carboxypeptidase A inhibitor, is expressed in rat peritoneal mast cells and is associated with granular structures distinct from secretory granules and lysosomes, *Biochem J.* 346 Pt 3, 817-826.

441. **Vaissiere, T., Sawan, C. and Herceg, Z.**, 2008. Epigenetic interplay between histone modifications and DNA methylation in gene silencing, *Mutat Res.* 659, 40-48.

442. **Valastyan, S. and Weinberg, R.A.**, 2011. Tumor metastasis: molecular insights and evolving paradigms, *Cell.* 147, 275-292.

443. **Van Den Berg, C., Guan, X.Y., Von Hoff, D., Jenkins, R., Bittner, Griffin, C., Kallioniemi, O., Visakorpi, McGill, Herath, J. and et al.**, 1995. DNA sequence amplification in human prostate cancer identified by chromosome microdissection: potential prognostic implications, *Clin Cancer Res.* 1, 11-18.

444. **van den Hoogen, C., van der Horst, G., Cheung, H., Buijs, J.T., Lippitt, J.M., Guzman-Ramirez, N., Hamdy, F.C., Eaton, C.L., Thalmann, G.N., Cecchini, M.G., Pelger, R.C. and van der Pluijm, G.**, 2010. High aldehyde dehydrogenase activity identifies tumor-initiating and metastasis-initiating cells in human prostate cancer, *Cancer Res.* 70, 5163-5173.

445. **van Leenders, G.J., Aalders, T.W., Hulsbergen-van de Kaa, C.A., Ruiter, D.J. and Schalken, J.A.**, 2001. Expression of basal cell keratins in human prostate cancer metastases and cell lines, *J Pathol.* 195, 563-570.

446. **van Leenders, G.J., Gage, W.R., Hicks, J.L., van Balken, B., Aalders, T.W., Schalken, J.A. and De Marzo, A.M.**, 2003. Intermediate cells in human prostate epithelium are enriched in proliferative inflammatory atrophy, *Am J Pathol.* 162, 1529-1537.

447. **van Leenders, G.J. and Schalken, J.A.**, 2001. Stem cell differentiation within the human prostate epithelium: implications for prostate carcinogenesis, *BJU Int.* 88 Suppl 2, 35-42; discussion 49-50.

448. **Varambally, S., Dhanasekaran, S.M., Zhou, M., Barrette, T.R., Kumar-Sinha, C., Sanda, M.G., Ghosh, D., Pienta, K.J., Sewalt, R.G., Otte, A.P., Rubin, M.A. and Chinnaiyan, A.M.**, 2002. The polycomb group protein EZH2 is involved in progression of prostate cancer, *Nature.* 419, 624-629.

449. **Vendrell, J., Querol, E. and Aviles, F.X.**, 2000. Metallocarboxypeptidases and their protein inhibitors. Structure, function and biomedical properties, *Biochim Biophys Acta*. 1477, 284-298.

450. **Verhagen, A.P., Aalders, T.W., Ramaekers, F.C., Debruyne, F.M. and Schalken, J.A.**, 1988. Differential expression of keratins in the basal and luminal compartments of rat prostatic epithelium during degeneration and regeneration, *Prostate*. 13, 25-38.

451. **Verhagen, A.P., Ramaekers, F.C., Aalders, T.W., Schaafsma, H.E., Debruyne, F.M. and Schalken, J.A.**, 1992. Colocalization of basal and luminal cell-type cytokeratins in human prostate cancer, *Cancer Res*. 52, 6182-6187.

452. **Verras, M., Brown, J., Li, X., Nusse, R. and Sun, Z.**, 2004. Wnt3a growth factor induces androgen receptor-mediated transcription and enhances cell growth in human prostate cancer cells, *Cancer Res*. 64, 8860-8866.

453. **Vezina, C.M., Allgeier, S.H., Fritz, W.A., Moore, R.W., Strerath, M., Bushman, W. and Peterson, R.E.**, 2008. Retinoic acid induces prostatic bud formation, *Dev Dyn*. 237, 1321-1333.

454. **Vire, E., Brenner, C., Deplus, R., Blanchon, L., Fraga, M., Didelot, C., Morey, L., Van Eynde, A., Bernard, D., Vanderwinden, J.M., Bollen, M., Esteller, M., Di Croce, L., de Launoit, Y. and Fuks, F.**, 2006. The Polycomb group protein EZH2 directly controls DNA methylation, *Nature*. 439, 871-874.

455. **Visakorpi, T., Hyytinen, E., Koivisto, P., Tanner, M., Keinanen, R., Palmberg, C., Palotie, A., Tammela, T., Isola, J. and Kallioniemi, O.P.**, 1995. In vivo amplification of the androgen receptor gene and progression of human prostate cancer, *Nat Genet*. 9, 401-406.

456. **Voeller, H.J., Sugars, L.Y., Pretlow, T. and Gelmann, E.P.**, 1994. p53 oncogene mutations in human prostate cancer specimens, *J Urol*. 151, 492-495.

457. **Vogelstein, B. and Kinzler, K.W.**, 1993. The multistep nature of cancer, *Trends Genet*. 9, 138-141.

458. **Vukovic, B., Park, P.C., Al-Maghrabi, J., Beheshti, B., Sweet, J., Evans, A., Trachtenberg, J. and Squire, J.**, 2003. Evidence of multifocality of telomere erosion in high-grade prostatic intraepithelial neoplasia (HPIN) and concurrent carcinoma, *Oncogene*. 22, 1978-1987.

459. **Waghray, A. and Webber, M.M.**, 1995. Retinoic acid modulates extracellular urokinase-type plasminogen activator activity in DU-145 human prostatic carcinoma cells, *Clin Cancer Res*. 1, 747-753.

460. **Walsh, C.P. and Bestor, T.H.**, 1999. Cytosine methylation and mammalian development, *Genes Dev*. 13, 26-34.

461. **Wang, Q., Williamson, M., Bott, S., Brookman-Amissah, N., Freeman, A., Nariculam, J., Hubank, M.J., Ahmed, A. and Masters, J.R.**, 2007. Hypomethylation of WNT5A, CRIP1 and S100P in prostate cancer, *Oncogene*. 26, 6560-6565.

462. **Wang, X., Kruithof-de Julio, M., Economides, K.D., Walker, D., Yu, H., Halili, M.V., Hu, Y.P., Price, S.M., Abate-Shen, C. and Shen, M.M.**, 2009. A luminal epithelial stem cell that is a cell of origin for prostate cancer, *Nature*. 461, 495-500.

463. **Waters, D.J. and Bostwick, D.G.**, 1997. The canine prostate is a spontaneous model of intraepithelial neoplasia and prostate cancer progression, *Anticancer Res*. 17, 1467-1470.

464. **Watt, F.M. and Hogan, B.L.**, 2000. Out of Eden: stem cells and their niches, *Science*. 287, 1427-1430.

465. **Webber, M.M. and Waghray, A.**, 1995. Urokinase-mediated extracellular matrix degradation by human prostatic carcinoma cells and its inhibition by retinoic acid, *Clin Cancer Res*. 1, 755-761.

466. **Weber, M., Davies, J.J., Wittig, D., Oakeley, E.J., Haase, M., Lam, W.L. and Schubeler, D.**, 2005. Chromosome-wide and promoter-specific analyses identify sites of differential DNA methylation in normal and transformed human cells, *Nat Genet*. 37, 853-862.

467. **Whipple, R.A., Matrone, M.A., Cho, E.H., Balzer, E.M., Vitolo, M.I., Yoon, J.R., Ioffe, O.B., Tuttle, K.C., Yang, J. and Martin, S.S.**, 2010. Epithelial-to-mesenchymal transition promotes tubulin detyrosination and microtentacles that enhance endothelial engagement, *Cancer Res*. 70, 8127-8137.

468. **Widschwendter, M., Fiegl, H., Egle, D., Mueller-Holzner, E., Spizzo, G., Marth, C., Weisenberger, D.J., Campan, M., Young, J., Jacobs, I. and Laird, P.W.**, 2007. Epigenetic stem cell signature in cancer, *Nat Genet*. 39, 157-158.

469. **Wilson, J.G., Roth, C.B. and Warkany, J.**, 1953. An analysis of the syndrome of malformations induced by maternal vitamin A deficiency. Effects of restoration of vitamin A at various times during gestation, *Am J Anat*. 92, 189-217.

470. **Witte, J.S., Goddard, K.A., Conti, D.V., Elston, R.C., Lin, J., Suarez, B.K., Broman, K.W., Burmester, J.K., Weber, J.L. and Catalona, W.J.**, 2000. Genomewide scan for prostate cancer-aggressiveness loci, *Am J Hum Genet*. 67, 92-99.

471. **Wolf, G.**, 2000. Cellular retinoic acid-binding protein II: a coactivator of the transactivation by the retinoic acid receptor complex RAR.RXR, *Nutr Rev*. 58, 151-153.

472. **Wood, R.J., Tchack, L., Angelo, G., Pratt, R.E. and Sonna, L.A.**, 2004. DNA microarray analysis of vitamin D-induced gene expression in a human colon carcinoma cell line, *Physiol Genomics*. 17, 122-129.

473. **Woodson, K., Gillespie, J., Hanson, J., Emmert-Buck, M., Phillips, J.M., Linehan, W.M. and Tangrea, J.A.**, 2004. Heterogeneous gene methylation patterns among pre-invasive and cancerous lesions of the prostate: a histopathologic study of whole mount prostate specimens, *Prostate*. 60, 25-31.

474. **Woychik, N.A. and Hampsey, M.**, 2002. The RNA polymerase II machinery: structure illuminates function, *Cell*. 108, 453-463.

475. **Wu, C.C., Hsu, C.W., Chen, C.D., Yu, C.J., Chang, K.P., Tai, D.I., Liu, H.P., Su, W.H., Chang, Y.S. and Yu, J.S.**, 2010. Candidate serological biomarkers for cancer identified

from the secretomes of 23 cancer cell lines and the human protein atlas, *Mol Cell Proteomics*. 9, 1100-1117.

476. **Wu, C.C., Shyu, R.Y., Chou, J.M., Jao, S.W., Chao, P.C., Kang, J.C., Wu, S.T., Huang, S.L. and Jiang, S.Y.**, 2006. RARRES1 expression is significantly related to tumour differentiation and staging in colorectal adenocarcinoma, *Eur J Cancer*. 42, 557-565.

477. **Wu, C.C., Tsai, F.M., Shyu, R.Y., Tsai, Y.M., Wang, C.H. and Jiang, S.Y.**, 2011. G protein-coupled receptor kinase 5 mediates Tazarotene-induced gene 1-induced growth suppression of human colon cancer cells, *BMC Cancer*. 11, 175.

478. **Wu, H. and Zhang, Y.**, 2011. Mechanisms and functions of Tet protein-mediated 5-methylcytosine oxidation, *Genes Dev*. 25, 2436-2452.

479. **Xi, R. and Xie, T.**, 2005. Stem cell self-renewal controlled by chromatin remodeling factors, *Science*. 310, 1487-1489.

480. **Xue, Y., Smedts, F., Debruyne, F.M., de la Rosette, J.J. and Schalken, J.A.**, 1998. Identification of intermediate cell types by keratin expression in the developing human prostate, *Prostate*. 34, 292-301.

481. **Yamanaka, M., Watanabe, M., Yamada, Y., Takagi, A., Murata, T., Takahashi, H., Suzuki, H., Ito, H., Tsukino, H., Katoh, T., Sugimura, Y. and Shiraishi, T.**, 2003. Altered methylation of multiple genes in carcinogenesis of the prostate, *Int J Cancer*. 106, 382-387.

482. **Yanatatsaneejit, P., Chalermchai, T., Kerekhanjanarong, V., Shotelersuk, K., Supiyaphun, P., Mutirangura, A. and Sriuranpong, V.**, 2008. Promoter hypermethylation of CCNA1, RARRES1, and HRASLS3 in nasopharyngeal carcinoma, *Oral Oncol*. 44, 400-406.

483. **Yap, T.A., Zivi, A., Omlin, A. and de Bono, J.S.**, 2011. The changing therapeutic landscape of castration-resistant prostate cancer, *Nat Rev Clin Oncol*. 8, 597-610.

484. **Yegnasubramanian, S., Kowalski, J., Gonzalgo, M.L., Zahurak, M., Piantadosi, S., Walsh, P.C., Bova, G.S., De Marzo, A.M., Isaacs, W.B. and Nelson, W.G.**, 2004. Hypermethylation of CpG islands in primary and metastatic human prostate cancer, *Cancer Res*. 64, 1975-1986.

485. **Yi, R., Poy, M.N., Stoffel, M. and Fuchs, E.**, 2008. A skin microRNA promotes differentiation by repressing 'stemness', *Nature*. 452, 225-229.

486. **Yilmaz, M. and Christofori, G.**, 2009. EMT, the cytoskeleton, and cancer cell invasion, *Cancer Metastasis Rev*. 28, 15-33.

487. **Youssef, E.M., Chen, X.Q., Higuchi, E., Kondo, Y., Garcia-Manero, G., Lotan, R. and Issa, J.P.**, 2004. Hypermethylation and silencing of the putative tumor suppressor Tazarotene-induced gene 1 in human cancers, *Cancer Res*. 64, 2411-2417.

488. **Yu, C., Yao, Z., Dai, J., Zhang, X., Escara-Wilke, J. and Keller, E.**, 2007a. Aldehyde dehydrogenase is a marker of prostate cancer stem cell-like cells in cell lines[abstract 1300]. *In: American Association for Cancer Research Annual Meeting: Proceedings: Los Angeles, CA.*

489. **Yu, F., Yao, H., Zhu, P., Zhang, X., Pan, Q., Gong, C., Huang, Y., Hu, X., Su, F., Lieberman, J. and Song, E.**, 2007b. let-7 regulates self renewal and tumorigenicity of breast cancer cells, *Cell*. 131, 1109-1123.

490. **Yvon, A.M., Wadsworth, P. and Jordan, M.A.**, 1999. Taxol suppresses dynamics of individual microtubules in living human tumor cells, *Mol Biol Cell*. 10, 947-959.

491. **Zenklusen, J.C., Thompson, J.C., Troncoso, P., Kagan, J. and Conti, C.J.**, 1994. Loss of heterozygosity in human primary prostate carcinomas: a possible tumor suppressor gene at 7q31.1, *Cancer Res*. 54, 6370-6373.

492. **Zhang, J., Liu, L. and Pfeifer, G.P.**, 2004. Methylation of the retinoid response gene TIG1 in prostate cancer correlates with methylation of the retinoic acid receptor beta gene, *Oncogene*. 23, 2241-2249.

493. **Zhang, S., Balch, C., Chan, M.W., Lai, H.C., Matei, D., Schilder, J.M., Yan, P.S., Huang, T.H. and Nephew, K.P.**, 2008. Identification and characterization of ovarian cancer-initiating cells from primary human tumors, *Cancer Res*. 68, 4311-4320.

494. **Zhang, Y. and Reinberg, D.**, 2001. Transcription regulation by histone methylation: interplay between different covalent modifications of the core histone tails, *Genes Dev*. 15, 2343-2360.

495. **Zhou, S., Schuetz, J.D., Bunting, K.D., Colapietro, A.M., Sampath, J., Morris, J.J., Lagutina, I., Grosveld, G.C., Osawa, M., Nakauchi, H. and Sorrentino, B.P.**, 2001. The ABC transporter Bcrp1/ABCG2 is expressed in a wide variety of stem cells and is a molecular determinant of the side-population phenotype, *Nat Med*. 7, 1028-1034.